

Targeting anti-cancer drug resistance in mouse models of breast cancer

Janneke E. Jaspers

ISBN: 978-90-393-6049-1

Copyright © 2013 by Janneke E. Jaspers, The Netherlands. All rights reserved.

The research described in this thesis was performed at the Division of Molecular Biology, Molecular Oncology and Molecular Pathology of the Netherlands Cancer Institute, Amsterdam, The Netherlands. This work was funded by a Toptalent fellowship from the Netherlands Organization for Scientific Research (NWO, 021.002.104) and the Dutch Cancer Society (KWF, NKI 2011-5220).

Layout and printing: Gildeprint Drukkerijen, Enschede. Publication of this thesis was financially supported by the Netherlands Cancer Institute, the Dutch Cancer Society, Roche Nederland and Teva Nederland.

Cover design: Studio Refill Ltd by Adrienne Simons
(www.adriennesimons.com)

TARGETING ANTI-CANCER DRUG RESISTANCE IN MOUSE MODELS OF BREAST CANCER

Studies naar resistentie tegen anti-kanker medicijnen in
muismodellen voor borstkanker
(met een samenvatting in het Nederlands)

Proefschrift

ter verkrijging van de graad van doctor
aan de Universiteit Utrecht
op gezag van de rector magnificus, prof.dr. G.J. van der Zwaan,
ingevolge het besluit van het college voor promoties
in het openbaar te verdedigen
op dinsdag 12 november 2013
des middags te 2.30 uur

door

Janneke Elisabeth Jaspers

geboren op 25 november 1983 te Eindhoven

Promotoren: Prof.dr. R.H. Medema
Prof.dr. J. Jonkers

Co-promotor: Dr. S. Rottenberg

TABLE OF CONTENTS

List of abbreviations	7
Chapter 1	11
Therapeutic options for triple-negative breast cancers with defective homologous recombination (<i>Biochim Biophys Acta 2009, 1796(2):266-80</i>)	
Chapter 2	49
High sensitivity of BRCA1-deficient mammary tumors to the PARP inhibitor AZD2281 alone and in combination with platinum drugs (<i>Proc Natl Acad Sci USA 2008, 105(44):17079-84</i>)	
Chapter 3	71
Loss of 53BP1 causes PARP inhibitor resistance in <i>Brca1</i> -mutated mouse mammary tumors (<i>Cancer Disc 2013, 3(1):68-81</i>)	
Chapter 4	107
Multi-drug resistance of sarcomatoid BRCA2-deficient mouse mammary tumors (<i>Manuscript in preparation</i>)	
Chapter 5	131
The mammary stem cell markers CD24 and CD49f are less effective to identify tumor-initiating cells in mesenchymal than in epithelial mouse mammary tumors (<i>Manuscript in preparation</i>)	
Chapter 6	147
Proteomics of mouse BRCA1-deficient mammary tumors identifies DNA repair proteins with potential diagnostic and prognostic value in human breast cancer (<i>Mol Cell Proteomics 2012, 11(7):M111.013334</i>)	
Chapter 7	191
Proteomics of genetically engineered mouse mammary tumors identifies fatty acid metabolism members as potential predictive markers for cisplatin resistance (<i>Mol Cell Proteomics 2013, 12(5):1319-34</i>)	
Chapter 8	221
General discussion	

Summary	245
Appendices	
Nederlandse samenvatting	252
Curriculum Vitae	256
List of publications	257
Dankwoord	259



List of abbreviations

LIST OF ABBREVIATIONS

53BP1	tumor suppressor p53-binding protein 1
ABCB1	ATP-binding cassette sub-family B member 1 (also known as MDR1 or Pgp)
ABCG2	ATP-binding cassette sub-family G member 2 (also known as BCRP)
ACACA	acetyl-CoA carboxylase 1
aCGH	array comparative genomic hybridization
ATM	ataxia telangiectasia mutated
BCRP	breast cancer resistance protein (also known as ABCG2)
BER	base-excision repair
BiNGO	biological networks gene ontology
BRCA1	breast cancer susceptibility protein 1
BRCA2	breast cancer susceptibility protein 2
CDH1	cadherin-1 (also known as E-cadherin)
CK	cytokeratin
CAN	copy number aberrations
CSC	cancer stem cell
DDR	DNA damage response
DNA	deoxyribonucleic acid
DSB	double-strand break
EGFR	epithelial growth factor receptor
EMT	epithelial-to-mesenchymal transition
ER	estrogen receptor
ERBB2	receptor tyrosine-protein kinase 2 (also known as HER2)
FA	Fanconi anaemia
FASN	fatty acid synthase
FFPE	formalin-fixed paraffin-embedded
GEMM	genetically engineered mouse model
GO	gene ontology
GSI	γ -secretase inhibitor
HDAC	histone deacetylase
HER2	tyrosin-kinase type cell surface receptor HER2 (also known as ERBB2)
HMLE	human mammary epithelial cells
HR	homologous recombination
HRD	homologous recombination-deficient
IPA	ingenuity pathways analysis
IR	ionizing radiation

IRIF	ionizing radiation-induced foci
K14	keratin 14
KB1P	<i>K14cre;Brca1^{F/F};p53^{F/F}</i>
KB1PM	<i>K14cre;Brca1^{F/F};p53^{F/F};Mdr1^{-/-}</i>
KB2P	<i>K14cre;Brca2^{F/F};p53^{F/F}</i>
KEP	<i>K14cre;Cdh1^{F/F};p53^{F/F}</i>
KP	<i>K14cre;p53^{F/F}</i>
LC-MS/MS	liquid chromatography-tandem mass spectrometry
LOH	loss of heterozygosity
MDR	multi-drug resistance
MDR1	multi-drug resistance 1 (also known as ABCB1 or Pgp)
MRP	multi-drug resistance protein
MTD	maximum-tolerable dose
NER	nucleotide excision repair
NHEJ	non-homologous end joining
ORF	open-reading frame
PAR	poly(ADP-ribose)
PARP	poly(ADP-ribose) polymerase
PARPi	PARP inhibitor
Pgp	P-glycoprotein
Pi3K	phosphatidylinositol 3-kinase
PR	progesterone receptor
PTEN	phosphatase and tensin homolog on chromosome ten
RNA	ribonucleic acid
RTV	relative tumor volume
SD	standard deviation
SDS-PAGE	sodium dodecyl sulfate poly-acrylamide gel electrophoresis
SELDI-TOF-MS	surface enhanced laser desorption ionization time of flight mass spectrometry
shRNA	short hairpin RNA
SRM-MS	selected reaction monitoring mass spectrometry
SSB	single-strand break repair
STRING	search tool for the retrieval of interacting genes
TGFβ	transforming growth factor beta
TIC	tumor-initiating cells
TNBC	triple-negative breast cancer
TOP	DNA topoisomerase
ZEB1	zinc finger E-box binding homeobox 1

CHAPTER 1



Therapeutic options for triple-negative breast cancers with defective homologous recombination

Janneke E. Jaspers, Sven Rottenberg, Jos Jonkers

Division of Molecular Biology, Netherlands Cancer Institute,
Plesmanlaan 121, 1066 CX Amsterdam, The Netherlands

Biochimica et Biophysica Acta 2009, 1796(2):266-80

ABSTRACT

Breast cancer is the most common malignancy among women in developed countries, affecting more than a million women per year worldwide. Over the last decades, our increasing understanding of breast cancer biology has led to the development of endocrine agents against hormone receptor-positive tumors and targeted therapeutics against HER2-expressing tumors. However, no targeted therapy is available for patients with triple-negative breast cancer, lacking expression of hormone receptors and HER2. Overlap between *BRCA1*-mutated breast cancers and triple-negative tumors suggests that an important part of the triple-negative tumors may respond to therapeutics targeting *BRCA1*-deficient cells. Here, we review the features shared between triple-negative, basal-like and *BRCA1*-related breast cancers. We also discuss the development of novel therapeutic strategies to target *BRCA1*-mutated tumors and triple-negative tumors with *BRCA1*-like features. Finally, we highlight the utility of mouse models for *BRCA1*-mutated breast cancer to optimize (combination) therapy and to understand drug resistance.

1.1 Triple-negative and basal-like breast cancer

Breast tumors are usually classified by immunohistochemical staining for the estrogen receptor (ER), progesterone receptor (PR) and HER2 receptor (also known as HER2/neu or ERBB2). Expression of these receptors gives an indication about prognosis and treatment possibilities. The presence of hormone receptors is a good predictor of response to endocrine agents such as the estrogen receptor antagonist tamoxifen and aromatase inhibitors^{1,2}. Amplification of HER2 is a strong predictor for response to HER2 targeting drugs such as trastuzumab (Herceptin, a monoclonal antibody against HER2) and lapatinib (a dual specificity EGFR/HER2 inhibitor)^{3,4}. However, no specific treatment is available for the third group of so called triple-negative tumors, which are negative for ER, PR and HER2.

Triple-negative breast cancer

Triple-negative breast cancer (TNBC) has a high prevalence in premenopausal African-American women, compared to postmenopausal African-American and non-African-American women⁵. TNBCs have an aggressive phenotype and African-American women with late stage TNBC show the poorest survival of all US patient groups⁶. This may also explain the paradoxical finding that African American women have a lower breast cancer incidence but higher mortality than Caucasian American women⁷. Compared to other breast cancer patient groups, women with TNBC have a lower recurrence-free and overall survival, regardless of disease stage at diagnosis^{6,8,9}. On average, TNBCs are larger and show a higher rate of node positivity at the time of diagnosis than other breast cancers⁸, although there is no correlation between these two parameters as seen in other tumors¹⁰. Despite their poor prognosis and survival, TNBC patients have significantly higher rates of pathological complete remission (pCR) than non-TNBC patients, following neoadjuvant chemotherapy^{11,12}. Also, TNBC patients have increased frequency of distant metastasis formation, but not of local relapse¹³, indicating that these tumors are generally sensitive to the (loco)regional adjuvant radiotherapy. Together, these observations suggest that TNBCs are very sensitive to chemotherapy or irradiation.

Basal-like breast cancer

Besides classification by histopathology, gene expression profiling has also been used for breast tumor classification. Perou *et al.* and Sørli *et al.* have identified five subtypes of breast cancer¹⁴⁻¹⁶. Luminal subtypes A and B are characterized by ER expression and high expression of genes associated with luminal epithelial cells. Their luminal phenotype was confirmed by immunohistochemical staining for cytokeratin (CK) 8/18. These tumors usually do not express HER2 at high levels. Luminal B tumors show low to moderate expression of genes associated with luminal differentiation and are sometimes called the ER⁺HER2⁺ subgroup. The ER-negative tumors can be divided into three groups: the HER2⁺ subtype, the

normal breast-like subtype and the basal-like subtype. The HER2⁺ tumors are characterized by high expression of a subset of genes associated with overexpression of the *HER2* oncogene. The gene expression profiles of normal breast-like tumors show many similarities with normal breast tissue. The basal-like subtype is characterized by high expression of basal *keratins 5* and *17*, *laminin* and *fatty acid binding protein 7*. The basal phenotype of these tumors was confirmed by immunohistochemical staining for the basal cytokeratins CK5/6 and CK17; however, not all basal-like tumors showed immunoreactivity for CK5/6 (ref. ¹⁷). A large proportion of basal-like breast cancers lacks expression of ER, PR and HER2, and can therefore also be classified as TNBC^{9,17,18}. Although the tumor dendrograms in individual studies are slightly different due to differences in the intrinsic gene sets used for hierarchical clustering, all studies show that immunohistochemically characterized TNBCs share distinctive features with the basal-like subtype¹⁶. In a set of 97 TNBCs, all tumors expressed the basal-like genotype¹⁹. However, when gene expression of ER, PR and HER2 in basal-like breast tumors is analyzed by microarray profiling, not all tumors are negative for all three markers²⁰⁻²². This indicates that the TNBC phenotype alone is not sufficient to identify basal-like tumors.

Similar to TNBCs, basal-like breast cancers are more sensitive to preoperative or neoadjuvant chemotherapy than luminal tumors^{21,23}, whereas they show a worse relapse-free or overall patient survival than other molecular subtypes^{9,18}. In a neoadjuvant chemotherapy study for basal-like breast cancer, Carey *et al.*²³ showed that patients who achieved a pathologic complete response had a good outcome whereas patients without a pathologic complete response had a poor outcome with a high chance of relapse. This indicates that there are at least two subgroups among basal-like breast cancer; one that is likely to give a complete response to standard therapy and a good outcome, and one that gives residual disease with a higher chance of relapse and death. Hence, it is of clinical importance to further characterize these subtypes of basal-like breast cancer.

1.2 *BRCA1*-related breast cancer

The breast cancer susceptibility genes 1 and 2 (*BRCA1/2*) were identified and cloned in 1994 and 1995, respectively^{24,25}. Heterozygous *BRCA1* mutation carriers have a high lifetime risk of breast and ovarian cancer²⁶. The breast and ovarian cancer risk among *BRCA2* mutation carriers is almost as high as for *BRCA1*, but with a later onset of the disease²⁷. The likelihood of *BRCA1* or *BRCA2* mutations in families with breast and ovarian cancer correlates with the number of affected relatives, lower age at the time of diagnosis and ethnicity. The majority of pathogenic *BRCA1* and *BRCA2* founder mutations are small insertions, deletions or nonsense mutations that result in a premature stop codon and a shortened, non-functional BRCA protein²⁸. *BRCA1* and *BRCA2* mutations are especially prevalent in Ashkenazi Jews, with *BRCA1-185delAG*, *BRCA1-5382insC* and *BRCA2-6174delT* as most common founder mutations^{29,30}.

BRCA1-related breast cancers are associated with a triple-negative and basal-like tumor phenotype

The majority of *BRCA1*-related breast tumors share many phenotypic features with TNBCs and basal-like tumors³¹. *BRCA1*-related tumors are mostly negative for ER and HER2 (ref. ³²) and express basal CK5/6 (ref. ^{15,33}). Also the gene expression profiles of *BRCA1*-related breast cancers are similar to those of sporadic TNBCs and basal-like tumors¹⁶. A basal-like breast tumor phenotype may, in addition to family history and low age at onset of the cancer, select patients for *BRCA1* mutation screening. Significant predictors for *BRCA1*-mutated breast cancer are expression of CK14 (61% positive *BRCA1* tumors vs. 12% controls) and CK5/6 (58% vs. 7%), and absence of ER expression (90% vs. 33%)³⁴. Similar to TNBC, *BRCA1*-related breast cancer is associated with poor disease outcome¹³. The 5-year survival of *BRCA1*-related breast cancer compared to non-*BRCA1*-related breast cancer is 49% vs. 85% respectively^{35,36}. As in TNBCs, there is no correlation between primary tumor size and rate of node positivity in *BRCA1*-related tumors¹⁰.

The strong phenotypic similarities between *BRCA1*-related breast cancers and triple-negative/basal-like sporadic tumors suggest that the latter may also harbor mutations in *BRCA1* or genes acting in the same DNA repair pathway³⁷. However, *BRCA1* mutations are very rare in sporadic breast cancer^{38,39}, despite frequent loss of heterozygosity (LOH) at the *BRCA1* locus and reduced *BRCA1* mRNA expression^{40,41}. Alternative mechanisms such as epigenetic silencing of *BRCA1* might result in decreased *BRCA1* protein levels. There is indeed evidence for *BRCA1* promoter methylation in sporadic breast and ovarian cancers^{40,42-44}. Other mechanisms for epigenetic *BRCA* inactivation might include transcriptional repression of *BRCA1* by *ID4* (ref. ⁴⁰) and amplification of *EMSY*, an inhibitor of *BRCA2* transcription⁴⁵. The *BRCA*/Fanconi Anemia (FA) pathway can also be inactivated by methylation of the *FANCF* promoter^{46,47} or by mutations in *BRIP1*⁴⁸ or *PALB2*^{49,50}. In contrast to *BRCA1*-mutated breast cancers, most *BRCA2*-mutated tumors do not have a TNBC phenotype^{51,52}, suggesting that there is no direct link between *BRCA2* loss of function and TNBC. The reason for this difference remains unclear, since *BRCA2* is, like *BRCA1*, an essential component of the homology-directed DNA repair pathway. In this review we will focus on TNBC and basal-like breast cancers with special emphasis on *BRCA1*-associated tumors.

The role of BRCA1 in DNA damage repair

BRCA1 binds to numerous cellular proteins and has multiple functions depending on the cellular context^{53,54}. A central function of *BRCA1* concerns the regulation and promotion of error-free repair of DNA double strand breaks (DSBs) by the process of homologous recombination (HR). In the absence of HR, DSBs that may arise during DNA replication and after exogenous induction of DNA damage are repaired by error-prone mechanisms such as non-homologous end-joining (NHEJ) and single-strand annealing (SSA), leading to

chromosomal rearrangements and genomic instability, a hallmark of cancer⁵⁵. BRCA1 co-localizes with RAD51 and is required for its nuclear assembly⁵⁶. Upon DNA damage BRCA1 and RAD51 localize to the damaged region. During this process BRCA1 is phosphorylated by several kinases, including ataxia telangiectasia mutated (ATM)⁵⁷, ATM and Rad3-related (ATR)⁵⁸ and checkpoint kinase 2 (ref. ⁵⁹), which are sensors and transducers in the DNA damage response network. BRCA2 interacts directly with RAD51 via its BRC repeats and is also required for RAD51 foci formation, which is a key step in HR⁶⁰⁻⁶³.

BRCA1 also interacts with other DNA damage proteins, such as RAD50. RAD50 is part of the MRN (Mre11/RAD50/NBS1) complex, which plays a role in HR and NHEJ⁶⁴⁻⁶⁶. Furthermore, BRCA1 is involved in the G2/M cell cycle checkpoint^{67,68}, the spindle assembly checkpoint⁶⁹, transcription-coupled repair (*i.e.* repair of single-stranded DNA damage utilizing base-excision repair)^{70,71} and ionizing radiation (IR)-induced apoptosis⁵³. BRCA1 might also indirectly regulate response to DNA damage by regulating gene expression of proteins involved in DNA repair and cell cycle check points⁶⁵. Interestingly, the ubiquitin ligase activity of BRCA1 (ref. ^{72,73}) is not essential for its role in HR⁷⁴. In contrast, complete loss-of-function of BRCA1 due to protein truncating mutations leads to loss of DNA damage repair by HR. Unrepaired damage normally triggers cell cycle arrest to allow repair or cell death to eliminate repair-deficient cells. However, *BRCA1*-mutated tumor cell lines show defects in intra-S-phase and G2/M checkpoints in response to IR⁶⁷, suggesting that these cells can progress through the cell cycle with unrepaired damage. BRCA1-deficient cell lines also fail to arrest in G2/M upon incubation with spindle poisons such as paclitaxel⁷⁵.

Mouse models for BRCA1-related breast cancer

When the *BRCA1* breast cancer gene was identified, many groups tried to mimic the effects of BRCA1 loss in genetically engineered mouse (GEM) models⁷⁶. These models are of importance for studying the *in vivo* functions of BRCA1, its role in tumorigenesis, its genetic interactions, and for testing potential therapies. First, conventional *Brca1* knockout mice were generated. However, most homozygous mouse mutants turned out to be embryonic lethal and heterozygous mutants were not tumor prone. To overcome these limitations, conditional mutagenesis of *Brca1* in mammary gland epithelium has been used to model hereditary breast cancer. Tissue-specific *Cre* recombinase expression, driven by the mouse mammary tumor virus long terminal repeat (*MMTV-LTR*), whey acidic protein (*WAP*), CK14 (*K14*) or β -lactoglobulin (*BLG*) promoter, has been used to delete *Brca1* in mammary epithelial cells⁷⁷⁻⁸⁰. Although mammary gland-specific *Brca1* knockout mice develop mammary tumors only after a long latency, additional loss of *p53* markedly accelerates tumor formation^{77,78,81}. This interaction is in line with the fact that *p53* is frequently mutated in *BRCA1*-related breast cancer⁸²⁻⁸⁵. This interaction also raises the possibility that BRCA1-deficient cells are normally cleared via *p53*-mediated apoptosis.

Mammary tumors arising in conditional BRCA1-deficient mouse models have been characterized for several properties, including histopathology, p53 mutation status, ER expression, HER2 expression, genomic instability and tumor incidence⁷⁶. Some models mimic several aspects of human *BRCA1*-related tumors^{77,80,86-88}. Liu *et al.* generated a *K14cre;Brca1^{F/F};p53^{F/F}* mouse model⁷⁷. These mice develop high-grade ductal adenocarcinomas with pushing-borders. The tumors are ER-negative and CK8-positive, and show a high degree of genomic instability, as determined by the extent of DNA copy number alterations (CNAs) measured by comparative genomic hybridization (CGH). Gene expression analysis indicated high activity of genes normally expressed in basal epithelial cells. Unsupervised hierarchical clustering of gene expression profiles showed significant co-clustering of mouse and human BRCA1-deficient tumors. Importantly, *Brca1^{-/-};p53^{-/-}* mammary tumors from *K14cre;Brca1^{F/F};p53^{F/F}* mice can be orthotopically transplanted without changing their basal-like phenotype, their gene expression profile or their sensitivity to anti-cancer drugs⁸⁹. In summary, the *K14cre;Brca1^{F/F};p53^{F/F}* mammary tumor model closely mimics human BRCA1-deficient breast tumors. This model may be useful for predicting responses of *BRCA1*-mutated tumors and *BRCA1*-like TNBCs to conventional and targeted therapies, and for studying mechanisms of acquired drug resistance.

1.3 Therapeutic strategies for BRCA-related breast cancer

A hallmark of *BRCA1* and *BRCA2*-related cancers is their deficiency in DSB repair via HR. Also basal-like breast cancers may be frequently HR-deficient, supported by their high degree of genomic instability⁹⁰. HR deficiency can be effectively targeted by certain DNA-damaging agents or by poly(ADP-ribose) polymerase (PARP) inhibitors that suppress DNA single-strand break (SSB) repair (see below). Loss-of-function of the HR pathway is limited to the tumor, which makes it an ideal target for therapy.

DNA-damaging agents

HR is particularly important for repair of DNA DSBs induced by DNA-damaging anti-cancer drugs (Figure 1). There are three groups of DNA-targeting agents that are currently used for the treatment of women with breast or ovarian cancer. The first group are alkylating agents that cause DNA interstrand cross links (ICLs), leading to arrest of DNA replication forks and subsequently to DSBs^{91,92}. The second category are inhibitors of topoisomerase I and II, which stabilize the topoisomerase-DNA complex and thereby cause arrest of DNA replication forks and DSBs^{93,94}. The third class of drugs are platinum-based compounds, which induce DSBs by forming intra-strand and ICLs⁹⁵. Another group of anti-cancer drugs are the spindle poisons, such as taxanes or vinca alkaloids. Taxanes bind to β -tubulin and stabilize microtubules, whereas vinca alkaloids also bind to β -tubulin but promote depolymerization of microtubules. Both types of spindle poisons arrest cells in mitosis and induce apoptotic cell death⁹⁶.

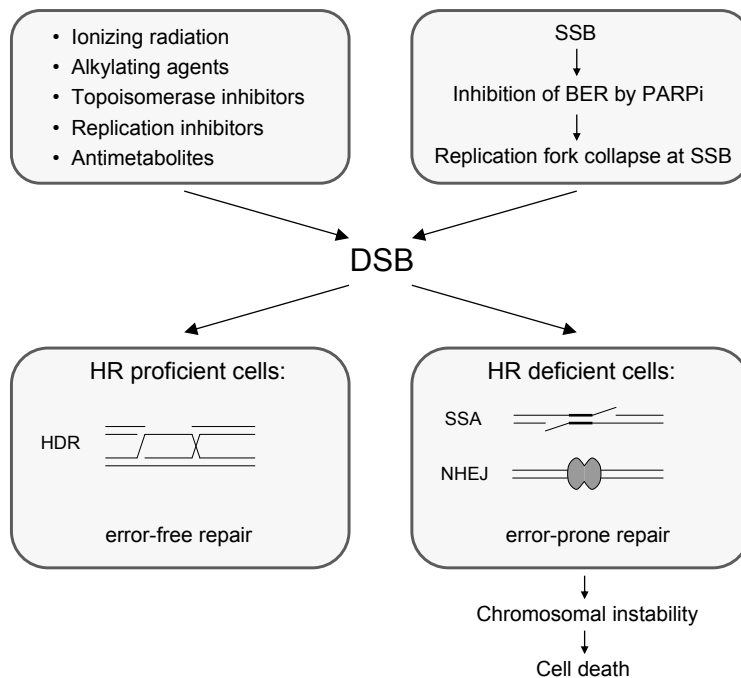


Figure 1. Several classes of anti-cancer agents induce double-strand breaks (DSBs) in replicating cells (top left). Also inhibition of single strand break (SSB) repair, e.g. by inhibiting the critical enzyme PARP1, will lead to DSBs when the cell encounters a replication fork (top right). Homologous recombination (HR) is important for error-free repair of DSBs. BRCA1/2-deficient cells lack homology-directed repair (HDR) and rely on error-prone repair mechanisms single-strand annealing (SSA) and non-homologous end joining (NHEJ). Thus, direct or indirect induction of DSBs will specifically kill familial *BRCA1/2*-related and sporadic HR-deficient breast cancer cells and not the HR-proficient normal tissue of the patient.

Preclinical experiments have indicated that BRCA1 inhibits apoptosis after treatment with DNA-damaging agents^{56,97,98}, but also that BRCA1 plays a role in regulating mitosis and is required for induction of apoptosis in response to spindle damage^{75,99}. This suggests that BRCA1-deficient cells are more sensitive to DNA-damaging agents and less sensitive to the spindle poisons⁷⁵, although the effectiveness of treating patients with BRCA1-deficient breast cancer with taxanes is still unresolved^{100,101}. BRCA1, BRCA2 or FA protein-deficient cells are extremely sensitive to the bifunctional alkylating agent mitomycin C and the platinum compounds cisplatin and carboplatin, that all generate ICLs^{56,102,103}. Recently a small study with ten breast cancer patients with a BRCA1 mutation has shown that nine patients had a pathologic complete response after neoadjuvant platinum therapy¹⁰⁴. Small molecule inhibitors of the FA/BRCA pathway sensitize cells to cisplatin¹⁰⁵, and cisplatin is even more toxic in BRCA1/2-deficient cells that also lack p53¹⁰⁶. In contrast, *BRCA1* downregulation in breast cancer cell lines was found to induce resistance to the spindle poison paclitaxel

through inactivation of the spindle checkpoint¹⁰⁷. To investigate the clinical implications of these observations, a randomized clinical trial is ongoing in which *BRCA1/2*-mutation carriers with metastatic breast cancer are treated either with the common breast cancer chemotherapy drug docetaxel or with carboplatin, which is currently not used to treat breast cancer patients¹⁰⁸. In a preclinical study in a GEM model for *BRCA1*-associated breast cancer, all *Brca1*^{-/-};*p53*^{-/-} mouse mammary tumors show high sensitivity to doxorubicin and cisplatin⁸⁹. These results support the earlier findings that *BRCA1* deficiency increases sensitivity to DNA-damaging agents¹⁰⁹. In contrast, HR-proficient *E-cadherin*^{-/-};*p53*^{-/-} mouse mammary tumors¹¹⁰ hardly respond to cisplatin and doxorubicin (unpublished results). In the clinic, high-dose alkylating chemotherapy regimens in combination with autologous peripheral blood progenitor cell transplantation were introduced almost two decades ago^{111,112}. High-dose alkylating chemotherapy improved relapse-free survival in patients with advanced breast cancer¹¹¹. Other studies, however, found that treatment of early-diagnosed poor prognosis breast cancer patients with high-dose alkylating chemotherapy had no effect on overall survival, but instead resulted in increased treatment-related morbidity and a worse quality of life immediately after treatment¹¹³. These results suggest that high-dose alkylating chemotherapy may not be beneficial in all patients with advanced breast cancer; however, it might be effective in selected populations. Indeed, patients with HER2-negative, triple-negative or basal-like breast cancer seem to benefit most from high-dose alkylating chemotherapy¹¹⁴⁻¹¹⁶. Also, breast tumors with a *BRCA1*-like array-CGH profile¹¹⁷ show a high complete remission rate and long progression-free survival in response to high-dose alkylating chemotherapy¹¹⁸. This suggests that a favorable response of TNBC patients to high-dose alkylating chemotherapy may be due to defective HR.

Poly(ADP-ribose) polymerase inhibitors

In the absence of homology-directed repair (HDR), *BRCA*-deficient tumors rely on error-prone NHEJ and SSA for repair of DSBs. Endogenous or therapy-induced SSBs are usually repaired by enzymes involved in the base excision repair pathway (BER). Chemical inhibition of SSB repair causes SSBs, which lead to formation of DSBs by replication fork collapse. In *BRCA*-deficient cells these DSBs can only be repaired by error-prone mechanisms, leading to chromosomal instability, cell cycle arrest and apoptosis.

An enzyme critical to the BER pathway is poly(ADP-ribose) polymerase 1 (PARP1). PARP1 inhibitors are seen as highly potent chemotherapeutics against *BRCA*-mutated breast and ovarian cancer⁸¹. PARP1 is a member of the PARP superfamily, which is responsible for the poly(ADP-ribosyl)ation (PAR-ylation) of nuclear proteins, a DNA damage-dependent post-translational modification¹¹⁹. PARP1 is activated by DNA damage. It binds to DNA strand breaks and synthesizes PAR chains covalently coupled to various acceptor proteins or to itself by transfer of ADP-ribose from NAD⁺ (ref. ^{120,121}). It plays an important role in DNA repair

and is therefore implicated in DNA recombination, cell proliferation and tumor suppression. In addition, the interplay between PARP1 and p53 may have a synergistic role in maintaining telomere length and genomic stability¹²². This is highlighted by the observation that PARP1 and p53 double knockout mice have an increased number of carcinomas in comparison to single knockouts¹²³. PARP-deficient cells are more sensitive to environmental stress. Lack of PARP in fibroblasts or lymphoid cells results in increased numbers of sister chromatid exchanges and micronuclei (a consequence of genomic instability) in the presence of the DNA cross-linking agent mitomycin C or γ -irradiation¹²⁴. PARP1 does not co-localize with RAD51 and in *PARP1*^{-/-} cells RAD51 foci, important in HR, are formed. Even spontaneous RAD51 foci are formed in *PARP1*^{-/-} cells¹²⁵. Thus, loss of PARP1 might increase the formation of DNA strand breaks that are repaired by HR without directly regulating the process of HR itself^{125,126}. PARP1 was also found to be important for reactivation of DNA synthesis and re-entry into G2/M phase of hydroxyurea-arrested embryonic fibroblasts¹²⁶. In spite of the numerous functions of PARP, *PARP*^{-/-} mice are healthy and fertile and do not develop early onset tumors¹²⁷. They are, however, sensitive to alkylating agents and γ -irradiation¹²⁸, due to their inability to repair SSBs. Two groups hypothesized that cells with deficiencies in both SSB and DSB repair would undergo massive DNA damage, genomic instability and cell death^{129,130} (Figure 1). They tested this concept by treating BRCA-deficient cells with PARP inhibitors (PARPi). Farmer *et al.* used BRCA1- and BRCA2-deficient ES cells. Bryant *et al.* used isogenic V-C8 (BRCA2-deficient) and V-C8+B2 (BRCA2 complemented) Chinese hamster cells. PARP1 inhibition by siRNAs or by small molecule inhibitors strongly reduced clonogenic survival of BRCA-deficient cells compared to wild-type cells. PARP1 inhibitors had no effect on BRCA heterozygous cells, which is important for *BRCA1* and *BRCA2* mutation carriers. PARP inhibitors have relatively limited side effects (Yap TA 2007 JCO ASCO, part I 25, 3529), probably because normal cells have an intact HDR pathway for error-free DSB repair. Induction of G2 arrest and apoptosis leads to the reduced survival of PARPi-treated BRCA-deficient cells. The formation of γ -H2AX foci, a marker of DSBs and stalled replication forks, was induced in both wild-type and BRCA-deficient cells, but the formation of RAD51 foci, a marker of BRCA-dependent DSB repair, was completely absent in BRCA-deficient cells. Both studies showed that in transplantation models PARP inhibition resulted in inhibition of tumor formation by BRCA2-deficient tumor cells. Bryant *et al.* showed that sensitivity of BRCA2-depleted cell lines to PARP inhibition is independent of their p53 status and that PARP1 rather than PARP2 is responsible for the repair of spontaneous recombinogenic lesions. Sensitivity to PARP inhibition is not limited to cells that are deficient for BRCA1 or BRCA2. Also deficiencies in various other proteins involved in HR, DNA damage signaling proteins and FA proteins induce sensitivity to PARP inhibition^{129,131}. This may have important consequences for treatment of sporadic tumors with a 'BRCAness' phenotype³⁷.

After the landmark studies of Bryant and Farmer, other groups have tested the effect of PARP inhibition in BRCA-deficient xenograft breast tumors^{132,133}. However, treatment with PARPi alone had little or no effect on tumor growth in xenografts. We have tested sensitivity to PARP inhibition of BRCA1- and p53-deficient mammary tumors which arise 'spontaneously' in *K14cre;Brca1^{F/F};p53^{F/F}* mice with tissue-specific loss of *Brca1* and *p53*¹³⁴. All tumors initially responded to the drug (AZD2281/olaparib), but when treatment stopped after 28 days, these tumors relapsed and had acquired resistance to a second treatment course of olaparib (Figure 2B). Extension of the treatment to 100 days increased the survival, but eventually all mice developed resistance to olaparib. Even after 100 days of continuous treatment no toxicity was observed. Thus, although they could not be eradicated, all spontaneous BRCA1-deficient mouse mammary tumors were initially sensitive to the PARP inhibitor olaparib¹³⁴. Also the recently published results of the Phase I trial showed selective activity of olaparib against *BRCA*-mutated cancers, resulting in disease stabilization or anti-tumor responses in 12 out of 19 patients with *BRCA*-associated ovarian, breast or prostate cancers¹³⁵.

Inhibition of PARP sensitizes cells to ionizing radiation *in vitro*^{136,137} and *in vivo*^{133,136}. PARP inhibition also enhances the sensitivity of tumor cells to conventional DNA damaging chemotherapy drugs *in vitro* and *in vivo*^{138,139}. *In vitro*, PARP-inhibiting compounds enhance the anti-proliferative effects of temozolomide (DNA alkylating agent)^{136,140,141}, topotecan (topoisomerase I inhibitor)^{136,142} and cisplatin¹⁴³⁻¹⁴⁵. In xenograft tumors, PARP inhibition increases the anti-tumor effect of temozolomide^{133,136,146}, topotecan¹³⁶, cisplatin¹³³, carboplatin¹³³ and cyclophosphamide (DNA alkylating agent)¹³³. PARP inhibition potentiates the cytotoxic effects of doxorubicin in p53-deficient breast cancer cell lines¹⁴⁷ as well as in p53-deficient mammary xenograft tumors¹⁴⁸. In BRCA1-deficient 'spontaneous' mouse mammary tumors, PARP inhibition potentiates the effect of cisplatin and carboplatin, resulting in prolonged relapse-free and overall survival¹³⁴. *In vitro*, PARP inhibition, either alone or in combination with cisplatin, is specifically effective in BRCA2-deficient cell lines compared to BRCA2-proficient cell lines¹⁴⁴. Besides radio-sensitization and chemopotiation, PARP inhibition has been shown to reduce chemotherapy-induced toxicity caused by oxidative stress, such as doxorubicin-induced heart failure¹⁴⁹ and cisplatin-induced nephrotoxicity¹⁵⁰. This may be drug dependent as we do not see this in our model with the combination of olaparib and cisplatin¹³⁴. It remains to be seen, however, how well combinations of PARP inhibitors with cytotoxic drugs are tolerated in patients. One can anticipate that also HR-proficient cells do not easily tolerate additive or synergistic DNA damage caused by PARP inhibition plus a cytotoxic drug.

In conclusion, therapy based on PARP inhibition has selective activity against HR-deficient tumors and may potentiate conventional therapies, such as radiation and DNA-damaging chemotherapy. There is overwhelming preclinical evidence for beneficial therapeutic

effects of PARP inhibition in selected tumors. Clearly, preclinical studies in realistic mouse models and clinical studies in selected patients are needed to determine optimal treatment regimens involving PARP inhibitors.

Receptor kinase inhibitors

There is evidence that the basal-like phenotype as well as *BRCA1*-mutation status of breast cancer correlate with increased CK5/6 and EGFR expression^{17,151}. The addition of these two markers can identify more specifically basal-like breast cancers in the TNBC patient group and the five markers together (ER, PR, HER2, CK5/6, EGFR) are significantly more prognostic than triple-negative status alone¹⁵². Expression of EGFR by TNBCs is associated with poor clinical outcome^{5,9}. Thus, EGFR may be a potential therapeutic target in *BRCA1*-mutated and basal-like breast cancers. Indeed, inhibition of EGFR by gefitinib (ZD1839/ Iressa, a receptor tyrosine kinase small molecule inhibitor) inhibits growth of basal-like and *BRCA1*-mutated breast cancer cells *in vitro*¹⁵³. Also the combination of EGFR inhibitors gefitinib or cetuximab (IMC-C225, monoclonal antibody against EGFR) with cytotoxic agents, such as carboplatin, 5-fluorouracil, paclitaxel and doxorubicin has a synergistic growth inhibitory effect on basal-like breast cancer cells¹⁵⁴.

The stem cell factor (SCF) receptor KIT is expressed in 12-14% of the breast cancers. It correlates with positivity for CK5 and CK17 and negativity for ER and HER2: the basal-like phenotype¹⁵⁵. About 30 % of the basal-like cancers are positive for KIT⁹, but no data are available about KIT expression in *BRCA1*-mutated breast cancers. KIT inhibition by STI571 (imatinib) reduces growth and invasion of aggressive ER-negative (MDA-MB-231) and ER-positive (ZR-75-1) breast cancer cell lines¹⁵⁶. Imatinib, an inhibitor of KIT, ABL and platelet-derived growth factor receptor (PDGFR), did not show clinical effect in 13 metastatic breast cancer patients¹⁵⁷. However, only one tumor was positive for KIT and four cases were PDGFR positive. To determine the clinical relevance of KIT inhibition in basal-like breast cancer, a patient group with KIT positive, basal-like tumors should be selected. Finn *et al.* showed that dasatinib, a small molecule inhibitor of Src and Abl, is specifically effective in basal-like breast cancer cell lines¹⁵⁸. However, the anti-proliferative effect of dasatinib in these basal-like breast cancer cell lines might also be mediated by KIT inhibition¹⁵⁹, since dasatinib also shows affinity for KIT¹⁶⁰.

1.4 Why can *BRCA1*-related breast tumors not be eradicated?

Both clinical data¹⁶¹ and preclinical studies^{89,109} indicate that *BRCA1*-mutated breast cancers are relatively sensitive to chemotherapy. Nevertheless, in metastatic patients and also in mice, *BRCA1*-mutated mammary tumors can almost never be completely eradicated; after various times most of them eventually grow back. Survival of a small number of tumor cells might be explained by several mechanisms. In this section mechanisms are discussed that

are relevant for *BRCA1*-related breast cancer and for the drugs that are extensively being studied in these tumors.

Intrinsic therapy resistance of tumor-initiating cells

The cancer stem cell theory postulates that only a subset of tumor cells drive tumor growth, give rise to metastases and confer resistance to anti-cancer drugs. These cells are thought to share important properties with normal stem cells and are therefore often referred to as cancer stem cells (CSCs), or tumor-initiating cells (TICs). The cancer stem cell hypothesis implies that cancer arises from and is driven by tissue stem or progenitor cells or more differentiated cells that have acquired stem cell properties, including long-term self-renewal capacity, the ability to differentiate, expression of telomerase, activation of anti-apoptotic pathways, increased membrane transporter activity and the ability to migrate¹⁶². However, it remains unclear whether these TICs arise from normal stem cells or from differentiated cells that acquire self-renewal capacity, or both. TICs are functionally defined by their capacity to regenerate the bulk of non-tumorigenic tumor cells, of which the molecular and histopathological profile closely resembles that of the original tumor. While TICs have originally been defined in haematopoietic cancers, they have more recently also been identified in several solid tumors, including colon, breast, liver, pancreatic and prostate cancers, brain tumors and melanomas¹⁶³⁻¹⁶⁹. However, the hypothesis that only a subset of tumor cells has tumorigenic capacity is still under debate and appears to depend very much on the assay that is used for identification of TICs. Quintana *et al.* showed that in the highly immunocompromised NOD/SCID;*Il2rg*^{-/-} mice most, if not all, human melanoma cells have tumor-initiating capacity¹⁷⁰. It remains however unclear if this is tumor-type specific. Several studies have investigated the role of TICs in resistance against chemotherapy and radiation. Woodward *et al.*¹⁷¹ showed in the MCF7 breast cancer cell line that radiation induces enrichment of progenitor cells. The enrichment was mediated by active β -catenin, an important player in the Wnt signaling pathway that regulates stem cell maintenance. In a small study on human breast tumor biopsies, Li *et al.*¹⁷² found that neoadjuvant chemotherapy increased the percentage of TICs in HER2-negative tumors. However, treatment of HER2-positive tumors with lapatinib, an inhibitor of EGFR and HER2, did not enrich for TICs. HER2 has been shown to be important in self-renewal and, as the authors state, the observation that TICs and non-TICs are equally sensitive to lapatinib may contribute to the higher response rate of HER2-positive tumors treated with chemotherapy in combination with trastuzumab (a recombinant monoclonal antibody against HER2) compared to chemotherapy alone¹⁷³. In a mouse model in which *BRCA1*-mutated mammary tumor formation is driven by a hypomorphic mutation of *Brca1* (deletion of exon 11, resulting in production of a truncated protein), TICs were significantly enriched in platinum-resistant secondary tumor transplants compared to the platinum-sensitive primary transplants¹⁷⁴. *BRCA1* has been reported to play an important role in the

differentiation of mammary epithelial cells. One could speculate that *BRCA1*-associated breast tumors contain a relatively high proportion of TICs and that these contribute to chemoresistance, frequently observed in these tumors. In the *BRCA1*- and *p53*-deficient mouse mammary tumor model developed in our lab⁷⁷ resistance to cisplatin never develops due to complete and irreversible inactivation of *BRCA1* (Figure 2C). Still, the tumors cannot be eradicated⁸⁹.

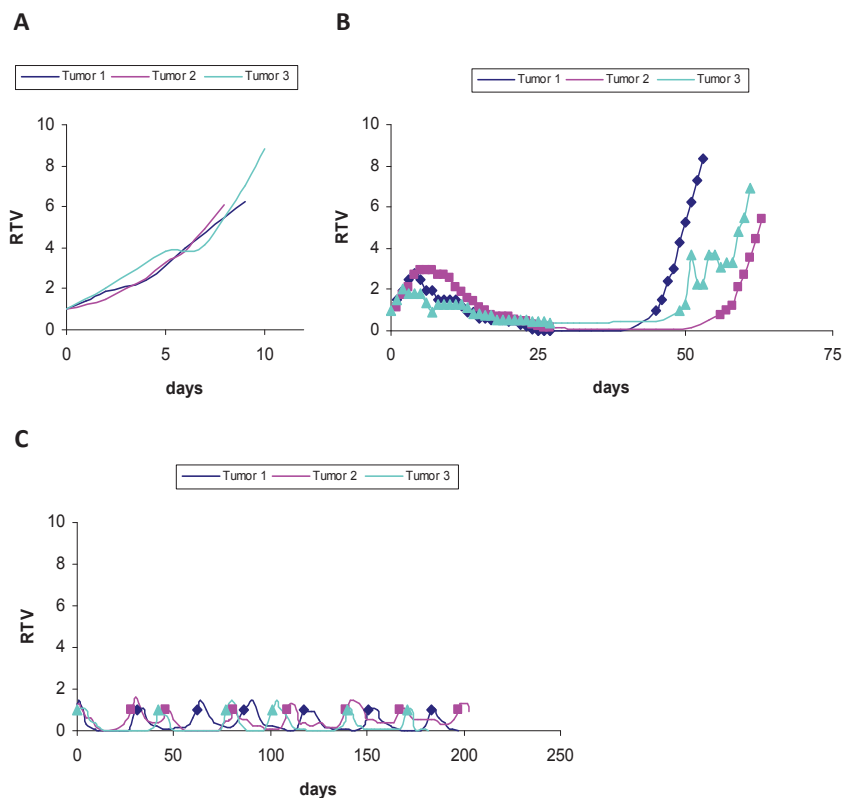


Figure 2. Responses of *K14cre;Brca1^{F/F};p53^{F/F}* mouse mammary tumors to PARP inhibition and platinum treatment. A) Tumor growth of untreated tumors. **B)** Growth of tumors treated with the PARP inhibitor olaparib. Tumors initially respond to the first treatment course of daily injections for 28 days. Treatment is resumed upon tumor relapse, but all tumors acquire resistance to olaparib during the second treatment course. **C)** Growth of tumors treated with cisplatin. A single dose of cisplatin is given on day 0 and 14 and resumed upon tumor relapse. The tumors repetitively respond to cisplatin and do not become resistant, but are also not eradicated by the treatment. Tumor growth is expressed as relative tumor volume (RTV, ratio of tumor volume to initial size at start of treatment). Treatment was given on days indicated by a square, triangle or rhombus.

Therapy-induced cell cycle arrest

Most of the commonly used chemotherapy agents are especially effective against rapidly dividing cells, because they interfere with the cell cycle or cause DNA damage which is especially toxic to dividing cells. This implicates that non-dividing (quiescent or senescent) cells are not effectively targeted by these drugs. However, several studies show that chemotherapy or radiotherapy itself can induce senescence in cancer cells¹⁷⁵⁻¹⁷⁸. Therapy-induced senescence might, like induction of apoptosis or mitotic catastrophe, explain why the tumor stops growing. A model of therapy resistance proposed by Stewart¹⁷⁹ states that cells with sufficient active resistance mechanisms to withstand initial chemotherapy will continue to divide between therapy cycles. If active resistance mechanisms are insufficient for protection, non-cycling cells will nevertheless survive based on their intrinsic passive resistance. Cells that have insufficient active resistance mechanisms to permit continued growth would arrest and remain quiescent until treatment cessation. It is conceivable that the latter scenario occurs in *BRCA*-deficient tumors to give cells more time to repair the damaged DNA. Senescence was always thought to be an irreversible state of growth arrest, but more and more data have been published on reversible induction of senescence^{178,180,181}. Recently, Puig *et al.*¹⁸² reported that cisplatin treatment induces mitotic aberrations and asymmetric divisions, giving rise to β -galactosidase positive, multinucleated giant cells. These cells were able to give rise to normal, diploid cells that started to proliferate and were increasingly cisplatin-resistant. It remains unclear how exactly the giant cells give rise to the normal, diploid cells.

Acquired resistance via upregulation of drug efflux transporters

In section 3 we discussed that PARP inhibitors are potent agents against *BRCA1*-deficient tumors. Especially in combination with cytotoxic agents, they induce a remarkable tumor regression. *Brca1*- and *p53*-deficient mouse mammary tumors respond very well to PARP inhibition alone and in combination with cisplatin, but none of them are completely eradicated and eventually all tumors relapse¹³⁴. Gene expression analysis shows that the murine P-glycoprotein (Pgp) genes *Abcb1a* and *Abcb1b* are up-regulated in several tumors with acquired resistance to the PARP inhibitor olaparib (Figure 3). Up-regulation of Pgp might be the most important cause of resistance to olaparib in these mice, since co-administration of olaparib with the Pgp inhibitor tariquidar could re-sensitize relapsed tumors to this PARP inhibitor. Increased expression of *Abcb1* genes was also detected as the cause of doxorubicin resistance in the *K14cre;Brca1^{F/F};p53^{F/F}* mouse mammary tumor model^{89,183,184}. These preclinical results show the need for development of new generations of PARP inhibitors that are not Pgp substrates to lower the chance of acquired resistance in patients. However, upregulation of Pgp does not seem to be the only mechanisms by which resistance to olaparib develops. Tumors in which Pgp activity was suppressed by

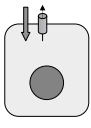
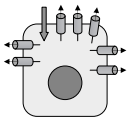
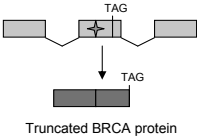
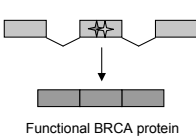
tariquidar still developed resistance to olaparib, suggesting other mechanisms that remain to be elucidated. In contrast to several preclinical models, the role of human Pgp as cause of multidrug resistance in breast cancer patients remains controversial because several studies gave conflicting results^{185,186}. A meta-analysis of 31 studies indicated that 41% of all tumors express Pgp, which was associated with a 3-fold reduction in chemotherapy response¹⁸⁷. In spite of this, attempts to use Pgp expression to predict chemotherapy response failed^{188,189}. A complicating factor in several clinical trials is the fact that drug combinations also contain compounds (e.g. several alkylating agents), that are not substrates for Pgp. Another caveat is that it might be difficult to identify drug-resistant tumors based on analysis of *MDR1* gene expression in pre-treatment tumor samples, because this trait might not be 'hard-wired'. Instead, drug-sensitive or -resistant tumor cells could have different kinetics in inducing *MDR1* gene expression following exposure to drugs. This can only be detected by analyzing tumor samples early after treatment onset, which is unpractical in the clinic. In addition to Pgp, other members of the ATP-binding cassette (ABC) transporter family may contribute to chemotherapy resistance. Of particular interest are the multidrug resistance protein 1 (MRP1)¹⁹⁰ and breast cancer resistance protein (BCRP)^{191,192}, which cover a broad range of substrates¹⁹³. In addition to these intensively studied ABC drug transporters, MRP7 has recently been found to confer resistance to several natural product anti-cancer drugs and also to the nontaxane anti-microtubular agent epothilone B, which is not a Pgp substrate¹⁹⁴.

Acquired resistance via genetic reversion

Two groups recently identified a new possible mechanism of acquired resistance in *BRCA1*- and *BRCA2*-associated ovarian tumors. As discussed in section 3, loss of the functional *BRCA1* or *BRCA2* allele, which is an important step in *BRCA*-associated tumorigenesis, sensitizes the tumor to DNA damaging agents, such as cisplatin, and to PARP inhibition. The groups of Ashworth and Taniguchi^{193,194} observed secondary mutations in PARPi- or cisplatin-resistant clones of the *BRCA2*-mutated pancreatic cancer cell line Capan1. These secondary mutations involved deletions or insertions, which restored the open reading frame (ORF) resulting in the synthesis of functional BRCA2 protein and reduced sensitivity to cisplatin and PARP inhibition (Figure 3). The same phenomenon of genetic reversion was observed in cisplatin- or carboplatin-resistant *BRCA1*- or *BRCA2*-mutated ovarian tumors¹⁹⁵⁻¹⁹⁷. This mechanism of secondary mutations that restore protein function has been previously reported for *FANCA*¹⁹⁸, *BRCA2*¹⁹⁹, and *PALB2*, a *BRCA2*-interacting protein²⁰⁰. Hence, treatment of HR-deficient tumors with DNA-damaging agents or PARP inhibitors might select for the presence of ORF-restoring secondary mutations, resulting in tumors with restored HR. Interestingly, *BRCA1*-deficient mouse mammary tumors with a deletion of *Brca1* exons 5-13 (which cannot be restored by a secondary mutation), never develop resistance to cisplatin^{89,201} (Figure 2C), supporting the notion that (partial) *BRCA* activity is an

absolute requirement for cells to develop resistance to platinum drugs²⁰¹. The fact that re-expression of BRCA1 or BRCA2 is tolerated suggests that BRCA loss-of-function is important for tumor initiation but not essential for maintenance of established tumors. It remains to be determined if some mutations in *BRCA1* or *BRCA2* are more prone to reversion by secondary ORF-restoring mutations than others. In this context, it would be interesting to see if there are differences in response to platinum therapy between ovarian cancer patients with different *BRCA* founder mutations, *e.g.* the three most prevalent Ashkenazi founder mutations (*BRCA1-185delAG*, *BRCA1-5382insC* and *BRCA2-6174delT*) in the National Israeli Study of Ovarian Cancer²⁰², which has been studied for survival²⁰³. It would also be interesting to screen platinum resistant tumors in *BRCA*-mutation carriers for the presence of functional BRCA proteins.

A

Mechanism of resistance	Drug sensitive	Drug resistant
Drug transport by P-gp	 Normal P-gp expression	 High P-gp expression
Genetic reversion of truncating mutation in <i>BRCA</i> gene	 Truncated BRCA protein	 Functional BRCA protein

B

Model	<i>BRCA</i> mutation	Platinum treatment		PARPi treatment		
		Resistance	Genetic reversion	Resistance	Genetic reversion	P-gp over-expression
<i>BRCA2</i> -mutated cell lines [195,196]	6174delT	+	+	+	+	n.d.
<i>BRCA2</i> -mutated ovarian tumors [195,196]	6174delT	+	+	n.d.	n.d.	n.d.
<i>BRCA1</i> -mutated ovarian tumors [197]	185delAG	+	+	n.d.	n.d.	n.d.
<i>BRCA1</i> -deficient mouse mammary tumors [76,132]	Δ exon 5-13	-	-	+	-	+
<i>BRCA1</i> -deficient mouse mammary tumors [171]	Δ exon 11	+	n.d.	n.d.	n.d.	n.d.

Figure 3. Recently, genetic reversion of *BRCA*-deficiency by a second mutation that restores the open-reading frame has been reported to mediate resistance against platinum drugs and PARP inhibition. The observation that resistance against platinum drugs does not occur in mouse tumor where a functional *BRCA1* protein cannot be restored due to the large deletion of exon 5-13, supports this mechanism of resistance. Resistance of *BRCA1*- and p53-deficient mouse mammary tumors to the PARP inhibitor olaparib has shown to be mediated by upregulation of the multidrug transporter P-glycoprotein (Pgp). (n.d. = not determined)

1.5 How to overcome chemotherapy resistance?

Since many mechanisms may underlie drug resistance, overcoming it is a complex issue. Several approaches have been investigated extensively, such as drug transporter inhibition and targeting tumor-initiating cells.

Targeting tumor-initiating cells

The cancer stem cell hypothesis postulates that conventional anti-cancer therapies fail to eradicate tumors because they mainly target the bulk of the tumor but not the TICs that are capable of regrowing a tumor after the therapy ends. If therapies could be targeted against these TICs, they would eliminate the 'roots' of the tumor and eventually lead to cures, even if they do not shrink tumors²⁰⁴. In order to eliminate the TICs, these cells have to be fully characterized and strategies must be developed to eradicate the TICs without excessive toxicity to normal stem cells. Several pathways that are linked to normal stem cell growth and maintenance are investigated as potential target to eliminate TICs. Prime candidates are the Hedgehog (HH), Wnt and Notch signaling pathways. These pathways are extensively studied in cancer research, but it remains to be seen whether they are essential for breast cancer-initiating cells. *HH* genes play a key role in embryogenesis and the mammalian *HH* genes are highly expressed in many cancer cell lines²⁰⁵⁻²⁰⁷. Patched (PTCH) is the receptor for HH molecules and is mutated in many basal cell carcinomas^{208,209}. In many epithelial tumors, ligand-dependent activation of the HH pathway does not occur in the tumor cells but in the stromal microenvironment, suggesting a paracrine requirement for HH signaling²¹⁰. Cyclopamine, a steroid-like compound, binds to Smoothened (SMO), which is regulated by PTCH, and inhibits the growth of cells and tumors with activated HH signaling²¹¹. Wnt signaling proteins bind to the Frizzled (Fz) family of transmembrane proteins and initiate various signaling pathways, leading to regulation of gene expression and changes in cell behavior. Activation of Fz receptors by Wnt ligand results in accumulation and nuclear translocation of β -catenin, formation of β -catenin/TCF complexes and transcriptional activation of β -catenin/TCF target genes. Wnt signaling plays an important role in the stem cell microenvironment in various haematopoietic and epithelial tissues²¹²⁻²¹⁴. Activation of Wnt signaling seems to be a generic step in carcinogenesis²¹⁵. Wnt pathway activation through APC loss in intestinal crypt stem cells rapidly induces formation of adenomas²¹⁶. Sulindac abrogates Wnt signaling by targeting β -catenin and seems to sensitize tumors to chemotherapeutics²¹⁷. Notch signaling is initiated by ligand binding followed by cleavage of the Notch receptor by the γ -secretase complex. Inhibition of Notch signaling by γ -secretase inhibitors (GSIs) results in reduced tumor growth and depletion of the tumor-forming cell fraction²¹⁸. GSIs are also reported to have activity against breast cancer cells that overexpress Notch^{219,220}. Inhibition of the Notch pathway by GSI or by deletion of the Notch pathway transcription factor CSL/RBP-J induces differentiation of stem and progenitor cells into goblet cells in a mouse model for adenomatous polyposis coli (APC)²²¹.

Much effort is spent on the characterization of TICs. When specific markers will be found, these might serve as new therapeutic targets. An ideal therapeutic target would be a cell surface marker that is specifically expressed on TICs and not on normal cells, to prevent severe long-term toxicity in organs with an active stem cell population, such as the haematopoietic system, gastrointestinal tract, skin and hair. The bulk of the tumor might then be eradicated with a less specific cytotoxic drug and the residual TICs with a new highly specific drug. Targeting a cell surface molecule might also avoid drug resistance caused by drug transporters. TIC markers that have been identified to date include CD133, CD44 and c-Kit. However, these markers are also expressed on normal (stem) cells. It is therefore unlikely that drugs can be designed to target specifically TICs through these markers. Clearly, further characterization of TICs is required before we will be able to target them and eventually eradicate the tumor.

Inhibition of drug transporters

The broad substrate specificity of ABC drug efflux transporters such as Pgp, MRP1 or BCRP makes them attractive targets to be chemically blocked in combination with anti-cancer agents. This straight-forward strategy has driven the pharmaceutical industry to develop inhibitors of ABC transporters, in particular Pgp. Whereas preclinical studies presented strong evidence for the utility of such inhibitors, three “generations” of Pgp inhibitors have yielded only little clinical benefit up to now (reviewed by Szakacs *et al.*²²²). This negative experience has frustrated further attempts to refine their development or clinical use. What lessons can be learned from the previous attempts to block Pgp? First-generation, nonspecific inhibitors, such as verapamil and cyclosporine A did not reach clinically effective plasma levels necessary for effective Pgp inhibition²²³. Second-generation inhibitors, such as PSC 833 (valsopodar) were more potent and selective. Unfortunately, their pharmacokinetic interactions with drugs often increased the toxic side effects of chemotherapy agents. Dose reductions decreased toxicity, but also efficacy of the anti-cancer drugs^{224,225}. More selective third-generation Pgp inhibitors include tariquidar (XR9576)²²⁶, elacridar (GF120918)²²⁷, and zosuquidar (LY335979)²²⁸. Their advantage is that in several studies no or only moderate interactions with pharmacokinetics of chemotherapy agents such as doxorubicin, vincristine, paclitaxel, docetaxel or vinorelbine were detected²²⁹⁻²³³. Clinical trials with these new generation inhibitors are still ongoing; however, the first results do not favor a major breakthrough in the treatment of breast cancer. A randomized placebo-controlled, double-blind phase 2 trial on metastatic or locally recurrent breast cancer did not reveal a benefit in progression-free survival, overall survival or response rate when docetaxel was combined with zosuquidar²³⁴. The authors suggest that there might be a benefit of administering zosuquidar plus docetaxel to patients who show relapses within 12 months after neoadjuvant or adjuvant treatment. If this is true, one could speculate that induction

of Pgp expression by prior chemotherapy has only a limited “memory” and declines back to low levels within months after therapy. Pusztai *et al.*²³⁵ found that only 1 of 17 patients with stable or progressive breast cancer disease benefited from the addition of tariquidar to a doxorubicin or taxane-based chemotherapy. Importantly, this was the patient in which scintigraphy using the ^{99m}Tc-labeled Pgp substrate sestamibi showed the highest increase in radiotracer uptake upon Pgp blockage by tariquidar. These limited data suggest that 3rd generation Pgp inhibitors may only be beneficial for a limited group of breast cancer patients. The challenge remains to identify these women. Given the lack of reliable assays for immunohistochemical detection of Pgp activity, functional imaging with a Pgp substrate like sestamibi in combination with a Pgp inhibitor may be more predictive for such a selection.

While more details need to be learned regarding the use of chemical ABC transporter inhibitors, the effect of Pgp inhibition can be tested unambiguously in preclinical models: mice with *Mdr1* or *Bcrp* null alleles are viable and fertile^{236,237} and can be bred into genetically engineered mouse models for breast cancer. The response to chemotherapy of MDR1- or BCRP-deficient mammary tumors can be directly compared to the response of MDR1- or BCRP-proficient tumors. Such clean tumor-specific genetic alterations can serve as baseline to evaluate the effect of chemical drug efflux transporter inhibition and can also be valuable to identify Pgp- or BCRP-independent resistance mechanisms.

1.6 Predictors for chemotherapy response of triple-negative and basal-like tumors

As described in section 1, TNBCs and basal-like breast cancers are a heterogeneous group of tumors. Additional markers are required to identify new subgroups and to predict clinical response. Because of the strong overlap between *BRCA1*-related breast cancers and TNBCs, the latter group is thought to include a significant fraction of ‘BRCA-like’ sporadic cancers with defective HR³⁷. It will therefore be important to identify markers that characterize HR deficiency, also in sporadic cancers. Moreover, since *BRCA2*-deficient tumors do not segregate with basal-like tumors, a molecular profile or biomarker for HR deficiency might be predictive for a broad range of breast cancers and perhaps other cancers.

Molecular classifiers for HR deficiency

Microarray-based gene expression profiling is a frequently used method to identify differential gene expression patterns between two or more sample sets. To characterize HR-deficient and HR-proficient TNBCs, a gene expression profile of well-defined samples should be determined. Miller *et al.* analyzed gene expression profiles of human breast cancer tumors with or without p53 mutation²³⁸. They found a gene expression signature which has prognostic significance and which is associated with a non-functional p53 pathway rather than the presence of a mutation in the p53 gene itself. Van ‘t Veer *et al.* used gene expression profiling for classification of ER-negative sporadic and *BRCA1*-related tumors²³⁹.

Because one sporadic tumor that was classified as BRCA1-related showed strong *BRCA1* promoter methylation (presumably resulting in *BRCA1* silencing), one could speculate that this signature might also be predictive for BRCA1-like sporadic tumors.

An important characteristic of BRCA-related breast cancer is the high degree of genomic instability which can be measured by CGH. Wessels *et al.*¹¹⁷ have built a CGH classifier for identification of BRCA1-related breast tumors. Sporadic tumors that fall into the BRCA1-tumor group might have an unknown BRCA1 mutation or other aberrations that make them HR deficient. Indeed, using an optimized BRCA1 CGH classifier, two of 48 breast tumors from patients with a family history of breast and ovarian cancer could be identified as BRCA1-associated tumors²⁴⁰. These CGH classifiers might also be useful for analyzing breast cancer samples to determine an optimal treatment strategy, given the targeted therapeutics now being developed for HR-deficient cancer.

In principle it might also be possible to identify HR deficiency by quantitative expression profiling and mutational analysis of genes known to be involved in DNA repair. Although this approach may be useful, it requires knowledge of all relevant genes, precise determination of expression levels and sequencing of each of the genes to detect mutations that do not affect expression level. Another potential limitation of this approach is that detection of reduced gene expression in tumor cells may be obscured by signals from the stromal cells present within the tumor samples.

Functional HR assays

Obviously, it would be preferable to have a clinical test that would directly assay HR function in breast tumors *in vivo* or in *ex vivo* breast tumor samples. Although methods are available to measure HR activity, these assays are not readily applicable to tumor specimens because they involve transfection of cultured cells with a plasmid containing the restriction enzyme gene *I-SceI* and an inactive selection gene containing an *I-SceI* recognition site. HDR of the DSB induced by the *I-SceI* restriction enzyme leads to activation of the selection gene and expression of antibiotic resistance or fluorescence markers²⁴¹.

A functional assay for HR deficiency that might be clinically applicable involves detection of γ -H2AX and RAD51 foci formation in tumor samples after *in vivo* or *ex vivo* induction of DNA damage by *e.g.* cisplatin or ionizing radiation. An increase in γ -H2AX foci indicates an increase in arrested replication forks and DSBs. RAD51 foci formation, on the other hand, is a hallmark of BRCA-dependent DSB repair. Thus, BRCA1/2-deficient cells should be positive for γ -H2AX, but negative for RAD51 foci upon DNA damage induction¹³⁰.

Another possible strategy to develop a surrogate marker for HR deficiency involves detection of DNA rearrangements that are frequent in HR deficient tumors by next-generation sequencing. It is conceivable that translocations, caused by illegitimate repair of DSBs, might be a frequent lesion in HR deficient tumors. These lesions might be effectively identified by genome-wide massively parallel paired-end sequencing of tumor DNA fragments²⁴².

1.7 Conclusions and future prospects

TNBCs are characterized by lack of hormone receptors and of HER2 expression. Since no targeted treatment is available, patients with TNBCs have limited therapeutic options and a worse clinical outcome compared to patients with cancers that are ER⁺ or HER2⁺. TNBCs largely overlap with the gene expression-based subgroup of basal-like breast cancer and with familial *BRCA1*-related breast cancer. The HR deficiency of *BRCA1*-related hereditary breast cancers and *BRCA1*-like sporadic TNBCs renders these tumors sensitive to anti-cancer drugs that directly or indirectly cause DNA DSBs. Although mutations in *BRCA1* are very rare in sporadic breast cancers, these cancers may have acquired epigenetic inactivation of *BRCA1* by *e.g.* promotor methylation⁴². New therapies that target HR-deficient cells are under extensive investigation. The most important one is PARP inhibition, which marks a new approach of cancer treatment in which the tumorigenic defect is targeted to induce synthetic lethality. PARP inhibition might also be effective against sporadic HR-deficient breast cancers; however, no good biomarkers are available to identify this patient group. Few functional HR assays are available, but these are not suitable for large scale clinical use. Other assays, such as γ H2AX or RAD51 staining and an HR deficiency gene expression or CGH profile, may be more useful in the clinic.

Targeting HR-deficient tumors with DNA-damaging agents might be even more potent in combination therapies. Treatment with DNA cross-linking agents and a PARP inhibitor increases synthetic lethality, but may also increase toxicity. Novel combination treatments will be required to target all tumor cells, including the tumor-initiating cells that give rise to tumor relapse and to resistance to current therapies. Resistance is a major problem in cancer treatment and ABC transporter-mediated resistance against specific PARP inhibitors has already been observed in mouse model systems. Another resistance mechanism that has recently been proposed is reversion of HR deficiency by restoration of *BRCA* function in platinum drug-resistant *BRCA*-deficient ovarian tumors. Therapy driven selection of cells that have restored functional expression of *BRCA1* or *BRCA2* might also cause resistance to PARP inhibition. This phenomenon makes the search for HR biomarkers even more urgent, because screening for *BRCA* germ-line mutations in familial breast/ovarian cancer patients will not identify tumors that have somehow regained HR function. It will also be important to determine which of the *BRCA1* and *BRCA2* founder mutations are able to acquire therapy resistance via genetic reversion.

In conclusion, familial and sporadic HR-deficient breast cancers can be targeted by induction of synthetic lethality by chemotherapeutics that directly or indirectly cause DSBs. However, in order to identify these patient groups, proper biomarkers for HR deficiency are needed. In addition, it can be expected that combination treatments with *e.g.* PARP inhibitors and conventional chemotherapeutic drugs will be required to fully eradicate HR-deficient tumors.

Acknowledgments

We thank Piet Borst, Bastiaan Evers, Sabine Linn, Marina Pajic and Marieke Vollebergh for their valuable comments on the manuscript. We acknowledge financial support from the Dutch Cancer Society, the Netherlands Organization for Scientific Research (NWO) and the European Union Framework Program. J.E. Jaspers is a recipient of the NWO TopTalent PhD fellowship.

REFERENCES

1. K.L.Cheung, Endocrine therapy for breast cancer: an overview, *Breast* 16 (2007) 327.
2. A.U.Buzdar, Advances in endocrine treatments for postmenopausal women with metastatic and early breast cancer, *Oncologist*. 8 (2003) 335.
3. R.Nahta and F.J.Esteva, Trastuzumab: triumphs and tribulations, *Oncogene* 26 (2007) 3637.
4. N.M.Diaz, Laboratory testing for HER2/neu in breast carcinoma: an evolving strategy to predict response to targeted therapy, *Cancer Control* 8 (2001) 415.
5. L.A.Carey, C.M.Perou, C.A.Livasy, L.G.Dressler, D.Cowan, K.Conway, G.Karaca, M.A.Troester, C.K.Tse, S.Edmiston, S.L.Deming, J.Geradts, M.C.Cheang, T.O.Nielsen, P.G.Moorman, H.S.Earp, and R.C.Millikan, Race, breast cancer subtypes, and survival in the Carolina Breast Cancer Study, *JAMA* 295 (2006) 2492.
6. K.R.Bauer, M.Brown, R.D.Cress, C.A.Parise, and V.Caggiano, Descriptive analysis of estrogen receptor (ER)-negative, progesterone receptor (PR)-negative, and HER2-negative invasive breast cancer, the so-called triple-negative phenotype: a population-based study from the California cancer Registry, *Cancer* 109 (2007) 1721.
7. L.A.Newman, Breast cancer in African-American women, *Oncologist*. 10 (2005) 1.
8. R.Dent, M.Trudeau, K.I.Pritchard, W.M.Hanna, H.K.Kahn, C.A.Sawka, L.A.Lickley, E.Rawlinson, P.Sun, and S.A.Narod, Triple-negative breast cancer: clinical features and patterns of recurrence, *Clin Cancer Res* 13 (2007) 4429.
9. T.O.Nielsen, F.D.Hsu, K.Jensen, M.Cheang, G.Karaca, Z.Hu, T.Hernandez-Boussard, C.Livasy, D.Cowan, L.Dressler, L.A.Akslen, J.Ragaz, A.M.Gown, C.B.Gilks, M.van de Rijn, and C.M.Perou, Immunohistochemical and clinical characterization of the basal-like subtype of invasive breast carcinoma, *Clin Cancer Res* 10 (2004) 5367.
10. W.D.Foulkes, J.S.Brunet, I.M.Stefansson, O.Straume, P.O.Chappuis, L.R.Begin, N.Hamel, J.R.Goffin, N.Wong, M.Trudel, L.Kapusta, P.Porter, and L.A.Akslen, The prognostic implication of the basal-like (cyclin E high/p27 low/p53+/glomeruloid-microvascular-proliferation+) phenotype of BRCA1-related breast cancer, *Cancer Res* 64 (2004) 830.
11. C.Liedtke, C.Mazouni, K.R.Hess, F.Andre, A.Tordai, J.A.Mejia, W.F.Symmans, A.M.Gonzalez-Angulo, B.Hennessy, M.Green, M.Cristofanilli, G.N.Hortobagyi, and L.Puszta, Response to neoadjuvant therapy and long-term survival in patients with triple-negative breast cancer, *J. Clin. Oncol.* 26 (2008) 1275.
12. M.E.Straver, A.M.Glas, J.Hannemann, J.Wesseling, M.J.Van De Vijver, E.J.Rutgers, M.J.Vrancken Peeters, H.van Tinteren, L.J.van't Veer, and S.Rodenhuis, The 70-gene signature as a response predictor for neoadjuvant chemotherapy in breast cancer, *Breast Cancer Res. Treat.* (2009).
13. B.G.Haffty, Q.Yang, M.Reiss, T.Kearney, S.A.Higgins, J.Weidhaas, L.Harris, W.Hait, and D.Toppmeyer, Locoregional relapse and distant metastasis in conservatively managed triple negative early-stage breast cancer, *J Clin Oncol* 24 (2006) 5652.
14. C.M.Perou, T.Sorlie, M.B.Eisen, M.van de Rijn, S.S.Jeffrey, C.A.Rees, J.R.Pollack, D.T.Ross, H.Johnsen, L.A.Akslen, O.Fluge, A.Pergamenschikov, C.Williams, S.X.Zhu, P.E.Lonning, A.L.Borresen-Dale, P.O.Brown, and D.Botstein, Molecular portraits of human breast tumours, *Nature* 406 (2000) 747.

15. T.Sorlie, C.M.Perou, R.Tibshirani, T.Aas, S.Geisler, H.Johnsen, T.Hastie, M.B.Eisen, M.van de Rijn, S.S.Jeffrey, T.Thorsen, H.Quist, J.C.Matese, P.O.Brown, D.Botstein, P.Eystein Lonning, and A.L.Borresen-Dale, Gene expression patterns of breast carcinomas distinguish tumor subclasses with clinical implications, *Proc Natl Acad Sci U S A* 98 (2001) 10869.
16. T.Sorlie, R.Tibshirani, J.Parker, T.Hastie, J.S.Marron, A.Nobel, S.Deng, H.Johnsen, R.Pesich, S.Geisler, J.Demeter, C.M.Perou, P.E.Lonning, P.O.Brown, A.L.Borresen-Dale, and D.Botstein, Repeated observation of breast tumor subtypes in independent gene expression data sets, *Proc Natl Acad Sci U S A* 100 (2003) 8418.
17. C.A.Livasy, G.Karaca, R.Nanda, M.S.Tretiakova, O.I.Olopade, D.T.Moore, and C.M.Perou, Phenotypic evaluation of the basal-like subtype of invasive breast carcinoma, *Mod Pathol* 19 (2006) 264.
18. M.van de Rijn, C.M.Perou, R.Tibshirani, P.Haas, O.Kallioniemi, J.Kononen, J.Torhorst, G.Sauter, M.Zuber, O.R.Kochli, F.Mross, H.Dieterich, R.Seitz, D.Ross, D.Botstein, and P.Brown, Expression of cytokeratins 17 and 5 identifies a group of breast carcinomas with poor clinical outcome, *Am J Pathol* 161 (2002) 1991.
19. B.Kreike, M.van Kouwenhove, H.Horlings, B.Weigelt, H.Peterse, H.Bartelink, and M.J.Van De Vijver, Gene expression profiling and histopathological characterization of triple-negative/basal-like breast carcinomas, *Breast Cancer Res* 9 (2007) R65.
20. M.Jumppanen, S.Gruvberger-Saal, P.Kauraniemi, M.Tanner, P.O.Bendahl, M.Lundin, M.Krogh, P.Kataja, A.Borg, M.Ferno, and J.Isola, Basal-like phenotype is not associated with patient survival in estrogen-receptor-negative breast cancers, *Breast Cancer Res* 9 (2007) R16.
21. R.Rouzier, C.M.Perou, W.F.Symmans, N.Ibrahim, M.Cristofanilli, K.Anderson, K.R.Hess, J.Stec, M.Ayers, P.Wagner, P.Morandi, C.Fan, I.Rabiul, J.S.Ross, G.N.Hortobagyi, and L.Pusztai, Breast cancer molecular subtypes respond differently to preoperative chemotherapy, *Clin Cancer Res* 11 (2005) 5678.
22. C.Sotiriou, S.Y.Neo, L.M.McShane, E.L.Korn, P.M.Long, A.Jazaeri, P.Martiat, S.B.Fox, A.L.Harris, and E.T.Liu, Breast cancer classification and prognosis based on gene expression profiles from a population-based study, *Proc. Natl Acad. Sci. U. S. A* 100 (2003) 10393.
23. L.A.Carey, E.C.Dees, L.Sawyer, L.Gatti, D.T.Moore, F.Collichio, D.W.Ollila, C.I.Sartor, M.L.Graham, and C.M.Perou, The triple negative paradox: primary tumor chemosensitivity of breast cancer subtypes, *Clin Cancer Res* 13 (2007) 2329.
24. R.Wooster, G.Bignell, J.Lancaster, S.Swift, S.Seal, J.Mangion, N.Collins, S.Gregory, C.Gumbs, and G.Micklem, Identification of the breast cancer susceptibility gene BRCA2, *Nature* 378 (1995) 789.
25. Y.Miki, J.Swensen, D.Shattuck-Eidens, P.A.Futreal, K.Harshman, S.Tavtigian, Q.Liu, C.Cochran, L.M.Bennett, W.Ding, and A strong candidate for the breast and ovarian cancer susceptibility gene BRCA1, *Science* 266 (1994) 66.
26. M.C.King, J.H.Marks, and J.B.Mandell, Breast and ovarian cancer risks due to inherited mutations in BRCA1 and BRCA2, *Science* 302 (2003) 643.
27. E.L.Schubert, M.K.Lee, H.C.Mefford, R.H.Argonza, J.E.Morrow, J.Hull, J.L.Dann, and M.C.King, BRCA2 in American families with four or more cases of breast or ovarian cancer: recurrent and novel mutations, variable expression, penetrance, and the possibility of families whose cancer is not attributable to BRCA1 or BRCA2, *Am J Hum Genet* 60 (1997) 1031.
28. R.Ferla, V.Calo, S.Cascio, G.Rinaldi, G.Badalamenti, I.Carreca, E.Surmacz, G.Colucci, V.Bazan, and A.Russo, Founder mutations in BRCA1 and BRCA2 genes, *Ann Oncol* 18 Suppl 6 (2007) vi93-vi98.
29. J.Simard, P.Tonin, F.Durocher, K.Morgan, J.Rommens, S.Gingras, C.Samson, J.F.LebLANC, C.Belanger, F.Dion, and, Common origins of BRCA1 mutations in Canadian breast and ovarian cancer families, *Nat Genet* 8 (1994) 392.
30. C.Oddoux, J.P.Struewing, C.M.Clayton, S.Neuhausen, L.C.Brody, M.Kaback, B.Haas, L.Norton, P.Borgen, S.Jhanwar, D.Goldgar, H.Ostrer, and K.Offit, The carrier frequency of the BRCA2 6174delT mutation among Ashkenazi Jewish individuals is approximately 1%, *Nat Genet* 14 (1996) 188.
31. N.C.Turner and J.S.Reis-Filho, Basal-like breast cancer and the BRCA1 phenotype, *Oncogene* 25 (2006) 5846.

32. T.A.Grushko, M.A.Blackwood, P.L.Schumm, F.G.Hagos, M.O.Adeyanju, M.D.Feldman, M.O.Sanders, B.L.Weber, and O.I.Olopade, Molecular-cytogenetic analysis of HER-2/neu gene in BRCA1-associated breast cancers, *Cancer Res* 62 (2002) 1481.
33. W.D.Foulkes, I.M.Stefansson, P.O.Chappuis, L.R.Begin, J.R.Goffin, N.Wong, M.Trudel, and L.A.Akslen, Germline BRCA1 mutations and a basal epithelial phenotype in breast cancer, *J Natl Cancer Inst* 95 (2003) 1482.
34. S.R.Lakhani, J.S.Reis-Filho, L.Fulford, F.Penault-Llorca, M.van der Vijver, S.Parry, T.Bishop, J.Benitez, C.Rivas, Y.J.Bignon, J.Chang-Claude, U.Hamann, C.J.Cornelisse, P.Devilee, M.W.Beckmann, C.Nestle-Kramling, P.A.Daly, N.Haites, J.Varley, F.Laloo, G.Evans, C.Maugard, H.Meijers-Heijboer, J.G.Klijn, E.Olah, B.A.Gusterson, S.Pilotti, P.Radice, S.Scherneck, H.Sobol, J.Jacquemier, T.Wagner, J.Peto, M.R.Stratton, L.McGuffog, and D.F.Easton, Prediction of BRCA1 status in patients with breast cancer using estrogen receptor and basal phenotype, *Clin Cancer Res* 11 (2005) 5175.
35. M.E.Robson, P.O.Chappuis, J.Satagopan, N.Wong, J.Boyd, J.R.Goffin, C.Hudis, D.Roberge, L.Norton, L.R.Begin, K.Offit, and W.D.Foulkes, A combined analysis of outcome following breast cancer: differences in survival based on BRCA1/BRCA2 mutation status and administration of adjuvant treatment, *Breast Cancer Res* 6 (2004) R8-R17.
36. D.Stoppa-Lyonnet, Y.Ansquer, H.Dreyfus, C.Gautier, M.Gauthier-Villars, E.Bourstyn, K.B.Clough, H.Magdelenat, P.Pouillart, A.Vincent-Salomon, A.Fourquet, and B.Asselain, Familial invasive breast cancers: worse outcome related to BRCA1 mutations, *J Clin Oncol* 18 (2000) 4053.
37. N.Turner, A.Tutt, and A.Ashworth, Hallmarks of 'BRCAness' in sporadic cancers, *Nat Rev Cancer* 4 (2004) 814.
38. P.A.Futreal, Q.Liu, D.Shattuck-Eidens, C.Cochran, K.Harshman, S.Tavtigian, L.M.Bennett, A.Haugen-Strano, J.Swensen, Y.Miki, and, BRCA1 mutations in primary breast and ovarian carcinomas, *Science* 266 (1994) 120.
39. J.M.Lancaster, R.Wooster, J.Mangion, C.M.Phelan, C.Cochran, C.Gumbs, S.Seal, R.Barfoot, N.Collins, G.Bignell, S.Patel, R.Hamoudi, C.Larsson, R.W.Wiseman, A.Berchuck, J.D.Iglehart, J.R.Marks, A.Ashworth, M.R.Stratton, and P.A.Futreal, BRCA2 mutations in primary breast and ovarian cancers, *Nat Genet* 13 (1996) 238.
40. N.C.Turner, J.S.Reis-Filho, A.M.Russell, R.J.Springall, K.Ryder, D.Steele, K.Savage, C.E.Gillett, F.C.Schmitt, A.Ashworth, and A.N.Tutt, BRCA1 dysfunction in sporadic basal-like breast cancer, *Oncogene* 26 (2007) 2126.
41. F.Magdinier, S.Ribieras, G.M.Lenoir, L.Frappart, and R.Dante, Down-regulation of BRCA1 in human sporadic breast cancer; analysis of DNA methylation patterns of the putative promoter region, *Oncogene* 17 (1998) 3169.
42. A.Catteau, W.H.Harris, C.F.Xu, and E.Solomon, Methylation of the BRCA1 promoter region in sporadic breast and ovarian cancer: correlation with disease characteristics, *Oncogene* 18 (1999) 1957.
43. M.Esteller, J.M.Silva, G.Dominguez, F.Bonilla, X.Matias-Guiu, E.Lerma, E.Bussaglia, J.Prat, I.C.Harkes, E.A.Repasky, E.Gabrielson, M.Schutte, S.B.Baylin, and J.G.Herman, Promoter hypermethylation and BRCA1 inactivation in sporadic breast and ovarian tumors, *J Natl Cancer Inst* 92 (2000) 564.
44. J.C.Rice, H.Ozcelik, P.Maxeiner, I.Andrulis, and B.W.Futscher, Methylation of the BRCA1 promoter is associated with decreased BRCA1 mRNA levels in clinical breast cancer specimens, *Carcinogenesis* 21 (2000) 1761.
45. L.Hughes-Davies, D.Huntsman, M.Ruas, F.Fuks, J.Bye, S.F.Chin, J.Milner, L.A.Brown, F.Hsu, B.Gilks, T.Nielsen, M.Schulzer, S.Chia, J.Ragaz, A.Cahn, L.Linger, H.Ozdogan, E.Cattaneo, E.S.Jordanova, E.Schuuring, D.S.Yu, A.Venkitaraman, B.Ponder, A.Doherty, S.Aparicio, D.Bentley, C.Theillet, C.P.Ponting, C.Caldas, and T.Kouzarides, EMSY links the BRCA2 pathway to sporadic breast and ovarian cancer, *Cell* 115 (2003) 523.
46. G.Narayan, H.Arias-Pulido, S.V.Nandula, K.Basso, D.D.Sugirtharaj, H.Vargas, M.Mansukhani, J.Villella, L.Meyer, A.Schneider, L.Gissmann, M.Durst, B.Pothuri, and V.V.Murty, Promoter hypermethylation of FANCF: disruption of Fanconi Anemia-BRCA pathway in cervical cancer, *Cancer Res* 64 (2004) 2994.

47. T.Taniguchi, M.Tischkowitz, N.Ameziane, S.V.Hodgson, C.G.Mathew, H.Joenje, S.C.Mok, and A.D.D'Andrea, Disruption of the Fanconi anemia-BRCA pathway in cisplatin-sensitive ovarian tumors, *Nat Med* 9 (2003) 568.
48. S.Seal, D.Thompson, A.Renwick, A.Elliott, P.Kelly, R.Barfoot, T.Chagtai, H.Jayatilake, M.Ahmed, K.Spanova, B.North, L.McGuffog, D.G.Evans, D.Eccles, D.F.Easton, M.R.Stratton, and N.Rahman, Truncating mutations in the Fanconi anemia J gene BRIP1 are low-penetrance breast cancer susceptibility alleles, *Nat. Genet.* 38 (2006) 1239.
49. N.Rahman, S.Seal, D.Thompson, P.Kelly, A.Renwick, A.Elliott, S.Reid, K.Spanova, R.Barfoot, T.Chagtai, H.Jayatilake, L.McGuffog, S.Hanks, D.G.Evans, D.Eccles, D.F.Easton, and M.R.Stratton, PALB2, which encodes a BRCA2-interacting protein, is a breast cancer susceptibility gene, *Nat. Genet.* 39 (2007) 165.
50. H.Erkko, B.Xia, J.Nikkila, J.Schleutker, K.Syrjakoski, A.Mannermaa, A.Kallioniemi, K.Pylkas, S.M.Karppinen, K.Rapakko, A.Miron, Q.Sheng, G.Li, H.Mattila, D.W.Bell, D.A.Haber, M.Grip, M.Reiman, A.Jukkola-Vuorinen, A.Mustonen, J.Kere, L.A.Aaltonen, V.M.Kosma, V.Kataja, Y.Soini, R.I.Drapkin, D.M.Livingston, and R.Winqvist, A recurrent mutation in PALB2 in Finnish cancer families, *Nature* 446 (2007) 316.
51. S.R.Lakhani, M.J.Van De Vijver, J.Jacquemier, T.J.Anderson, P.P.Osin, L.McGuffog, and D.F.Easton, The pathology of familial breast cancer: predictive value of immunohistochemical markers estrogen receptor, progesterone receptor, HER-2, and p53 in patients with mutations in BRCA1 and BRCA2, *J Clin Oncol* 20 (2002) 2310.
52. J.E.Armes, L.Trute, D.White, M.C.Southey, F.Hammet, A.Tesoriero, A.M.Hutchins, G.S.Dite, M.R.McCredie, G.G.Giles, J.L.Hopper, and D.J.Venter, Distinct molecular pathogeneses of early-onset breast cancers in BRCA1 and BRCA2 mutation carriers: a population-based study, *Cancer Res.* 59 (1999) 2011.
53. C.X.Deng and S.G.Brodie, Roles of BRCA1 and its interacting proteins, *Bioessays* 22 (2000) 728.
54. J.D.Parvin, BRCA1 at a branch point, *Proc Natl Acad Sci U S A* 98 (2001) 5952.
55. J.H.Hoeijmakers, Genome maintenance mechanisms for preventing cancer, *Nature* 411 (2001) 366.
56. A.Bhattacharyya, U.S.Ear, B.H.Koller, R.R.Weichselbaum, and D.K.Bishop, The breast cancer susceptibility gene BRCA1 is required for subnuclear assembly of Rad51 and survival following treatment with the DNA cross-linking agent cisplatin, *J Biol Chem* 275 (2000) 23899.
57. D.Cortez, Y.Wang, J.Qin, and S.J.Elledge, Requirement of ATM-dependent phosphorylation of brca1 in the DNA damage response to double-strand breaks, *Science* 286 (1999) 1162.
58. R.S.Tibbetts, D.Cortez, K.M.Brumbaugh, R.Scully, D.Livingston, S.J.Elledge, and R.T.Abraham, Functional interactions between BRCA1 and the checkpoint kinase ATR during genotoxic stress, *Genes Dev* 14 (2000) 2989.
59. J.S.Lee, K.M.Collins, A.L.Brown, C.H.Lee, and J.H.Chung, hCds1-mediated phosphorylation of BRCA1 regulates the DNA damage response, *Nature* 404 (2000) 201.
60. M.E.Moynahan, A.J.Pierce, and M.Jasin, BRCA2 is required for homology-directed repair of chromosomal breaks, *Mol Cell* 7 (2001) 263.
61. F.Xia, D.G.Taghian, J.S.DeFrank, Z.C.Zeng, H.Willers, G.Iliakis, and S.N.Powell, Deficiency of human BRCA2 leads to impaired homologous recombination but maintains normal nonhomologous end joining, *Proc Natl Acad Sci U S A* 98 (2001) 8644.
62. J.Chen, D.P.Silver, D.Walpita, S.B.Cantor, A.F.Gazdar, G.Tomlinson, F.J.Couch, B.L.Weber, T.Ashley, D.M.Livingston, and R.Scully, Stable interaction between the products of the BRCA1 and BRCA2 tumor suppressor genes in mitotic and meiotic cells, *Mol Cell* 2 (1998) 317.
63. P.L.Chen, C.F.Chen, Y.Chen, J.Xiao, Z.D.Sharp, and W.H.Lee, The BRC repeats in BRCA2 are critical for RAD51 binding and resistance to methyl methanesulfonate treatment, *Proc Natl Acad Sci U S A* 95 (1998) 5287.
64. L.Chen, C.J.Nievera, A.Y.Lee, and X.Wu, Cell Cycle-dependent Complex Formation of BRCA1-CtIP-MRN Is Important for DNA Double-strand Break Repair, *J Biol Chem* 283 (2008) 7713.
65. T.T.Paull, D.Cortez, B.Bowers, S.J.Elledge, and M.Gellert, Direct DNA binding by Brca1, *Proc Natl Acad Sci U S A* 98 (2001) 6086.

66. Q.Zhong, C.F.Chen, S.Li, Y.Chen, C.C.Wang, J.Xiao, P.L.Chen, Z.D.Sharp, and W.H.Lee, Association of BRCA1 with the hRad50-hMre11-p95 complex and the DNA damage response, *Science* 285 (1999) 747.
67. B.Xu, S.Kim, and M.B.Kastan, Involvement of Brca1 in S-phase and G(2)-phase checkpoints after ionizing irradiation, *Mol Cell Biol* 21 (2001) 3445.
68. X.Xu, Z.Weaver, S.P.Linke, C.Li, J.Gotay, X.W.Wang, C.C.Harris, T.Ried, and C.X.Deng, Centrosome amplification and a defective G2-M cell cycle checkpoint induce genetic instability in BRCA1 exon 11 isoform-deficient cells, *Mol Cell* 3 (1999) 389.
69. R.H.Wang, H.Yu, and C.X.Deng, A requirement for breast-cancer-associated gene 1 (BRCA1) in the spindle checkpoint, *Proc. Natl. Acad. Sci. U S A* 101 (2004) 17108.
70. L.C.Gowen, A.V.Avrutskaya, A.M.Latour, B.H.Koller, and S.A.Leadon, BRCA1 required for transcription-coupled repair of oxidative DNA damage, *Science* 281 (1998) 1009.
71. F.Le Page, V.Randrianarison, D.Marot, J.Cabannes, M.Perricaudet, J.Feunteun, and A.Sarasin, BRCA1 and BRCA2 are necessary for the transcription-coupled repair of the oxidative 8-oxoguanine lesion in human cells, *Cancer Res* 60 (2000) 5548.
72. J.R.Morris and E.Solomon, BRCA1: BARD1 induces the formation of conjugated ubiquitin structures, dependent on K6 of ubiquitin, in cells during DNA replication and repair, *Hum Mol Genet* 13 (2004) 807.
73. L.C.Wu, Z.W.Wang, J.T.Tsan, M.A.Spillman, A.Phung, X.L.Xu, M.C.Yang, L.Y.Hwang, A.M.Bowcock, and R.Baer, Identification of a RING protein that can interact in vivo with the BRCA1 gene product, *Nat Genet* 14 (1996) 430.
74. L.J.Reid, R.Shakya, A.P.Modi, M.Lokshin, J.T.Cheng, M.Jasin, R.Baer, and T.Ludwig, E3 ligase activity of BRCA1 is not essential for mammalian cell viability or homology-directed repair of double-strand DNA breaks, *Proc. Natl. Acad. Sci. U S A* 105 (2008) 20876.
75. J.E.Quinn, R.D.Kennedy, P.B.Mullan, P.M.Gilmore, M.Carty, P.G.Johnston, and D.P.Harkin, BRCA1 functions as a differential modulator of chemotherapy-induced apoptosis, *Cancer Res* 63 (2003) 6221.
76. B.Evers and J.Jonkers, Mouse models of BRCA1 and BRCA2 deficiency: past lessons, current understanding and future prospects, *Oncogene* 25 (2006) 5885.
77. X.Liu, H.Holstege, H.van der Gulden, M.Treur-Mulder, J.Zevenhoven, A.Velds, R.M.Kerkhoven, M.H.van Vliet, L.F.Wessels, J.L.Peterse, A.Berns, and J.Jonkers, Somatic loss of BRCA1 and p53 in mice induces mammary tumors with features of human BRCA1-mutated basal-like breast cancer, *Proc Natl Acad Sci U S A* 104 (2007) 12111.
78. X.Xu, K.U.Wagner, D.Larson, Z.Weaver, C.Li, T.Ried, L.Hennighausen, A.Wynshaw-Boris, and C.X.Deng, Conditional mutation of Brca1 in mammary epithelial cells results in blunted ductal morphogenesis and tumour formation, *Nat Genet* 22 (1999) 37.
79. A.J.Poole, Y.Li, Y.Kim, S.C.Lin, W.H.Lee, and E.Y.Lee, Prevention of Brca1-mediated mammary tumorigenesis in mice by a progesterone antagonist, *Science* 314 (2006) 1467.
80. A.McCarthy, K.Savage, A.Gabriel, C.Naceur, J.S.Reis-Filho, and A.Ashworth, A mouse model of basal-like breast carcinoma with metaplastic elements, *J. Pathol.* 211 (2007) 389.
81. L.C.Brody, Treating cancer by targeting a weakness, *N Engl J Med* 353 (2005) 949.
82. M.S.Greenblatt, P.O.Chappuis, J.P.Bond, N.Hamel, and W.D.Foulkes, TP53 mutations in breast cancer associated with BRCA1 or BRCA2 germ-line mutations: distinctive spectrum and structural distribution, *Cancer Res* 61 (2001) 4092.
83. H.Holstege, S.A.Joose, C.T.van Oostrom, P.M.Nederlof, A.de Vries, and J.Jonkers, High incidence of protein-truncating TP53 mutations in BRCA1-related breast cancer, *Cancer Res.* 69 (2009) 3625.
84. E.Manie, A.Vincent-Salomon, J.Lehmann-Che, G.Pierron, E.Turpin, M.Warcoin, N.Gruel, I.Lebigot, X.Sastre-Garau, R.Lidereau, A.Remenieras, J.Feunteun, O.Delattre, H.de The, D.Stoppa-Lyonnet, and M.H.Stern, High frequency of TP53 mutation in BRCA1 and sporadic basal-like carcinomas but not in BRCA1 luminal breast tumors, *Cancer Res.* 69 (2009) 663.
85. P.O.Chappuis, V.Nethercot, and W.D.Foulkes, Clinico-pathological characteristics of BRCA1- and BRCA2-related breast cancer, *Semin Surg Oncol* 18 (2000) 287.

86. S.G.Brodie, X.Xu, W.Qjiao, W.M.Li, L.Cao, and C.X.Deng, Multiple genetic changes are associated with mammary tumorigenesis in Brca1 conditional knockout mice, *Oncogene* 20 (2001) 7514.
87. T.Ludwig, P.Fisher, S.Ganesan, and A.Efstratiadis, Tumorigenesis in mice carrying a truncating Brca1 mutation, *Genes Dev* 15 (2001) 1188.
88. T.Ludwig, P.Fisher, V.Murty, and A.Efstratiadis, Development of mammary adenocarcinomas by tissue-specific knockout of Brca2 in mice, *Oncogene* 20 (2001) 3937.
89. S.Rottenberg, A.O.Nygren, M.Pajic, F.W.van Leeuwen, I.van der Heijden, K.van de Wetering, X.Liu, K.E.de Visser, K.G.Gilhuijs, O.van Tellinggen, J.P.Schouten, J.Jonkers, and P.Borst, Selective induction of chemotherapy resistance of mammary tumors in a conditional mouse model for hereditary breast cancer, *Proc Natl Acad Sci U S A* 104 (2007) 12117.
90. A.Bergamaschi, Y.H.Kim, P.Wang, T.Sorlie, T.Hernandez-Boussard, P.E.Lonning, R.Tibshirani, A.L.Borresen-Dale, and J.R.Pollack, Distinct patterns of DNA copy number alteration are associated with different clinicopathological features and gene-expression subtypes of breast cancer, *Genes Chromosomes Cancer* 45 (2006) 1033.
91. P.J.McHugh, W.R.Sones, and J.A.Hartley, Repair of intermediate structures produced at DNA interstrand cross-links in *Saccharomyces cerevisiae*, *Mol Cell Biol* 20 (2000) 3425.
92. J.A.Tercero and J.F.Diffley, Regulation of DNA replication fork progression through damaged DNA by the Mec1/Rad53 checkpoint, *Nature* 412 (2001) 553.
93. G.Minotti, P.Menna, E.Salvatorelli, G.Cairo, and L.Gianni, Anthracyclines: molecular advances and pharmacologic developments in antitumor activity and cardiotoxicity, *Pharmacol Rev* 56 (2004) 185.
94. R.G.Shao, C.X.Cao, H.Zhang, K.W.Kohn, M.S.Wold, and Y.Pommier, Replication-mediated DNA damage by camptothecin induces phosphorylation of RPA by DNA-dependent protein kinase and dissociates RPA:DNA-PK complexes, *EMBO J* 18 (1999) 1397.
95. Z.Z.Zdraveski, J.A.Mello, M.G.Marinus, and J.M.Essigmann, Multiple pathways of recombination define cellular responses to cisplatin, *Chem Biol* 7 (2000) 39.
96. T.H.Wang, H.S.Wang, and Y.K.Soong, Paclitaxel-induced cell death: where the cell cycle and apoptosis come together, *Cancer* 88 (2000) 2619.
97. A.Husain, G.He, E.S.Venkatraman, and D.R.Spriggs, BRCA1 up-regulation is associated with repair-mediated resistance to cis-diamminedichloroplatinum(II), *Cancer Res* 58 (1998) 1120.
98. V.Sylvain, S.Lafarge, and Y.J.Bignon, Dominant-negative activity of a Brca1 truncation mutant: effects on proliferation, tumorigenicity in vivo, and chemosensitivity in a mouse ovarian cancer cell line, *Int J Oncol* 20 (2002) 845.
99. P.B.Mullan, J.E.Quinn, P.M.Gilmore, S.McWilliams, H.Andrews, C.Gervin, N.McCabe, S.McKenna, P.White, Y.H.Song, S.Maheswaran, E.Liu, D.A.Haber, P.G.Johnston, and D.P.Harkin, BRCA1 and GADD45 mediated G2/M cell cycle arrest in response to antimicrotubule agents, *Oncogene* 20 (2001) 6123.
100. S.J.Kim, Y.Miyoshi, T.Taguchi, Y.Tamaki, H.Nakamura, J.Yodoi, K.Kato, and S.Noguchi, High thioredoxin expression is associated with resistance to docetaxel in primary breast cancer, *Clin. Cancer Res.* 11 (2005) 8425.
101. R.Torrisi, A.Balduzzi, R.Ghisini, A.Rocca, L.Bottiglieri, F.Giovanardi, P.Veronesi, A.Luini, L.Orlando, G.Viale, A.Goldhirsch, and M.Colleoni, Tailored preoperative treatment of locally advanced triple negative (hormone receptor negative and HER2 negative) breast cancer with epirubicin, cisplatin, and infusional fluorouracil followed by weekly paclitaxel, *Cancer Chemother. Pharmacol.* 62 (2008) 667.
102. N.G.Howlett, T.Taniguchi, S.Olson, B.Cox, Q.Waisfisz, C.Die-Smulders, N.Persky, M.Grompe, H.Joenje, G.Pals, H.Ikeda, E.A.Fox, and A.D.D'Andrea, Biallelic inactivation of BRCA2 in Fanconi anemia, *Science* 297 (2002) 606.
103. M.Kraakman-van der Zwet, W.J.Overkamp, R.E.van Lange, J.Essers, A.Duijn-Goedhart, I.Wiggers, S.Swaminathan, P.P.van Buul, A.Errami, R.T.Tan, N.G.Jaspers, S.K.Sharan, R.Kanaar, and M.Z.Zdzienicka, Brca2 (XRCC11) deficiency results in radioresistant DNA synthesis and a higher frequency of spontaneous deletions, *Mol Cell Biol* 22 (2002) 669.
104. T.Byrski, T.Huzarski, R.Dent, J.Gronwald, D.Zuziak, C.Cybulski, J.Kladny, B.Gorski, J.Lubinski, and S.A.Narod, Response to neoadjuvant therapy with cisplatin in BRCA1-positive breast cancer patients, *Breast Cancer Res. Treat.* 115 (2009) 359.

105. D.Chirnomas, T.Taniguchi, M.de la Vega, A.P.Vaidya, M.Vasserman, A.R.Hartman, R.Kennedy, R.Foster, J.Mahoney, M.V.Seiden, and A.D.D'Andrea, Chemosensitization to cisplatin by inhibitors of the Fanconi anemia/BRCA pathway, *Mol Cancer Ther* 5 (2006) 952.
106. S.R.Bartz, Z.Zhang, J.Burchard, M.Imakura, M.Martin, A.Palmieri, R.Needham, J.Guo, M.Gordon, N.Chung, P.Warrener, A.L.Jackson, M.Carleton, M.Oatley, L.Looco, F.Santini, T.Smith, P.Kunapuli, M.Ferrer, B.Strulovici, S.H.Friend, and P.S.Linsley, Small interfering RNA screens reveal enhanced cisplatin cytotoxicity in tumor cells having both BRCA network and TP53 disruptions, *Mol Cell Biol* 26 (2006) 9377.
107. C.Chabaliere, C.Lamare, C.Racca, M.Privat, A.Valette, and F.Larminat, BRCA1 downregulation leads to premature inactivation of spindle checkpoint and confers paclitaxel resistance, *Cell Cycle* 5 (2006) 1001.
108. L.S.Kilburn, 'Triple negative' breast cancer: a new area for phase III breast cancer clinical trials, *Clin. Oncol. (R Coll. Radiol.)* 20 (2008) 35.
109. R.D.Kennedy, J.E.Quinn, P.B.Mullan, P.G.Johnston, and D.P.Harkin, The role of BRCA1 in the cellular response to chemotherapy, *J. Natl. Cancer Inst.* 96 (2004) 1659.
110. P.W.Derksen, X.Liu, F.Saridin, H.van der Gulden, J.Zevenhoven, B.Evers, J.R.van Beijnum, A.W.Griffioen, J.Vink, P.Krimpenfort, J.L.Peterse, R.D.Cardiff, A.Berns, and J.Jonkers, Somatic inactivation of E-cadherin and p53 in mice leads to metastatic lobular mammary carcinoma through induction of anoikis resistance and angiogenesis, *Cancer Cell* 10 (2006) 437.
111. S.Rodenhuis, M.Bontenbal, L.V.Beex, J.Wagstaff, D.J.Richel, M.A.Nooij, E.E.Voest, P.Hupperets, H.van Tinteren, H.L.Peterse, E.M.TenVergert, and E.G.de Vries, High-dose chemotherapy with hematopoietic stem-cell rescue for high-risk breast cancer, *N Engl. J. Med.* 349 (2003) 7.
112. E.van der Wall, J.H.Beijnen, and S.Rodenhuis, High-dose chemotherapy regimens for solid tumors, *Cancer Treat. Rev.* 21 (1995) 105.
113. C.M.Farquhar, J.Marjoribanks, A.Lethaby, and R.Basser, High dose chemotherapy for poor prognosis breast cancer: systematic review and meta-analysis, *Cancer Treat. Rev.* 33 (2007) 325.
114. S.Rodenhuis, M.Bontenbal, Q.G.van Hoesel, W.M.Smit, M.A.Nooij, E.E.Voest, E.van der Wall, P.Hupperets, H.van Tinteren, J.L.Peterse, M.J.Van De Vijver, and E.G.de Vries, Efficacy of high-dose alkylating chemotherapy in HER2/neu-negative breast cancer, *Ann. Oncol.* 17 (2006) 588.
115. O.Gluz, U.A.Nitz, N.Harbeck, E.Ting, R.Kates, A.Herr, W.Lindemann, C.Jackisch, W.E.Berdel, H.Kirchner, B.Metzner, F.Werner, G.Schutt, M.Frick, C.Poremba, R.Diallo-Danebrock, and S.Mohrmann, Triple-negative high-risk breast cancer derives particular benefit from dose intensification of adjuvant chemotherapy: results of WSG AM-01 trial, *Ann. Oncol.* 19 (2008) 861.
116. R.Diallo-Danebrock, E.Ting, O.Gluz, A.Herr, S.Mohrmann, H.Geddert, A.Rody, K.L.Schaefer, S.E.Baldus, A.Hartmann, P.J.Wild, M.Burson, H.E.Gabbert, U.Nitz, and C.Poremba, Protein expression profiling in high-risk breast cancer patients treated with high-dose or conventional dose-dense chemotherapy, *Clin. Cancer Res.* 13 (2007) 488.
117. L.F.Wessels, T.van Welsem, A.A.Hart, L.J.van't Veer, M.J.Reinders, and P.M.Nederlof, Molecular classification of breast carcinomas by comparative genomic hybridization: a specific somatic genetic profile for BRCA1 tumors, *Cancer Res.* 62 (2002) 7110.
118. M.A.Vollebergh, E.H.Lips, P.M.Nederlof, L.F.Wessels, M.K.Schmidt, E.H.van Beers, S.Cornelissen, M.Holtkamp, F.E.Froklage, E.G.de Vries, J.G.Schrama, J.Wesseling, M.J.van de Vijver, H.van Tinteren, M.de Bruin, M.Hauptmann, S.Rodenhuis, and S.C.Linn, An aCGH classifier derived from BRCA1-mutated breast cancer and benefit of high-dose platinum-based chemotherapy in HER2-negative breast cancer patients, *Ann Oncol.* 22 (2011) 1561.
119. J.C.Ame, C.Spenlehauer, and G.de Murcia, The PARP superfamily, *Bioessays* 26 (2004) 882.
120. D.D'Amours, S.Desnoyers, I.D'Silva, and G.G.Poirier, Poly(ADP-ribosyl)ation reactions in the regulation of nuclear functions, *Biochem J* 342 (Pt 2) (1999) 249.
121. V.Schreiber, F.Dantzer, J.C.Ame, and G.de Murcia, Poly(ADP-ribose): novel functions for an old molecule, *Nat. Rev. Mol. Cell Biol.* 7 (2006) 517.
122. H.Vaziri, M.D.West, R.C.Allsopp, T.S.Davison, Y.S.Wu, C.H.Arrowsmith, G.G.Poirier, and S.Benchimol, ATM-dependent telomere loss in aging human diploid fibroblasts and DNA damage lead to the post-translational activation of p53 protein involving poly(ADP-ribose) polymerase, *EMBO J* 16 (1997) 6018.

123. W.M.Tong, M.P.Hande, P.M.Lansdorp, and Z.Q.Wang, DNA strand break-sensing molecule poly(ADP-Ribose) polymerase cooperates with p53 in telomere function, chromosome stability, and tumor suppression, *Mol Cell Biol* 21 (2001) 4046.
124. Z.Q.Wang, L.Stingl, C.Morrison, M.Jantsch, M.Los, K.Schulze-Osthoff, and E.F.Wagner, PARP is important for genomic stability but dispensable in apoptosis, *Genes Dev* 11 (1997) 2347.
125. N.Schultz, E.Lopez, N.Saleh-Gohari, and T.Helleday, Poly(ADP-ribose) polymerase (PARP-1) has a controlling role in homologous recombination, *Nucleic Acids Res* 31 (2003) 4959.
126. Y.G.Yang, U.Cortes, S.Patnaik, M.Jasin, and Z.Q.Wang, Ablation of PARP-1 does not interfere with the repair of DNA double-strand breaks, but compromises the reactivation of stalled replication forks, *Oncogene* 23 (2004) 3872.
127. C.Conde, M.Mark, F.J.Oliver, A.Huber, G.de Murcia, and J.Menissier-de Murcia, Loss of poly(ADP-ribose) polymerase-1 causes increased tumour latency in p53-deficient mice, *EMBO J* 20 (2001) 3535.
128. M.Masutani, T.Nozaki, K.Nakamoto, H.Nakagama, H.Suzuki, O.Kusuoka, M.Tsutsumi, and T.Sugimura, The response of Parp knockout mice against DNA damaging agents, *Mutat Res* 462 (2000) 159.
129. H.E.Bryant, N.Schultz, H.D.Thomas, K.M.Parker, D.Flower, E.Lopez, S.Kyle, M.Meuth, N.J.Curtin, and T.Helleday, Specific killing of BRCA2-deficient tumours with inhibitors of poly(ADP-ribose) polymerase, *Nature* 434 (2005) 913.
130. H.Farmer, N.McCabe, C.J.Lord, A.N.Tutt, D.A.Johnson, T.B.Richardson, M.Santarosa, K.J.Dillon, I.Hickson, C.Knights, N.M.Martin, S.P.Jackson, G.C.Smith, and A.Ashworth, Targeting the DNA repair defect in BRCA mutant cells as a therapeutic strategy, *Nature* 434 (2005) 917.
131. N.McCabe, N.C.Turner, C.J.Lord, K.Kluzek, A.Bialkowska, S.Swift, S.Giavara, M.J.O'Connor, A.N.Tutt, M.Z.Zdzienicka, G.C.Smith, and A.Ashworth, Deficiency in the repair of DNA damage by homologous recombination and sensitivity to poly(ADP-ribose) polymerase inhibition, *Cancer Res* 66 (2006) 8109.
132. J.A.De Soto, X.Wang, Y.Tominaga, R.H.Wang, L.Cao, W.Qiao, C.Li, X.Xu, A.P.Skoumbourdis, S.A.Prindiville, C.J.Thomas, and C.X.Deng, The inhibition and treatment of breast cancer with poly (ADP-ribose) polymerase (PARP-1) inhibitors, *Int J Biol Sci* 2 (2006) 179.
133. C.K.Donawho, Y.Luo, Y.Luo, T.D.Penning, J.L.Bauch, J.J.Bouska, V.D.Bontcheva-Diaz, B.F.Cox, T.L.DeWeese, L.E.Dillehay, D.C.Ferguson, N.S.Ghoreishi-Haack, D.R.Grimm, R.Guan, E.K.Han, R.R.Holley-Shanks, B.Hristov, K.B.Idler, K.Jarvis, E.F.Johnson, L.R.Kleinberg, V.Klinghofer, L.M.Lasko, X.Liu, K.C.Marsh, T.P.McGonigal, J.A.Meulbroek, A.M.Olson, J.P.Palma, L.E.Rodriguez, Y.Shi, J.A.Stavropoulos, A.C.Tsurutani, G.D.Zhu, S.H.Rosenberg, V.L.Giranda, and D.J.Frost, ABT-888, an orally active poly(ADP-ribose) polymerase inhibitor that potentiates DNA-damaging agents in preclinical tumor models, *Clin Cancer Res* 13 (2007) 2728.
134. S.Rottenberg, J.E.Jaspers, A.Kersbergen, E.van der Burg, A.O.Nygren, S.A.Zander, P.W.Derksen, M.de Bruin, J.Zevenhoven, A.Lau, R.Boulter, A.Cranston, M.J.O'Connor, N.M.Martin, P.Borst, and J.Jonkers, High sensitivity of BRCA1-deficient mammary tumors to the PARP inhibitor AZD2281 alone and in combination with platinum drugs, *Proc. Natl. Acad. Sci. U S A* 105 (2008) 17079.
135. P.C.Fong, D.S.Boss, T.A.Yap, A.Tutt, P.Wu, M.Mergui-Roelvink, P.Mortimer, H.Swaisland, A.Lau, M.J.O'Connor, A.Ashworth, J.Carmichael, S.B.Kaye, J.H.Schellens, and J.S.de Bono, Inhibition of Poly(ADP-Ribose) Polymerase in Tumors from BRCA Mutation Carriers, *N Engl. J. Med.* (2009).
136. C.R.Calabrese, R.Almassy, S.Barton, M.A.Batey, A.H.Calvert, S.Canan-Koch, B.W.Durkacz, Z.Hostomsky, R.A.Kumpf, S.Kyle, J.Li, K.Maegley, D.R.Newell, E.Notarianni, I.J.Stratford, D.Skalitzky, H.D.Thomas, L.Z.Wang, S.E.Webber, K.J.Williams, and N.J.Curtin, Anti-cancer chemosensitization and radiosensitization by the novel poly(ADP-ribose) polymerase-1 inhibitor AG14361, *J Natl Cancer Inst* 96 (2004) 56.
137. S.J.Veuger, N.J.Curtin, C.J.Richardson, G.C.Smith, and B.W.Durkacz, Radiosensitization and DNA repair inhibition by the combined use of novel inhibitors of DNA-dependent protein kinase and poly(ADP-ribose) polymerase-1, *Cancer Res* 63 (2003) 6008.
138. L.Tentori and G.Graziani, Chemopotentialization by PARP inhibitors in cancer therapy, *Pharmacol Res* 52 (2005) 25.

139. E.R.Plummer, Inhibition of poly(ADP-ribose) polymerase in cancer, *Curr. Opin. Pharmacol.* 6 (2006) 364.
140. N.J.Curtin, L.Z.Wang, A.Yiakouvaki, S.Kyle, C.A.Arris, S.Canan-Koch, S.E.Webber, B.W.Durkacz, H.A.Calvert, Z.Hostomsky, and D.R.Newell, Novel poly(ADP-ribose) polymerase-1 inhibitor, AG14361, restores sensitivity to temozolomide in mismatch repair-deficient cells, *Clin Cancer Res* 10 (2004) 881.
141. L.Tentori, P.M.Lacal, E.Benincasa, D.Franco, I.Faraoni, E.Bonmassar, and G.Graziani, Role of wild-type p53 on the antineoplastic activity of temozolomide alone or combined with inhibitors of poly(ADP-ribose) polymerase, *J Pharmacol Exp Ther* 285 (1998) 884.
142. C.A.Delaney, L.Z.Wang, S.Kyle, A.W.White, A.H.Calvert, N.J.Curtin, B.W.Durkacz, Z.Hostomsky, and D.R.Newell, Potentiation of temozolomide and topotecan growth inhibition and cytotoxicity by novel poly(adenosine diphosphoribose) polymerase inhibitors in a panel of human tumor cell lines, *Clin Cancer Res* 6 (2000) 2860.
143. P.A.Nguewa, M.A.Fuertes, V.Cepeda, C.Alonso, C.Quevedo, M.Soto, and J.M.Perez, Poly(ADP-ribose) polymerase-1 inhibitor 3-aminobenzamide enhances apoptosis induction by platinum complexes in cisplatin-resistant tumor cells, *Med Chem* 2 (2006) 47.
144. B.Evers, R.Drost, E.Schut, M.de Bruin, E.van der Burg, P.W.Derksen, H.Holstege, X.Liu, E.van Drunen, H.B.Beverloo, G.C.Smith, N.M.Martin, A.Lau, M.J.O'Connor, and J.Jonkers, Selective inhibition of BRCA2-deficient mammary tumor cell growth by AZD2281 and cisplatin, *Clin. Cancer Res.* 14 (2008) 3916.
145. N.Gambi, F.Tramontano, and P.Quesada, Poly(ADPR)polymerase inhibition and apoptosis induction in cDDP-treated human carcinoma cell lines, *Biochem. Pharmacol.* 75 (2008) 2356.
146. L.Tentori, C.Leonetti, M.Scarsella, G.D'Amati, M.Vergati, I.Portarena, W.Xu, V.Kalish, G.Zupi, J.Zhang, and G.Graziani, Systemic administration of GPI 15427, a novel poly(ADP-ribose) polymerase-1 inhibitor, increases the antitumor activity of temozolomide against intracranial melanoma, glioma, lymphoma, *Clin Cancer Res* 9 (2003) 5370.
147. J.A.Munoz-Gamez, D.Martin-Oliva, R.Aguilar-Quesada, A.Canuelo, M.I.Nunez, M.T.Valenzuela, J.M.Ruiz de Almodovar, G.de Murcia, and F.J.Oliver, PARP inhibition sensitizes p53-deficient breast cancer cells to doxorubicin-induced apoptosis, *Biochem J* 386 (2005) 119.
148. K.A.Mason, D.Valdecanas, N.R.Hunter, and L.Milas, INO-1001, a novel inhibitor of poly(ADP-ribose) polymerase, enhances tumor response to doxorubicin, *Invest New Drugs* (2007).
149. P.Pacher, L.Liaudet, P.Bai, L.Virag, J.G.Mabley, G.Hasko, and C.Szabo, Activation of poly(ADP-ribose) polymerase contributes to development of doxorubicin-induced heart failure, *J Pharmacol Exp Ther* 300 (2002) 862.
150. I.Racz, K.Tory, F.Gallyas, Jr., Z.Berente, E.Osz, L.Jaszlits, S.Bernath, B.Sumegi, G.Rabloczky, and P.Literati-Nagy, BGP-15 - a novel poly(ADP-ribose) polymerase inhibitor - protects against nephrotoxicity of cisplatin without compromising its antitumor activity, *Biochem Pharmacol* 63 (2002) 1099.
151. J.B.Arnes, L.R.Begin, I.Stefansson, J.S.Brunet, T.O.Nielsen, W.D.Foulkes, and L.A.Akslen, Expression of epidermal growth factor receptor in relation to BRCA1 status, basal-like markers and prognosis in breast cancer, *J. Clin. Pathol.* 62 (2009) 139.
152. M.C.Cheang, D.Voduc, C.Bajdik, S.Leung, S.McKinney, S.K.Chia, C.M.Perou, and T.O.Nielsen, Basal-like breast cancer defined by five biomarkers has superior prognostic value than triple-negative phenotype, *Clin. Cancer Res.* 14 (2008) 1368.
153. A.L.Stratford, G.Habibi, A.Astanehe, H.Jiang, K.Hu, E.Park, A.Shadeo, T.P.Buys, W.Lam, T.Pugh, M.Marra, T.O.Nielsen, U.Klinge, P.R.Mertens, S.Aparicio, and S.E.Dunn, Epidermal growth factor receptor (EGFR) is transcriptionally induced by the Y-box binding protein-1 (YB-1) and can be inhibited with Iressa in basal-like breast cancer, providing a potential target for therapy, *Breast Cancer Res* 9 (2007) R61.
154. K.A.Hoadley, V.J.Weigman, C.Fan, L.R.Sawyer, X.He, M.A.Troester, C.I.Sartor, T.Rieger-House, P.S.Bernard, L.A.Carey, and C.M.Perou, EGFR associated expression profiles vary with breast tumor subtype, *BMC Genomics* 8 (2007) 258.

155. S.Azoulay, M.Lae, P.Freneaux, S.Merle, A.Al Ghuzlan, C.Chnecker, C.Rosty, J.Klijanienko, B.Sigal-Zafrani, R.Salmon, A.Fourquet, X.Sastre-Garau, and A.Vincent-Salomon, KIT is highly expressed in adenoid cystic carcinoma of the breast, a basal-like carcinoma associated with a favorable outcome, *Mod Pathol* 18 (2005) 1623.
156. A.E.Roussidis, T.N.Mitropoulou, A.D.Theocharis, C.Kiamouris, S.Papadopoulos, D.Kletsas, and N.K.Karamanos, STI571 as a potent inhibitor of growth and invasiveness of human epithelial breast cancer cells, *Anti-cancer Res* 24 (2004) 1445.
157. S.Modi, A.D.Seidman, M.Dickler, M.Moasser, G.D'Andrea, M.E.Moynahan, J.Menell, K.S.Panageas, L.K.Tan, L.Norton, and C.A.Hudis, A phase II trial of imatinib mesylate monotherapy in patients with metastatic breast cancer, *Breast Cancer Res Treat* 90 (2005) 157.
158. R.S.Finn, J.Dering, C.Ginther, C.A.Wilson, P.Glaspy, N.Tchekmedyan, and D.J.Slamon, Dasatinib, an orally active small molecule inhibitor of both the src and abl kinases, selectively inhibits growth of basal-type/"triple-negative" breast cancer cell lines growing in vitro, *Breast Cancer Res Treat* 105 (2007) 319.
159. O.Dizdar, D.S.Dede, N.Bulut, and K.Altundag, Dasatinib may also inhibit c-Kit in triple negative breast cancer cell lines, *Breast Cancer Res Treat* (2007).
160. L.J.Lombardo, F.Y.Lee, P.Chen, D.Norris, J.C.Barrish, K.Behnia, S.Castaneda, L.A.Cornelius, J.Das, A.M.Doweyko, C.Fairchild, J.T.Hunt, I.Inigo, K.Johnston, A.Kamath, D.Kan, H.Klei, P.Marathe, S.Pang, R.Peterson, S.Pitt, G.L.Schieven, R.J.Schmidt, J.Tokarski, M.L.Wen, J.Wityak, and R.M.Borzilleri, Discovery of N-(2-chloro-6-methyl-phenyl)-2-(6-(4-(2-hydroxyethyl)-piperazin-1-yl)-2-methylpyrimidin-4-ylamino)thiazole-5-carboxamide (BMS-354825), a dual Src/Abl kinase inhibitor with potent antitumor activity in preclinical assays, *J Med Chem* 47 (2004) 6658.
161. G.Rennert, S.Bisland-Naggan, O.Barnett-Griness, N.Bar-Joseph, S.Zhang, H.S.Rennert, and S.A.Narod, Clinical outcomes of breast cancer in carriers of BRCA1 and BRCA2 mutations, *N Engl. J. Med.* 357 (2007) 115.
162. M.S.Wicha, S.Liu, and G.Dontu, Cancer stem cells: an old idea--a paradigm shift, *Cancer Res* 66 (2006) 1883.
163. C.A.O'Brien, A.Pollett, S.Gallinger, and J.E.Dick, A human colon cancer cell capable of initiating tumour growth in immunodeficient mice, *Nature* 445 (2007) 106.
164. M.Al Hajj, M.S.Wicha, A.Benito-Hernandez, S.J.Morrison, and M.F.Clarke, Prospective identification of tumorigenic breast cancer cells, *Proc. Natl Acad. Sci. U. S. A* 100 (2003) 3983.
165. Z.F.Yang, D.W.Ho, M.N.Ng, C.K.Lau, W.C.Yu, P.Ngai, P.W.Chu, C.T.Lam, R.T.Poon, and S.T.Fan, Significance of CD90+ cancer stem cells in human liver cancer, *Cancer Cell* 13 (2008) 153.
166. P.C.Hermann, S.L.Huber, T.Herrler, A.Aicher, J.W.Ellwart, M.Guba, C.J.Bruns, and C.Heeschen, Distinct populations of cancer stem cells determine tumor growth and metastatic activity in human pancreatic cancer, *Cell Stem Cell* 1 (2007) 313.
167. A.T.Collins, P.A.Berry, C.Hyde, M.J.Stower, and N.J.Maitland, Prospective identification of tumorigenic prostate cancer stem cells, *Cancer Res.* 65 (2005) 10946.
168. S.K.Singh, C.Hawkins, I.D.Clarke, J.A.Squire, J.Bayani, T.Hide, R.M.Henkelman, M.D.Cusimano, and P.B.Dirks, Identification of human brain tumour initiating cells, *Nature* 432 (2004) 396.
169. T.Schatton, G.F.Murphy, N.Y.Frank, K.Yamaura, A.M.Waaga-Gasser, M.Gasser, Q.Zhan, S.Jordan, L.M.Duncan, C.Weishaupt, R.C.Fuhlbrigge, T.S.Kupper, M.H.Sayegh, and M.H.Frank, Identification of cells initiating human melanomas, *Nature* 451 (2008) 345.
170. E.Quintana, M.Shackleton, M.S.Sabel, D.R.Fullen, T.M.Johnson, and S.J.Morrison, Efficient tumour formation by single human melanoma cells, *Nature* 456 (2008) 593.
171. W.A.Woodward, M.S.Chen, F.Behbod, M.P.Alfaro, T.A.Buchholz, and J.M.Rosen, WNT/beta-catenin mediates radiation resistance of mouse mammary progenitor cells, *Proc. Natl. Acad. Sci. U S A* 104 (2007) 618.
172. X.Li, M.T.Lewis, J.Huang, C.Gutierrez, C.K.Osborne, M.F.Wu, S.G.Hilsenbeck, A.Pavlick, X.Zhang, G.C.Chamness, H.Wong, J.Rosen, and J.C.Chang, Intrinsic resistance of tumorigenic breast cancer cells to chemotherapy, *J. Natl. Cancer Inst.* 100 (2008) 672.
173. M.J.Piccart-Gebhart, M.Procter, B.Leyland-Jones, A.Goldhirsch, M.Untch, I.Smith, L.Gianni, J.Baselga, R.Bell, C.Jackisch, D.Cameron, M.Dowsett, C.H.Barrios, G.Steger, C.S.Huang, M.Andersson, M.Inbar, M.Lichinitser, I.Lang, U.Nitz, H.Iwata, C.Thomssen, C.Lohrisch, T.M.Suter,

- J.Ruschoff, T.Suto, V.Greatorex, C.Ward, C.Straehle, E.McFadden, M.S.Dolci, and R.D.Gelber, Trastuzumab after adjuvant chemotherapy in HER2-positive breast cancer, *N Engl. J. Med.* 353 (2005) 1659.
174. N.Shafee, C.R.Smith, S.Weil, Y.Kim, G.B.Mills, G.N.Hortobagyi, E.J.Stanbridge, and E.Y.Lee, Cancer stem cells contribute to cisplatin resistance in Brca1/p53-mediated mouse mammary tumors, *Cancer Res.* 68 (2008) 3243.
 175. B.D.Chang, Y.Xuan, E.V.Broude, H.Zhu, B.Schott, J.Fang, and I.B.Roninson, Role of p53 and p21waf1/cip1 in senescence-like terminal proliferation arrest induced in human tumor cells by chemotherapeutic drugs, *Oncogene* 18 (1999) 4808.
 176. M.Suzuki and D.A.Boothman, Stress-induced premature senescence (SIPS)--influence of SIPS on radiotherapy, *J. Radiat. Res. (Tokyo)* 49 (2008) 105.
 177. X.Wang, S.C.Wong, J.Pan, S.W.Tsao, K.H.Fung, D.L.Kwong, J.S.Sham, and J.M.Nicholls, Evidence of cisplatin-induced senescent-like growth arrest in nasopharyngeal carcinoma cells, *Cancer Res.* 58 (1998) 5019.
 178. R.S.Roberson, S.J.Kussick, E.Vallieres, S.Y.Chen, and D.Y.Wu, Escape from therapy-induced accelerated cellular senescence in p53-null lung cancer cells and in human lung cancers, *Cancer Res.* 65 (2005) 2795.
 179. D.J.Stewart, Mechanisms of resistance to cisplatin and carboplatin, *Crit Rev Oncol Hematol* 63 (2007) 12.
 180. C.M.Beausejour, A.Krtolica, F.Galimi, M.Narita, S.W.Lowe, P.Yaswen, and J.Campisi, Reversal of human cellular senescence: roles of the p53 and p16 pathways, *EMBO J.* 22 (2003) 4212.
 181. L.W.Elmore, X.Di, C.Dumur, S.E.Holt, and D.A.Gewirtz, Evasion of a single-step, chemotherapy-induced senescence in breast cancer cells: implications for treatment response, *Clin. Cancer Res.* 11 (2005) 2637.
 182. P.E.Puig, M.N.Guilly, A.Bouchot, N.Droin, D.Cathelin, F.Bouyer, L.Favier, F.Ghiringhelli, G.Kroemer, E.Solary, F.Martin, and B.Chauffert, Tumor cells can escape DNA-damaging cisplatin through DNA endoreduplication and reversible polyploidy, *Cell Biol. Int* 32 (2008) 1031.
 183. F.W.van Leeuwen, T.Buckle, A.Kersbergen, S.Rottenberg, and K.G.Gilhuijs, Noninvasive functional imaging of P-glycoprotein-mediated doxorubicin resistance in a mouse model of hereditary breast cancer to predict response, and assign Pgp inhibitor sensitivity, *Eur. J. Nucl. Med. Mol. Imaging* 36 (2009) 406.
 184. M.Pajic, J.K.Iyer, A.Kersbergen, E.van der Burg, A.O.H.Nygren, J.Jonkers, P.Borst, and S.Rottenberg, A moderate increase in *Mdr1a/1b* expression causes *in vivo* resistance to doxorubicin in a mouse model for hereditary breast cancer, *Cancer Research*, in press (2009).
 185. L.O'Driscoll and M.Clynes, Biomarkers and multiple drug resistance in breast cancer, *Curr. Cancer Drug Targets* 6 (2006) 365.
 186. I.F.Faneyte, P.M.Kristel, and M.J.Van De Vijver, Determining MDR1/P-glycoprotein expression in breast cancer, *Int J. Cancer* 93 (2001) 114.
 187. B.J.Trock, F.Leonessa, and R.Clarke, Multidrug resistance in breast cancer: a meta-analysis of MDR1/gp170 expression and its possible functional significance, *J. Natl. Cancer Inst.* 89 (1997) 917.
 188. M.Rudas, M.Filipits, S.Taucher, T.Stranzl, G.G.Steger, R.Jakesz, R.Pirker, and G.Pohl, Expression of MRP1, LRP and Pgp in breast carcinoma patients treated with preoperative chemotherapy, *Breast Cancer Res. Treat.* 81 (2003) 149.
 189. S.C.Linn, H.M.Pinedo, J.Ark-Otte, P.van der Valk, K.Hoekman, A.H.Honkoop, J.B.Vermorken, and G.Giaccone, Expression of drug resistance proteins in breast cancer, in relation to chemotherapy, *Int J. Cancer* 71 (1997) 787.
 190. M.Filipits, G.Pohl, M.Rudas, O.Dietze, S.Lax, R.Grill, R.Pirker, C.C.Zielinski, H.Hausmaninger, E.Kubista, H.Samonigg, and R.Jakesz, Clinical role of multidrug resistance protein 1 expression in chemotherapy resistance in early-stage breast cancer: the Austrian Breast and Colorectal Cancer Study Group, *J. Clin. Oncol.* 23 (2005) 1161.
 191. L.A.Doyle, W.Yang, L.V.Abruzzo, T.Krogmann, Y.Gao, A.K.Rishi, and D.D.Ross, A multidrug resistance transporter from human MCF-7 breast cancer cells, *Proc. Natl. Acad. Sci. U S A* 95 (1998) 15665.

192. Y.Honjo, C.A.Hrycyna, Q.W.Yan, W.Y.Medina-Perez, R.W.Robey, A.van de Laar, T.Litman, M.Dean, and S.E.Bates, Acquired mutations in the MXR/BCRP/ABCP gene alter substrate specificity in MXR/BCRP/ABCP-overexpressing cells, *Cancer Res.* 61 (2001) 6635.
193. P.Borst and R.Oude Elferink, Mammalian ABC transporters in health and disease, *Annu Rev Biochem* 71 (2002) 537.
194. E.Hopper-Borge, X.Xu, T.Shen, Z.Shi, Z.S.Chen, and G.D.Kruh, Human multidrug resistance protein 7 (ABCC10) is a resistance factor for nucleoside analogues and epothilone B, *Cancer Res.* 69 (2009) 178.
195. S.L.Edwards, R.Brough, C.J.Lord, R.Natrajan, R.Vatcheva, D.A.Levine, J.Boyd, J.S.Reis-Filho, and A.Ashworth, Resistance to therapy caused by intragenic deletion in BRCA2, *Nature* 451 (2008) 1111.
196. W.Sakai, E.M.Swisher, B.Y.Karlan, M.K.Agarwal, J.Higgins, C.Friedman, E.Villegas, C.Jacquemont, D.J.Farrugia, F.J.Couch, N.Urban, and T.Taniguchi, Secondary mutations as a mechanism of cisplatin resistance in BRCA2-mutated cancers, *Nature* 451 (2008) 1116.
197. E.M.Swisher, W.Sakai, B.Y.Karlan, K.Wurz, N.Urban, and T.Taniguchi, Secondary BRCA1 mutations in BRCA1-mutated ovarian carcinomas with platinum resistance, *Cancer Res.* 68 (2008) 2581.
198. Q.Waisfisz, N.V.Morgan, M.Savino, J.P.de Winter, C.G.van Berkel, M.E.Hoatlin, L.Ianzano, R.A.Gibson, F.Arwert, A.Savoia, C.G.Mathew, J.C.Pronk, and H.Joenje, Spontaneous functional correction of homozygous fanconi anaemia alleles reveals novel mechanistic basis for reverse mosaicism, *Nat. Genet.* 22 (1999) 379.
199. H.Ikeda, M.Matsushita, Q.Waisfisz, A.Kinoshita, A.B.Oostra, A.W.Nieuwint, J.P.de Winter, M.E.Hoatlin, Y.Kawai, M.S.Sasaki, A.D.D'Andrea, Y.Kawakami, and H.Joenje, Genetic reversion in an acute myelogenous leukemia cell line from a Fanconi anemia patient with biallelic mutations in BRCA2, *Cancer Res* 63 (2003) 2688.
200. B.Xia, J.C.Dorsman, N.Ameziane, Y.de Vries, M.A.Rooimans, Q.Sheng, G.Pals, A.Errami, E.Gluckman, J.Llera, W.Wang, D.M.Livingston, H.Joenje, and J.P.de Winter, Fanconi anemia is associated with a defect in the BRCA2 partner PALB2, *Nat. Genet.* 39 (2007) 159.
201. P.Borst, S.Rottenberg, and J.Jonkers, How do real tumors become resistant to cisplatin?, *Cell Cycle* 7 (2008) 1353.
202. A.Chetrit, G.Hirsh-Yechezkel, Y.Ben David, F.Lubin, E.Friedman, and S.Sadetzki, Effect of BRCA1/2 mutations on long-term survival of patients with invasive ovarian cancer: the national Israeli study of ovarian cancer, *J Clin Oncol* 26 (2008) 20.
203. Y.Ben David, A.Chetrit, G.Hirsh-Yechezkel, E.Friedman, B.D.Beck, U.Beller, G.Ben Baruch, A.Fishman, H.Levavi, F.Lubin, J.Menczer, B.Piura, J.P.Struewing, and B.Modan, Effect of BRCA mutations on the length of survival in epithelial ovarian tumors, *J. Clin. Oncol.* 20 (2002) 463.
204. T.Reya, S.J.Morrison, M.F.Clarke, and I.L.Weissman, Stem cells, cancer, and cancer stem cells, *Nature* 414 (2001) 105.
205. D.M.Berman, S.S.Karhadkar, A.Maitra, R.Montes De Oca, M.R.Gerstenblith, K.Briggs, A.R.Parker, Y.Shimada, J.R.Eshleman, D.N.Watkins, and P.A.Beachy, Widespread requirement for Hedgehog ligand stimulation in growth of digestive tract tumours, *Nature* 425 (2003) 846.
206. S.S.Karhadkar, G.S.Bova, N.Abdallah, S.Dhara, D.Gardner, A.Maitra, J.T.Isaacs, D.M.Berman, and P.A.Beachy, Hedgehog signalling in prostate regeneration, neoplasia and metastasis, *Nature* 431 (2004) 707.
207. D.N.Watkins, D.M.Berman, S.G.Burkholder, B.Wang, P.A.Beachy, and S.B.Baylin, Hedgehog signalling within airway epithelial progenitors and in small-cell lung cancer, *Nature* 422 (2003) 313.
208. A.E.Bale and K.P.Yu, The hedgehog pathway and basal cell carcinomas, *Hum. Mol Genet.* 10 (2001) 757.
209. M.R.Gailani, M.Stahle-Backdahl, D.J.Leffell, M.Glynn, P.G.Zaphiropoulos, C.Pressman, A.B.Unden, M.Dean, D.E.Brash, A.E.Bale, and R.Toftgard, The role of the human homologue of *Drosophila* patched in sporadic basal cell carcinomas, *Nat. Genet.* 14 (1996) 78.
210. R.L.Yauch, S.E.Gould, S.J.Scales, T.Tang, H.Tian, C.P.Ahn, D.Marshall, L.Fu, T.Januario, D.Kallop, M.Nannini-Pepe, K.Kotkow, J.C.Marsters, L.L.Rubin, and F.J.de Sauvage, A paracrine requirement for hedgehog signalling in cancer, *Nature* 455 (2008) 406.

211. J.K.Chen, J.Taipale, M.K.Cooper, and P.A.Beachy, Inhibition of Hedgehog signaling by direct binding of cyclopamine to Smoothened, *Genes Dev.* 16 (2002) 2743.
212. T.Byun, M.Karimi, J.L.Marsh, T.Milovanovic, F.Lin, and R.F.Holcombe, Expression of secreted Wnt antagonists in gastrointestinal tissues: potential role in stem cell homeostasis, *J Clin Pathol.* 58 (2005) 515.
213. K.A.Moore, Recent advances in defining the hematopoietic stem cell niche, *Curr. Opin. Hematol.* 11 (2004) 107.
214. T.Reya and H.Clevers, Wnt signalling in stem cells and cancer, *Nature* 434 (2005) 843.
215. M.Ilyas, Wnt signalling and the mechanistic basis of tumour development, *J Pathol.* 205 (2005) 130.
216. N.Barker, R.A.Ridgway, J.H.van Es, M.van de Wetering, H.Begthel, M.van den Born, E.Danenbergh, A.R.Clarke, O.J.Sansom, and H.Clevers, Crypt stem cells as the cells-of-origin of intestinal cancer, *Nature* 457 (2009) 608.
217. N.Barker and H.Clevers, Mining the Wnt pathway for cancer therapeutics, *Nat. Rev. Drug Discov.* 5 (2006) 997.
218. X.Fan, W.Matsui, L.Khaki, D.Stearns, J.Chun, Y.M.Li, and C.G.Eberhart, Notch pathway inhibition depletes stem-like cells and blocks engraftment in embryonal brain tumors, *Cancer Res* 66 (2006) 7445.
219. S.Pece, M.Serresi, E.Santolini, M.Capra, E.Hulleman, V.Galimberti, S.Zurrida, P.Maisonneuve, G.Viale, and P.P.Di Fiore, Loss of negative regulation by Numb over Notch is relevant to human breast carcinogenesis, *J Cell Biol* 167 (2004) 215.
220. S.Weijzen, P.Rizzo, M.Braid, R.Vaishnav, S.M.Jonkheer, A.Zlobin, B.A.Osborne, S.Gottipati, J.C.Aster, W.C.Hahn, M.Rudolf, K.Siziopikou, W.M.Kast, and L.Miele, Activation of Notch-1 signaling maintains the neoplastic phenotype in human Ras-transformed cells, *Nat. Med* 8 (2002) 979.
221. J.H.van Es, M.E.van Gijn, O.Riccio, M.van den Born, M.Vooijs, H.Begthel, M.Cozijnsen, S.Robine, D.J.Winton, F.Radtke, and H.Clevers, Notch/gamma-secretase inhibition turns proliferative cells in intestinal crypts and adenomas into goblet cells, *Nature* 435 (2005) 959.
222. G.Szakacs, J.K.Paterson, J.A.Ludwig, C.Booth-Genthe, and M.M.Gottesman, Targeting multidrug resistance in cancer, *Nat Rev Drug Discov* 5 (2006) 219.
223. M.Raderer and W.Scheithauer, Clinical trials of agents that reverse multidrug resistance. A literature review, *Cancer* 72 (1993) 3553.
224. C.Wandel, R.B.Kim, S.Kajiji, P.Guengerich, G.R.Wilkinson, and A.J.Wood, P-glycoprotein and cytochrome P-450 3A inhibition: dissociation of inhibitory potencies, *Cancer Res.* 59 (1999) 3944.
225. S.Bates, Solving the Problem of Multidrug Resistance: ABC Transporters in Clinical Oncology., in: I.B.Holland, S.P.C.Cole, K.Kuchler, and C.F.Higgins (Eds.), *ABC Proteins: From Bacteria to Man*, Academic Press, London, 2002, pp.359-391.
226. P.Mistry, A.J.Stewart, W.Dangerfield, S.Okiji, C.Liddle, D.Bootle, J.A.Plumb, D.Templeton, and P.Charlton, In vitro and in vivo reversal of P-glycoprotein-mediated multidrug resistance by a novel potent modulator, XR9576, *Cancer Res.* 61 (2001) 749.
227. F.Hyafil, C.Vergely, P.Du Vignaud, and T.Grand-Perret, In vitro and in vivo reversal of multidrug resistance by GF120918, an acridonecarboxamide derivative, *Cancer Res.* 53 (1993) 4595.
228. R.L.Shepard, J.Cao, J.J.Starling, and A.H.Dantzig, Modulation of P-glycoprotein but not, *Int J. Cancer* 103 (2003) 121.
229. E.Fox and S.E.Bates, Tariquidar (XR9576): a P-glycoprotein drug efflux pump inhibitor, *Expert Rev. Anti-cancer Ther.* 7 (2007) 447.
230. L.H.Le, M.J.Moore, L.L.Siu, A.M.Oza, M.MacLean, B.Fisher, A.Chaudhary, D.P.de Alwis, C.Slapak, and L.Seymour, Phase I study of the multidrug resistance inhibitor zosuquidar administered in combination with vinorelbine in patients with advanced solid tumours, *Cancer Chemother. Pharmacol.* 56 (2005) 154.
231. P.M.Fracasso, L.J.Goldstein, D.P.de Alwis, J.S.Rader, M.A.Arquette, S.A.Goodner, L.P.Wright, C.L.Fears, R.J.Gazak, V.A.Andre, M.F.Burgess, C.A.Slapak, and J.H.Schellens, Phase I study of docetaxel in combination with the P-glycoprotein inhibitor, zosuquidar, in resistant malignancies, *Clin. Cancer Res.* 10 (2004) 7220.

232. A.Sandler, M.Gordon, D.P.de Alwis, I.Pouliquen, L.Green, P.Marder, A.Chaudhary, K.Fife, L.Battiato, C.Sweeney, C.Jordan, M.Burgess, and C.A.Slapak, A Phase I trial of a potent P-glycoprotein inhibitor, zosuquidar trihydrochloride (LY335979), administered intravenously in combination with doxorubicin in patients with advanced malignancy, *Clin. Cancer Res.* 10 (2004) 3265.
233. A.S.Planting, P.Sonneveld, A.van der Gaast, A.Sparreboom, M.E.van der Burg, G.P.Luyten, K.de Leeuw, M.Boer-Dennert, P.S.Wissel, R.C.Jewell, E.M.Paul, N.B.Purvis, Jr., and J.Verweij, A phase I and pharmacologic study of the MDR converter GF120918 in combination with doxorubicin in patients with advanced solid tumors, *Cancer Chemother. Pharmacol.* 55 (2005) 91.
234. P.Ruff, D.A.Vorobiof, J.P.Jordaan, G.S.Demetriou, S.D.Moodley, A.L.Nosworthy, I.D.Werner, J.Raats, and L.J.Burgess, A randomized, placebo-controlled, double-blind phase 2 study of docetaxel compared to docetaxel plus zosuquidar (LY335979) in women with metastatic or locally recurrent breast cancer who have received one prior chemotherapy regimen, *Cancer Chemother. Pharmacol.* (2009).
235. L.Pusztai, P.Wagner, N.Ibrahim, E.Rivera, R.Theriault, D.Booser, F.W.Symmans, F.Wong, G.Blumenschein, D.R.Fleming, R.Rouzier, G.Boniface, and G.N.Hortobagyi, Phase II study of tariquidar, a selective P-glycoprotein inhibitor, in patients with chemotherapy-resistant, advanced breast carcinoma, *Cancer* 104 (2005) 682.
236. A.H.Schinkel, U.Mayer, E.Wagenaar, C.A.Mol, L.van Deemter, J.J.Smit, M.A.Van Der Valk, A.C.Voordouw, H.Spits, O.van Tellingen, J.M.Zijlmans, W.E.Fibbe, and P.Borst, Normal viability and altered pharmacokinetics in mice lacking *mdr1*-type (drug-transporting) P-glycoproteins, *Proc. Natl. Acad. Sci. U S A* 94 (1997) 4028.
237. J.W.Jonker, M.Buitelaar, E.Wagenaar, M.A.Van Der Valk, G.L.Scheffer, R.J.Scheper, T.Plosch, F.Kuipers, R.P.Elferink, H.Rosing, J.H.Beijnen, and A.H.Schinkel, The breast cancer resistance protein protects against a major chlorophyll-derived dietary phototoxin and protoporphyria, *Proc. Natl. Acad. Sci. U S A* 99 (2002) 15649.
238. L.D.Miller, J.Smeds, J.George, V.B.Vega, L.Vergara, A.Ploner, Y.Pawitan, P.Hall, S.Klaar, E.T.Liu, and J.Bergh, An expression signature for p53 status in human breast cancer predicts mutation status, transcriptional effects, and patient survival, *Proc. Natl Acad. Sci. U. S. A* 102 (2005) 13550.
239. L.J.van 't Veer, H.Dai, M.J.Van De Vijver, Y.D.He, A.A.Hart, M.Mao, H.L.Peterse, K.van der Kooy, M.J.Marton, A.T.Witteveen, G.J.Schreiber, R.M.Kerkhoven, C.Roberts, P.S.Linsley, R.Bernards, and S.H.Friend, Gene expression profiling predicts clinical outcome of breast cancer, *Nature* 415 (2002) 530.
240. S.A.Joose, E.H.van Beers, I.H.Tielen, H.Horlings, J.L.Peterse, N.Hoogerbrugge, M.J.Ligtenberg, L.F.Wessels, P.Axwijk, S.Verhoef, F.B.Hogervorst, and P.M.Nederlof, Prediction of BRCA1-association in hereditary non-BRCA1/2 breast carcinomas with array-CGH, *Breast Cancer Res. Treat.* (2008).
241. D.M.Weinstock, K.Nakanishi, H.R.Helgadottir, and M.Jasin, Assaying double-strand break repair pathway choice in mammalian cells using a targeted endonuclease or the RAG recombinase, *Methods Enzymol.* 409 (2006) 524.
242. P.J.Campbell, P.J.Stephens, E.D.Pleasance, S.O'Meara, H.Li, T.Santarius, L.A.Stebbins, C.Leroy, S.Edkins, C.Hardy, J.W.Teague, A.Menzies, I.Goodhead, D.J.Turner, C.M.Clee, M.A.Quail, A.Cox, C.Brown, R.Durbin, M.E.Hurles, P.A.Edwards, G.R.Bignell, M.R.Stratton, and P.A.Futreal, Identification of somatically acquired rearrangements in cancer using genome-wide massively parallel paired-end sequencing, *Nat. Genet.* 40 (2008) 722.

CHAPTER 2



High sensitivity of BRCA1-deficient mammary tumors to the PARP inhibitor AZD2281 alone and in combination with platinum drugs

Sven Rottenberg¹, Janneke E. Jaspers¹, Ariena Kersbergen¹, Eline van der Burg¹, Anders O.H. Nygren²,
Serge A.L. Zander¹, Patrick W.B. Derksen^{1,a}, Michiel de Bruin¹, John Zevenhoven³, Alan Lau⁴,
Robert Boulter⁴, Aaron Cranston⁴, Mark J. O'Connor⁴, Niall M.B. Martin⁴, Piet Borst¹, Jos Jonkers¹

¹ Divisions of Molecular Biology and ³ Molecular Genetics, Netherlands Cancer Institute, Plesmanlaan
121, 1066 CX Amsterdam, The Netherlands; ² MRC-Holland, Willem Schoutenstraat 6, 1057 DN
Amsterdam, The Netherlands; ⁴ KuDOS Pharmaceuticals, Ltd., 410 Cambridge Science Park, Milton
Road, Cambridge, CB4 0PE, United Kingdom

Proceedings of the National Academy of Sciences 2008, 105(44):17079-84

ABSTRACT

Whereas target-specific drugs are available for treating ERBB2-overexpressing and hormone receptor-positive breast cancers, no tailored therapy exists for hormone receptor- and ERBB2-negative (“triple-negative”) mammary carcinomas. Triple-negative tumors account for 15% of all breast cancers, and frequently harbor defects in DNA double-strand break repair through homologous recombination (HR), such as BRCA1 dysfunction. The DNA-repair defects characteristic of BRCA1-deficient cells confer sensitivity to poly(ADP-ribose) polymerase 1 (PARP1) inhibition, which could be relevant to treatment of triple-negative tumors. To evaluate PARP1 inhibition in a realistic *in vivo* setting, we tested the PARP inhibitor AZD2281 in a genetically engineered mouse model (GEMM) for BRCA1-associated breast cancer. Treatment of tumor-bearing mice with AZD2281 inhibited tumor growth without signs of toxicity, resulting in strongly increased survival. Long-term treatment with AZD2281 in this model did result in the development of drug resistance, caused by up-regulation of *Abcb1a/b* genes encoding P-glycoprotein efflux pumps. This resistance to AZD2281 could be reversed by co-administration of the P-glycoprotein inhibitor tariquidar. Combination of AZD2281 with cisplatin or carboplatin increased the recurrence-free and overall survival, suggesting that AZD2281 potentiates the effect of these DNA-damaging agents. Our results demonstrate *in vivo* efficacy of AZD2281 against BRCA1-deficient breast cancer, and illustrate how GEMMs of cancer can be used for preclinical evaluation of novel therapeutics and for testing ways to overcome or circumvent therapy resistance.

INTRODUCTION

Poly(ADP-ribose) polymerase 1 (PARP1) is involved in surveillance and maintenance of genome integrity and functions as a key molecule in the repair of DNA single-strand breaks (SSBs)¹⁻³. Inactivation of SSB repair by PARP1 inhibition during S-phase induces DNA double-strand breaks (DSBs), and may thus confer synthetic lethality to cells with defective homology-directed DSB repair⁴⁻⁵. Mutations in *BRCA1* or *BRCA2* predispose to hereditary breast and ovarian cancer, which accounts for 3-5% of all breast cancers and a greater proportion of ovarian cancers⁶. *BRCA1* and *BRCA2* function are critical for homologous recombination (HR)⁶⁻⁷, and *BRCA*-deficient cells appear to be highly sensitive to PARP inhibition, resulting in increased genomic instability, cell cycle arrest and apoptosis⁴⁻⁵. PARP1 inhibition might, therefore, be a specific therapy for cancers with defects in *BRCA1/2* or other HR pathway components (clinically relevant PARP inhibitors are reviewed in ref. 8). Recently, Donawho *et al.*⁹ have reported that the PARP inhibitor ABT-888 in combination with platinum drugs or cyclophosphamide, but not alone, causes regression of *BRCA1*-deficient MX-1 xenografts. However, this study uses only a single *BRCA1*-mutated tumor line without isogenic controls to address the impact of *BRCA1* mutation on response to PARP inhibition. In addition, xenografts in immunodeficient mice do not sufficiently mimic the tumor-host interactions of real breast cancers in women¹⁰. To assess the therapeutic potential of PARP1 inhibition in a more realistic *in vivo* model, we tested the PARP inhibitor AZD2281¹¹ in our *K14cre;Brca1^{F/F};p53^{F/F}* mouse model for hereditary breast cancer. The *Brca1^{-/-};p53^{-/-}* mammary adenocarcinomas arising in this model recapitulate several key features of human *BRCA1*-associated breast cancer, including a basal-like phenotype, lack of ER-, PR- and ERBB2-expression and a high degree of genomic instability¹², and may therefore be a good predictor for clinical responses of *BRCA1*-deficient cancers to AZD2281.

RESULTS

***Brca1^{-/-};p53^{-/-}* mammary tumors respond to the PARP inhibitor AZD2281**

An important feature of the spontaneous *Brca1^{-/-};p53^{-/-}* mammary tumors in the *K14cre;Brca1^{F/F};p53^{F/F}* mouse model is that they can be transplanted orthotopically into wild-type female mice without losing their basal-like phenotype, their gene expression profile or their sensitivity to anti-cancer agents¹³. Figure 1 illustrates how this orthotopic transplantation system was used to test various treatment regimens of AZD2281 as single agent or in combination therapy on genetically identical tumors. We first determined the PARP inhibitory dose of AZD2281 in tumor-bearing mice.

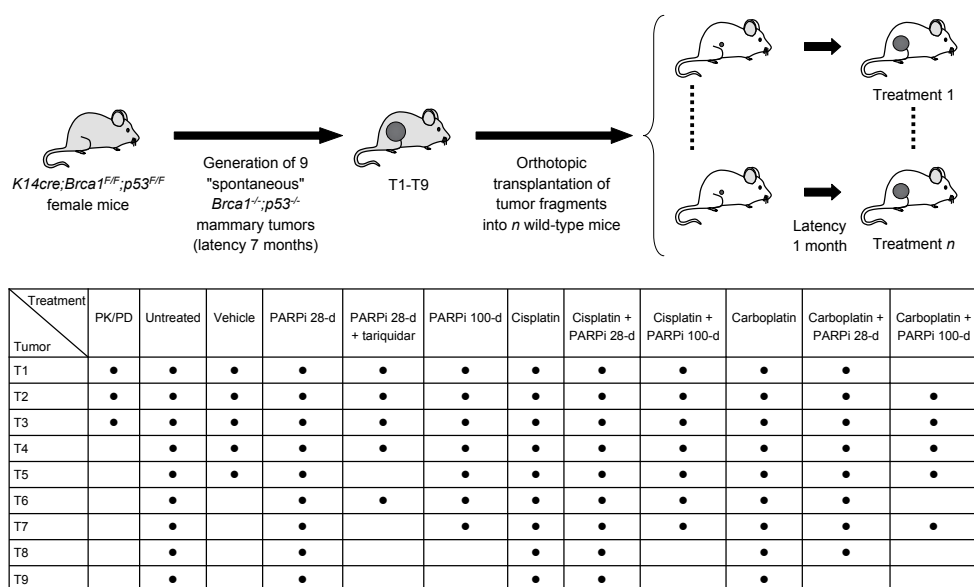


Figure 1. Overview of tumor transplantations and drug treatments in this study. Small tumor fragments of 9 spontaneous mammary tumors (T1-T9), which developed in *K14cre;Brca1^{F/F};p53^{F/F}* mice¹² were transplanted orthotopically into syngeneic wild-type female mice. After a mean latency of ≈ 4 weeks, when tumors reached a size of 150-250 mm³ ($V = \text{length} \times \text{width}^2 \times 0.5$), the indicated drug treatments were carried out. Dosing was as follows: 50 mg of AZD2281 per kg i.p. daily for 28 days (28-d) or daily for 100 days (100-d), 6 mg cisplatin per kg i.v. on day 0 (30 min after the first AZD2281 injection), 100 mg carboplatin per kg i.v. on day 0 (30 min after the first AZD2281 injection), 2 mg tariquidar per kg every other day (if combined with AZD2281, tariquidar was given 30 min in advance). Treatment of tumors was resumed once the tumor relapsed to its original size (100 %).

As shown in Figure 2A, AZD2281 given at 50 mg/kg per day is rapidly taken up by the tumor, but is also quickly cleared. However, compared with the plasma concentration (data not shown), the intratumoral levels of AZD2281 were ≈ 2 -fold and 6- to 8-fold higher at 2 and 6 h after injection, respectively, suggesting tumor loading of AZD2281. Importantly, we observed a reduction of the intratumoral PARP1 activity to ≈ 25 % of pre-dose levels 30 min after treatment, which returned back to 77 % after 24 h (Figure 2A).

Next, we treated animals harboring 9 individual *Brca1^{-/-};p53^{-/-}* tumors (T1-T9) with AZD2281 (50 mg/kg i.p. per day) for 28 consecutive days once the tumor volume was between 150 and 250 mm³ (Figure 2C). Compared with untreated (Figure 2B) and vehicle-treated controls (Supplementary Figure S1), all tumors responded to AZD2281. After a lag time of ≈ 5 days, T1-T7 stopped growing and showed a substantial shrinkage ranging from non-palpable to a nodule of ≈ 40 % of the initial size. As additional control for the selective targeting of HR-deficient cells by AZD2281, we treated 5 individual *Ecad^{-/-};p53^{-/-}* tumors from a mouse model for pleomorphic invasive lobular carcinoma (ref. 14 and P.W.B.D. and J.J., unpublished results). None of these HR-proficient tumors responded to AZD2281

(Supplementary Figure S2). The lag phase we observed in *Brca1*^{-/-};*p53*^{-/-} tumors might be explained by the fact that PARP1 inhibition is not cytotoxic by itself, but acts by forcing BRCA1-deficient cells to employ error-prone repair pathways which eventually result in cell death⁵. This notion is supported by our finding that DNA damage-associated γ H2AX foci and cleaved caspase 3-positive cells are significantly increased after 7 days of daily AZD2281 treatment compared with untreated *Brca1*^{-/-};*p53*^{-/-} tumors or AZD2281-treated HR-proficient *Ecad*^{-/-};*p53*^{-/-} mammary tumors (Figure 3 and Supplementary Table S1). After withdrawal of treatment, tumors began to grow again with various lag times (Figure 2C) and when tumors reached 100% of the original volume at the time of treatment initiation, a second course of AZD2281 (50 mg/kg i.p. per day x28) was administered. The relapsing tumors, however, did not respond to AZD2281 treatment at this point and lacked the increased numbers of γ H2AX and cleaved caspase 3-positive cells detected during the first course of AZD2281 administration (Figure 3).

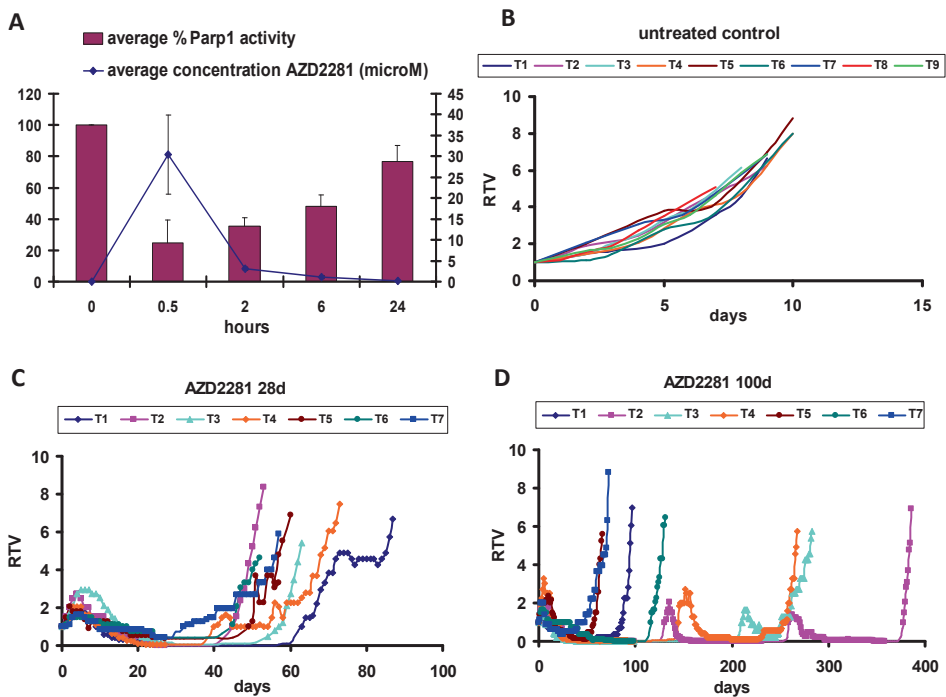


Figure 2. Treatment of mice carrying orthotopically transplanted *Brca1*^{-/-};*p53*^{-/-} tumors with 50 mg AZD2281 per kg i.p. **A**, Intratumoral concentration of AZD2281 and PARP1 activity over time. Error bars indicate SEM. **B-D**, Animals carrying 9 individually transplanted tumors (T1-T9) were either left untreated, or received AZD2281 daily for 28 days or 100 days. Graphs show relative tumor volume (RTV, ratio of tumor volume to initial size at start of treatment) as a function of time. T8 and T9 showed stable disease and received continuous dosing beyond the 28 days (see Supplementary Figure S1). Once the tumors relapsed, treatment was resumed when the tumor size reached 100 % of the original volume. Days on which AZD2281 was given are indicated by circles, triangles or squares.

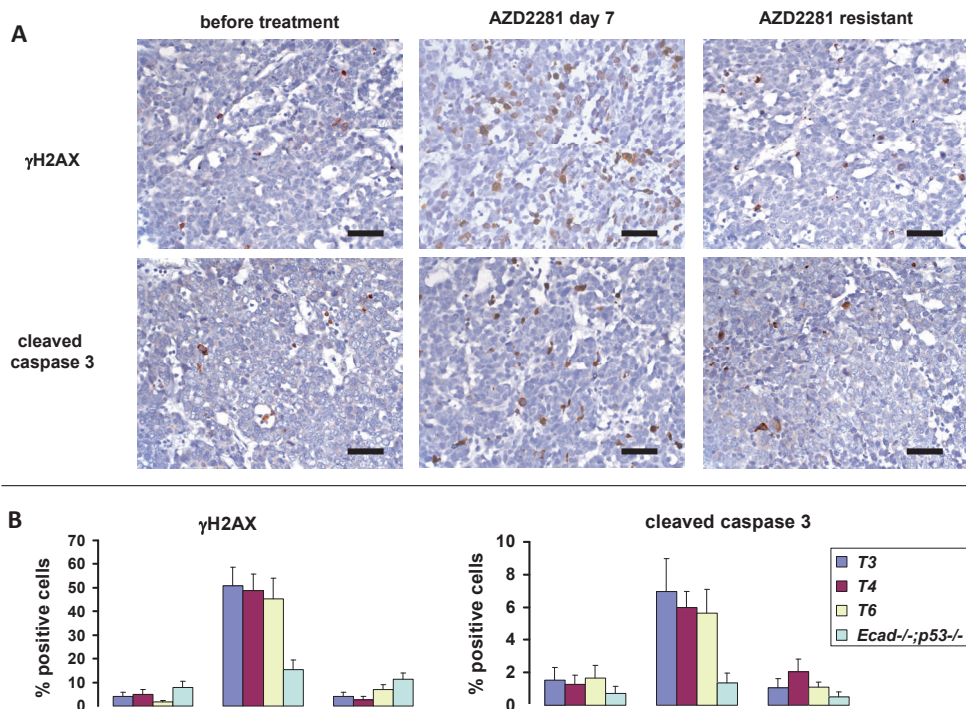


Figure 3. AZD2281 treatment induces DNA damage-associated foci and caspase 3-mediated apoptosis. **A**, Example of the IHC analysis of T4 using anti-activated caspase 3 and anti-γH2AX-specific antibodies. Sections of the sensitive tumor (before or 7 days after daily injection of 50 mg AZD2281 per kg i.p.) and resistant tumor (day 73 after unsuccessful daily treatment of the relapsing tumor, see Figure 2C) are shown. Bar = 50 μm. **B**, Quantification of γH2AX or cleaved caspase 3-positive cells of 3 individual *Brca1*^{-/-};*p53*^{-/-} tumors (T3, T4, T6) and *Ecad*^{-/-};*p53*^{-/-} tumor 1 before, 7 days after daily AZD2281 treatment, or of the outgrown AZD2281-resistant tumor (see Figure 2C and Supplementary Figure S2). For *P* values see Supplementary Table S1.

Prolonged AZD2281 treatment increases the overall survival without obvious signs of toxicity

In the two cases where mice engrafted with tumors (T8 and T9) exhibited stable disease, continuous dosing beyond the 28 days was carried out with AZD2281 (Supplementary Figure S1). Eventually, these tumors also failed to respond to AZD2281. Importantly, continuous treatment for 58d (T8) and 156d (T9) did not result in any obvious signs of toxicity such as weight loss, apathy, or pathological abnormalities at necropsy. Therefore, in an attempt to eradicate *Brca1*^{-/-};*p53*^{-/-} tumors, we repeated the experiments with tumors T1-T7 but extended AZD2281 treatment to 100 days (Figure 2D). Again, all tumors shrunk to small or non-palpable remnants. For tumors T1, T5 and T7, resistance was acquired during treatment, whereas T6 relapsed to 100 % of the pretreatment volume on day 116 without responding to a second course of AZD2281. Notably, relapsed tumors T2, T3 and T4 were sensitive to

the resumption of AZD2281 administration, but developed resistance during the second (T3 and T4) or third 100-day cycle of AZD2281 (T2). Hence, compared with the 28-day dosing schedule the 100-day schedule significantly increased the median survival of the mice from 60 to 131 days (Figure 5B). Also in animals undergoing extended AZD2281 treatment, no signs of toxicity were observed.

AZD2281 resistance is frequently caused by increased expression of *Abcb1a/b*

To investigate mechanisms of acquired resistance to AZD2281, which arose in all tumors investigated, we analyzed the expression levels of several drug efflux transporter genes in addition to the drug target gene *Parp1* in AZD2281-sensitive tumors and their AZD2281-resistant counterparts using reverse transcriptase-multiplex ligation-dependent probe amplification (RT-MLPA; Figure 4A and Supplementary Table S2). Most strikingly, the expression of the drug efflux transporters *Abcb1a* or *Abcb1b*¹⁵, which encode the murine P-glycoproteins, was increased by 2- to 85-fold in 11 of 15 AZD2281-resistant tumors. Approximately a 2.5-fold increased expression of *Abcg2* (*Bcrp1*)¹⁶ was observed in 3 tumors (T2-28, T3-100 and T6-100), while no change in the *Abcc1* or *Hprt1* expression was detected. Up-regulation of the drug target *Parp1* was found in tumors T6-28 (2.7-fold) and T6-100 (4.2-fold).

Because acquired doxorubicin resistance in the *K14cre;Brca1^{F/F};p53^{F/F}* model is frequently caused by increased *Abcb1a* and *Abcb1b* expression¹³, we studied the effects of AZD2281 on doxorubicin-resistant tumors with or without increased *Abcb1a/b* expression (Figure 4B). Of 3 doxorubicin-resistant tumors analyzed, only those with increased *Abcb1a/b* expression showed primary resistance to AZD2281. The doxorubicin-resistant tumor without altered drug transporter expression responded initially to drug, but eventually developed AZD2281 resistance, which was characterized by a 3.6-fold increase in *Abcb1b* expression. To test whether acquired AZD2281 resistance could be reversed by blocking drug transporter activity, we combined AZD2281 treatment with the specific third-generation P-glycoprotein (Pgp) inhibitor tariquidar (XR9576)¹⁷. For this purpose, tumors T1-T4 and T6 were first treated with AZD2281 for 28 days, resulting in complete regression (Figure 4C). When tumors relapsed following the withdrawal of the PARP inhibitor, tariquidar was applied alone or in combination with a second cycle of AZD2281. In contrast to relapsed tumors T1-T3 and T6 treated with AZD2281 alone, tumor recurrences again became sensitive to AZD2281 by concurrent inhibition of Pgp using tariquidar. T4 showed stable disease, suggesting that other mechanisms of resistance may also evolve. Such mechanisms might explain AZD2281 resistance of T1-100, T5-28 and T4-28, which do not show marked up-regulation of drug transporter gene expression. Of note, T6 (showing marked up-regulation of *Abcb1b*) responded to Pgp inhibition using tariquidar despite an increased mRNA expression of the drug target *Parp1*, indicating that AZD2281 resistance in this tumor is primarily caused by Pgp overexpression.

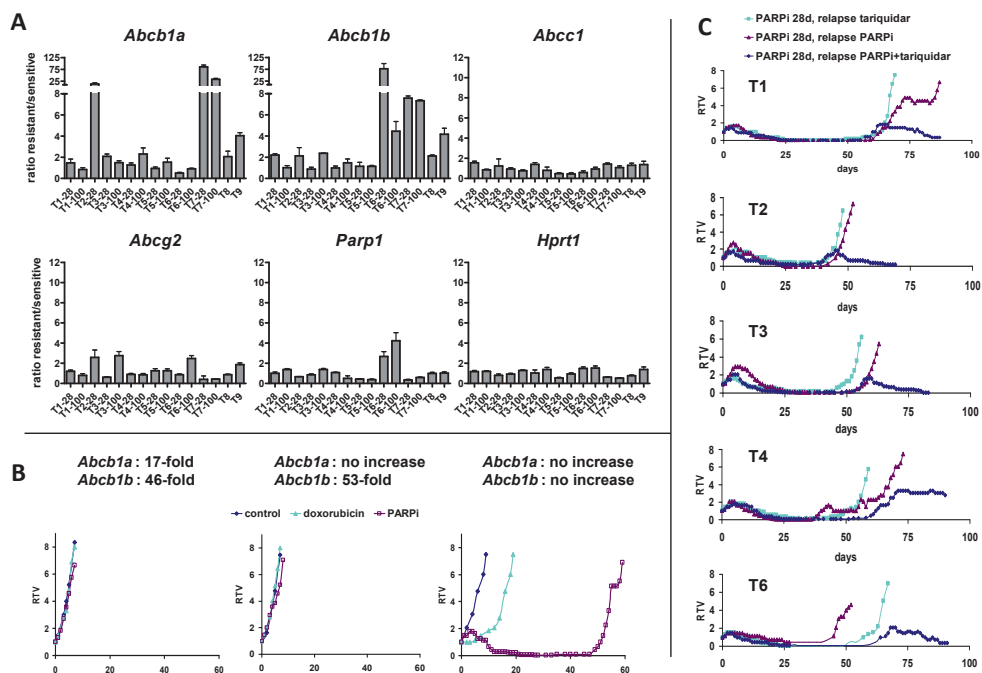


Figure 4. Increased expression of *Abcb1a* and *Abcb1b* is associated with AZD2281 resistance *in vivo*. **A**, RT-MLPA analysis of the ratios of *Abcb1a*, *Abcb1b*, *Abcc1*, *Abcg2*, *Parp1* and *Hprt1* expression in AZD2281-resistant tumors and samples from the corresponding untreated tumors. *Actin- β* expression was used as internal reference. The values presented are the mean ratio of 3 independent reactions. The suffix 28 indicates the 28-day schedule of AZD2281 and 100 the 100-day schedule. Error bars indicate standard deviation. For the complete data set see Supplementary Table S2. **B**, Three *Brca1*^{-/-};*p53*^{-/-} doxorubicin-resistant tumors (2 with up-regulation of *Abcb1a/b* and 1 without; ref. ¹³) were tested for their response to AZD2281. Days on which 50 mg AZD2281 per kg were given have open squares. **C**, T1-T4 and T6 were treated with a daily injection of 50 mg AZD2281 per kg for 28 days. When tumors relapsed to 100 % of their original volume, they were retreated by i.p. injection of 2 mg of tariquidar per kg every other day (light blue line), or 50 mg AZD2281 per kg daily (red line) or both (dark blue line). Days on which animals were treated are indicated by rhombi, triangles or squares. Graphs in **B** and **C** show relative tumor volume (RTV, ratio of tumor volume to initial size at start of treatment) as a function of time.

Combination of AZD2281 with platinum drugs increases the recurrence-free and overall survival

Inhibition of PARP has also been reported to enhance the effects of DNA-damaging anti-cancer drugs such as temozolomide, platinum and cyclophosphamide in BRCA1-deficient cells⁹. Indeed, *in vitro* combination studies showed strong and selective synergy between AZD2281 and cisplatin in suppressing BRCA2-deficient mammary tumor cell growth¹⁸. From a previous study, we already know that mammary tumors in our *K14cre;Brca1^{F/F};p53^{F/F}* model are sensitive to the MTD of cisplatin and do not acquire resistance¹³. We therefore tested the combination of AZD2281 with cisplatin and carboplatin in this model according

to a defined treatment schedule (see Methods). Compared with cisplatin or carboplatin monotherapy, combination treatment with cisplatin and 28- or 100-day cycles of AZD2281 significantly prolonged both recurrence-free survival (Figure 5A and Supplementary Table S3) and overall survival (Figure 5B and Supplementary Table S4). These results indicate that AZD2281 potentiates the effect of these platinum drugs. Nevertheless, most tumors could not be eradicated with the current AZD2281-platinum combination schedules and tended to relapse (Figure 5A and Supplementary Figure S1). Moreover, we observed increased toxicity of cisplatin in combination with AZD2281. Mice tolerated an average of 6.7 cycles of cisplatin (6 mg/kg i.v., SD = 1, n = 9) before they had to be sacrificed due to accumulating nephrotoxicity. In contrast, mice tolerated only 3 cycles of cisplatin (6 mg/kg i.v. day 0) + 100 daily injections of 50 mg AZD2281 per kg (SD = 0.7, n = 5).

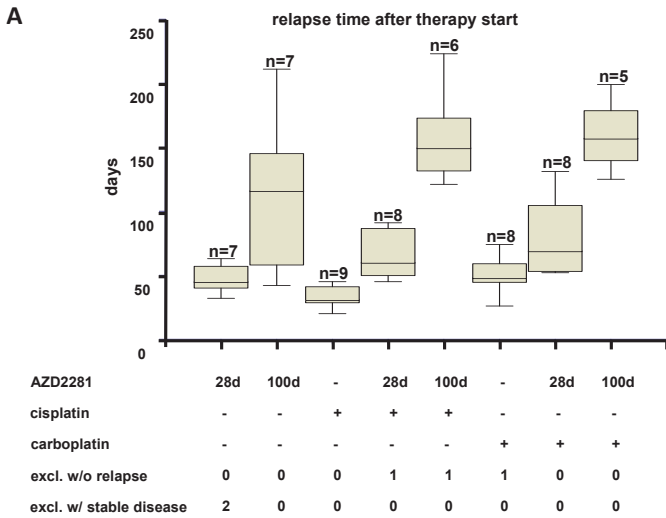
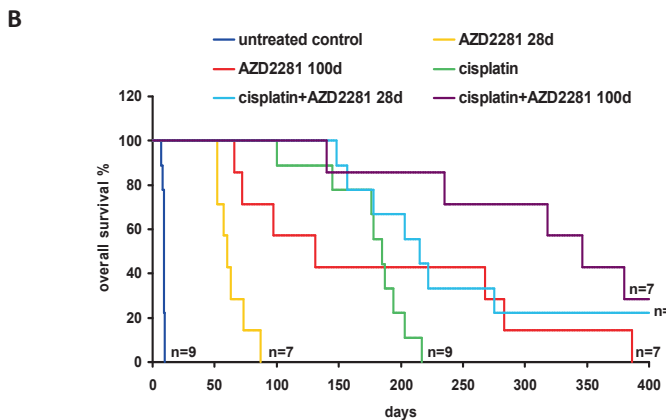


Figure 5. Combination of AZD2281 with carboplatin and cisplatin prolongs recurrence-free survival and overall survival. **A**, Box plots indicate the time after therapy start before tumors relapse back to the size when treatment was initiated. Dosing was as follows: 50 mg AZD2281 per kg i.p. daily for 28 days (28d) or daily for 100 days (100d), 6 mg cisplatin per kg i.v. on day 0 (30 min after the first AZD2281 injection), 100 mg carboplatin per kg i.v. (30 min after the first AZD2281 injection). **B**, Kaplan-Meier curves showing the overall survival after 400 days. Wilcoxon signed rank tests: control versus AZD2281-28d: $P < 0.009$ ($n = 7$); control versus AZD2281-100d: $P < 0.009$ ($n = 7$); AZD2281-28d versus AZD2281-100d: $P < 0.009$ ($n = 7$); cisplatin versus cisplatin+AZD2281-28d: $P < 0.019$ ($n = 9$); cisplatin versus cisplatin+AZD2281-100d: $P < 0.014$ ($n = 7$).



DISCUSSION

Here we show that the *K14cre;Brca1^{F/F};p53^{F/F}* mouse model is useful for preclinical evaluation of novel therapeutics, such as the clinical PARP inhibitor AZD2281. We found that BRCA1-deficient “spontaneous” mouse mammary tumors show an impressive and prolonged response to AZD2281. This is consistent with the reported hypersensitivity of BRCA1-deficient cells to PARP1 inhibition⁵. An important advantage of AZD2281 is its excellent therapeutic index. Even after prolonged daily treatment with a PARP1-inhibitory dose of AZD2281, no dose-limiting toxicity is observed in tumor-bearing mice. Because also BRCA2-deficient mouse mammary cells demonstrate selective sensitivity to AZD2281¹⁸, this PARP inhibitor may represent a promising drug against BRCA-associated breast and ovarian cancer in humans. In addition, sporadic cancers with HR pathway defects may also be expected to show selective sensitivity to AZD2281. In particular, treatment of patients with triple-negative breast cancers, which account for 15% of all breast cancers¹⁹ and frequently harbor BRCA1 pathway defects²⁰⁻²³, might be useful, because no targeted therapy exists thus far for this subgroup of breast cancers. Preliminary data from Phase I clinical trials with AZD2281 also indicate a favorable toxicity profile and objective responses in several patients with BRCA1-associated ovarian cancer²⁴. Regarding administration of AZD2281 as a single agent, our data suggest that continuous dosing of the PARP inhibitor may be more effective than intermittent treatment. Continuous AZD2281 treatment might result in increased toxicity in non-tumor cells carrying heterozygous *BRCA* mutations compared with wild-type non-tumor cells, but continuous dosing of AZD2281 in *BRCA1* mutation carriers does not suggest this to be the case²⁴.

Genetically engineered mouse models (GEMMs) of BRCA-associated breast cancer also enable preclinical evaluation of combination treatments that increase the types of DNA damage for which repair will be abrogated following PARP1 inhibition in a BRCA-deficient genetic background. A promising therapeutic strategy involves combination treatment with PARP inhibitors and platinum drugs, which induce, in addition to interstrand cross-links, intrastrand cross-links that are removed by nucleotide-excision repair (NER)²⁵. Because PARP1 might be involved in both base-excision repair (BER) and NER²⁶, synergy between PARP inhibitors and platinum drugs could be anticipated. Indeed, *in vitro* drug combination studies showed selective synergy between AZD2281 and cisplatin in BRCA2-deficient mammary tumor cell lines¹⁸. In line with this, we found that AZD2281 may enhance the efficacy of platinum drugs against BRCA1-deficient mammary tumors, suggesting this drug combination might be beneficial in the clinic. Additional preclinical studies in the *K14cre;Brca1^{F/F};p53^{F/F}* mouse model can be performed to optimize AZD2281-platinum combination therapy, *e.g.* by applying AZD2281 in combination with multiple low-dose platinum treatments or by applying triple combinations of AZD2281 with tariquidar and

platinum drugs. Repeated treatment of animals with cisplatin alone or in combination with AZD2281 resulted in accumulating nephrotoxicity. In the *K14cre;Brca1^{F/F};p53^{F/F}* mouse model different schedules of AZD2281-platinum combinations that maximize tumor cell kill without increasing toxicity can be explored.

As for all new anti-cancer agents that enter the clinic, one can expect the development of resistance to occur. Using the *K14cre;Brca1^{F/F};p53^{F/F}* mammary tumor model, we were able to model acquired resistance to AZD2281 and to investigate the mechanistic basis of this resistance²⁷. The most frequently observed mechanism of acquired resistance to AZD2281, up-regulation of Pgp, could be effectively blocked by the Pgp inhibitor tariquidar, suggesting that this might be a suitable strategy to reverse Pgp-related clinical resistance to AZD2281 should it occur. Interestingly, Pgp expression might also be directly modulated by PARP1 inhibition, as mouse embryonic fibroblasts from *Parp1^{-/-}* mice were found to have increased Pgp expression and doxorubicin resistance which could be reversed by the Pgp modulator verapamil²⁸. To identify alternative Pgp-independent resistance mechanisms, we are currently crossing the *K14cre;Brca1^{F/F};p53^{F/F}* model onto an *Abcb1a/b* null background²⁹. In human *BRCA*-mutated breast cancer, acquired resistance to AZD2281 might also be mediated by genetic reversion of the *BRCA1* or *BRCA2* mutations³⁰⁻³². This possibility can not be investigated in our current mouse model, in which *BRCA1* function is irreversibly abolished by Cre-mediated deletion of exons 5-13 (ref. ¹²), disabling the development of platinum resistance by genetic reconstitution of *BRCA1* function^{13,33}. New mouse models containing *Brca1* frame shift mutations that mimic common human *BRCA1* founder mutations are required to investigate whether such a resistance mechanism does occur *in vivo*.

Our study shows that GEMMs of human cancer may be useful not only for assessment of tumor response and toxicity, but also for modeling acquired resistance, analysis of resistance mechanisms, and evaluation of reversal strategies or second-generation drugs in resistant tumors. Hence, intervention studies in GEMMs may help to predict the basis of resistance to novel therapeutics well in advance of the human experience, thereby providing the possibility to more adequately respond to clinical resistance. Ultimately, this may improve the clinical success rate for novel anti-cancer drugs.

METHODS

Animals, generation of mammary tumors, and orthotopic transplantations

Brca1^{-/-};p53^{-/-} mammary tumors were generated in *K14cre;Brca1^{F/F};p53^{F/F}* mice, genotyped and orthotopically transplanted into syngeneic wild-type mice as described^{12,13,34}. *Ecad^{-/-};p53^{-/-}* mammary tumors were generated in *WAPcre;Ecdh^{F/F};p53^{F/F}* mice (P.W.B.D. and J.J., unpublished results) and transplanted as *Brca1^{-/-};p53^{-/-}* tumors. Starting 2 weeks after tumor grafting, the onset of tumor growth

was checked at least 3 times per week. Mammary tumor size was determined by caliper measurements (length and width in millimeters) and tumor volume (in mm³) was calculated by using the following formula: $0.5 \times \text{length} \times \text{width}^2$. Animals were killed with CO₂ when the tumor volume reached 1500mm³. In addition to sterile collection of multiple tumor pieces for grafting experiments, tumor samples were snap-frozen in liquid nitrogen and fixed in 4 % formaline. All experimental procedures on animals were approved by the Animal Ethics Committee of the Netherlands Cancer Institute.

Drugs

AZD2281 was used by diluting 50 mg/ml stocks in DMSO with 10% 2-hydroxyl-propyl- β -cyclodextrine/PBS such that the final volume administered by i.p. injection was 10 μ l/g of body weight. Cisplatin (1 mg/ml in saline-mannitol) and carboplatin (10 mg/ml in mannitol-H₂O) originated from Mayne Pharma (Brussels, Belgium). Tariquidar (Avaant) was diluted in 5 % glucose such that the final volume administered by i.p. injection was 10 μ l/g of body weight.

Treatment of mammary tumor-bearing animals

When mammary tumors reached a size of \approx 200 mm³, 50 mg/kg AZD2281 was given i.p. daily for 28 or 100 consecutive days. Controls were left untreated or were dosed with vehicle only. Cisplatin (6 mg/kg) and carboplatin (100 mg/kg) were injected i.v. When combined with platinum drugs, AZD2281 was given 30 min in advance. Following the initial treatment, the tumor size was determined at least 3 times per week. The relative tumor volume was calculated as the ratio between the tumor volume at time t and the tumor volume at the start of treatment. To avoid accumulating toxicity of repeated drug injections, an additional treatment was not given after the recovery time of 14 days when the tumor responded to the treatment (tumor size <50 % of the original volume, partial response). In this case treatment was resumed once the tumor relapsed to its original size (100 %).

AZD2281 PK/PD analysis

Three primary *Brca1*^{-/-};*p53*^{-/-} tumors (T1-T3) were transplanted into 5 animals each and 4 of these mice were treated with 50 mg AZD2281 per kg i.p. when the tumor volume reached 500 mm³. Tumor and plasma samples were harvested 30 min, 2 h, 6 h, and 24 h. The tumor of the fifth animal was used as control when 500 mm³ in size. Tumors were homogenized for 1 min in 3 volumes of ice-cold PBS and tumor and plasma samples snap frozen on dry-ice. The concentration of AZD2281 was determined by liquid chromatography-tandem mass spectrometry (LC-MS/MS) on an Agilent 1100 series LC system linked to a Sciex 2000 triple Quad Mass Spectrometer (Applied Biosystems). After thawing, the compound was extracted from the sample by protein precipitation with acetonitrile and injected on an acetonitrile (0.01 % Formic Acid): 0.01 % Formic Acid gradient. Calibration standards were prepared in mouse plasma and tumor as proxy matrices. To measure PARP1 activity tumor whole cell extracts (WCE) were first analyzed by Western Blots using the anti-PARP1 mouse monoclonal 7D3-6 (BD Bioscience) followed by ECL detection and quantitative image capture analysis (LAS-3000,

Fuji/Raytek). The PARP1 protein concentration for each extract was determined by 2D densitometry against PARP1 standards using AIDA (Advanced Image Data Analyzer) imaging software. The equivalent of 20 pg PARP1 of mouse tumor WCEs were then activated *ex vivo* by incubating with dsDNA oligos and NAD⁺ to stimulate PARP1 activity and poly-ADP-ribosylation (PAR formation). PAR formation was then quantified by electrochemiluminescence with a Meso Scale assay using the anti-PAR mouse monoclonal 10H (Serotec) primary antibody followed by a goat anti-mouse IgG SULFO-TAG (Meso Scale) secondary antibody.

RT-MLPA analysis

From the snap frozen tumor samples total RNA was isolated with Trizol (Invitrogen) and the integrity of RNA was verified by denaturing gel electrophoresis. Reverse transcription, hybridization, ligation, PCR amplification and fragment analysis by capillary electrophoresis were performed as described^{13,35}.

Immunohistochemical analysis

Immunohistochemical stainings of tumors were carried out using anti- γ H2AX (rabbit polyclonal, Cell Signaling, #2577, 1:50 in 1 % bovine serum albumin diluted in phosphate saline buffer (PBSA)) and anti-cleaved caspase 3 (rabbit polyclonal, Cell Signaling, #9661, 1:100 in 1 % PBSA) antibodies. Antigen retrieval was performed by boiling for 15 min in citrate buffer (pH 6.0). After overnight probing at 4°C with the primary antibodies, slides were incubated with a biotinylated goat-anti-rabbit secondary antibody (Dakocytomation, # E043201, 1:800 in 1 % PBSA) for 30 min at room temperature. For detection, we used a standard StreptABC amplified staining procedure with DAB (Dakocytomation, # K037711) and haematoxylin counterstaining. Positive and negative (no antibody) controls were included for each slide and staining procedure. Positively labeled cells (in the case of γ H2AX ≥ 1 dot per nucleus) were counted in the tumor sections in 10 standardized microscopic fields (650x650 μ m). These fields were defined by using an ocular morphometric grid and a 40x lens.

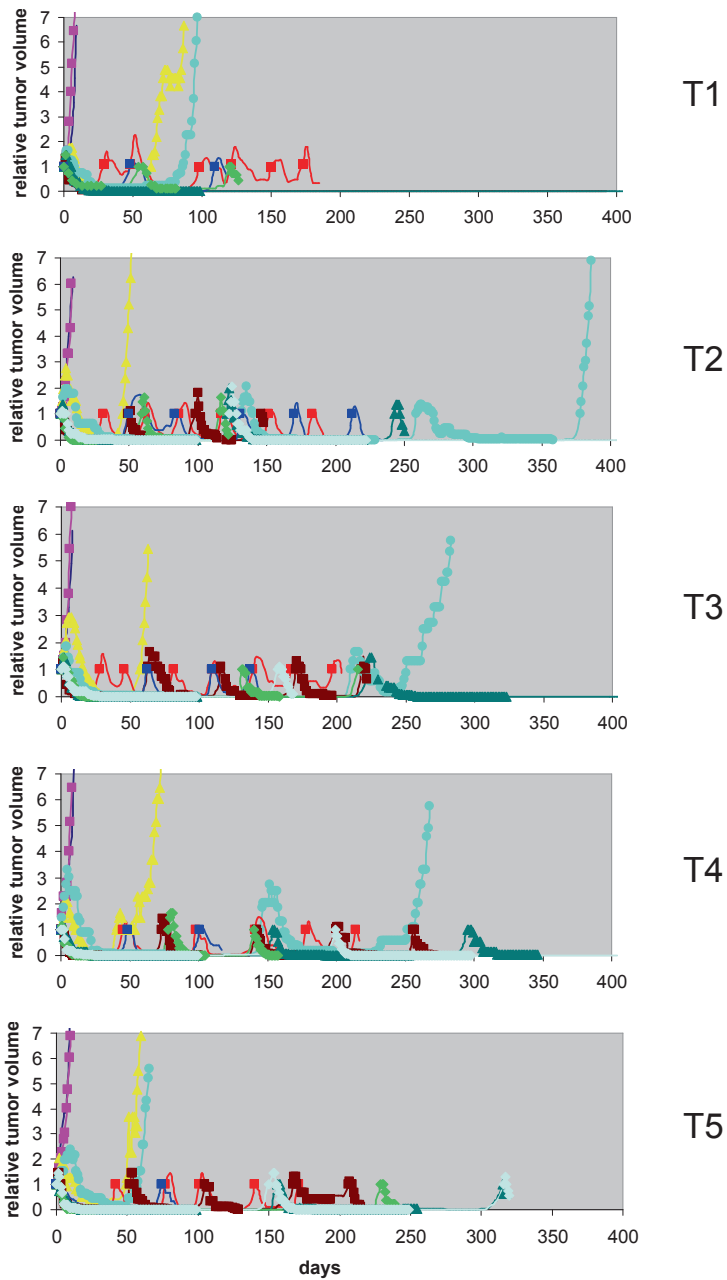
ACKNOWLEDGMENTS

We thank Anton Berns, Maarten van Lohuizen and Jan Schellens for critical reading of the manuscript and Susan Bates and Tito Fojo from the NIH in Bethesda (USA) for providing tariquidar. This work was supported by grants of the Dutch Cancer Society (2002-2635 to J.J. and A. Berns; 2006-3566 to P.B., S.R. and J.J.; 2007-3772 to J.J., S.R. and J.H.M. Schellens), the Netherlands Organization for Scientific Research (NWO-Veni 916.56.135 to P.W.B.D.) and the European Union (FP6 Integrated Project 037665-CHEMORES to P. B. and S. R.). S.R. was supported by fellowships from the Swiss National Science Foundation (PBBEB-104429) and the Swiss Foundation for Grants in Biology and Medicine.

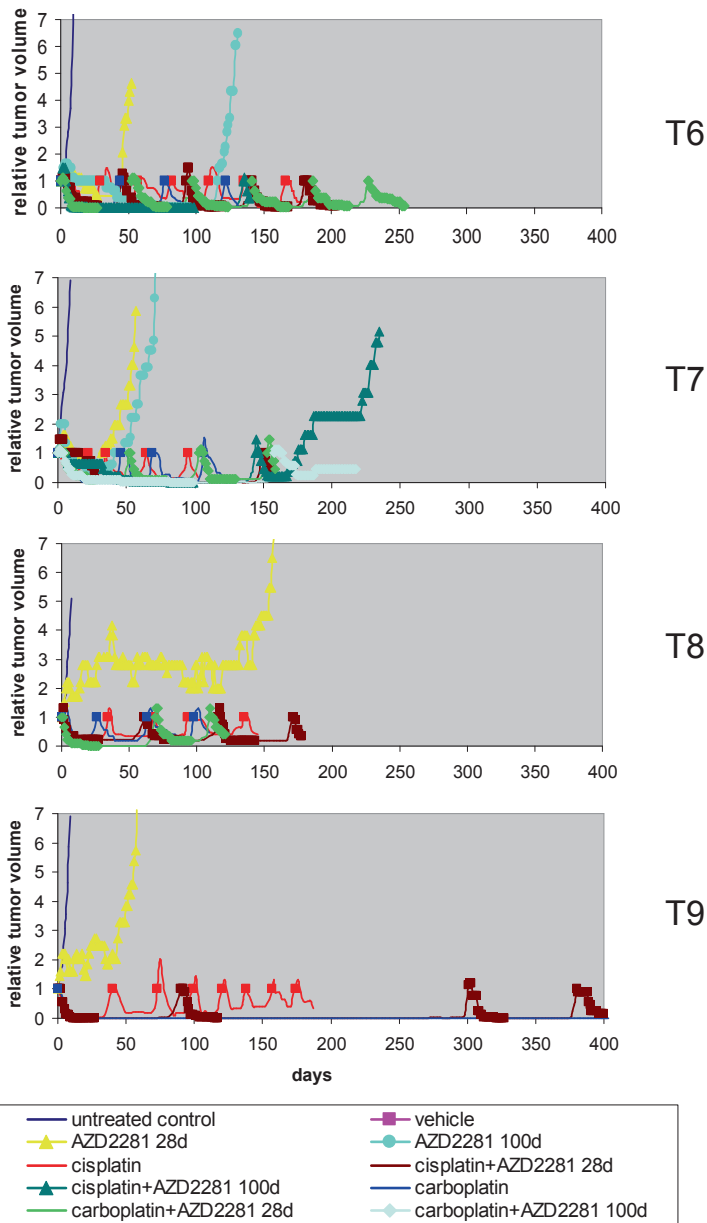
REFERENCES

1. De Murcia J, *et al.* (1997) Requirement of poly(ADP-ribose) polymerase in recovery from DNA damage in mice and in cells. *Proc Natl Acad Sci U S A* 94:7303-7307.
2. Schreiber V, Dantzer F, Ame JC, de Murcia G (2006) Poly(ADP-ribose): novel functions for an old molecule. *Nat Rev Mol Cell Biol* 7:517-528.
3. Wang ZQ, *et al.* (1997) PARP is important for genomic stability but dispensable in apoptosis. *Genes Dev* 11:2347-2358.
4. Bryant HE, *et al.* (2005) Specific killing of BRCA2-deficient tumours with inhibitors of poly(ADP-ribose) polymerase. *Nature* 434:913-917.
5. Farmer H, *et al.* (2005) Targeting the DNA repair defect in BRCA mutant cells as a therapeutic strategy. *Nature* 434:917-921.
6. Narod SA, Foulkes WD (2004) BRCA1 and BRCA2: 1994 and beyond. *Nat Rev Cancer* 4:665-76.
7. Gudmundsdottir K, Ashworth A (2006) The roles of BRCA1 and BRCA2 and associated proteins in the maintenance of genomic stability. *Oncogene* 25:5864-5874.
8. Helleday T, *et al.* (2008) DNA repair pathways as targets for cancer therapy. *Nat Rev Cancer* 8:193-204.
9. Donawho CK, *et al.* (2007) ABT-888, an orally active poly(ADP-ribose) polymerase inhibitor that potentiates DNA-damaging agents in preclinical tumor models. *Clin Cancer Res* 13:2728-2737.
10. Sharpless NE, DePinho RA (2006) The mighty mouse: genetically engineered mouse models in cancer drug development. *Nat Rev Drug Disc* 5:741-54.
11. Menear KA, *et al.* (2008) 4-[3-(4-cyclopropanecarbonyl)piperazine-1-carbonyl]-4-fluorobenzyl]-2H-phthalazin-1-one: a novel bioavailable inhibitor of poly(ADP-ribose) polymerase-1. *J Med Chem* 51:6581-91
12. Liu X, *et al.* (2007) Somatic loss of BRCA1 and p53 in mice induces mammary tumors with features of human BRCA1-mutated basal-like breast cancer. *Proc Natl Acad Sci U S A* 104:12111-12116.
13. Rottenberg S, *et al.* (2007) Selective induction of chemotherapy resistance of mammary tumors in a conditional mouse model for hereditary breast cancer. *Proc Natl Acad Sci U S A* 104:12117-12122.
14. Derksen P, *et al.* (2006) Somatic inactivation of E-cadherin and p53 in mice leads to metastatic lobular mammary carcinoma through induction of anoikis resistance and angiogenesis. *Cancer Cell* 10:437-449.
15. Raymond M, Rose E, Housman DE, Gros P (1990) Physical mapping, amplification, and overexpression of the mouse *mdr* gene family in multidrug-resistant cells. *Mol Cell Biol* 10:1642-1651.
16. Allen JD, Brinkhuis RF, Wijnholds J, Schinkel AH (1999) The mouse *Bcrp1/Mxr/Abcp* gene: amplification and overexpression in cell lines selected for resistance to topotecan, mitoxantrone, or doxorubicin. *Cancer Res* 59:4237-4241.
17. Mistry P, *et al.* (2001) In vitro and in vivo reversal of P-glycoprotein-mediated multidrug resistance by a novel potent modulator, XR9576. *Cancer Res* 61:749-758.
18. Evers B, *et al.* (2008) Selective inhibition of BRCA2-deficient mammary tumor cell growth by AZD2281 and cisplatin. *Clin Cancer Res* 14:3916-3925.
19. Cleator S, Heller W, Coombes RC (2007) Triple-negative breast cancer: therapeutic options. *Lancet Oncol* 8:235-244.
20. Sorlie T, *et al.* (2001) Gene expression patterns of breast carcinomas distinguish tumor subclasses with clinical implications. *Proc Natl Acad Sci U S A* 98:10869-10874.
21. Foulkes WD, *et al.* (2003) Germline BRCA1 mutations and a basal epithelial phenotype in breast cancer. *J Natl Cancer Inst* 95:1482-1485.
22. Turner N, Tutt A, Ashworth A (2004) Hallmarks of 'BRCAness' in sporadic cancers. *Nat Rev Cancer* 4:814-819.
23. Turner NC, *et al.* (2007) BRCA1 dysfunction in sporadic basal-like breast cancer. *Oncogene* 26:2126-2132.

24. Yap TA, *et al.* (2007) First in human phase I pharmacokinetic (PK) and pharmacodynamic (PD) study of KU-0059436 (Ku), a small molecule inhibitor of poly ADP-ribose polymerase (PARP) in cancer patients (p), including BRCA1/2 mutation carriers. *Journal of Clinical Oncology*, ASCO Annual Meeting Proceedings Part I 25:3529.
25. Kelland L (2007) The resurgence of platinum-based cancer chemotherapy. *Nat Rev Cancer* 7:573-584.
26. Flohr C, Bürkle A, Radicella JP, Epe B (2003) Poly(ADP-ribosyl)ation accelerates DNA repair in a pathway dependent on Cockayne syndrome B protein. *Nucleic Acids Res* 31:5332-5337.
27. Rottenberg S, Jonkers J (2008) Modeling therapy resistance in genetically engineered mouse cancer models. *Drug Resist Updat* 11:51-60.
28. Wurzer G, Herceg Z, Wesierska-Gadek J (2000) Increased resistance to anticancer therapy of mouse cells lacking the poly(ADP-ribose) polymerase attributable to up-regulation of the multidrug resistance gene product P-glycoprotein. *Cancer Res* 60:4238-4244.
29. Schinkel AH, *et al.* (1997) Normal viability and altered pharmacokinetics in mice lacking mdr1-type (drug-transporting) P-glycoproteins. *Proc Natl Acad Sci U S A* 94:4028-4033.
30. Sakai W, *et al.* (2008) Secondary mutations as a mechanism of cisplatin resistance in BRCA2-mutated cancers. *Nature* 451:1116-1120.
31. Swisher EM, *et al.* (2008) Secondary BRCA1 mutations in BRCA1-mutated ovarian carcinomas with platinum resistance. *Cancer Research* 68:2581-2586.
32. Edwards SL, *et al.* (2008) Resistance to therapy caused by intragenic deletion in BRCA2. *Nature* 451:1111-1115.
33. Borst,P., Rottenberg,S. and Jonkers,J (2008). How do real tumors become resistant to cisplatin? *Cell Cycle* 7:1353-1359.
34. Jonkers J, *et al.* (2001) Synergistic tumor suppressor activity of BRCA2 and p53 in a conditional mouse model for breast cancer. *Nat Genet* 29:418-425.
35. Eldering E, *et al.* (2003) Expression profiling via novel multiplex assay allows rapid assessment of gene regulation in defined signalling pathways. *Nucleic Acids Res* 31:e153



Supplementary Figure S1.



Supplementary Figure S1. Overview of the treatments administered into animals carrying 9 individual Brca1- and p53-deficient mammary tumors (T1-T9). Graphs show relative tumor volume (ratio of tumor volume to initial size at start of treatment) as a function of time. For the different drugs the following doses were applied: AZD2281: 50 mg/kg i.p. daily for 28 or 100 consecutive days; cisplatin: 6 mg/kg i.v. day 0; carboplatin: 100 mg/kg i.v. day 0. Once the tumors relapsed, treatment was resumed when the tumor size reached 100 % of the original volume. Treatments are indicated by rhombi, triangles, squares or circles. In combination therapies, AZD2281 was given 30 min before the platinum drug.

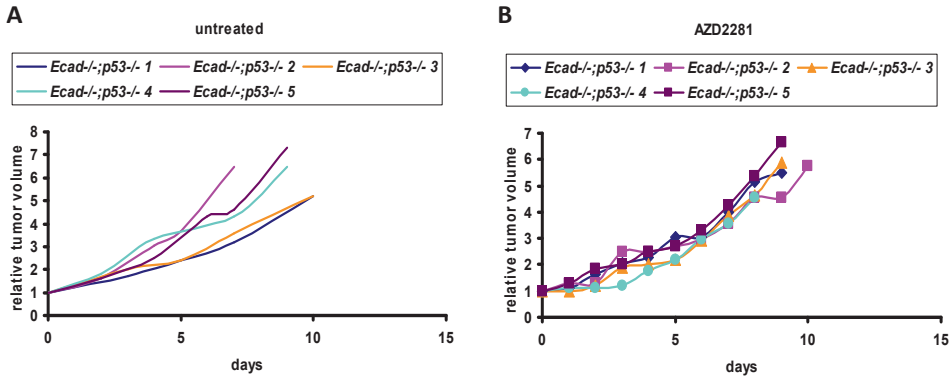
Supplementary Table S1. Wilcoxon Signed Rank Tests for the IHC analysis of Figure 3B

Hypothesis	P<	n =
γH2AX		
T3 untreated – T3 7days < 0	0.0001	10
T3 resistant – T3 7days < 0	0.0001	10
T4 untreated – T4 7days < 0	0.0001	10
T4 resistant – T4 7days < 0	0.0001	10
T6 untreated – T6 7days < 0	0.0001	10
T6 resistant – T6 7days < 0	0.0001	10
Ecad/p53 untreated – Ecad/p53 7days < 0	0.0001	10
Ecad/p53 resistant – Ecad/p53 7days < 0	0.01	10
Ecad/p53 7 days – T3 7days < 0	0.0001	10
Ecad/p53 7 days – T4 7days < 0	0.0001	10
Ecad/p53 7 days – T6 7days < 0	0.0001	10
Cleaved caspase 3		
T3 untreated – T3 7days < 0	0.0001	10
T3 resistant – T3 7days < 0	0.0001	10
T4 untreated – T4 7days < 0	0.0001	10
T4 resistant – T4 7days < 0	0.0001	10
T6 untreated – T6 7days < 0	0.0001	10
T6 resistant – T6 7days < 0	0.0001	10
Ecad/p53 untreated – Ecad/p53 7days < 0	0.01	10
Ecad/p53 resistant – Ecad/p53 7days < 0	0.001	10
Ecad/p53 7 days – T3 7days < 0	0.0001	10
Ecad/p53 7 days – T4 7days < 0	0.0001	10
Ecad/p53 7 days – T6 7days < 0	0.0001	10

Supplementary Table S2. Semi-quantitative RT-MLPA analysis of 15 AZD2281-resistant tumors

	T1-28	T1-100	T2-28	T3-28	T3-100	T4-28	T4-100	T5-28
<i>Abcb1a</i>	1.47 +/- 0.36	0.84 +/- 0.17	13.6 +/- 4.40	2.09 +/- 0.22	1.49 +/- 0.18	1.27 +/- 0.19	2.31 +/- 0.58	0.95 +/- 0.13
<i>Abcb1b</i>	2.18 +/- 0.12	1.01 +/- 0.20	2.13 +/- 0.78	0.88 +/- 0.17	2.38 +/- 0.01	0.99 +/- 0.18	1.47 +/- 0.36	1.15 +/- 0.37
<i>Abcc1</i>	1.56 +/- 0.16	0.85 +/- 0.06	1.23 +/- 0.70	0.94 +/- 0.13	0.76 +/- 0.09	1.40 +/- 0.18	0.80 +/- 0.33	0.48 +/- 0.07
<i>Abcg1</i>	1.20 +/- 0.12	0.79 +/- 0.17	2.59 +/- 0.73	0.61 +/- 0.06	2.75 +/- 0.41	0.90 +/- 0.09	0.85 +/- 0.13	1.25 +/- 0.21
<i>Parp1</i>	1.01 +/- 0.13	1.37 +/- 0.10	0.66 +/- 0.03	0.85 +/- 0.09	1.39 +/- 0.09	1.07 +/- 0.04	0.51 +/- 0.25	0.44 +/- 0.04
<i>Parp2</i>	1.47 +/- 0.26	3.02 +/- 0.52	0.79 +/- 0.27	1.78 +/- 0.43	0.99 +/- 0.09	0.76 +/- 0.04	1.17 +/- 0.10	0.70 +/- 0.13
<i>CD24</i>	1.40 +/- 0.27	1.99 +/- 0.66	0.44 +/- 0.35	0.88 +/- 0.09	3.55 +/- 0.28	0.88 +/- 0.13	1.34 +/- 0.38	0.31 +/- 0.05
<i>CD29</i>	0.97 +/- 0.18	1.64 +/- 0.17	0.62 +/- 0.27	1.05 +/- 0.19	0.96 +/- 0.03	0.91 +/- 0.21	0.92 +/- 0.12	0.68 +/- 0.14
<i>CD49f</i>	1.06 +/- 0.13	2.10 +/- 0.58	0.92 +/- 0.39	1.45 +/- 0.27	1.88 +/- 0.25	1.78 +/- 0.09	0.76 +/- 0.12	0.73 +/- 0.09
<i>Hprt1</i>	1.20 +/- 0.11	1.19 +/- 0.06	0.80 +/- 0.14	0.92 +/- 0.08	1.29 +/- 0.06	1.04 +/- 0.30	1.39 +/- 0.20	0.54 +/- 0.06

Per tumor, the fluorescence peak value of the indicated gene (left axis) was divided by the internal reference *Actinβ*. The presented values give the mean ratio (three independent reactions) +/- standard deviation of a AZD2281-resistant tumor in comparison to the matched untreated control tumor. A *P* value was calculated using the nonparametric Wilcoxon rank sum test to measure significant differences between the median gene expression values in comparison to those of the housekeeping gene *Hprt1*.



Supplementary Figure S2. Five individual spontaneous *Ecad^{-/-};p53^{-/-}* mammary tumors were generated in *WAPcre;Ecad^{F/F};p53^{F/F}* animals (ref. ¹² and P.W.B.D and J.J., unpublished results). Like *Brca1^{-/-};p53^{-/-}* tumors, small tumor fragments were transplanted orthotopically into syngeneic mice and left untreated (A) or treated with 50 mg AZD2281 per kg mouse i.p. daily (filled boxes) once the outgrown tumor volume reached 200 mm³ (B).

	T5-100	T6-28	T6-100	T7-28	T7-100	T8	T9	P =
	1.54 +/- 0.37	0.51 +/- 0.07	0.91 +/- 0.06	85.48 +/- 7.58	33.42 +/- 3.60	2.06 +/- 0.52	4.04 +/- 0.29	0.011
	1.14 +/- 0.08	76.9 +/- 22.49	4.46 +/- 0.92	7.59 +/- 0.20	7.34 +/- 0.07	2.12 +/- 0.09	4.18 +/- 0.56	0.004
	0.45 +/- 0.10	0.59 +/- 0.16	0.93 +/- 0.18	1.43 +/- 0.11	1.07 +/- 0.17	1.31 +/- 0.21	1.37 +/- 0.33	0.820
	1.25 +/- 0.19	0.86 +/- 0.08	2.47 +/- 0.30	0.41 +/- 0.33	0.44 +/- 0.02	0.86 +/- 0.06	1.86 +/- 0.18	0.920
	0.38 +/- 0.06	2.67 +/- 0.48	4.23 +/- 0.79	0.34 +/- 0.07	0.59 +/- 0.05	0.99 +/- 0.11	1.03 +/- 0.12	0.380
	0.71 +/- 0.18	1.32 +/- 0.49	1.57 +/- 0.38	0.75 +/- 0.11	1.16 +/- 0.15	0.68 +/- 0.10	1.48 +/- 0.16	0.650
	0.45 +/- 0.03	2.13 +/- 0.22	1.88 +/- 0.19	0.36 +/- 0.05	0.84 +/- 0.04	0.63 +/- 0.06	1.30 +/- 0.17	0.983
	0.39 +/- 0.02	0.88 +/- 0.20	0.53 +/- 0.08	0.78 +/- 0.02	1.34 +/- 0.02	1.38 +/- 0.37	1.33 +/- 0.55	0.468
	1.24 +/- 0.16	1.01 +/- 0.03	1.44 +/- 0.14	0.42 +/- 0.04	0.22 +/- 0.04	0.86 +/- 0.09	1.37 +/- 0.11	0.983
	0.94 +/- 0.11	1.48 +/- 0.16	1.53 +/- 0.20	0.62 +/- 0.03	0.53 +/- 0.04	0.77 +/- 0.07	1.39 +/- 0.25	

2

Supplementary Table S3. Wilcoxon Signed Rank Tests for Figure 5A

Hypothesis	<i>P</i> =	<i>n</i> =
AZD2281_28d - AZD2281_100d < 0	0.009	7
cisplatin – cisplatin + AZD2281_28d < 0	0.006	8
cisplatin – cisplatin + AZD2281_100d < 0	0.014	6
carboplatin – carboplatin + AZD2281_28d < 0	0.006	8
carboplatin – carboplatin + AZD2281_100d < 0	0.022	5

Supplementary Table S4. Wilcoxon Signed Rank Tests for the overall survival of mice treated with carboplatin alone or in combination with AZD2281

Hypothesis	<i>P</i> =	<i>n</i> =
carboplatin – carboplatin + AZD2281_28d < 0	0.047	8
carboplatin – carboplatin + AZD2281_100d < 0	0.022	5



Loss of 53BP1 causes PARP inhibitor resistance in *Brca1*-mutated mouse mammary tumors

Janneke E. Jaspers^{1,2}, Ariena Kersbergen¹, Ute Boon², Wendy Sol¹, Liesbeth van Deemter¹, Serge A.L. Zander¹, Rinske Drost², Ellen Wientjens², Jiuping Ji³, Amal Aly⁴, James H. Doroshov⁵, Aaron Cranston⁶, Niall M.B. Martin⁶, Alan Lau⁷, Mark J. O'Connor⁷, Shridar Ganesan⁵, Piet Borst¹, Jos Jonkers², Sven Rottenberg¹

¹ Divisions of Molecular Biology and ² Molecular Pathology, Netherlands Cancer Institute, Plesmanlaan 121, 1066 CX Amsterdam, The Netherlands; ³ National Clinical Target Validation Laboratory, National Cancer Institute, Frederick; and ⁵ Division of Cancer Treatment and Diagnosis and Laboratory of Molecular Pharmacology, National Cancer Institute, Bethesda, Maryland; ⁴ Cancer Institute of New Jersey, New Brunswick, New Jersey; ⁶ KuDOS Pharmaceuticals, Cambridge and ⁷ AstraZeneca, Macclesfield, United Kingdom

***Cancer Discovery* 2013, 3(1):68-81**

(<http://cancerdiscovery.aacrjournals.org/content/3/1/68.abstract?sid=63d4c83e-c4fb-415c-a1ca-018f935ccd26>)

ABSTRACT

Inhibition of poly(ADP-ribose) polymerase (PARP) is a promising therapeutic strategy for homologous recombination-deficient tumors, such as BRCA1-associated cancers. We previously reported that BRCA1-deficient mouse mammary tumors may acquire resistance to the clinical PARP inhibitor (PARPi) olaparib through activation of the P-glycoprotein drug efflux transporter. Here we show that tumor-specific genetic inactivation of P-glycoprotein increases the long-term response of BRCA1-deficient mouse mammary tumors to olaparib, but these tumors eventually developed PARPi resistance. In a fraction of cases this is caused by partial restoration of homologous recombination due to somatic loss of 53BP1. Importantly, PARPi resistance was minimized by long-term treatment with the novel PARP inhibitor AZD2461, which is a poor P-glycoprotein substrate. Together, our data suggest that restoration of homologous recombination is an important mechanism for PARPi resistance in BRCA1-deficient mammary tumors and that the risk of relapse of BRCA1-deficient tumors can be effectively minimized by using optimized PARP inhibitors.

Statement of significance

In this study we show that loss of 53BP1 causes resistance to PARP inhibition in mouse mammary tumors that are deficient in BRCA1. We hypothesize that low expression or absence of 53BP1 also reduces the response of patients with BRCA1-deficient tumors to PARP inhibitors.

INTRODUCTION

Inhibition of poly (ADP-ribose) polymerase 1 (PARP1) induces synthetic lethality in cells that are defective in homologous recombination (HR) due to loss of BRCA1 or BRCA2 or other HR-associated proteins¹⁻³. PARP1 inhibition results in unrepaired DNA single-strand breaks (SSBs), which are eventually converted into double strand breaks (DSBs) during DNA replication. Whereas HR-proficient cells can repair these DSBs in an error-free manner, HR-deficient cells cannot, and die. Preclinical studies and phase I and II clinical trials have demonstrated potent anti-tumor efficacy of the PARP inhibitor (PARPi) olaparib (AZD2281) as a single agent in BRCA1- or BRCA2-associated cancers with only modest side effects⁴⁻¹⁰. Unfortunately, not all cancer patients carrying *BRCA1* or *BRCA2* mutations respond to PARPi therapy^{4,10}, which is impeding further clinical development of this promising therapeutic approach. Identification of the mechanisms underlying PARPi resistance is therefore important for improving treatment and for prediction of tumor response prior to treatment.

Since pre- or post-PARPi-treatment tumor samples from patients with BRCA1-deficient cancers are still limited, we studied the response and resistance to the clinical PARPi olaparib in a validated genetically engineered mouse model for *BRCA1*-mutated breast cancer^{9,11,12}. Mammary tumors that arise in these mice were highly sensitive to olaparib⁹. Nevertheless, long-term olaparib response was frequently hampered by increased expression of the *Mdr1a/b* (also known as *Abcb1a/b*) genes, which encode the drug efflux transporter P-glycoprotein (Pgp)⁹. Also the MRE11A-deficient human colon cancer cell line HCT-15, which expresses Pgp, could be sensitized to olaparib by combining it with the Pgp-inhibitor verapamil¹³. However, the relevance of Pgp in clinical drug resistance is still controversial, and there may be a difference in the induction of Pgp expression between mice and humans¹⁴.

Recently, we have also shown that mouse mammary tumors that contain the *Brca1*^{C61G} mutation still show hypomorphic BRCA1 activity that explains the modest responses to olaparib or cisplatin treatment¹⁵. Using BRCA2-deficient cell lines, another PARPi resistance mechanism has previously been identified: genetic reversion of the *BRCA2* mutation causes resistance to PARP inhibition or cisplatin^{16,17}. Secondary mutations that restore BRCA1/2 function have subsequently been found in platinum-resistant hereditary ovarian cancers^{18,19}.

Here, we set out to identify novel mechanisms of PARPi resistance that cannot be explained by Pgp-mediated drug efflux, residual BRCA1 activity or restoration of BRCA1 function. For this purpose we have used a mouse model, in which mammary tumors arise that contain a large, irreversible *Brca1* mutation on a Pgp-deficient background. We report on inactivation of p53 binding protein 1 (53BP1) as a causal factor in PARPi resistance, and on the successful circumvention of drug resistance of Pgp-proficient tumors using AZD2461, a novel PARPi with lower affinity to Pgp.

RESULTS

Elimination of Pgp prolongs the response of BRCA1-deficient mouse mammary tumors to olaparib, but tumors still develop drug resistance

Using the *K14cre;Brca1^{F/F};p53^{F/F}* (KB1P) mouse model for BRCA1-associated breast cancer, we have previously shown that activation of Pgp induces resistance to the PARPi olaparib⁹. To study olaparib sensitivity of KB1P mammary tumors in the absence of functional Pgp, we bred the *Mdr1a/b* null alleles^{20;21} to homozygosity into our KB1P model (Supplementary Figure S1A). Eleven individual mammary tumors from *K14cre;Brca1^{F/F};p53^{F/F};Mdr1a/b^{-/-}* (KB1PM) mice were orthotopically transplanted into syngeneic FVB mice, which were subsequently treated with olaparib and monitored for survival (Figure 1A and Supplementary Figure S1B). All tumors were initially highly sensitive to olaparib. Moreover, the response of tumors derived from the same original donor tumor was comparable (Supplementary Figure S2), showing that initial heterogeneity in PARPi response is limited. The survival of mice bearing Pgp-deficient KB1PM tumors increased, compared with mice carrying Pgp-proficient KB1P tumors, following 28 days of treatment with olaparib ($p = 0.0392$, Figure 1A and Supplementary Figure S1B,C). This result confirms that Pgp plays a pivotal role in the development of olaparib resistance in the KB1P model, as we have shown previously using the Pgp inhibitor tariquidar⁹. Despite this increased survival all mice eventually developed tumor recurrences that no longer responded to olaparib (Supplementary Figure S1B). Due to the large intragenic deletion of *Brca1* in our model¹¹, PARPi resistance can not be caused by restoration of BRCA function, as was found previously for BRCA2-deficient CAPAN1 cells¹⁶. Hence, PARPi resistance can arise *in vivo* in the absence of two known resistance mechanisms: drug efflux by Pgp and genetic reversion of the *Brca1* mutation.

The characteristics of olaparib-resistant KB1PM tumors suggest activation of DNA damage repair

We transplanted nine individual olaparib-resistant KB1PM tumors into syngeneic mice and found that the resistance was stable (Figure 1B). To exclude that olaparib resistance in KB1PM tumors is driven by alterations of the drug target PARP resulting in restoration of poly(ADP-ribose) (PAR) formation, we tested the effects of olaparib on PARP activity in control versus olaparib-resistant tumors from three different donors (Figure 1C). PAR levels were low or undetectable in olaparib-resistant tumors 30 minutes after olaparib administration and after 7 days of daily treatment with olaparib, showing that PARP function is still inhibited by olaparib, thus excluding alteration of the drug target as PARPi resistance mechanism. As a consequence of the inhibition of PARP activity in both control and olaparib-resistant tumors there is an increase in DNA DSBs, as measured by γ H2AX staining (Supplementary Figure S3).

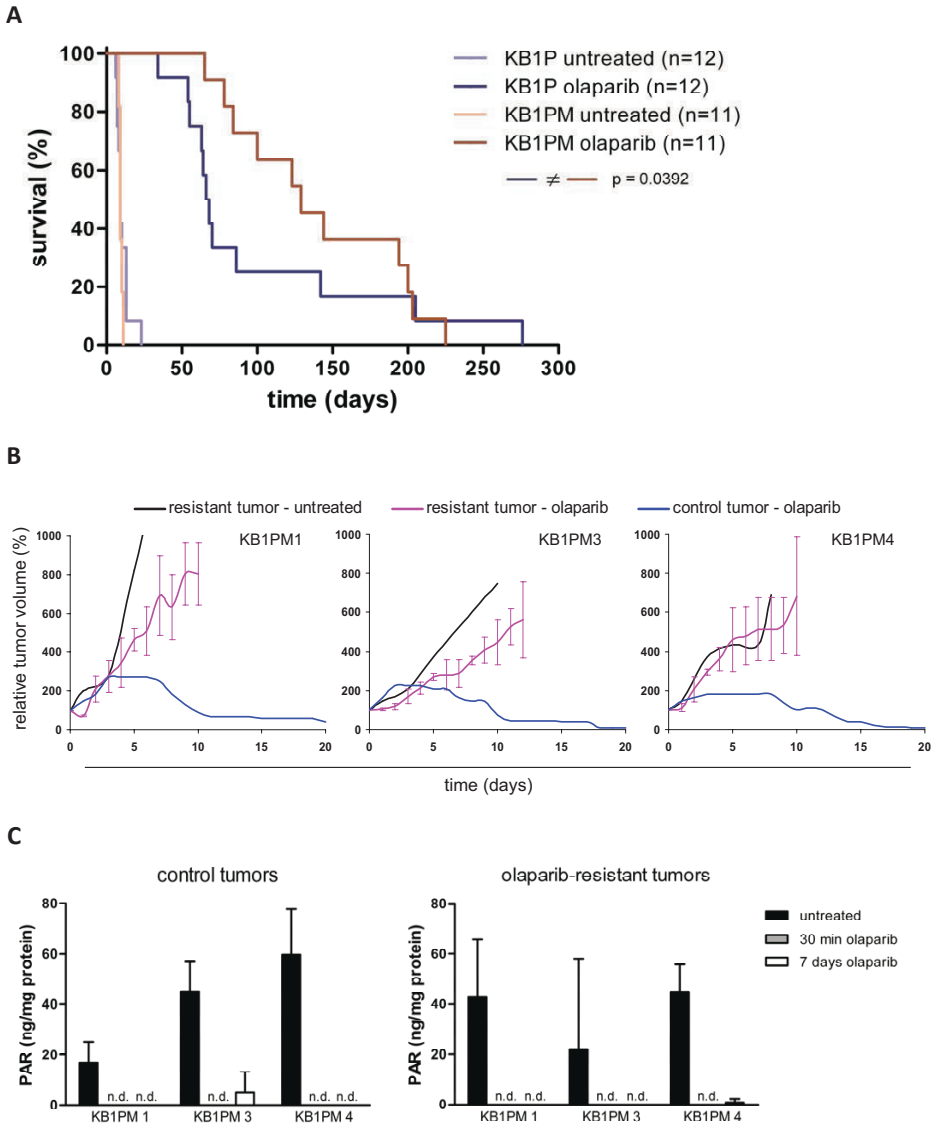


Figure 1. Acquired resistance of P-glycoprotein-deficient *Brca1*^{Δ/Δ};*p53*^{Δ/Δ} (KB1PM) mouse mammary tumors to the PARPi olaparib. **A**, Kaplan-Meier curve showing survival of mice bearing Pgp-proficient KB1P or Pgp-deficient KB1PM tumors, either untreated or treated with 50 mg olaparib per kg i.p. for 28 consecutive days. Treatment was resumed when a relapsing tumor reached a size of 100% (the tumor size at the start of the treatment). Individual tumor responses are shown in Supplementary Figure S1. The Gehan-Breslow-Wilcoxon *p* value is indicated. **B**, response to daily treatment with 50 mg olaparib per kg i.p. of olaparib-resistant tumors from three donor tumors (KB1PM1, 3 and 4) and drug-naive control tumors from the corresponding donors. **C**, levels of poly(ADP-ribose) (PAR) detected in whole tumor extracts from olaparib-resistant and control tumors derived from KB1PM1, 3 and 4. The tumors were harvested either without treatment, 30 minutes after one dose of 50 mg olaparib per kg i.p. or 2 hours after the last dose of 7 days of daily treatment. n.d. = not detectable (lower than 2*SD above background). Data are presented as mean+SD of three mice per donor per treatment.

To test whether the sensitivity to DNA damage inflicted by other DNA-targeting anti-cancer drugs would also be altered, we transplanted olaparib-resistant and corresponding control tumors from five individual KB1PM donors. The tumor-bearing mice were treated with the topoisomerase I inhibitor topotecan, the DNA adduct-forming agent cisplatin or the topoisomerase II inhibitor doxorubicin. Almost all drug-naïve KB1PM tumors responded well to cisplatin or doxorubicin and about half of the tumors showed high topotecan sensitivity (Figure 2A). In contrast, none of the olaparib-resistant KB1PM tumors shrunk more than 50 % following treatment with topotecan (Figure 2A,B). Although olaparib-resistant KB1PM tumors were usually still sensitive to cisplatin or doxorubicin, the time to relapse of these tumors was reduced in comparison to the drug-naïve KB1PM tumors (Figure 2C,D). The fact that olaparib-resistant KB1PM tumors are cross-resistant to topotecan and recover more quickly from cisplatin- or doxorubicin-mediated DNA damage supports the hypothesis that olaparib-resistant KB1PM tumors have an altered DNA damage response compared to control tumors.

Loss of 53BP1 causes olaparib resistance by restoration of HR

We and others have recently identified p53-binding protein 1 (53BP1) as a factor for maintaining the growth defect of *Brca1*-deficient cell lines^{22;23}. Loss of 53BP1 partially restores HR in BRCA1-deficient cells, thereby reducing their hypersensitivity to PARP inhibition and DNA-damaging agents. Using immunohistochemistry we tested whether 53BP1 was lost in any of our KB1PM tumors which acquired olaparib resistance *in vivo*. We found that three out of 11 olaparib-resistant KB1PM tumors at least partly lost 53BP1 protein, whereas all untreated KB1PM tumors were positive (Figure 3A,B). Besides these differences between individual olaparib-resistant tumors, we also observed intra-tumor heterogeneity: 53BP1-positive and -negative cell nests were both present in olaparib-resistant tumors KB1PM3 (Figure 3B) and KB1PM8 (data not shown). In two olaparib-resistant KB1PM tumors we identified somatic mutations in the *Trp53bp1* gene that explain loss of 53BP1 protein. We found two genomic rearrangements in olaparib-resistant KB1PM5 in intron 24 of *Trp53bp1* (Supplementary Figure S4A,B). By cDNA sequencing, however, we only detected a duplication of exons 25 and 26 (Figure 3C and Supplementary Figure S4C), indicating that the duplication of a part of exon and intron 24 leads to non-sense mediated mRNA decay. The duplication of exon 25 and 26 results in a frame shift and premature stop codon (Figure 3C). In the 53BP1-negative tumor nests of the olaparib-resistant KB1PM8 we detected a heterozygous mutation in exon 12 (Figure 3D). cDNA sequencing only showed the truncating mutation Q626*, suggesting that the wild-type allele is silenced, possibly by promoter methylation.

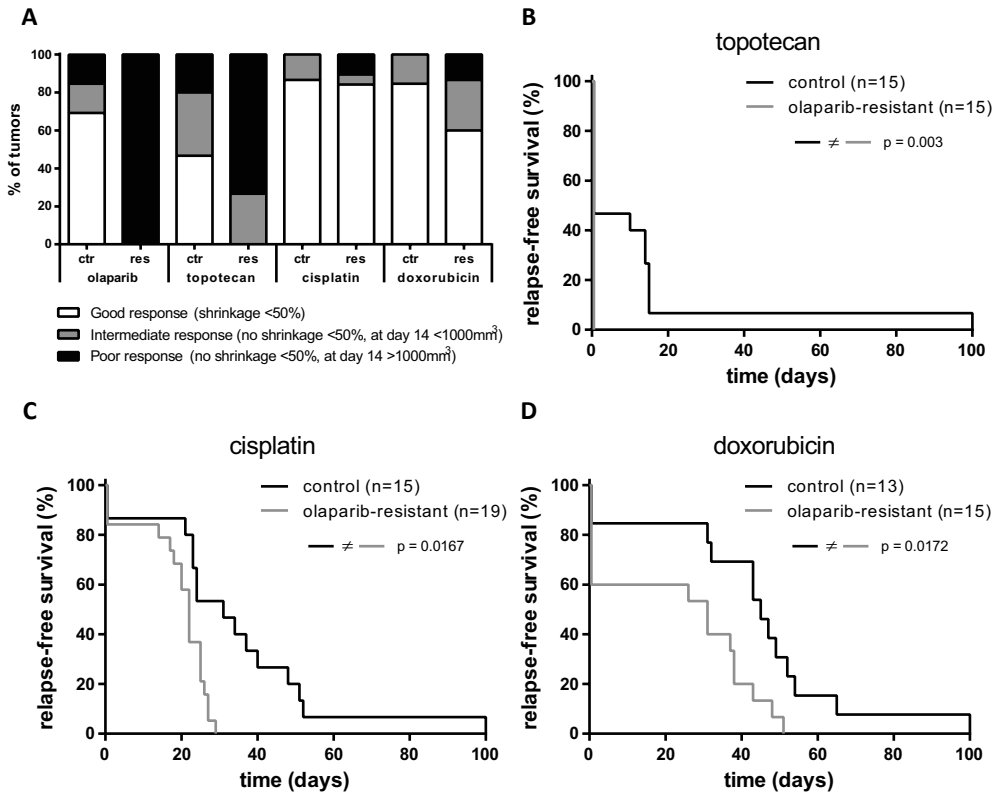
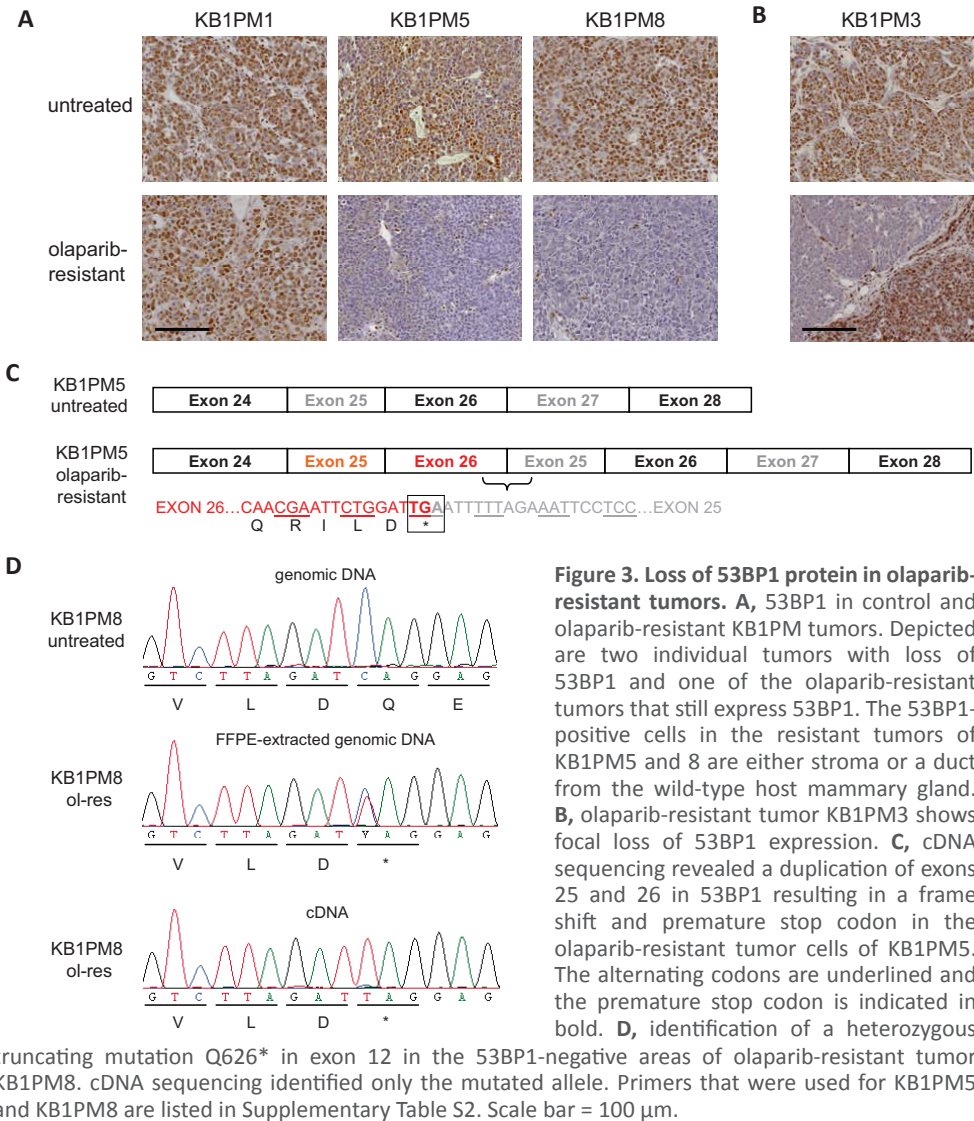


Figure 2. Response of olaparib-resistant tumors to DNA-damaging agents. **A**, classification of the response of olaparib-resistant and control tumors from five individual donors (KB1PM1, 3, 4, 5 and 8) to olaparib (50 mg/kg, daily for 28 days), topotecan (2 mg/kg, day 0-4 and 14-18), cisplatin (6 mg/kg, day 0) and doxorubicin (5 mg/kg, day 0, 7 and 14). Untreated tumors would be classified as 'poor responders'. **B-D**, for the same group of mice the relapse-free survival is shown in response to topotecan, cisplatin or doxorubicin. The poor and intermediate responders of figure **A** have a relapse-free survival of 0 days since the tumor did not shrink below 50% of the original size. Day 0 is the start of the treatment. The Gehan-Breslow-Wilcoxon p values are indicated.

To test whether HR is restored in 53BP1-deficient KB1PM tumors, we derived cell lines from olaparib-sensitive and -resistant KB1PM5 tumors. The deletions of *Brca1*, *p53* and *Mdr1* were confirmed by genotyping PCR (Supplementary Figure S5A) and the array comparative genomic hybridization (aCGH) profiles of the cell lines resembled those of the original tumors (Supplementary Figure S5B). Western Blotting confirmed the complete lack of 53BP1 in the resistant cells, whereas it was still present in sensitive KB1PM5 cells (Supplementary Figure S5C). In a clonogenic assay the cell lines derived from the olaparib-resistant KB1PM5 tumor retained their resistance *in vitro* (Supplementary Figure S5D).



Importantly, we found that irradiation-induced RAD51 foci (IRIFs) were present in olaparib-resistant KB1PM5 tumor cells, but absent in olaparib-sensitive KB1PM5 cells, indicating that DNA repair by HR is restored in the 53BP1-deficient KB1PM tumors (Figure 4A). However, the 53BP1-deficient KB1PM5 tumor cells did not contain as many RAD51 IRIFs as 53BP1- and BRCA1-proficient KP3.33 cells (Figure 4B), suggesting that HR restoration by 53BP1 loss in KB1PM tumors is only partial, which may explain the lack of cross-resistance

to cisplatin and doxorubicin. In addition to the cell lines, we have analyzed the ability to form RAD51 IRIFs in short-term tumor cell cultures derived from 53BP1-negative olaparib-resistant KB1PM tumors and their controls (Figure 4C). Olaparib-resistant tumor cells from KB1PM5 and 8 form RAD51 IRIFs and are negative for 53BP1 (Supplementary Figure S6). Interestingly, olaparib-resistant tumor cells from the heterogeneous olaparib-resistant tumor KB1PM3 form RAD51 IRIFs, but also have functional 53BP1 in all cells tested, shown by the 53BP1 IRIFs. This indicates the presence of a 53BP1-independent mechanism of HR-restoration in the 53BP1-positive tumor cell nests. In addition to the KB1PM3, 5 and 8, we measured RAD51 and 53BP1 IRIFs in KB1PM1 and 9. Similar to KB1PM3, the olaparib-resistant cells of KB1PM9 form 53BP1 IRIFs, but also RAD51 IRIFs. Tumor cells derived from olaparib-resistant KB1PM1 have functional 53BP1 and do not show RAD51 IRIFs, indicating an HR-independent mechanism of PARPi resistance.

We next tested whether inactivation of 53BP1 is causal to PARPi resistance. To this end, we transduced two cell lines derived from an untreated KB1P tumor (KB1P-B11 and KB1P-G3) with lentiviral vectors encoding two individual short-hairpin RNAs (shRNAs) against *Trp53bp1* (Figure 5A). Also in these cell lines depletion of 53BP1 partially restored the formation of RAD51 IRIFs (Supplementary Figure S7A). A decrease of 53BP1 indeed resulted in reduced sensitivity to olaparib (Figure 5B), indicating that 53BP1 loss causes olaparib resistance. This notion was confirmed by experiments with the olaparib-resistant cell line KB1P-3.12 in which a point mutation in *Trp53bp1* intron 22 leads to a cryptic splice acceptor site before exon 23 and production of a frame-shifted mRNA (Supplementary Figure S7B). When we reconstituted functional 53BP1 in this cell line we observed increased olaparib sensitivity, further supporting the relevance of 53BP1 expression for olaparib sensitivity (Figure 5C,D).

We also tested KB1P-B11 cells with stable shRNA-mediated depletion of 53BP1 *in vivo* after orthotopic transplantation of these cells in mice. The resulting outgrowths did not respond to olaparib anymore, whereas the control tumors were still sensitive (Figure 5E). IHC analysis confirmed the complete loss of 53BP1 expression in tumors derived from KB1P-B11 cells with stable 53BP1 depletion (Supplementary Figure S7C). This directly proves that absence of 53BP1 in KB1P tumors is sufficient for complete resistance to olaparib. In line with our cross-resistance experiments (Figure 2C), all tumor cell line outgrowths responded well to cisplatin treatment, but 53BP1-negative outgrowths tended to relapse earlier (Figure 5F).

In view of the complete cross-resistance of olaparib-resistant tumors to topotecan (Figure 2A,B), we tested whether loss of 53BP1 also contributes to drug resistance of tumors that were only treated with topotecan. As the drug efflux transporter ABCG2 contributes to topotecan resistance of KB1P mouse mammary tumors²⁴, we used ABCG2-deficient KB1P tumors from *K14cre;Brca1^{F/F};p53^{F/F};Abcg2^{-/-}* mice for these experiments.

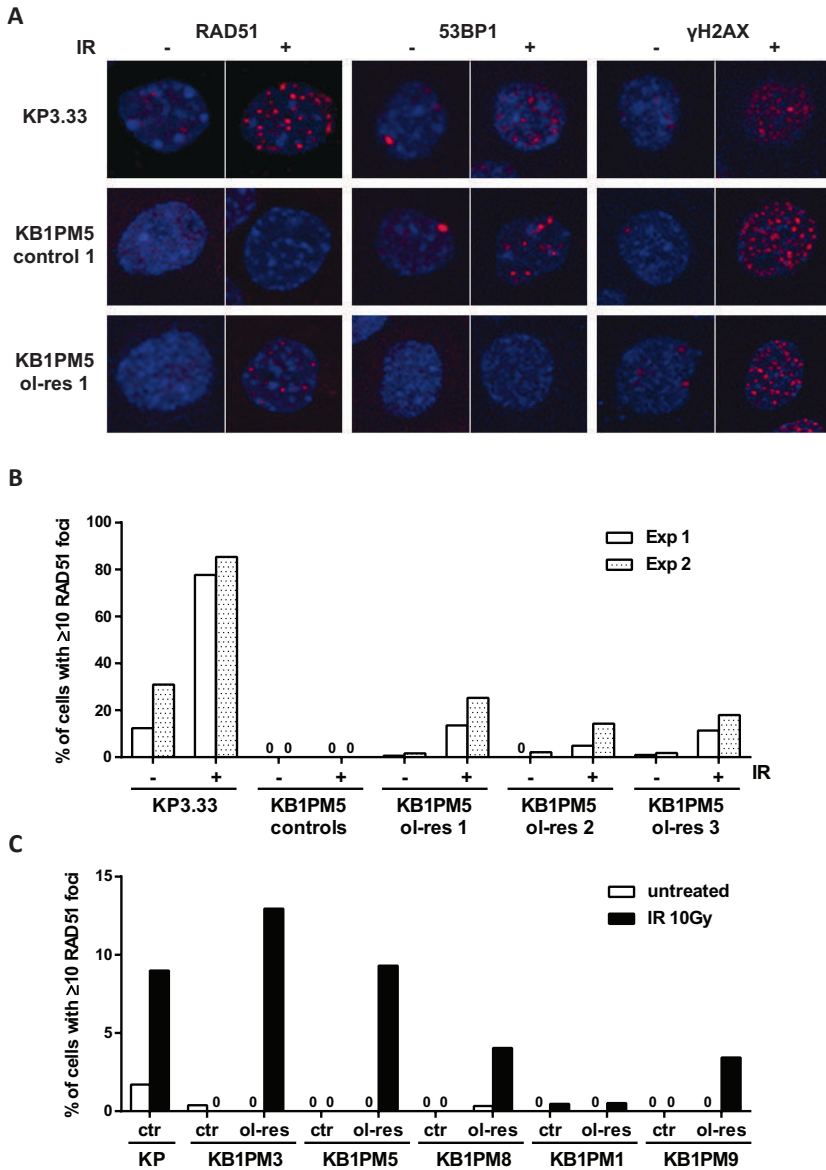


Figure 4. DNA damage foci in irradiated cells. A, detection of ionizing radiation-induced RAD51, 53BP1 and γ H2AX foci in BRCA1-proficient KP3.33 cells⁵, a cell line derived from a KB1PM5 control tumor (control 1), and a 53BP1-negative cell line derived from the olaparib-resistant KB1PM5 tumor (ol-res 1). For characterization of the cell lines, see also Supplementary Figure S5. Images show the maximum projection, covering the whole cell in the z-direction. **B**, quantification of RAD51 focus formation of three KB1PM5 control cell lines and three KB1PM5 olaparib-resistant cell lines in two independent experiments. The three control cell lines are combined in one bar and each olaparib-resistant cell line is shown separately for both experiments. **C**, quantification of RAD51 IRIFs in a control KP tumor and in matched olaparib-sensitive and -resistant KB1PM tumors. See also Supplementary Figure S6. IR = ionizing radiation.

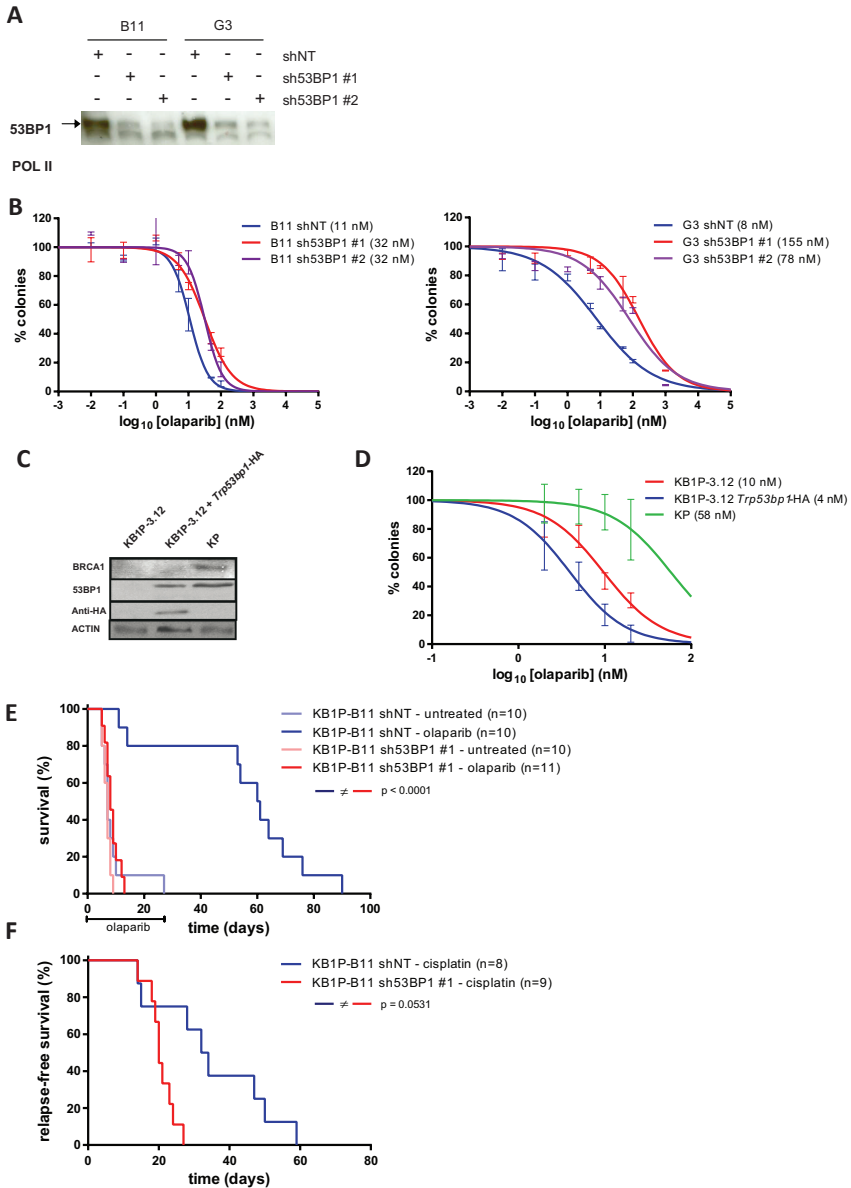


Figure 5. The effect of 53BP1 loss on olaparib sensitivity. **A**, Western blot showing 53BP1 levels in KB1P-B11 and KB1P-G3 cells that express a non-targeting hairpin (NT) or a hairpin against *Trp53bp1*. **B**, clonogenic assay with olaparib. The IC₅₀ is indicated between brackets. **C**, Western blot showing the reconstitution of 53BP1 in 53BP1-deficient KB1P-3.12 cells. KP cells are used as positive control for the BRCA1 western blot. **D**, clonogenic assay of 53BP1-negative KB1P-3.12 cells, h53BP1-reconstituted KB1P-3.12 cells and BRCA-proficient KP cells. **E**, overall survival of mice with a 53BP1-positive (shNT) or -negative (sh53BP1) tumor treated with one regimen of olaparib daily for 28 days and the untreated control mice. 53BP1 expression in these tumors is shown in Supplementary Figure S7C. **F**, Relapse-free survival of mice with a 53BP1-positive (shNT) or -negative (sh53BP1) tumor treated with one dose of cisplatin. The Gehan-Breslow-Wilcoxon *p* values are indicated.

Indeed, we found that 53BP1 expression was absent in 3 out of 20 topotecan-resistant tumors, whereas 53BP1 was still fully present in the corresponding tumors before treatment (Supplementary Figure S8). This strongly suggests that 53BP1 loss is not exclusively a mechanism of olaparib resistance, but may also play a role in resistance to other commonly used anti-cancer agents.

Long-term PARP inhibition by AZD2461 suppresses the development of resistance

To circumvent the development of PARPi resistance we investigated whether long-term dosing of a PARPi would be capable of causing eradication or chronic suppression of KB1P tumors. We have previously shown that long-term olaparib treatment of 100 consecutive days significantly increased the overall survival of mice with KB1P tumors compared to 28 days of treatment, but we also found that several of these tumors acquired Pgp-mediated resistance⁹. Therefore we tested the response of KB1P tumors to the novel PARPi AZD2461 (Supplementary Figure S9A), which has lower affinity for Pgp than olaparib¹³. Both AZD2461 and olaparib completely inhibited the PARP activity for several hours and the amount of PAR returned to baseline levels 24 hours after treatment (Supplementary Figure S9B). 6 hours after drug administration we observed a small difference in PARP activity. This may be caused by a higher potency of AZD2461 or a faster Pgp-mediated washout of olaparib. We confirmed the low affinity of AZD2461 to Pgp by testing the inhibitor on olaparib-resistant KB1P tumor T6-28, which has an 80-fold increased *Mdr1b* expression⁹. This tumor is sensitized to olaparib by pre-treatment with the Pgp inhibitor tariquidar and it also responds well to AZD2461 without inhibition of Pgp (Figure 6A). In contrast, Pgp-deficient olaparib-resistant KB1PM tumors do not respond to AZD2461 (Figure 6B). These data show that AZD2461 is a novel PARPi with potential to bypass Pgp-mediated resistance to olaparib.

We first studied short-term AZD2461 treatment in mice with KB1P tumors using daily dosing for 28 consecutive days as we did for olaparib. Although mice treated with AZD2461 clearly showed increased survival compared to olaparib-treated mice ($p = 0.0061$), all mice eventually developed relapsing tumors that were refractory to PARPi treatment (Figure 6C and Supplementary Figure S9C). Three out of twelve AZD2461-resistant KB1P tumors also showed loss of 53BP1 expression (Figure 6D). In the AZD2461-resistant tumor KB1P2 we found a deletion of 94 base pairs in exon 21 of *Trp53bp1* (Figure 6E and Supplementary Figure S9D), which leads to a stop-codon in this exon. We also identified a deletion of 34 base pairs on the boundary of intron 24 and exon 25 of *Trp53bp1* in AZD2461-resistant tumor KB1P8 (Figure 6F and Supplementary Figure S9E).

When we increased the AZD2461 treatment to 100 consecutive days, we found that 8 out of 9 mice engrafted with fragments from 3 individual KB1P tumors did not develop refractory tumors within 300 days after treatment start (Figure 7A and Supplementary Figure S10A-C). In contrast, 6 out of 7 KB1P tumor-bearing mice that received 100 days

of consecutive olaparib treatment acquired drug resistance in this time (Figure 7A and Rottenberg *et al.*⁹). The tumor that acquired AZD2461 resistance during the first treatment cycle had an epithelial-to-mesenchymal transition (EMT) phenotype (Supplementary Figure S10D), which is frequently linked to drug resistance²⁵.

Long-term AZD2461 treatment was well tolerated and doubled the median relapse-free survival from 64 days to 132 days ($p < 0.0001$, Figure 7B). Intriguingly, long-term AZD2461 treatment did not result in tumor eradication: although tumor remnants were not palpable during AZD2461 treatment, we found tumor relapse once treatment was stopped on day 100 (Supplementary Figure S10A-C). Nevertheless, KB1P tumor recurrences were still sensitive when AZD2461 treatment was resumed.

DISCUSSION

Despite the induction of synthetic lethality of BRCA1-deficient cells by PARP inhibition^{1,2}, a heterogeneous response of breast or ovarian cancer patients who carry a *BRCA1* mutation has been observed recently^{4,10}. This shows that there is an urgent need to identify mechanisms that thwart the success of this promising therapeutic approach. We have studied PARPi resistance using a mouse model for BRCA1-deleted breast cancer in which two known mechanisms, BRCA1 re-expression by genetic reversion and increased drug efflux by P-glycoprotein, were eliminated by genetic engineering. We show that loss of 53BP1 causes resistance to PARP inhibition in BRCA1-deficient mouse mammary tumors. As underlying mechanism, 53BP1-deficient KB1PM cells appear to have partially restored HR-mediated DNA repair, as evidenced by the presence of DNA damage-induced RAD51 foci. Hence, our data demonstrate that HR restoration by 53BP1 loss is a relevant drug resistance mechanism that occurs in real tumors.

Our results are consistent with recent *in vitro* data from the group of A. Nussenzweig²³ and our own group²² showing that 53BP1 loss in BRCA1-deficient cells increases resistance to DNA-damaging agents and partially restores HR activity. While the underlying mechanisms are still under investigation, data from *in vitro* studies show that 53BP1 loss promotes end resection of DNA DSBs in the absence of BRCA1, resulting in RAD51 recruitment and subsequent HR²³. The importance of end resection for promoting HR over NHEJ has been shown earlier²⁶⁻²⁸.

Loss of 53BP1 adds a novel *in vivo* mechanism of PARPi resistance to two other resistance mechanisms that have previously been identified in preclinical models: restoration of BRCA function^{16,17,19} and increased *Mdr1* gene expression⁹. To what extent these mechanisms contribute to PARPi resistance in patients is still unclear, although secondary somatic mutations restoring BRCA1/2 function have been found in platinum resistant hereditary ovarian cancers¹⁸.

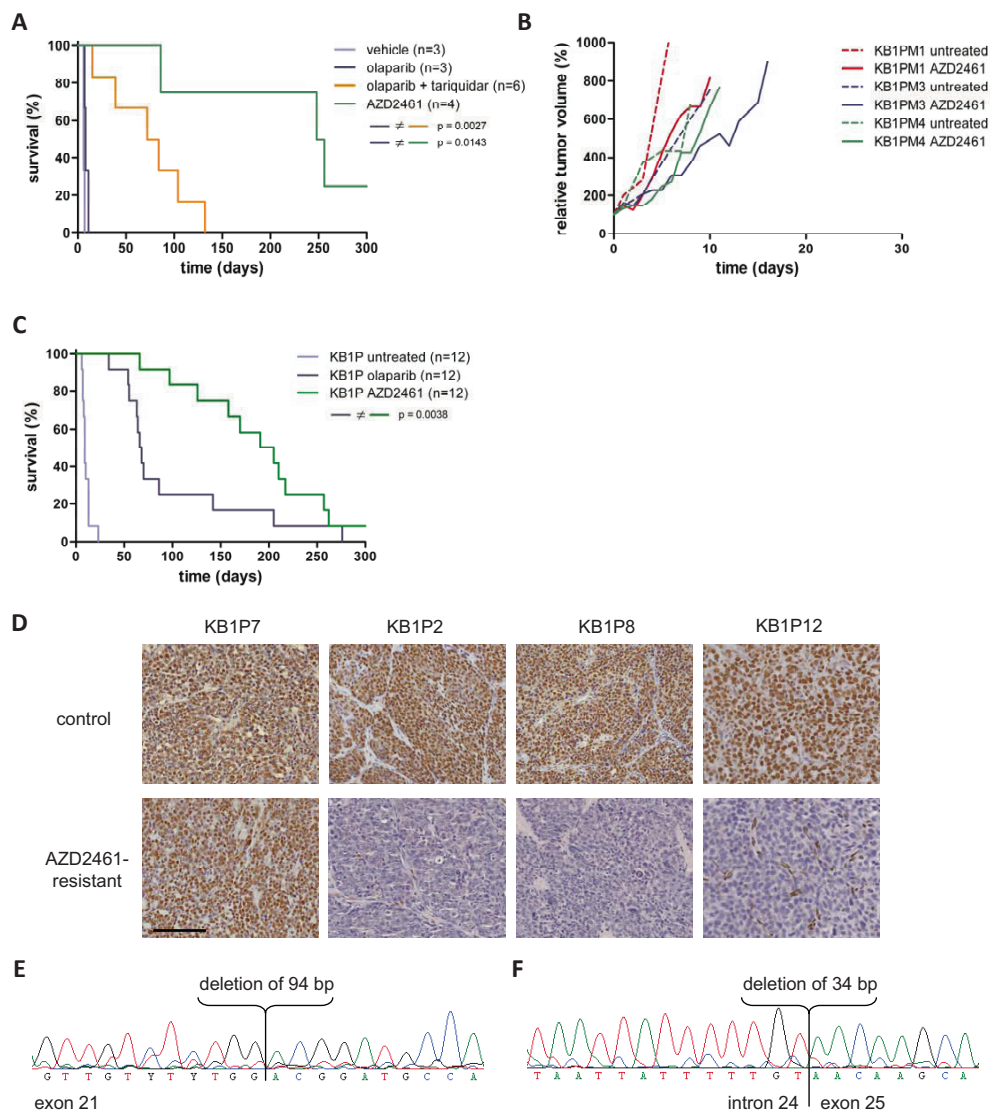


Figure 6. Non-Pgp-mediated resistance to the next generation PARP inhibitor AZD2461. **A**, overall survival of mice with an olaparib-resistant KB1P tumor with 80-fold increase in *Mdr1b* expression, that were treated with the vehicle of AZD2461 (0.5 % v/w HPMC), olaparib, olaparib in combination with the Pgp-inhibitor tariquidar or with AZD2461. **B**, tumor growth of the Pgp-deficient, olaparib-resistant tumors from KB1PM1, KB1PM3 and KB1PM4, either untreated or treated with AZD2461. **C**, Kaplan-Meier curve showing survival of mice with a Pgp-proficient KB1P tumor, either untreated or after treatment with olaparib or AZD2461. Individual tumor responses are shown in Supplementary Figs. S1C and S9C. The Gehan-Breslow-Wilcoxon p value is indicated. **D**, 53BP1 in control and AZD2461-resistant KB1P tumors. Depicted are three individual tumors with loss of 53BP1 and one of the AZD2461-resistant tumors that still express 53BP1. Scale bar = 100 μ m. **E**, identification of a 94bp deletion in exon 21 of *Trp53bp1* in AZD2461-resistant tumor KB1P2, leading to a frame shift and early stop codon in exon 21. **F**, identification of a 34bp deletion at the splice acceptor site of exon 25 of *Trp53bp1*.

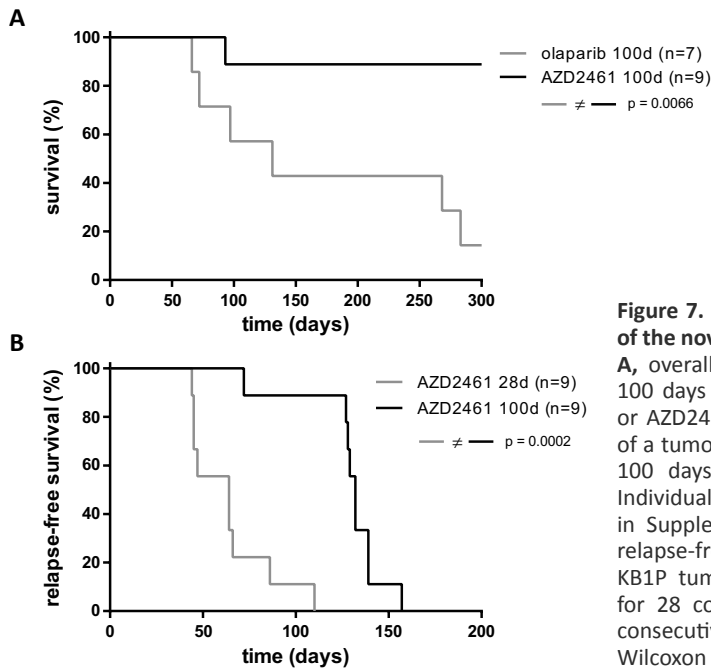


Figure 7. Chronic anti-tumor efficacy of the novel PARP inhibitor AZD2461.

A, overall survival of mice receiving 100 days of olaparib (see also ref. ⁹) or AZD2461 treatment. After relapse of a tumor to a size of 100 % another 100 days of treatment was given. Individual tumor responses are shown in Supplementary Figure S10A-C. **B**, relapse-free survival of mice with a KB1P tumor that received AZD2461 for 28 consecutive days or for 100 consecutive days. The Gehan-Breslow-Wilcoxon p values are indicated.

Interestingly, 53BP1 expression is frequently absent in *BRCA1/2*-mutated or triple negative breast cancers²². We therefore hypothesize that the poor overall survival of patients with 53BP1-negative breast cancer²² is partly due to increased resistance to DNA-damaging agents. It would therefore be useful to evaluate the utility of 53BP1 as a biomarker for predicting response of *BRCA1*-deficient cancers to PARPi therapy.

HR restoration due to 53BP1 loss induces not only resistance to PARPi, but also to the topoisomerase I inhibitor topotecan. In contrast, olaparib-resistant tumors were still sensitive to the DNA cross-linking agent cisplatin or the topoisomerase II inhibitor doxorubicin. Topotecan promotes SSBs which are converted into more cytotoxic DSBs during DNA replication. It is therefore conceivable that partial HR restoration is sufficient to antagonize this effect. Moreover, the topotecan cross-resistance suggests that PARP inhibition primarily targets SSB repair²⁹.

Despite the remarkable capability of 53BP1-deficient cells to carry out homology-directed DNA repair in the absence of *BRCA1*, our data suggest that this restoration is not complete: the number of RAD51 IRIF-positive 53BP1-deficient KB1P(M) tumor cells does not reach the level observed in 53BP1- and *BRCA1*-proficient KP3.33 tumor cells *in vitro*. The fact that we observe more heterogeneous levels of RAD51 foci using the short-term cell cultures of tumor cell suspensions may be due to the more complex nature of this assay. Several factors in the procedure of tumor cell dissociation and subsequent adhesion to cover slips may have an impact on RAD51 foci quantification.

We have previously reported that the amount of DNA damage inflicted by olaparib is not sudden, but accumulates over a short period of time⁹. As a result of this, tumors only shrink after a few days of PARP inhibition, which correlates with a peak of γ H2AX foci about a week after the start of treatment. In contrast, the number of γ H2AX foci is much higher shortly after cisplatin treatment (data not shown). Hence, partial restoration of HR by 53BP1 loss may not be sufficient for BRCA1-deficient tumor cells to cope with the profound and acute induction of DNA damage by cisplatin. This lack of complete cross-resistance is consistent with the recent findings of Bunting *et al.*³⁰: the absence of 53BP1 in *Brca1* ^{Δ 11/ Δ 11} MEFs does not rescue the hypersensitivity to cisplatin, in contrast to the sensitivity to PARP inhibition. BRCA1 has also functions in interstrand cross-link (ICL) repair that are not directly linked to the HR pathway, such as replication fork protection³¹ or recruitment of FANCD2^{30;32;33}. It is likely that such additional functions explain the partial sensitivity to cisplatin of our 53BP1- and BRCA1-deficient tumors.

The fact that 53BP1 loss only occurs in a fraction of the PARPi resistant mouse mammary tumors indicates that other resistance mechanisms should exist in 53BP1-positive tumors. These mechanisms might include impaired recruitment of 53BP1 to sites of DNA damage due to dysfunctional recruitment factors, such as RNF8 or RNF168, or prevention of PARPi-induced DNA damage through inhibition of other NHEJ-associated factors³⁴. We found at least two PARPi resistant tumors (KB1PM3 and 9) in which both RAD51 and 53BP1 IRIFs are formed (Figure 4C and Supplementary Figure S6). This strongly suggests a 53BP1-independent mechanism of HR restoration in BRCA1-deficient cells. In addition, the lack of RAD51 IRIF formation in olaparib-resistant KB1PM1 suggests an HR-independent resistance mechanism. We are currently investigating what other mechanisms may explain this outcome by using functional screens in our panel of BRCA1-deficient cell lines.

The observation that in several PARPi-resistant tumors 53BP1 expression is lost in only a fraction of tumor cells strongly suggests that different resistance mechanisms may be selected within an individual tumor. Distinct clonal subpopulations and their relation to metastasis were recently characterized in breast cancer³⁵. Our data suggest that distinct subpopulations of tumor cells utilizing different resistance mechanisms may evolve during PARPi treatment. This heterogeneity might complicate the design of novel therapeutic strategies to reverse PARPi resistance. Our model may be a useful tool to test such therapeutic approaches before they enter clinical trials.

As one strategy to minimize the risk of development of PARPi resistance we present continuous treatment with the novel PARPi AZD2461. Whereas 28-day treatment with AZD2461 resulted in induction of resistance (which was in several tumors mediated by 53BP1 loss), chronic treatment resulted in complete remission and suppression of refractory disease during a period of 300 days. Although chronic AZD2461 treatment did not result in tumor eradication, it inhibited the outgrowth of drug resistant clones. Apparently, the pool

of proliferating cells, in which new mutations can arise, is effectively reduced in size. While we cannot exclude that resistance to AZD2461 may develop at later time points, our data suggest that chronic PARP inhibition may be a promising strategy to achieve long-term tumor suppression in patients with HR-deficient tumors. Other PARPi's that are not Pgp substrates, such as veliparib (ABT888)³⁶, might have the same potential. In case Pgp-mediated olaparib resistance does not occur in humans, stable disease suppression might also be achieved using olaparib. In fact, in a phase II study, maintenance therapy using olaparib prolonged progression-free survival of patients with high-grade serous ovarian carcinoma³⁷. Of note, benefit from long-term PARPi treatment may not be restricted to *BRCA*-mutation carriers, as 51% of the high-grade serous ovarian carcinomas were found to have a genetic or epigenetic alteration in the HR pathway and may therefore respond to PARPi³⁸.

Collectively, our results further the understanding of PARPi resistance and underscore the relevance of HR restoration in *BRCA1*-deficient mammary tumors that cannot escape treatment by increased drug efflux, restoration of *BRCA1* function or residual activity of the *BRCA1* mutant protein¹⁵. Moreover, we show how preclinical evaluation of targeted therapeutics in genetically engineered mice can facilitate the development of therapeutic strategies that may prolong the treatment benefit in cancer patients.

METHODS

Mice, generation of mammary tumors and orthotopic transplantations

Brc1^{Δ/Δ};*p53*^{Δ/Δ} mammary tumors were generated in *K14cre;Brc1*^{F/F};*p53*^{F/F} (KB1P) female mice and genotyped as described previously¹¹. In this study we used KB1P mice that were backcrossed to a pure FVB/N background. To generate *Brc1*^{Δ/Δ};*p53*^{Δ/Δ};*Mdr1a*/*b*^{-/-} tumors we crossed *Mdr1a*/*b*^{-/-} mice^{20,21} with KB1P mice to produce *K14cre;Brc1*^{F/F};*p53*^{F/F};*Mdr1a*/*b*^{-/-} (KB1PM) mice. *Mdr1a* and *Mdr1b* genotypes were tested by PCR with specific primers (*Mdr1a* forward: 5'-GTGCATAGACCACCCTCAAGG-3'; *Mdr1b* forward: 5'-AAGCTGTGCATGATTCTGGG-3') for wild type (*Mdr1a* reverse: 5'-GTCATGCACATCAAACCAGCC-3'; *Mdr1b* reverse: 5'-GAGAAACGATGCCTTCCAG-3') and deleted alleles (*Mdr1a* reverse: 5'-GGAGCAAAGCTGCTATTGGC-3'). Orthotopic transplantations into wild-type FVB/N mice, tumor monitoring and sampling were performed as described¹². For the transplantation of cell lines 500,000 cells in PBS and matrigel (1:1) were injected in the fourth right mammary fat pad. All experimental procedures on animals were approved by the Animal Ethics Committee of the Netherlands Cancer Institute.

Drugs and treatment of tumor-bearing mice

Starting from two weeks after transplantation tumor size was monitored at least three times a week. All treatments were started when tumors reached a size of ≈200 mm³. Olaparib (50 mg/kg i.p.) and AZD2461 (100 mg/kg p.o.) were given for 28 consecutive days, unless otherwise indicated. If

tumors did not shrink below 50 % of the initial volume, treatment was continued for another 28 days; otherwise a new treatment cycle of 28 days was started when the relapsing tumor reached a size of 100% of the original volume (except for Figure 5E, where only one 28-day cycle of olaparib treatment was used). AZD2461 was diluted in 0.5 % w/v hydroxypropyl methylcellulose in deionized water to a concentration of 10 mg/ml. The synthesis of AZD2461 is described in international patent WO2009/093032, specifically compound number 2b. In brief, *O*-benzotriazol-1-yl-tetramethyluronium hexafluorophosphate (45.5 g, 119.86 mmol) was added portion wise to a solution of 2-fluoro-5-((4-oxo-3,4-dihydrophthalazin-1-yl)methyl)benzoic acid (1) (27.5 g, 92.20 mmol), 4-methoxypiperidine (11.68 g, 101.42 mmol) and triethylamine (30.8 mL, 221.28 mmol) in dimethyl acetamide (450 mL) at 20 °C under nitrogen. The resulting solution was stirred at 200 °C for 21 hours. The solution was poured into water (2.5 L) and extracted with EtOAc (x3), the combined extracts washed with brine (x3), dried (MgSO₄), filtered and evaporated to a gum. The crude product was purified by flash silica chromatography, elution gradient 0 to 100 % EtOAc in isohexane. Pure fractions were evaporated to dryness and slurred with EtOAc to afford 4-(4-fluoro-3-(4-methoxypiperidine-1-carbonyl)benzyl)phthalazin-1(2H)-one (2b) (22.45 g, 61.6 %) as a white solid after filtration and vacuum drying.

For testing cross-resistance, mice were treated with a single treatment regimen of topotecan (2 mg/kg i.p., days 0-4 and 14-18), cisplatin (Mayne Pharma, 6 mg/kg i.v., day 0) or doxorubicin (Amersham Pharmacia Netherlands, 5 mg/kg i.v., day 0, 7 and 14). Tariquidar (Avaant, 2 mg/kg i.p.) was administered 15 minutes prior to the olaparib injection for 28 consecutive days. Tumor volume was calculated with the following formula: $l \times b^2 \times 0.5$.

PAR Immunoassay

The ELISA for detecting poly-ADP-ribose was described before³⁹. In brief, tissue lysates are prepared in Cell Extraction Buffer (Invitrogen, FNN0011) supplemented with 1x protease inhibitor cocktail (Sigma-Aldrich P-2714 or Roche 11697498001) and 2 mM PMSF (Sigma-Aldrich, Cat#: 93482-50ML-F). Protein concentration is determined with BCA Protein Assay Kit (Thermo Scientific Pierce, Cat#: 23227 or 23225). PAR standards are prepared from pure PAR (BioMol International, Plymouth Meeting, PA, SW-311) and diluted in Superblock (Pierce 37535). Pierce Reactibind (15042) plates were coated with Trevigen Monoclonal anti-PAR (4335) diluted to a concentration of 4 µg/ml in pH 9.6 carbonate buffer, overnight at 4 °C and washed with PBS-0.1 % Tween (Sigma-Aldrich). Blocking was performed with Superblock at 37 °C for one hour. Samples, standards and controls were incubated in the plate for 16 hours at 4 °C. After washing 4 times, rabbit anti-PAR (Trevigen 4336, 1:500 in PBS, 2 % BSA, 1 % mouse serum) was incubated at 25 °C for 2 hours. Goat-anti-rabbit-HRP (KPL Inc., Gaithersburg, MD, 074-15-061, 1 µg/ml in PBS, 2 % BSA, 1 % mouse serum) was incubated at 25 °C for 1 hour. Detection was performed with Supersignal Pico Chemiluminescent Substrate (Pierce 37070) and plates were read on a Tecan Infinite or Tecan Genios Pro Luminometer (Tecan; Mannedorf, Switzerland). Detailed descriptions of the sample preparation and the protocol are available online^{40;41}.

Immunohistochemistry

For immunohistochemical stainings antigen retrieval was done by cooking in citrate buffer pH 6.0 (53BP1 and γ H2AX) or proteinase K digestion (vimentin). Furthermore, the stainings were carried out by using 3 % H₂O₂ for blocking endogenous peroxidase activity, 5 % goat serum plus 2.5 % bovine serum albumin (BSA) in phosphate buffered saline (PBS) as blocking buffer and antibody diluent, overnight first-antibody incubation and one hour incubation with the secondary antibody. For detection we used streptavidin-HRP (Dako K1016, 10 minutes incubation at room temperature), DAB (Dako K3468) and haematoxylin counterstaining.

Immunoblotting

Cells were harvested by trypsinization, washed in PBS, lysed in RIPA buffer (50 mM Tris pH 7.5, 150 mM NaCl, 1 mM EDTA, 1 % Nonidet-P40, 0.1 % SDS, 0.5 % Na-deoxycholate and 25x Complete protease inhibitor cocktail (Roche)), incubated on ice and sonicated. Equal amounts of protein were run on NuPAGE Novex Tris-Acetate 3-8 % (w/v) (Invitrogen) according to manufacturer's instructions, followed by Western blotting.

DNA damage-induced foci detection

Cryopreserved tumor pieces were digested with 3 mg/ml collagenase A and 0.1 % trypsin for two hours at 37 °C, filtered, seeded on coverslips and irradiated with 10 Gy after 48 hours. Cell lines were grown on coverslips for 16-24 hours before irradiation. Cells were fixed 6 hours after irradiation in 2 % paraformaldehyde in PBS⁺⁺ (with 1mM CaCl₂ and 0.5 mM MgCl₂). Cells were permeabilized in 0.2 % Triton-X100/PBS⁺⁺ for 20 minutes and incubated in staining buffer (1 % BSA, 0.15 % glycine and 0.1 % Triton-X100 in PBS⁺⁺) for 30 minutes at room temperature. The staining buffer was used for all washing steps and as solvent for antibodies. Incubation with primary and secondary antibodies was done for 2 hours and 1 hour respectively at room temperature. DNA was stained with To-Pro-3 (Molecular Probes, 1:2000). Images were taken with a Leica TCS SP2 (Leica Microsystems, Heidelberg, Germany) confocal system, equipped with an Ar Diode 561 and HeNe 633 laser system. Images were taken using a 63x NA 1.32 objective. Standard LCS software was used for processing. RAD51 foci were quantified by counting them in the maximum projection of z-images. At least 100 cells were counted blindly on four different fields per slide and every cell line has been measured in two independent experiments.

Antibodies

All antibodies and their dilutions are summarized in Supplementary Table S1.

Establishment and maintenance of tumor cell lines

Tumors were harvested, minced and digested in RPMI 1640 (Gibco) supplemented with 2 % FBS (Sigma), 3 mg/ml collagenase A and 0.1 % trypsin (Gibco) for 30 minutes at 37 °C. Cells were passed through a 40 μ m cell strainer (Falcon), washed three times and seeded in DMEM/F12 (Gibco)

supplemented with 20 ng/mL bFGF (Invitrogen), 20 ng/mL EGF (Invitrogen), B-27 supplement (1:50 dilution, Invitrogen) and 4 µg/mL heparin on ultra-low attachment plates (Corning Incorporated) to grow them as mammospheres. Established mammospheres were plated in cluster plates in DMEM/F12 culture medium (with 10 % FBS, 1 % penicillin/streptomycin (Gibco), 5 µg/ml insulin (Sigma), 5 ng/ml EGF (Invitrogen) and 5 ng/ml cholera toxin (Sigma)) under low oxygen (3 %) conditions to obtain epithelial cell populations. All mammosphere-derived BRCA1-deficient cell lines were continuously cultured under low oxygen conditions.

***Trp53bp1* knock down**

Brca1^{Δ/Δ};p53^{Δ/Δ} cell lines (KB1P-B11 and KB1P-G3) were transduced with lentiviral pLKO.1-puro vectors containing non-targeting shRNA (Sigma SHC002) or one of the *Trp53bp1*-targeting hairpins (TRCN0000081778 and TRCN0000081781) from the Sigma MISSION library. Infected cells were selected by growth in medium containing 2 µg/ml (B11) or 3 µg/ml (G3) puromycin for two weeks.

Reconstitution of *Trp53bp1*

For transfection of pCMH6K-*Trp53bp1* (a gift from K. Iwabuchi, Kanazawa Medical University, Ishikawa, Japan) 1 µg DNA in DMEM was used with lipofectamine reagent (Invitrogen) according to the manufacturers' instruction. After 18-24 hours the medium was replaced by complete medium. Hygromycin B (100 µg/ml) was added to the growing cells for 4 days.

Mutation analysis

Genomic DNA was isolated from frozen tumor pieces and cell pellets with phenol/chloroform and isopropanol precipitation. RNA was extracted from tumor pieces with trizol and isopropanol precipitation and from cell pellets with the High pure RNA isolation kit (Roche 11828665001). cDNA was prepared using the First strand synthesis system (Invitrogen 18080-051). For sequencing we used the Big Dye Terminator v3.1 cycle sequencing kit (Applied Biosystems). Primers that were used to detect the rearrangement in KB1PM5 and the mutations in KB1PM8, KB1P2 and KB1P8 are depicted in Supplementary Table S2.

Clonogenic assay

To measure the effect of olaparib on the colony-forming capacity we seeded cells at low density in 6-well plates. The next day olaparib was added and the concentration of dimethylsulfoxide (DMSO) was equalized for every well. After seven days the colonies are fixed and stained with Leishman's eosin methylene blue solution (Merck 105387). All concentrations are measured in duplo and each experiment is done three times.

Array comparative genomic hybridization (aCGH)

Genomic DNA was extracted with proteinase K and phenol-chloroform, fragmented and labeled with the Klenow kit (Roche). Tumor and spleen samples were labeled with the Nimblegen dual-color DNA labeling kit and hybridized to Nimblegen 12-plex 135K full genome mouse custom NKI array. The data are analyzed with NimbleScan software.

ACKNOWLEDGMENTS

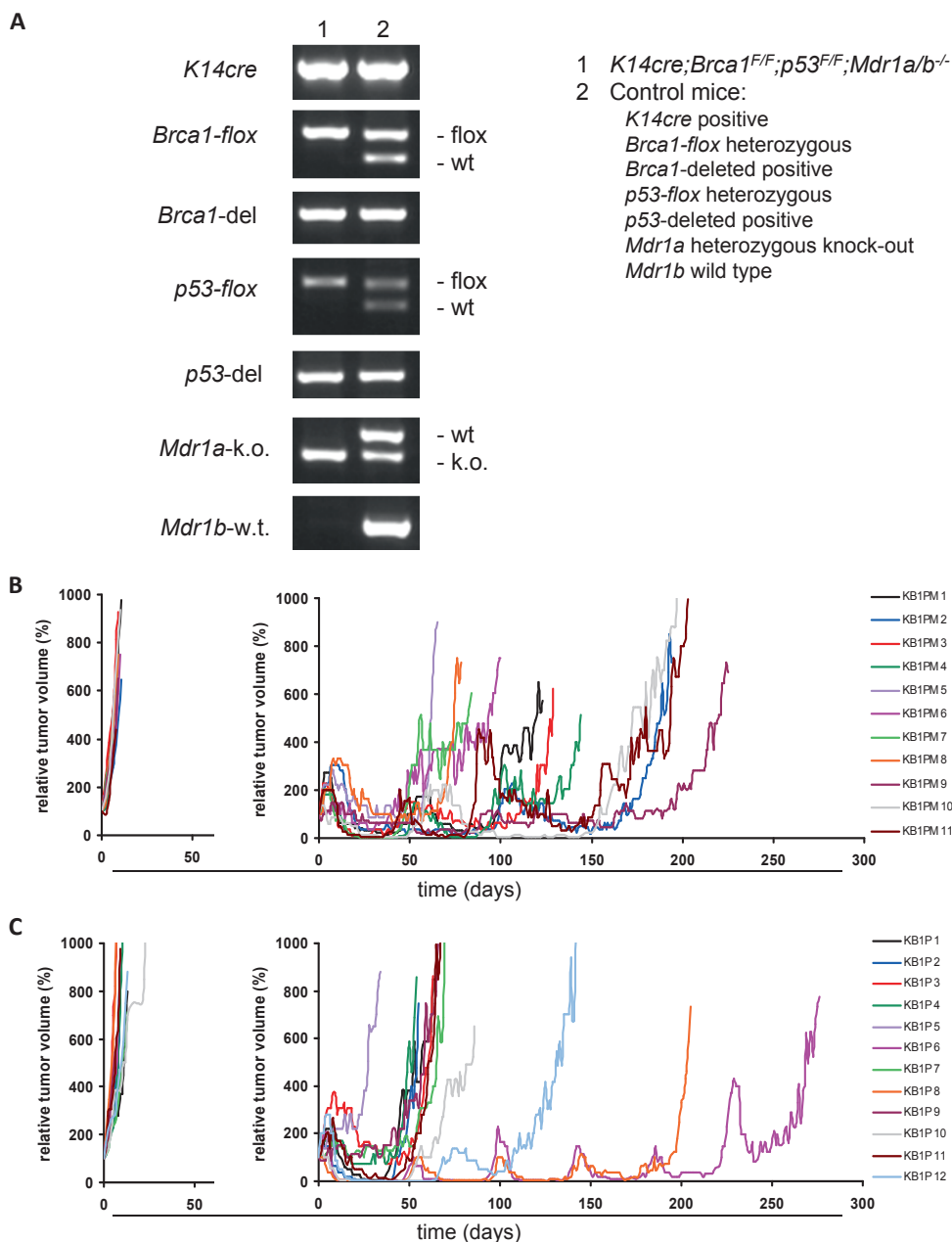
We would like to thank Anton Berns and Peter Bouwman for critical reading of the manuscript; Susan Bates from the National Institutes of Health, Bethesda, MD, for providing tariquidar; and Thijs Siegenbeek van Heukelom and Marieke Haenen for technical support. This work was supported by grants from the Netherlands Organization for Scientific Research (NWO-Toptalent 021.002.104 to J.E.J. and NWO-VIDI-91711302 to S.R.); the Dutch Cancer Society (projects NKI 2006-3566, NKI 2007-3772, NKI 2009-4303, and NKI 2011-5220); the European Union (EU) FP6 Integrated Project 037665-CHEMORES; the EU FP7 Project 260791-EurocanPlatform; CTMM Breast Care; and the NKI-AVL Cancer Systems Biology Centre.

REFERENCES

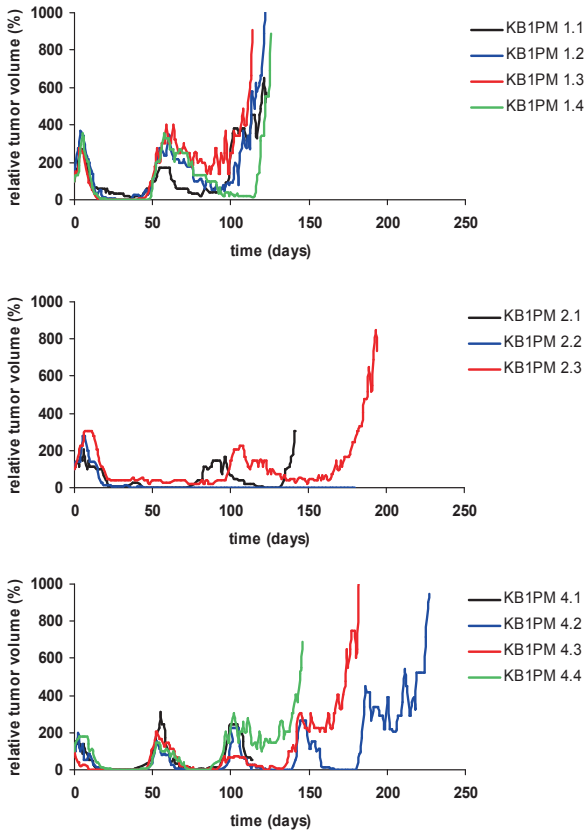
- 1 Bryant HE, Schultz N, Thomas HD, Parker KM, Flower D, Lopez E *et al.* Specific killing of BRCA2-deficient tumours with inhibitors of poly(ADP-ribose) polymerase. *Nature* 2005;434:913-7.
- 2 Farmer H, McCabe N, Lord CJ, Tutt AN, Johnson DA, Richardson TB *et al.* Targeting the DNA repair defect in BRCA mutant cells as a therapeutic strategy. *Nature* 2005;434:917-21.
- 3 McCabe N, Turner NC, Lord CJ, Kluzek K, Bialkowska A, Swift S *et al.* Deficiency in the repair of DNA damage by homologous recombination and sensitivity to poly(ADP-ribose) polymerase inhibition. *Cancer Res* 2006;66:8109-15.
- 4 Audeh MW, Carmichael J, Penson RT, Friedlander M, Powell B, Bell-McGuinn KM *et al.* Oral poly(ADP-ribose) polymerase inhibitor olaparib in patients with BRCA1 or BRCA2 mutations and recurrent ovarian cancer: a proof-of-concept trial. *Lancet* 2010;376:245-51.
- 5 Evers B, Schut E, van der Burg E, Braumuller TM, Egan DA, Holstege H *et al.* A high-throughput pharmaceutical screen identifies compounds with specific toxicity against BRCA2-deficient tumors. *Clin Cancer Res* 2010;16:99-108.
- 6 Fong PC, Boss DS, Yap TA, Tutt A, Wu P, Mergui-Roelvink M *et al.* Inhibition of poly(ADP-ribose) polymerase in tumors from BRCA mutation carriers. *N Engl J Med* 2009;361:123-34.
- 7 Hay T, Matthews JR, Pietzka L, Lau A, Cranston A, Nygren AO *et al.* Poly(ADP-ribose) polymerase-1 inhibitor treatment regresses autochthonous Brca2/p53-mutant mammary tumors in vivo and delays tumor relapse in combination with carboplatin. *Cancer Res* 2009;69:3850-5.
- 8 Menear KA, Adcock C, Boulter R, Cockcroft XL, Copley L, Cranston A *et al.* 4-[3-(4-cyclopropanecarbonylpiperazine-1-carbonyl)-4-fluorobenzyl]-2H-phth alazin-1-one: a novel bioavailable inhibitor of poly(ADP-ribose) polymerase-1. *J Med Chem* 2008;51:6581-91.
- 9 Rottenberg S, Jaspers JE, Kersbergen A, van der Burg E, Nygren AO, Zander SA *et al.* High sensitivity of BRCA1-deficient mammary tumors to the PARP inhibitor AZD2281 alone and in combination with platinum drugs. *Proc Natl Acad Sci U S A* 2008;105:17079-84.

- 10 Tutt A, Robson M, Garber JE, Domchek SM, Audeh MW, Weitzel JN *et al.* Oral poly(ADP-ribose) polymerase inhibitor olaparib in patients with BRCA1 or BRCA2 mutations and advanced breast cancer: a proof-of-concept trial. *Lancet* 2010;376:235-44.
- 11 Liu X, Holstege H, van der Gulden H, Treur-Mulder M, Zevenhoven J, Velds A *et al.* Somatic loss of BRCA1 and p53 in mice induces mammary tumors with features of human BRCA1-mutated basal-like breast cancer. *Proc Natl Acad Sci U S A* 2007;104:12111-6.
- 12 Rottenberg S, Nygren AO, Pajic M, van Leeuwen FW, van der Heijden I, van de Wetering K *et al.* Selective induction of chemotherapy resistance of mammary tumors in a conditional mouse model for hereditary breast cancer. *Proc Natl Acad Sci U S A* 2007;104:12117-22.
- 13 Oplustilova L, Rulten SL, Cranston AN, Odedra R, Jaspers JE, Jones L *et al.* Characterisation of a novel PARP inhibitor AZD2461 that overcomes the P-glycoprotein resistance associated with olaparib and demonstrates differential activity against PARP-3. 2012. Manuscript in preparation
- 14 Borst P. Cancer drug pan-resistance: pumps, cancer stem cells, quiescence, epithelial to mesenchymal transition, blocked cell death pathways, persists or what? *Open Biol* 2012;2:120066.
- 15 Drost R, Bouwman P, Rottenberg S, Boon U, Schut E, Klarenbeek S *et al.* BRCA1 RING Function Is Essential for Tumor Suppression but Dispensable for Therapy Resistance. *Cancer Cell* 2011;20:797-809.
- 16 Edwards SL, Brough R, Lord CJ, Natrajan R, Vatcheva R, Levine DA *et al.* Resistance to therapy caused by intragenic deletion in BRCA2. *Nature* 2008;451:1111-5.
- 17 Sakai W, Swisher EM, Karlan BY, Agarwal MK, Higgins J, Friedman C *et al.* Secondary mutations as a mechanism of cisplatin resistance in BRCA2-mutated cancers. *Nature* 2008;451:1116-20.
- 18 Norquist B, Wurz KA, Pennil CC, Garcia R, Gross J, Sakai W *et al.* Secondary Somatic Mutations Restoring BRCA1/2 Predict Chemotherapy Resistance in Hereditary Ovarian Carcinomas. *J Clin Oncol* 2011;29:3008-15.
- 19 Swisher EM, Sakai W, Karlan BY, Wurz K, Urban N, Taniguchi T. Secondary BRCA1 mutations in BRCA1-mutated ovarian carcinomas with platinum resistance. *Cancer Res* 2008;68:2581-6.
- 20 Schinkel AH, Mayer U, Wagenaar E, Mol CA, van Deemter L, Smit JJ *et al.* Normal viability and altered pharmacokinetics in mice lacking mdr1-type (drug-transporting) P-glycoproteins. *Proc Natl Acad Sci U S A* 1997;94:4028-33.
- 21 Schinkel AH, Smit JJ, van Tellingen O, Beijnen JH, Wagenaar E, van Deemter L *et al.* Disruption of the mouse mdr1a P-glycoprotein gene leads to a deficiency in the blood-brain barrier and to increased sensitivity to drugs. *Cell* 1994;77:491-502.
- 22 Bouwman P, Aly A, Escandell JM, Pieterse M, Bartkova J, van der Gulden H *et al.* 53BP1 loss rescues BRCA1 deficiency and is associated with triple-negative and BRCA-mutated breast cancers. *Nat Struct Mol Biol* 2010;17:688-95.
- 23 Bunting SF, Callen E, Wong N, Chen HT, Polato F, Gunn A *et al.* 53BP1 inhibits homologous recombination in Brca1-deficient cells by blocking resection of DNA breaks. *Cell* 2010;141:243-54.
- 24 Zander SA, Kersbergen A, van der Burg E, de Water N, van Tellingen O, Gunnarsdottir S *et al.* Sensitivity and acquired resistance of BRCA1;p53-deficient mouse mammary tumors to the topoisomerase I inhibitor topotecan. *Cancer Res* 2010;70:1700-10.
- 25 Singh A, Settleman J. EMT, cancer stem cells and drug resistance: an emerging axis of evil in the war on cancer. *Oncogene* 2010;29:4741-51.
- 26 Huertas P, Cortes-Ledesma F, Sartori AA, Aguilera A, Jackson SP. CDK targets Sae2 to control DNA-end resection and homologous recombination. *Nature* 2008;455:689-92.
- 27 Huertas P, Jackson SP. Human CtIP mediates cell cycle control of DNA end resection and double strand break repair. *J Biol Chem* 2009;284:9558-65.
- 28 Yun MH, Hiom K. CtIP-BRCA1 modulates the choice of DNA double-strand-break repair pathway throughout the cell cycle. *Nature* 2009;459:460-3.
- 29 Helleday T. The underlying mechanism for the PARP and BRCA synthetic lethality: Clearing up the misunderstandings. *Mol Oncol* 2011.
- 30 Bunting SF, Callen E, Kozak ML, Kim JM, Wong N, Lopez-Contreras AJ *et al.* BRCA1 functions independently of homologous recombination in DNA interstrand crosslink repair. *Mol Cell* 2012;46:125-35.

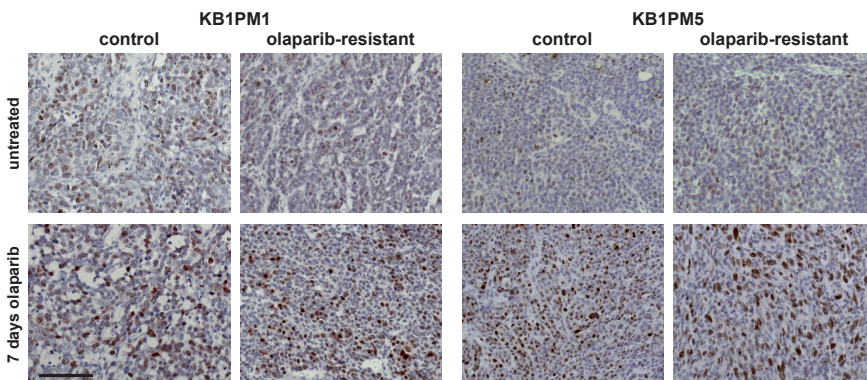
- 31 Schlacher K, Wu H, Jasin M. A Distinct Replication Fork Protection Pathway Connects Fanconi Anemia Tumor Suppressors to RAD51-BRCA1/2. *Cancer Cell* 2012;22:106-16.
- 32 Garcia-Higuera I, Taniguchi T, Ganesan S, Meyn MS, Timmers C, Hejna J *et al.* Interaction of the Fanconi anemia proteins and BRCA1 in a common pathway. *Mol Cell* 2001;7:249-62.
- 33 Vandenberg CJ, Gergely F, Ong CY, Pace P, Mallery DL, Hiom K *et al.* BRCA1-independent ubiquitination of FANCD2. *Mol Cell* 2003;12:247-54.
- 34 Patel AG, Sarkaria JN, Kaufmann SH. Nonhomologous end joining drives poly(ADP-ribose) polymerase (PARP) inhibitor lethality in homologous recombination-deficient cells. *Proc Natl Acad Sci U S A* 2011;108:3406-11.
- 35 Navin N, Kendall J, Troge J, Andrews P, Rodgers L, McIndoo J *et al.* Tumour evolution inferred by single-cell sequencing. *Nature* 2011;472:90-4.
- 36 Li X, Delzer J, Voorman R, de Morais SM, Lao Y. Disposition and drug-drug interaction potential of veliparib (ABT-888), a novel and potent inhibitor of poly(ADP-ribose) polymerase. *Drug Metab Dispos* 2011;39:1161-9.
- 37 Ledermann JA, Harter P, Gourley C, Friedlander M, Vergote IB, Rustin GJS *et al.* Phase II randomized placebo-controlled study of olaparib (AZD2281) in patients with platinum-sensitive relapsed serous ovarian cancer (PSR SOC). ASCO Annual Meeting, Abstract 5003. 2011.
- 38 Integrated genomic analyses of ovarian carcinoma. *Nature* 2011;474:609-15.
- 39 Kinders RJ, Hollingshead M, Khin S, Rubinstein L, Tomaszewski JE, Doroshow JH *et al.* Preclinical modeling of a phase 0 clinical trial: qualification of a pharmacodynamic assay of poly (ADP-ribose) polymerase in tumor biopsies of mouse xenografts. *Clin Cancer Res* 2008;14:6877-85.
40 http://dctd.cancer.gov/ResearchResources/biomarkers/docs/par/SOP340520_Biopsy_Tissue.pdf.
- 41 http://dctd.cancer.gov/ResearchResources/biomarkers/docs/par/SOP340505_PAR_IA.pdf.



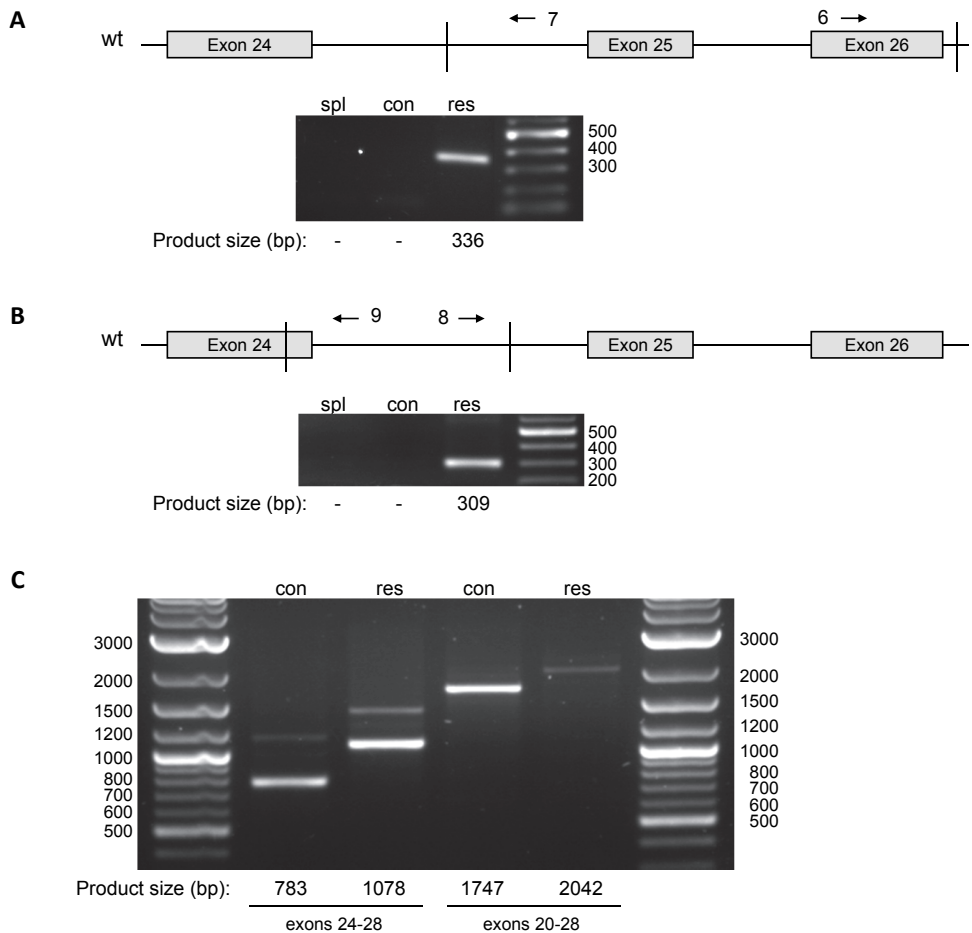
Supplementary Figure S1. A, genotyping PCR of genomic tail DNA from a *K14cre;Brca1^{F/F};p53^{F/F};Mdr1a/b^{-/-}* mouse (left lanes) and controls (right lanes). **B-C**, response curves of untreated tumors (left panels) and when treated with olaparib (50 mg/kg i.p., daily for 28 days). Figure **B** shows the response of 11 individual *Brca1^{Δ/Δ};p53^{Δ/Δ};Mdr1a/b^{-/-}* tumors (KB1PM) and figure **C** shows the response of 12 individual *Brca1^{Δ/Δ};p53^{Δ/Δ}* tumors (KB1P). The treatment of 28 consecutive days with olaparib was repeated when a tumor relapsed and reached the size of 200 mm³ (100 %).



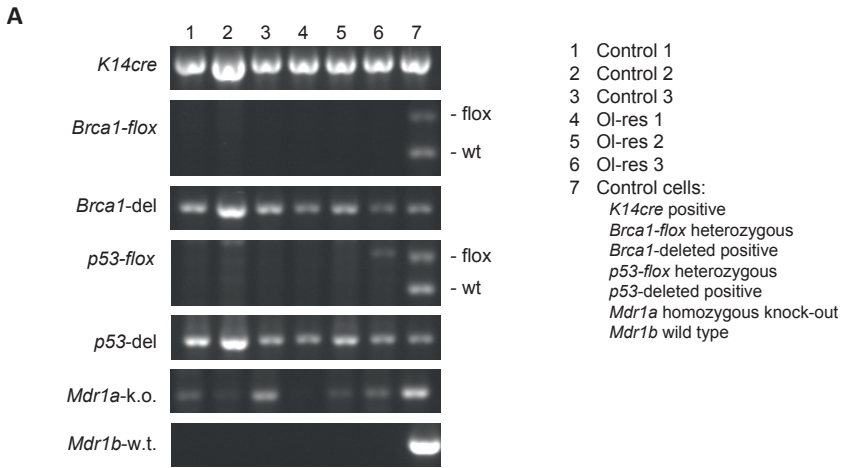
Supplementary Figure S2. Response of three or four tumors that originate from the same KB1PM donor tumor to olaparib (50 mg/kg i.p., daily for 28 days). The treatment of 28 consecutive days with olaparib was repeated when a tumor relapsed and reached the size of 200 mm³ (100 %).



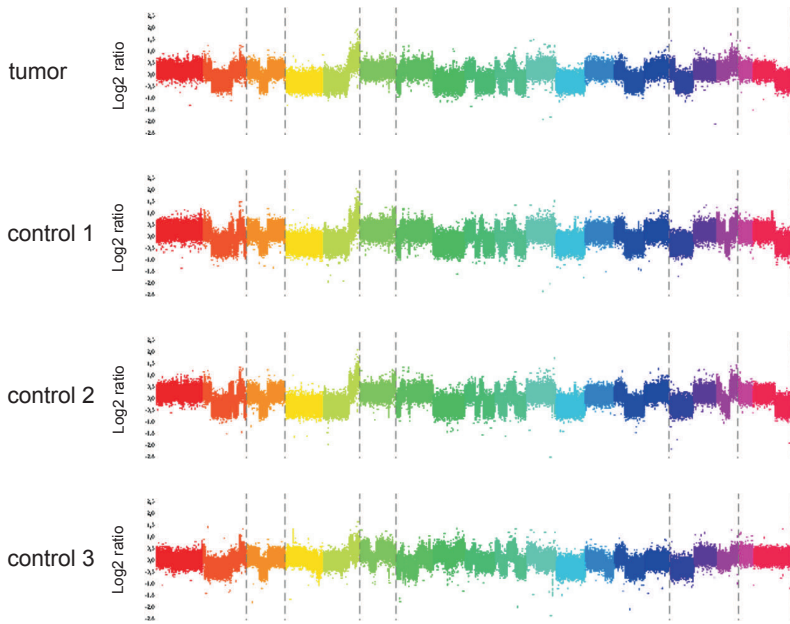
Supplementary Figure S3. γ H2AX immunohistochemistry after 7 days of PARP inhibition in control and olaparib-resistant tumors from KB1PM1 and 5. Tumors shown in the bottom row were treated daily for 7 days with olaparib (50 mg/kg i.p.) and the tumors were harvested 2 hours after the last treatment. Scale bar = 100 μ m.



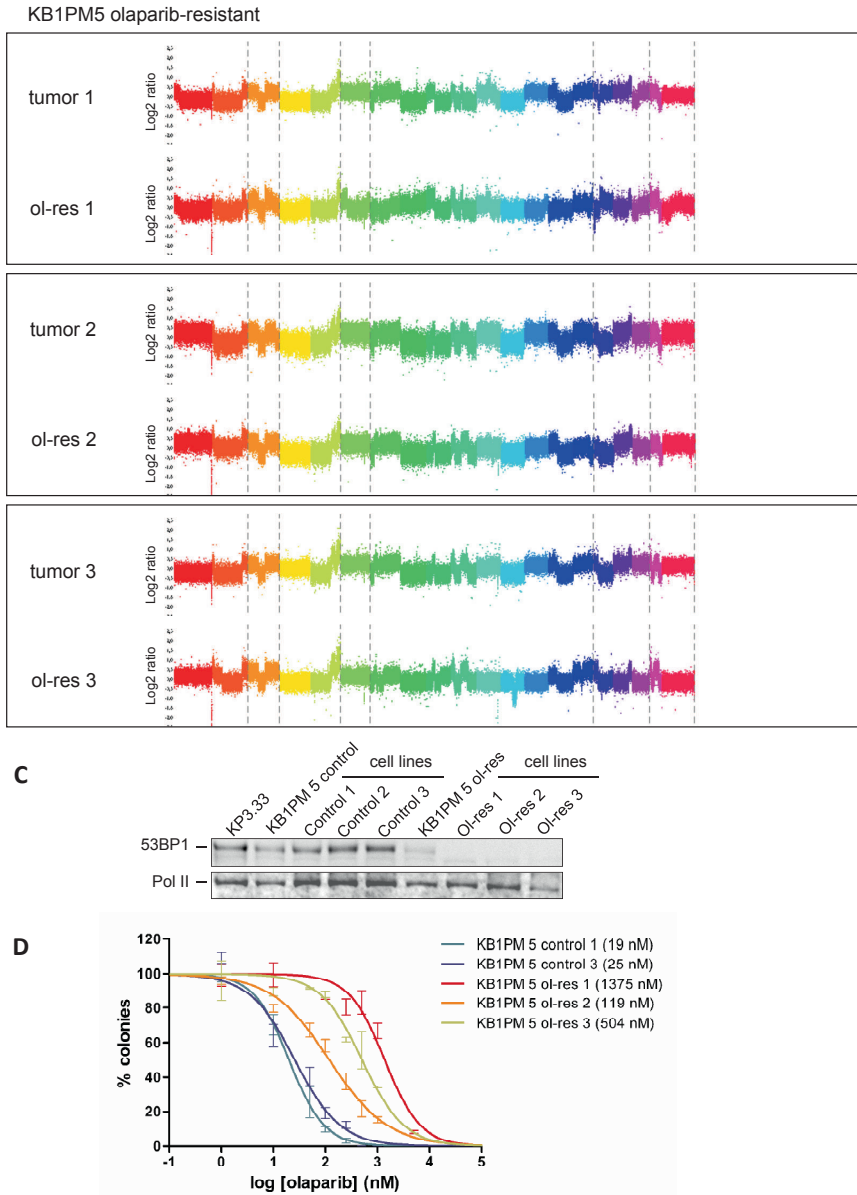
Supplementary Figure S4. To prevent stromal contamination we analyzed the mutations in the cell lines derived from the control and olaparib-resistant tumor of KB1PM5. **A-B**, PCR reactions on the genomic DNA of the spleen (spl), KB1PM5 cell line Control 3 (con) and Ol-res 2 (res) showing a rearrangement in *Trp53bp1* of exon 26 and intron 24 (**A**) and of exon 24 and intron 24 (**B**). **C**, PCR reactions on cDNA showed absence of the wild-type sequence in the resistant cells. Sequencing showed an exact duplication of exons 25 and 26 (295 bp, see also Figure 3C). For the primers that were used, see Supplementary Table S1.



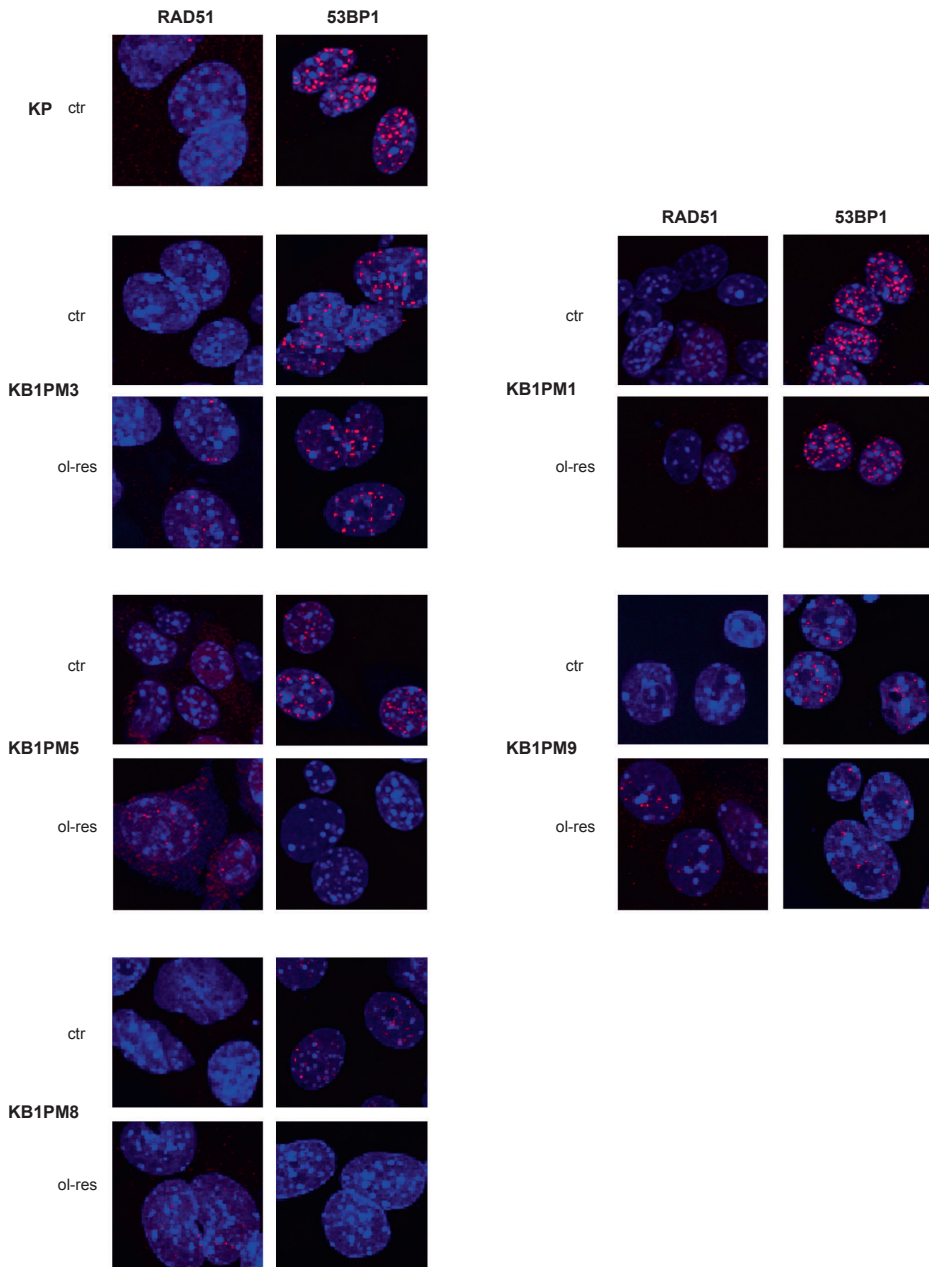
B KB1PM5 control



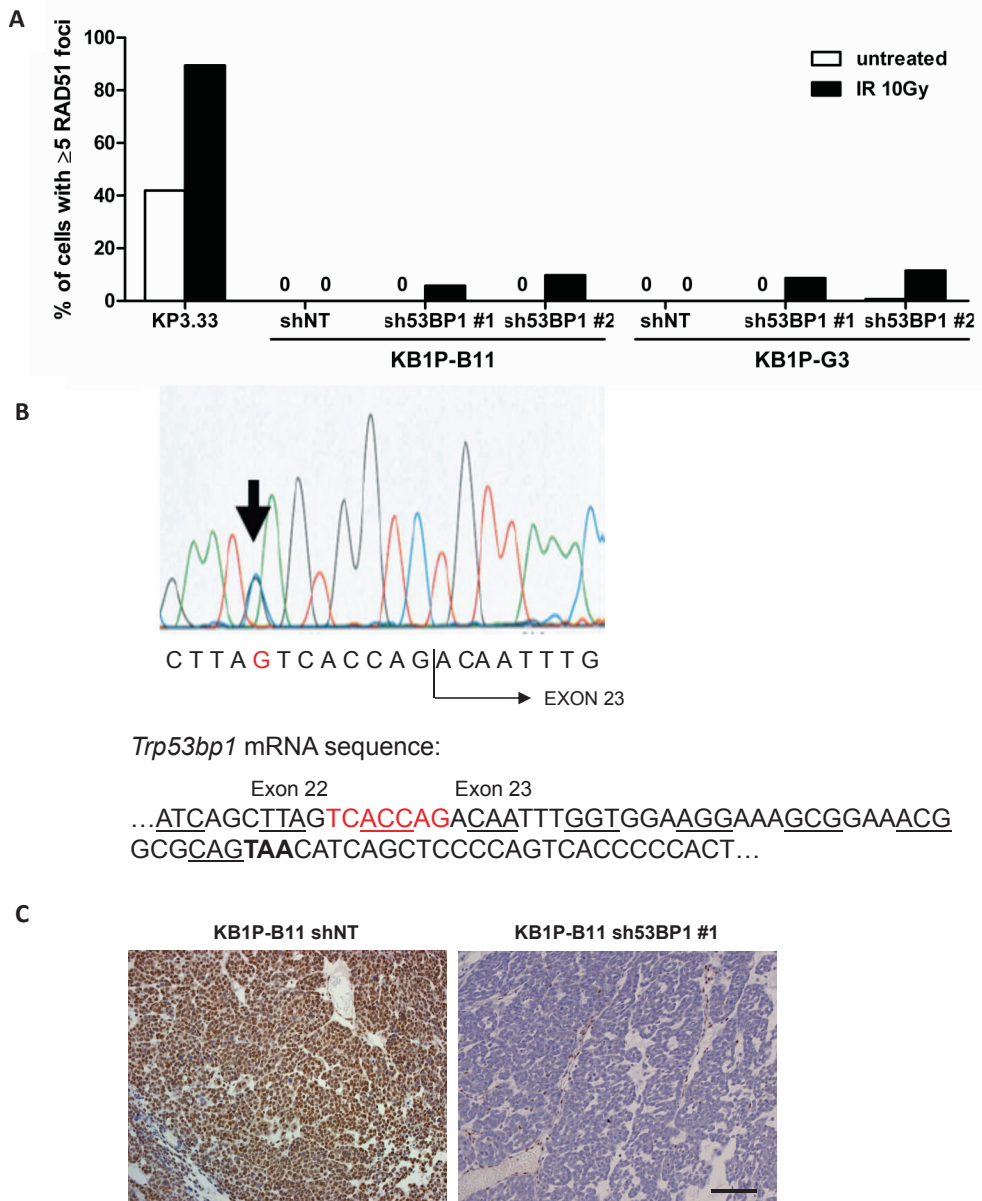
Supplementary Figure S5.



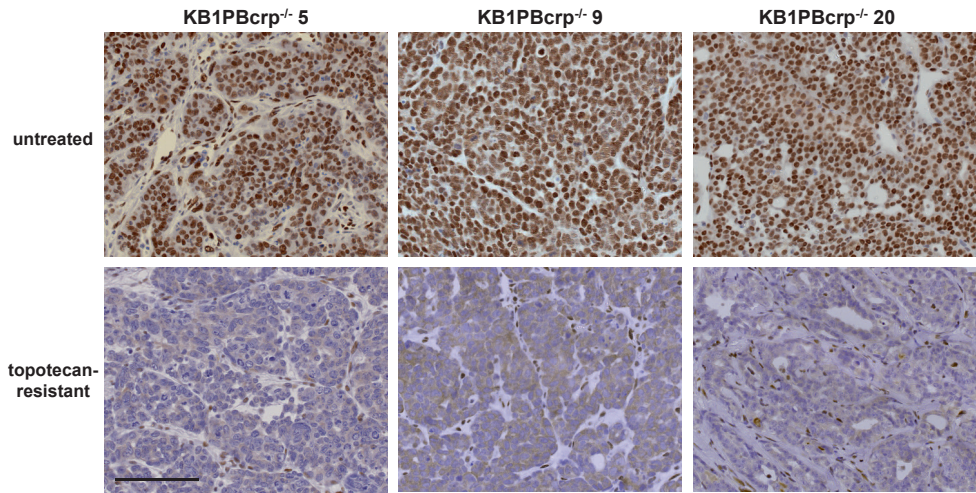
Supplementary Figure S5 Continued. **A**, genotyping PCR to confirm that the cell lines are derived from the KB1PM tumor cells and not contaminated with stromal cells. All six cell lines have deletions in *Brca1*, *p53* and *Mdr1a/b*, and have completely lost the flox bands of *Brca1* and *p53*, indicating complete Cre-mediated deletion in all cells. **B**, comparative genomic hybridization shows that the cell lines are highly similar to the tumor that they were derived from. The spleen from the *K14cre;Brca1^{F/F};p53^{F/F};Mdr1a/b^{-/-}* mouse that produced tumor KB1PM5 was used as reference DNA. **C**, the cell lines derived from olaparib-resistant tumor KB1PM5 are negative for 53BP1, whereas the cell lines from the control tumor express 53BP1. **D**, clonogenic assay for olaparib with tumor-derived cell lines. The IC₅₀ is indicated between brackets.



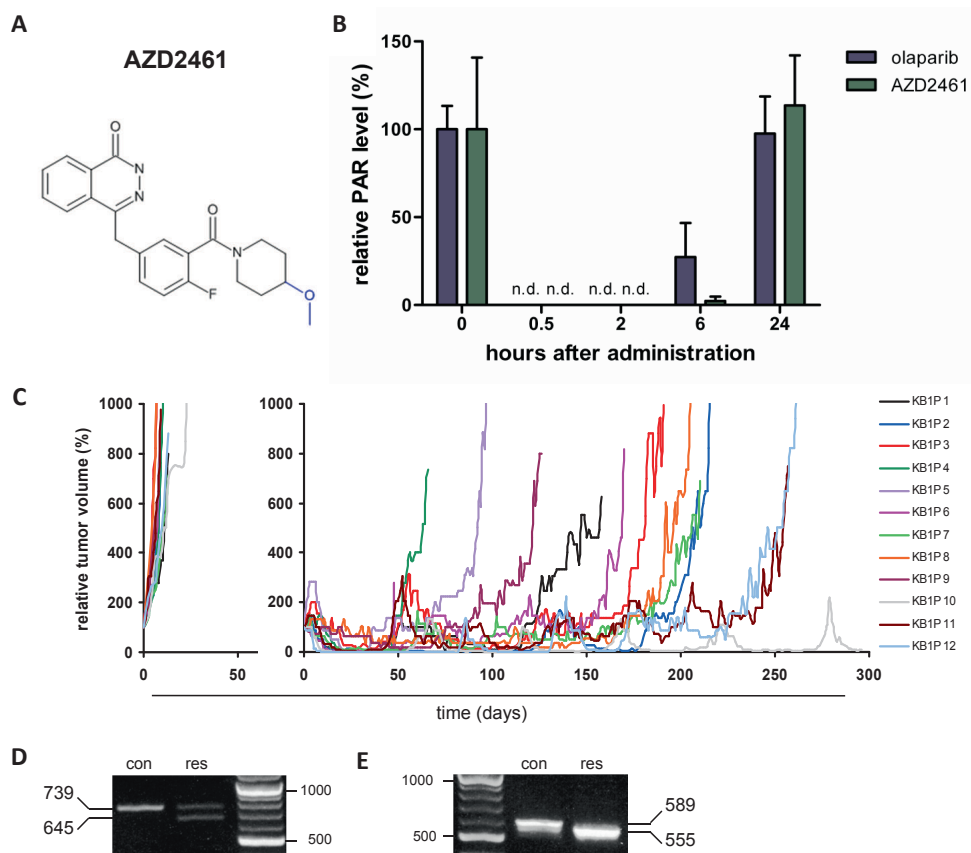
Supplementary Figure S6. Images of RAD51 and 53BP1 IRIFs measured 6 hours after irradiation with 10 Gy in short-term tumor cell suspension of a KP tumor and the control (ctr) and olaparib-resistant (ol-res) tumors of 5 KB1PM donors. Quantification of the RAD51 foci is presented in Figure 4C.



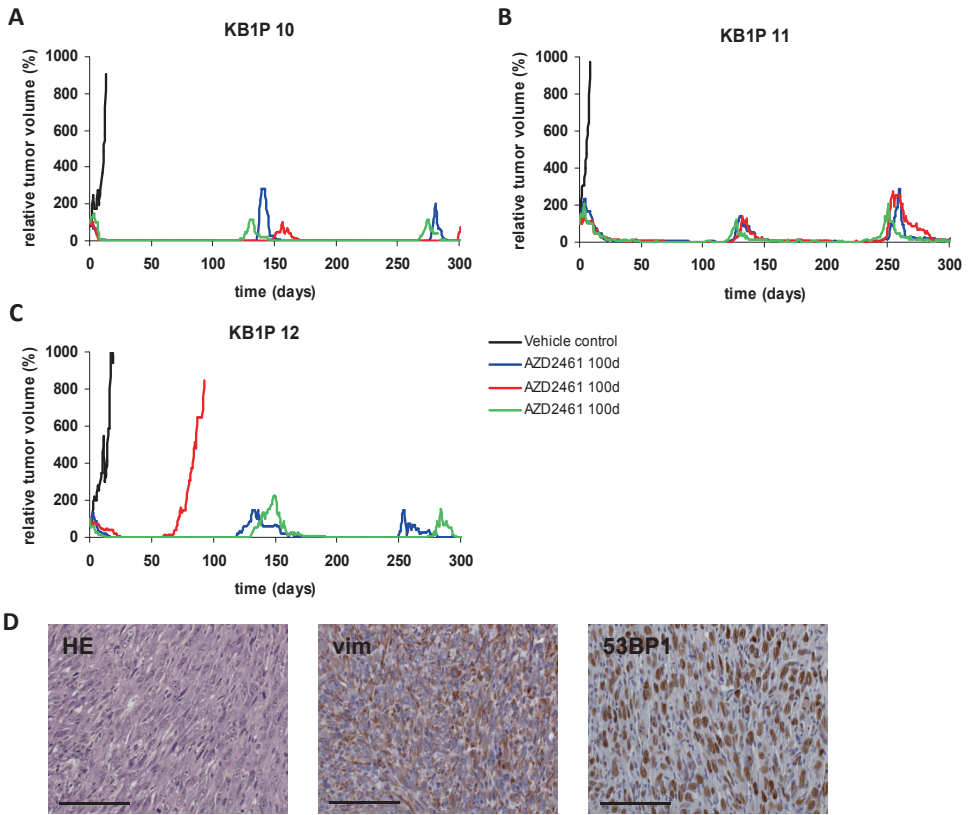
Supplementary Figure S7. A, Quantification of RAD51 IRIFs in KP cells and two KB1P cell lines expressing a non-targeting hairpin (shNT) or two different hairpins against 53BP1 (sh53BP1 #1 and #2). Cells were fixed 6 hours after irradiation with 10 Gy. **B**, spontaneous point mutation in intron 22 of *Trp53bp1* in KB1P-3.12 cells resulting in a cryptic splice acceptor site and the resulting mRNA sequence. The extra seven base pairs are highlighted in red. The alternating codons are underlined and the premature stop codon is indicated in bold. **C**, 53BP1 protein in tumors that grew out upon orthotopic transplantation of KB1P-B11 cells expressing either a non-targeting hairpin (shNT) or a hairpin against 53BP1 (sh53BP1 #1). Scale bar = 100 μ m.



Supplementary Figure S8. Absence of 53BP1 was detected in three *Brca1*^{Δ/Δ};*p53*^{Δ/Δ};*Bcrp*^{-/-} tumors that have acquired resistance to topotecan. Scale bar = 100 μm.



Supplementary Figure S9. A, chemical structure of AZD2461. **B**, pharmacodynamics of olaparib and AZD2461. PAR levels measured at several time points after a single administration of olaparib (50 mg/kg i.p.) or AZD2461 (100 mg/kg p.o.). At the indicated time points tumors were harvested and snap frozen. PAR levels were measured in whole tumor extracts with an ELISA. n.d. = not detectable (lower than 2*SD above background). Data are presented as mean+SD of five tumors per time point per treatment. **C**, response curves of 12 individual *Brca1*^{Δ/Δ};*p53*^{Δ/Δ} tumors (KB1P) tumors that were untreated (left panel) or treated with AZD2461 (100 mg/kg p.o., daily for 28 days). The treatment of 28 days with AZD2461 was repeated when the tumor relapsed and reached the size of 200 mm³ (100 %). **D**, PCR (primers 14 and 15) on genomic DNA of the control (con) and AZD2461-resistant (res) tumors KB1P2, showing a deletion in exon 21 of *Trp53bp1* in the AZD2461-resistant tumor, which has been confirmed by Sanger sequencing (see Figure 6E). **E**, PCR (primers 18 and 19) on genomic DNA of the control (con) and AZD2461-resistant (res) tumors KB1P8, showing a deletion at the border of intron 24 and exon 25 in *Trp53bp1* in the AZD2461-resistant tumor, which has been confirmed by Sanger sequencing (see Figure 6F).



Supplementary Figure S10. A-C, response of tumors from three individual donor tumors (KB1P 10-12) to 100 days of daily treatment with AZD2461 (100 mg/kg p.o.). The treatment of 100 days was repeated when the tumor relapsed and reached the size of 200 mm³ (100 %). Except one tumor (KB1P12-2) that acquired resistance during the first treatment cycle, all other tumors respond to three cycles of 100 days AZD2461. **D**, histology and immunohistochemical staining of vimentin and 53BP1 of the KB1P12-2 tumor that acquired resistance to AZD2461 during the first treatment cycle of 100 days (see red curve in (C)). HE = hematoxylin eosin, vim = vimentin. Scale bar = 100 μ m.

Supplementary Table S1. Primary and secondary antibodies that were used in this study

Antigen	Application	Antibody	Manufacturer	Dilution
53BP1	Western blotting (Fig. 5A and S4C)	1. rabbit-polyclonal	Abcam ab21083	1:1000
		2. goat-anti-rabbit-HRP	Dako P0448	1:1000
53BP1	Western blotting (Fig. 5C)	1. mouse-monoclonal	Chemicon International MAB3804	1:500
pol II	Western blotting	1. goat-polyclonal	Santa Cruz sc 5943	1:200
		2. rabbit-anti-goat-HRP	Dako P0160	1:1000
HA-tag	Western blotting	1. rabbit-polyclonal	Sigma H6908	1:500
BRCA1	Western blotting	1. rabbit-polyclonal	Upstate 07-434	1:500
actin	Western blotting	1. rabbit-polyclonal	Sigma A2066	1:200
RAD51	Immunofluorescence	1. rabbit-polyclonal	Santa Cruz sc8349	1:500
		2. goat-anti-rabbit-Alexa568	Molecular Probes A11011	1:400
53BP1	Immunofluorescence	1. rabbit-polyclonal	Bethyl A300-272A	1:4000
		2. goat-anti-rabbit-Alexa568	Molecular Probes A11011	1:400
γH2AX	Immunofluorescence	1. rabbit-polyclonal	Cell Signaling 2577	1:200
		2. goat-anti-rabbit-Alexa568	Molecular Probes A11011	1:400
γH2AX	Immunohistochemistry	1. rabbit-polyclonal	Cell Signaling 2577	1:50
		2. goat-anti-rabbit-biotin	Dako E043201	1:800
53BP1	Immunohistochemistry	1. rabbit-polyclonal	Bethyl A300-272A	1:1000
		2. goat-anti-rabbit-biotin	Dako E043201	1:800
vimentin	Immunohistochemistry	1. guinea pig-monoclonal	Research Diagnostics Inc. RDI	1:400
		2. goat-anti-guinea pig-biotin	Jackson ImmunoResearch Inc.	1:500

Supplementary Table S2. Overview of all primers that were used in this study

	Sequence (5' → 3')	Direction	Target	Application
1	GGCACCGGTGTGTGAGGAAG	Forward	exon 20	PCR cDNA KB1PM5
2	GGCAGCAGAGTTTGTGAGTC	Forward	exon 24	PCR cDNA KB1PM5
3	TCCAGTGCCTCATTGTTGGGGAGAG	Reverse	exon 28	PCR cDNA KB1PM5
4	CAGAGTTTGTGAGTC CCTGT	Forward	exon 24	sequencing PCR product cDNA KB1PM5
5	CACAAGAATGGGTGATCCAG	Reverse	exon 28	sequencing PCR product cDNA KB1PM5
6	GTCTCCTAATTGCGGACCAG	Forward	exon 26	PCR genomic DNA KB1PM5
7	CTGCCAGTGCCTAGCAAATA	Reverse	intron 24	PCR genomic DNA KB1PM5
8	TGGCATCTGCCTAGTGTCTG	Forward	intron 24	PCR genomic DNA KB1PM5
9	AGATGGTCTTGGTAGGCAGC	Reverse	intron 24	PCR genomic DNA KB1PM5
10	GCAGGACGACCAGGTAGAAA	Forward	exon 12	PCR genomic DNA KB1PM8
11	TCCATAGCTTCTGGGCATTC	Reverse	exon 12	PCR genomic DNA KB1PM8
12	GAAACGAGGACAGAGGTGA	Forward	exon 12	sequencing PCR product gDNA KB1PM8
13	CTTCTGGGCATTCTCTTTG	Reverse	exon 12	sequencing PCR product gDNA KB1PM8
14	ACAGGGGCACCGGTGTGTGA	Forward	exon 20	PCR genomic DNA KB1P2
15	CGTGACAGGAGGGAACAGCAGG	Reverse	intron 21	PCR genomic DNA KB1P2
16	CCGCCACCTTCTCGGACCA	Forward	exon 20	Sequencing PCR product gDNA KB1P2
17	ACAGGAGGGAACAGCAGGCACA	Reverse	intron 21	Sequencing PCR product gDNA KB1P2
18	TGGCATCTGCCTAGTGTCTG	Forward	intron 24	PCR genomic DNA KB1P8
19	AATGCCACTGGCAAGGCACAG	Reverse	exon 26	PCR genomic DNA KB1P8
20	CGTGTGGCTTGCAACAGA	Forward	intron 24	Sequencing PCR product gDNA KB1P8
21	CACACTGGCACATTACCCTGCACT	Reverse	intron 25	Sequencing PCR product gDNA KB1P8

CHAPTER 4



Multi-drug resistance of sarcomatoid BRCA2-deficient mouse mammary tumors

Janneke E. Jaspers^{1,2}, Wendy Sol¹, Ariena Kersbergen¹, Andreas Schlicker³, Charlotte Guyader¹,
Guotai Xu¹, Lodewyk Wessels³, Piet Borst¹, Jos Jonkers², Sven Rottenberg¹

¹Divisions of Molecular Oncology, ²Molecular Pathology and ³Molecular Carcinogenesis,
Netherlands Cancer Institute, Plesmanlaan 121, 1066 CX Amsterdam, The Netherlands

Manuscript in preparation

ABSTRACT

Pan- or multi-drug resistance is a central problem in clinical oncology. Here we use a genetically engineered mouse model of BRCA2-associated hereditary breast cancer to study drug resistance to several types of chemotherapy and PARP inhibition. We found that multi-drug resistance was strongly associated with an EMT-like sarcomatoid phenotype and high expression of the drug efflux transporters P-glycoprotein and BCRP. Inhibition of P-glycoprotein could partly re-sensitize sarcomatoid tumors to the PARP inhibitor olaparib, docetaxel and doxorubicin. We propose that multi-drug resistance is a multi-factorial process and that mouse models are useful to unravel this.

INTRODUCTION

A major clinical problem in cancer therapy is resistance of tumors to all available therapies, a phenomenon called pan-resistance¹. The frequently used term “multi-drug resistance” historically refers to resistance due to drug efflux transporters. After an initial response primary tumors and especially metastases do not respond anymore to treatment, including radiotherapy. Drug resistance is not only a problem for classical chemotherapeutics, but also for targeted therapeutics. Mechanisms can be drug specific, such as imatinib resistance caused by mutations in or overexpression of the drug target BCR-ABL² or down-regulation of *Top1* or *Top2* causing resistance to topoisomerase I or II poisons³. The precise mechanisms that cause resistance of tumors to multiple classes of drugs are not fully understood. One mechanism that has been put forward to explain pan-resistance of various types of cancer is epithelial-to-mesenchymal transition (EMT)^{1,4}. During EMT cells lose epithelial characteristics and acquire mesenchymal characteristics. EMT is a physiological process involved in, for example, embryogenesis and wound healing, but it has also been described for epithelial cancers when cells acquire a spindle-shaped (also called ‘mesenchymal’ or ‘sarcomatoid’) morphology and lose expression of cell adhesion molecules. *In vitro*, EMT was observed in various cell lines that acquired resistance to chemotherapeutic agents and targeted inhibitors^{5–12} and induction of EMT by recombinant TGF β treatment led to resistance tyrosine kinase inhibitors and cisplatin¹³, suggesting a role of EMT in pan-resistance.

Breast cancer is a heterogeneous disease, which comprises different histologic and molecular subtypes¹⁴. Among these is the subgroup of metaplastic breast cancer, a variant of triple-negative breast cancer, which includes different morphologic entities, including spindle-shaped tumor cells^{14–16}. A molecular subtype that is frequently observed in metaplastic cancers is the claudin-low signature^{17,18}. Since metaplastic cancers have a poor prognosis, we wondered whether EMT may contribute to poor drug response of these tumors.

To study the influence of EMT on pan-resistance, we made use of a unique mouse model of BRCA2-deficient breast cancer, *i.e.* the *K14cre;Brca2^{F/F};p53^{F/F}* mammary tumor model¹⁹. Female *K14cre;Brca2^{F/F};p53^{F/F}* mice develop mostly epithelial mammary carcinomas but also mesenchymal carcinosarcomas are formed. Since the K14 promoter drives Cre expression in epithelial cells¹⁹, it is conceivable that these mesenchymal mammary tumors originate from an epithelial-to-mesenchymal transition. The advantage of such an *in vivo* model is that no cell lines have to be used, which may be a poor representation of the original tumor²⁰. We and others have previously shown that the BRCA2-deficient mouse mammary tumors are sensitive to DNA damage-inducing drugs and PARP inhibitors due to deficiency in error-free repair of double strand DNA breaks by homologous recombination^{21–25}. In BRCA2-deficient breast cancer patients such an increased sensitivity was also observed after neoadjuvant

therapy with DNA-damaging agents^{26,27} or PARP inhibitors²⁸. We investigated whether this drug sensitivity is diminished in BRCA2-deficient carcinosarcomas. For this purpose, we compared the responses of epithelial carcinomas and mesenchymal carcinosarcomas to chemotherapy drugs and PARP inhibitors. We found that BRCA2-deficient carcinosarcomas are multi-drug resistant, which was, at least in part, due to high expression of the drug efflux transporters P-glycoprotein (Pgp) and breast cancer resistance protein (BCRP), which have affinity for a wide range of chemotherapeutic and targeted agents. In addition, we found that an EMT-like gene expression profile correlates with Pgp expression in multiple independent mouse mammary tumor data sets.

RESULTS

Two main mammary tumor phenotypes are produced in *K14cre;Brca2^{F/F};p53^{F/F}* mice

To study the effect of a mesenchymal morphology on therapy response we made use of the *K14cre;Brca2^{F/F};p53^{F/F}* mouse model¹⁹. K14cre-mediated deletion of exon 11 of *Brca2* and exon 2-10 of *Trp53* in mammary epithelial cells results in the development of mammary tumors with an average latency of 181 days. We used an established orthotopic transplantation model to study the response of each donor tumor to various chemotherapies²⁹. As described previously¹⁹, the predominant histopathological mammary tumor phenotype in *K14cre;Brca2^{F/F};p53^{F/F}* mice is a carcinoma with well-defined tumor cell nests. These tumors express epithelial markers such as E-cadherin and are negative for vimentin, a fibroblast and mesenchymal cell marker (Figure 1A, upper panel). A second phenotype present in the group of 14 *Brca2^{Δ/Δ};p53^{Δ/Δ}* (KB2P) mammary tumors used in this study, is a sarcomatoid tumor that has undergone a spindle cell metaplasia, characterized by bundles with elongated cells, absence of E-cadherin and expression of vimentin (Figure 1A, lower panel). This subtype is referred to as carcinosarcoma. In our tumor panel we identified ten carcinomas and four carcinosarcomas. In contrast to the clear histopathological separation, carcinosarcomas did not form a separate group at the genomic level when we tested array comparative genomic hybridization (aCGH) data of a larger panel of *Brca2^{Δ/Δ};p53^{Δ/Δ}* carcinomas and carcinosarcomas³⁰ by unsupervised hierarchical clustering (Supplementary Figure S1). Thus, these tumors do not form a clearly separate subgroup within this model for BRCA2-mutated breast cancer at the DNA level.

Due to the spindle-shaped morphology of the carcinosarcomas we suspected that these tumors have undergone epithelial-to-mesenchymal transition (EMT) after the initial induction of the *Brca2* and *p53* mutations in an epithelial cell. To test this we applied an EMT signature¹³ on our panel of BRCA2;p53-mutated mouse mammary tumors. As expected, the two histological subtypes were clearly separated in an unsupervised clustering analysis using this EMT signature (Figure 1B). Compared to carcinomas, carcinosarcomas show higher expression of mesenchymal genes and lower expression of epithelial genes.

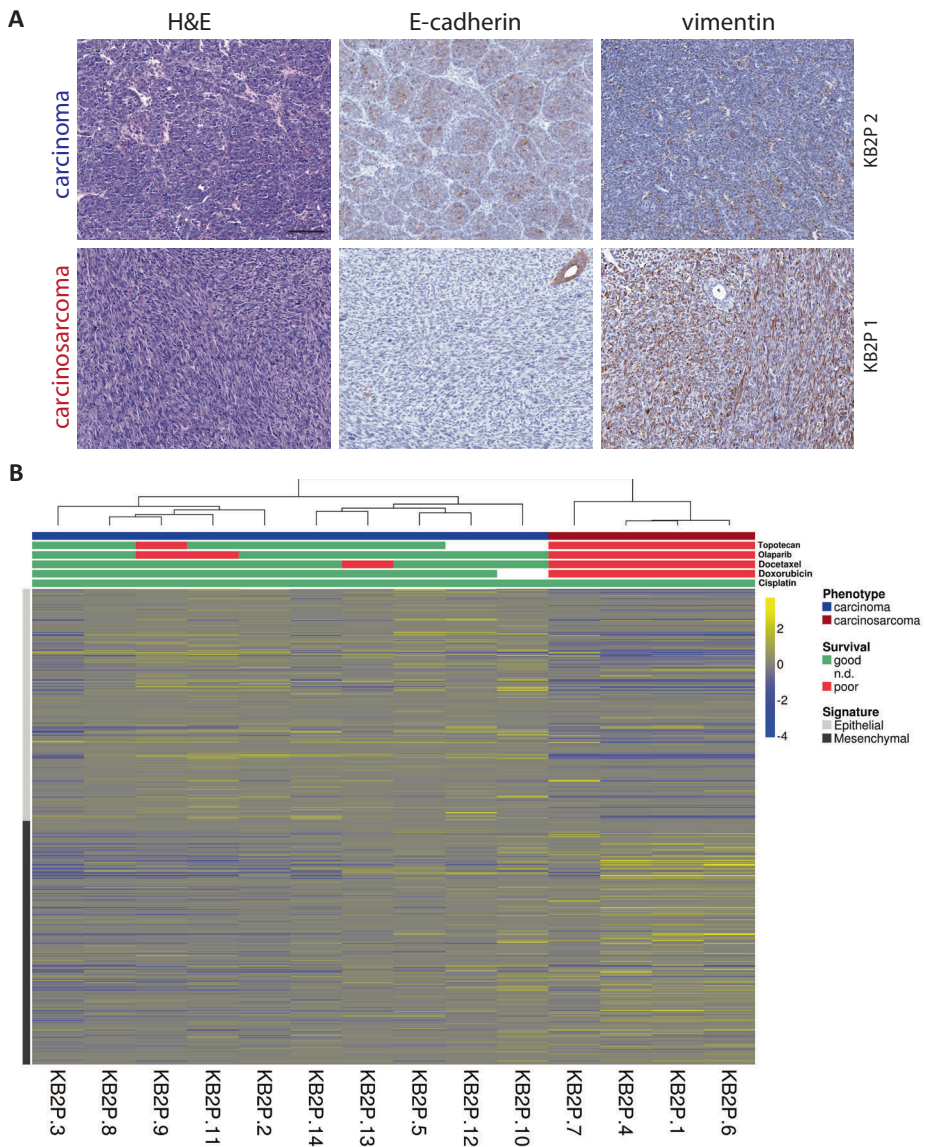


Figure 1. *Brca2*^{Δ/Δ};*p53*^{Δ/Δ} (KB2P) carcinosarcomas are characterized by epithelial-to-mesenchymal transition (EMT)-related proteins and gene expression pattern. **A**, Example of histology and E-cadherin and vimentin staining in a KB2P carcinoma with epithelial morphology and a KB2P carcinosarcoma with mesenchymal morphology. Scale bar = 100 μm. **B**, The mesenchymal tumors cluster together in an unsupervised hierarchical clustering using the EMT signature genes. The phenotype of each tumor is determined by histology and immunohistochemical stainings for E-cadherin and vimentin (see **A**). Genes indicated with the gray bar are related to an epithelial cellular state and genes indicated with the black bar are higher expressed in mesenchymal cells. Red and green bars indicate the response to the indicated treatments for the individual donor tumors. A poor response is defined as a survival of less than 31 days after start of the treatment. Mice carrying a tumor with a good response survived more than 30 days after start of the treatment.

Brca2^{Δ/Δ};p53^{Δ/Δ} carcinosarcomas are multi-drug resistant

To investigate differential drug sensitivities, we tested the response of 10 KB2P carcinomas versus 4 KB2P carcinosarcomas to the maximum tolerable dose (MTD) of the topoisomerase I inhibitor topotecan, the microtubule stabilizing agent docetaxel, the topoisomerase II inhibitor doxorubicin or the cross-linking agent cisplatin. As shown in Figure 2 and Supplementary Figure S2 the KB2P carcinomas responded to all drugs, even though they eventually acquired resistance to olaparib, topotecan, docetaxel and doxorubicin. In contrast, the four carcinosarcomas did not respond well to olaparib, topotecan, docetaxel, and doxorubicin, but were still sensitive to cisplatin. In Figure 1B the response to each drug is depicted per tumor and shows that a poor response is highly correlated with a mesenchymal gene expression profile. Carcinomas that acquired drug resistance have all retained their epithelial state, as measured by histology and gene expression (see Supplementary Figure S3 for the olaparib-resistant tumors).

Drug delivery is not impaired in *Brca2^{Δ/Δ};p53^{Δ/Δ} carcinosarcomas*

In a mouse model for pancreatic ductal adenocarcinoma (PDAC), the lack of response to gemcitabine was caused by a poor perfusion of the tumors³¹. We therefore checked the presence of blood vessels in KB2P carcinomas and carcinosarcomas. Both subtypes showed blood vessels throughout the tumor (Figure 3A). In the carcinomas blood vessels are mainly present between the cell nests, whereas in carcinosarcomas blood vessels lay in between the tumor cells. The vessels are functional, as shown by the presence of intravenously injected, fluorescently labelled Tomato-Lectin (Figure 3B), indicating that the drugs reach the tumor cells in both KB2P subtypes. These data are consistent with our observation that both carcinomas and carcinosarcomas respond to cisplatin.

Brca2^{Δ/Δ};p53^{Δ/Δ} carcinosarcomas can be re-sensitized to chemotherapy by co-administration of the Pgp inhibitor tariquidar

Each drug for which we observed primary resistance in the carcinosarcomas is known to be transported by drug efflux transporters: olaparib²⁹, docetaxel³² and doxorubicin³³ by ABCB1 (also known as Pgp) and topotecan mainly by ABCG2 (also known as BCRP)³⁴, whereas cisplatin has no strong affinity for any efflux transporter. This suggested to us that high expression of drug efflux transporters in KB2P carcinosarcomas could have contributed to their drug resistance phenotype. In the SAM analysis, expression of *Abcb1b* (which encodes Pgp together with *Abcb1a*) was indeed higher in carcinosarcomas compared to the carcinomas (Supplementary Figure S4). We tested expression of *Abcb1a*, *Abcb1b* and *Abcg2* in a semi-quantitative manner by RT-MLPA (Figure 4A). *Abcb1a* and *Abcb1b* were expressed at varying levels in the carcinosarcomas, but three out of four carcinosarcomas showed a higher expression than all carcinomas. All carcinosarcomas expressed increased levels of *Abcg2*.

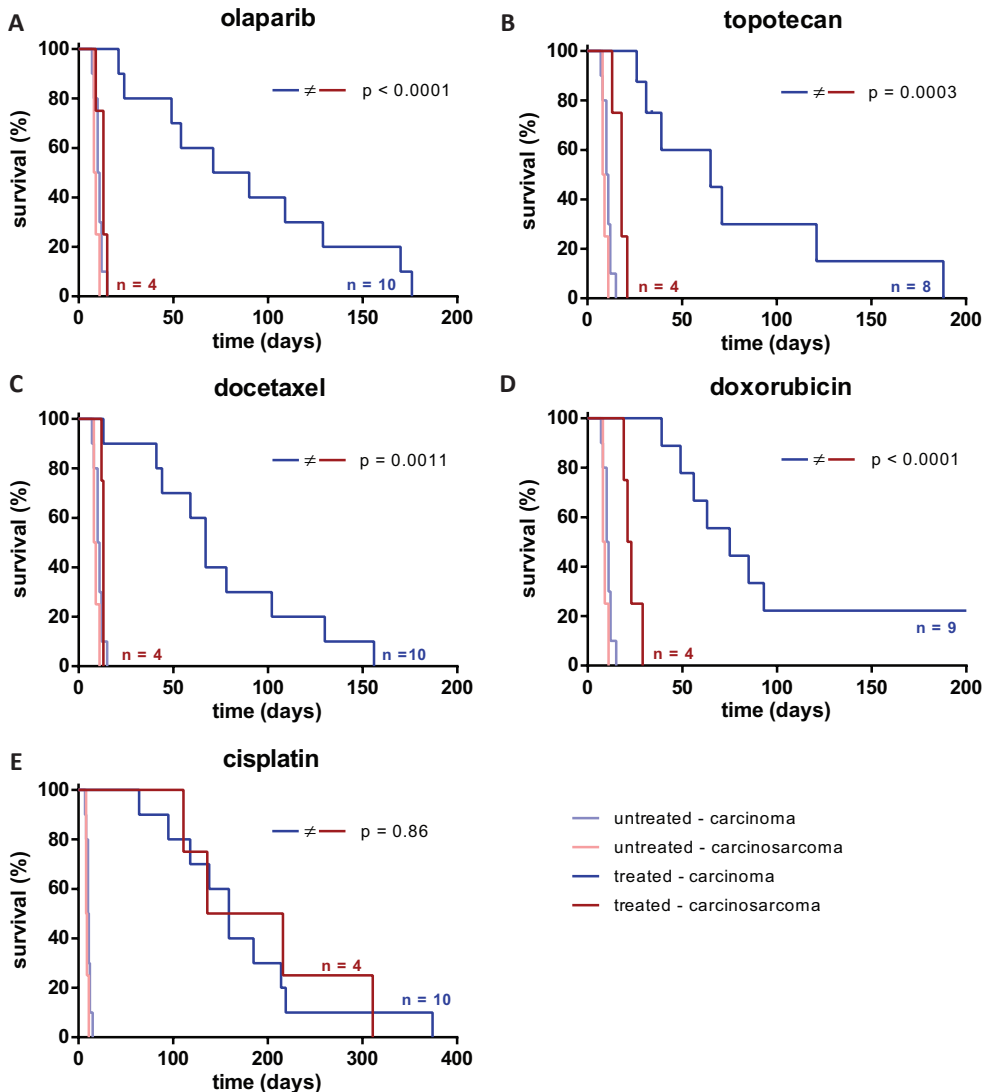


Figure 2. *Brca2*^{Δ/Δ};*p53*^{Δ/Δ} carcinosarcomas do not respond to treatment with the PARP inhibitor olaparib, topotecan, docetaxel or doxorubicin, but respond well to cisplatin treatment. Small tumor pieces from 14 individual KB2P donor tumors were transplanted orthotopically in wild-type syngeneic recipients. Treatment with olaparib (A), topotecan (B), docetaxel (C), doxorubicin (D) or cisplatin (E) was started when the tumor reached a volume of 200 mm³ (100%) and after relapse of the tumor to a size of 100% another treatment cycle was given. In the Kaplan-Meier curves overall survival is shown. All mice in A-D had to be sacrificed due to a large, resistant tumor. The treated mice in figure E were sacrificed due to cisplatin-induced cumulative toxicity. Note the difference in time scale with panels A-D. The relative tumor volume of each tumor is shown in Supplementary Figure S2.

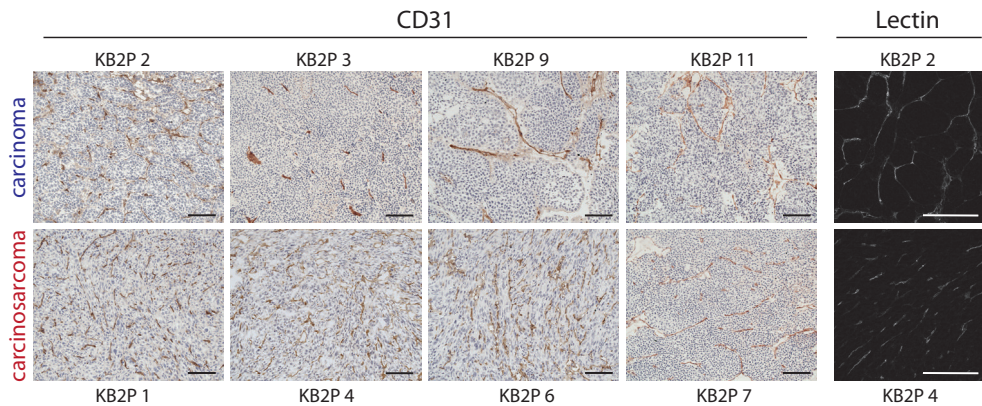


Figure 3. *Brca2*^{Δ/Δ};*p53*^{Δ/Δ} carcinomas and carcinosarcomas are well perfused. **A**, Immunohistochemical staining of the endothelial cell marker CD31. **B**, Perfused vasculature is visualized with labeled Lypersicon Esculentum Lectin. Scale bar = 100 μ m.

To determine whether increased expression of *Abcb1a* and *Abcb1b* was causally related to the drug insensitivity, we tested the effect of the Pgp inhibitor tariquidar on therapy responses of carcinosarcomas derived from donors KB2P4 and KB2P6. Tumors were treated with tariquidar alone; olaparib, docetaxel or doxorubicin alone; or the drug in combination with tariquidar. In addition, mice were treated with AZD2461, a novel PARP inhibitor with low affinity for Pgp³⁵. The effect of the combination therapy differed between the two donor tumors (Figure 4B). KB2P4 tumors showed no effect of tariquidar on olaparib sensitivity, a small delay in outgrowth when docetaxel was combined with tariquidar, and a clear delay in tumor growth for doxorubicin plus tariquidar. All KB2P6 tumors responded well to the combination therapies of tariquidar with olaparib, docetaxel or doxorubicin. Also, the response to AZD2461 was comparable to that of olaparib plus tariquidar. Taken together, these results show that Pgp contributed largely to the low drug sensitivity of KB2P6 and, in the case of doxorubicin, of KB2P4.

EMT status correlates with *Abcb1a* and *Abcb1b* expression in several mouse mammary tumor models

In several *in vitro* studies EMT has been linked to resistance for various classes of drugs⁴. As we observed in our KB2P mouse model a strong positive correlation between an “EMT-like” gene expression pattern and expression of *Abcb1a*, *Abcb1b* and *Abcg2*, we wondered whether this is also the case in other mouse mammary tumor models. In order to obtain a continuous value for EMT, we used an EMT score based on the EMT signature. The score is calculated by subtracting the average mean-centered \log_2 expression of the epithelial genes from the average mean-centered \log_2 expression of the mesenchymal genes.

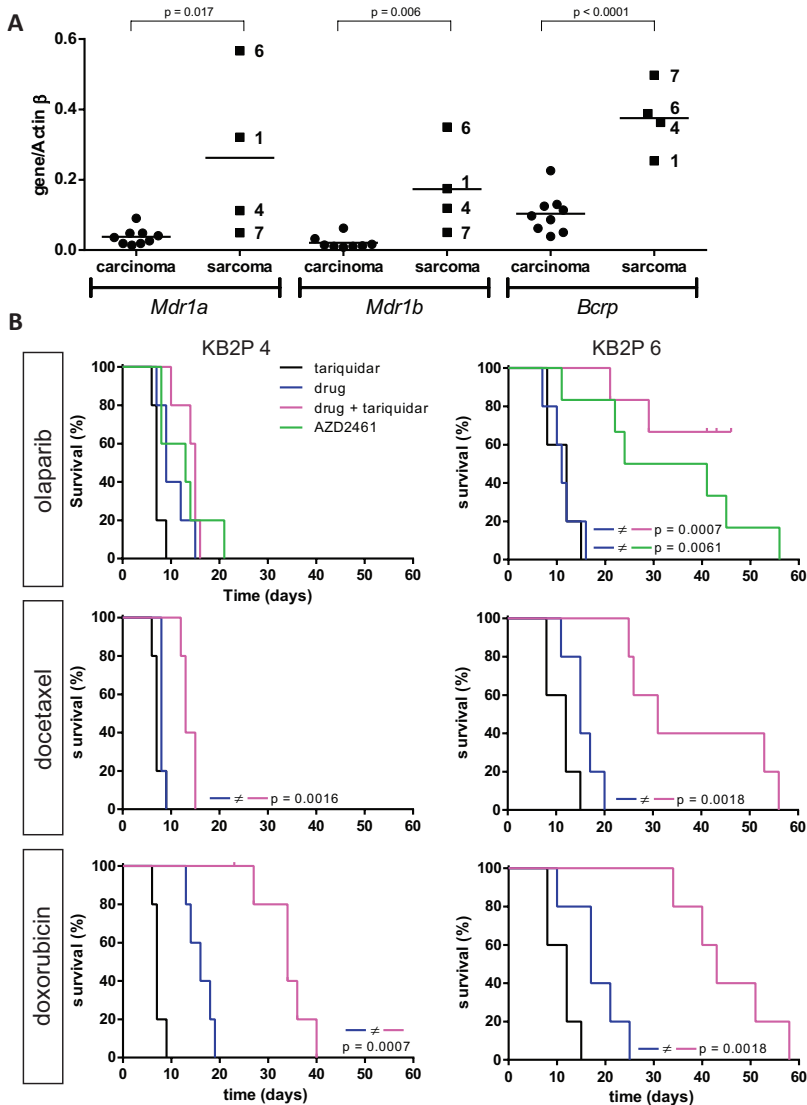


Figure 4. P-glycoprotein (Pgp) contributes to multi-drug resistance in *Brca2* ^{Δ/Δ} ;*p53* ^{Δ/Δ} carcinosarcomas.

A, sarcomatoid KB2P tumors have a higher expression of drug transporters *Abcb1a*, *Abcb1b* (which both encode Pgp) and *Abcg2*. Gene expression levels are measured by reverse transcriptase multiplex ligation-dependent probe amplification (RT-MLPA) and normalized for *Actb* expression. For the carcinosarcomas the expression level is indicated for each donor tumor. **B**, Kaplan-Meier curves, showing the survival of mice bearing sarcomatoid tumors from donor KB2P4 (left) or KB2P6 (right). Treatment was started on day 0. The mice received either the Pgp-inhibitor tariquidar (10 mg/kg i.p., daily), olaparib (50 mg/kg i.p., daily for 28 days), AZD2461 (100 mg/kg oral, daily for 28 days), docetaxel (25 mg/kg i.v., day 0, 7 and 14) or doxorubicin (5 mg/kg i.v., day 0, 7 and 14) or a combination of tariquidar with olaparib, docetaxel or doxorubicin. Tariquidar was given 15 minutes prior to olaparib, docetaxel or doxorubicin administration. The censored cases died due to unexpected toxicity. $n = 5$ or 6 per treatment group. The log-rank p -values are indicated.

We used four different gene expression data sets from mouse mammary tumors: two that were generated at the NKI and two publicly available data sets. The first one consists of 91 mammary tumors from K14cre or WAPcre driven mouse mammary tumor models with conditional deletion of *Trp53* alone³⁶ or in combination with *Cdh1*^{37,38}. Similar to the KB2P model, these models develop two main histopathologic tumor subtypes: carcinoma and carcinosarcoma. The EMT score of these tumors correlated with *Abcb1b* and to a lesser extent with *Abcb1a* and *Abcg2* (Figure 5A).

The second series is a set of *Brca1*^{Δ/Δ};*p53*^{Δ/Δ} (KB1P) tumors with or without overexpression of the MET oncogene (L. Henneman, M. van Miltenburg *et al.* manuscript in preparation). While KB1P tumors mostly have an epithelial phenotype³⁶, KB1P tumors with engineered overexpression of MET (KB1P-MET) tumors displayed a sarcomatoid phenotype in about half of the cases. Combined analysis of the KB1P and KB1P-MET tumors revealed a clear correlation between EMT score and *Abcb1a/b* expression, which is also present in the KB1P-MET group alone (Figure 5B). Due to the absence of carcinosarcomas in the KB1P tumor cohort there is no correlation between EMT score and transporter expression in this group. For *Abcg2* we did not find a correlation with EMT score.

The third and fourth data sets are publicly available from Herschkowitz *et al.*³⁹ and Zhu *et al.*⁴⁰ and contain a collection of thirteen and eight different genetically engineered mouse mammary tumor models respectively. Although both data sets contain mostly tumors with a low EMT score, a positive correlation between EMT score and *Abcb1b* expression could still be detected (Figure 5C and D).

DISCUSSION

In this study we investigated the role of EMT in anti-cancer drug sensitivity in the KB2P mouse model for BRCA2-deficient breast cancer. We found that a subset of tumors from this model has a mesenchymal, sarcomatoid phenotype and gene expression profile. While these BRCA2-deficient carcinosarcomas are hypersensitive to the alkylating agent cisplatin due to their homologous recombination deficiency, they do not respond to several other DNA-damaging chemotherapeutics or the PARP inhibitor olaparib. The high sensitivity and absence of resistance to cisplatin of KB2P carcinomas and carcinosarcomas is comparable to the response of BRCA1-deficient mouse mammary tumors to cisplatin⁴¹. We show in our KB2P model and four other mouse mammary tumor data sets that an EMT-related transcriptional profile (indicated by a high EMT score) correlates with high expression of the *Abcb1a* and *Abcb1b* genes which both encode the drug efflux transporter P-glycoprotein (Pgp). Moreover, KB2P carcinosarcomas could be sensitized to olaparib, docetaxel and doxorubicin by the Pgp inhibitor tariquidar. Taken together, these results indicate that EMT-associated multi-drug resistance is in part driven by increased activity of drug efflux transporters.

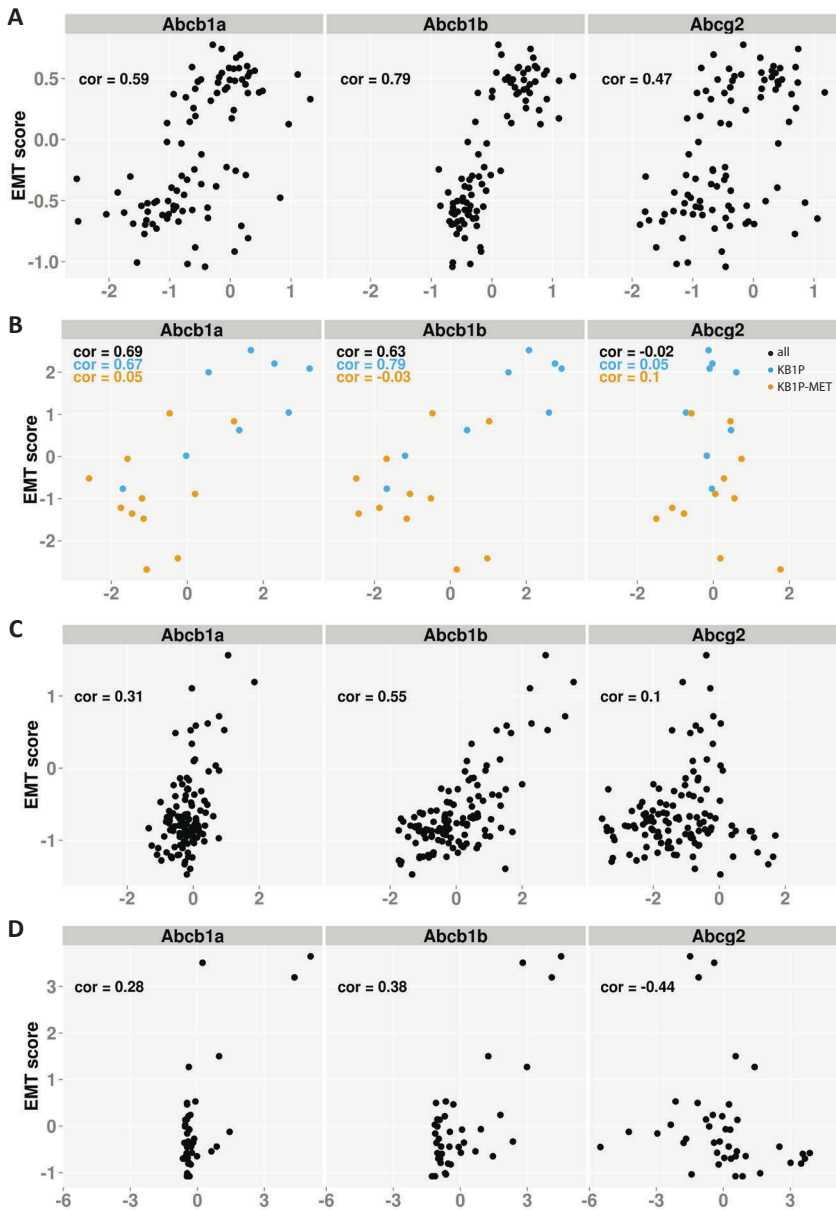


Figure 5. EMT score correlates with *Abcb1* expression in genetically engineered mouse mammary tumor models. Each plot shows the correlations between EMT score and the gene expression level of *Abcb1a*, *Abcb1b* and *Abcg2* in four different gene expression data sets with the correlation coefficient (cor). **A**, 91 tumors from *K14cre;p53^{F/F}*, *K14cre;Cdh1^{F/F};p53^{F/F}*, *WAPcre;p53^{F/F}* or *WAPcre;Cdh1^{F/F};p53^{F/F}* mice (Klijn et al. *in press*). **B**, 21 tumors from chimeric *K14cre;Brca1^{F/F};p53^{F/F}* mice with (KB1P-MET) or without (KB1P) overexpression of the MET oncogene. **C**, a publicly available dataset (GSE3165) with 108 mammary tumors from 13 different mouse models³⁹. **D**, a publicly available dataset (GSE23938) with 41 tumors from 8 different mouse models⁴⁰.

To date, only a few studies have investigated a link between EMT and drug transporter levels. Doxorubicin treatment can induce EMT in cultured breast cancer cells and up-regulate efflux transporters, which is mediated by EMT transcription factors TWIST1¹² and ZEB1⁴². Conversely, overexpression of *SNAI1* in MCF7 cells results in increased Pgp levels after doxorubicin treatment⁴³, and in increased BCRP levels⁴⁴. These studies also reported a positive correlation between SNAIL and Pgp⁴³, and between SNAIL and BCRP⁴⁴ respectively, in human breast cancer tissues. In contrast to the strong evidence for a causal role of Pgp in primary and acquired resistance to chemotherapy and targeted agents in mice^{29,41,45}, the relevance of drug efflux transporters for therapy response in breast cancer patients is still controversial. Pgp mRNA or protein expression is in some, but not all, studies related to worse outcome⁴⁶. It is however unclear whether these clinical studies measure only membranous, and not cytoplasmic, Pgp staining. In addition, Pgp (*ABCB1*) mRNA levels may be attributed to *ABCB1* expression in non-tumor cells, such as macrophages, in the tumor microenvironment⁴⁷. Over the last decades many clinical studies with transporter inhibitors have been conducted, with mostly negative results³³. This could be due to various reasons, but overall the impact of drug efflux transporters on patient outcome is likely to be small. Potentially, the human *ABCB1* gene promoter is not strong enough to reach sufficient levels of Pgp protein to acquire drug resistance and needs to be linked to a strong promoter by chromosomal rearrangements⁴⁸, which may be a rare event. It is possible that Pgp plays a role in a small subset of breast cancer such as metaplastic breast cancer. However, we did not find any correlation with *ABCB1* expression and a high EMT score in metaplastic tumors (Supplementary Figure S5). This does not mean that Pgp could not play a role in some patients with acquired or secondary resistance. Unfortunately, matched samples of initially sensitive and subsequently drug-refractory tumors are hardly available from individual breast cancer patients to address this issue.

Pgp contributes to multi-drug resistance in KB2P carcinosarcomas, but the finding that KB2P4 is still insensitive to PARP inhibition and only modestly responsive to docetaxel and doxorubicin when Pgp is inhibited by tariquidar, strongly suggest that other factors in the EMT program contribute as well. It is well possible that these other factors are responsible for the EMT-related drug resistance that is frequently observed in human cancer cells *in vitro*. In humans, metaplastic and claudin-low breast cancers are both associated with EMT. These (partly overlapping) breast cancer subtypes express EMT and tumor-initiating-cell (TIC)-associated genes^{18,49}. Both subtypes are also associated with a triple-negative phenotype, characterized by absence of hormone receptors and HER2/ERBB2 expression. Metaplastic breast cancers are often refractory to treatment and have a poor prognosis compared to other triple-negative breast cancers⁵⁰. The claudin-low subtype has a worse pCR rate than the basal-like group¹⁸. This is also the case when the claudin-low cancers are defined by absence of immunohistochemical staining of five claudin family members¹⁷.

Single EMT markers have been shown to predict prognosis in various cancer types⁵¹ and high SNAIL levels predict a shorter relapse-free survival of breast cancer patients⁵². Van Nes *et al.*⁵³ also showed a predictive role of combined high levels of SNAIL and TWIST for relapse-free survival in ER-positive breast cancer. Which proteins in the EMT program eventually cause low drug sensitivity in general and to which drugs specifically still requires further investigation.

In our model we show that a sarcomatoid tumor phenotype correlates with primary resistance to a range of drugs. It is possible that in the clinic EMT also plays an important role in acquired resistance. Even though several studies have shown that drug treatment, especially with doxorubicin, can induce EMT *in vitro*, we have not observed this phenomenon in any of our treated KB2P carcinomas. A possible explanation is that other resistance mechanisms are more easily activated, although it is not clear what these mechanisms might be, other than Pgp up-regulation. Another option is that the carcinomas and carcinosarcomas arise from a different cell of origin, for example a luminal or myoepithelial progenitor cell, respectively, in which K14 is expressed¹⁹ and therefore not easily switch from one type to another. This low plasticity is also illustrated by the small effect of *Snai1* or *Twist* overexpression on the phenotype of KB2P tumor cell lines *in vitro* and *in vivo* (data not shown).

In summary, we show the usefulness of studying multi-drug resistance in a realistic mouse model of BRCA2-deficient breast cancer. We found that enhanced expression of Pgp contributes to multi-drug resistance associated with a sarcomatoid tumor phenotype. In addition, our data suggest that the correlation between a high EMT signature score and high expression of Pgp is a general phenomenon in mouse models of breast cancer. Pan-resistance is likely to be an accumulation of multiple mechanisms and mouse models could be useful to unravel the different layers of resistance.

METHODS

Mice and tumor transplantations

Tumors were generated in *K14cre;Brca2^{F/F};p53^{F/F}* (KB2P) female mice¹⁹ and samples were taken for histology, RNA isolation and cryopreservation. Orthotopic transplantation of *BRCA2^{-/-};p53^{-/-}* tumors in wild-type FVB/Ola129 F1 mice was performed as previously described⁴¹. The tumor size was monitored at least three times a week by calliper measurements. The tumor volume was calculated with the following formula: $0.5 \times \text{length} \times \text{width}^2$. Animals were sacrificed with CO₂, when the tumor reached a size of 1500 mm³. All animal experiments were approved by the Animal Ethics Committee of the Netherlands Cancer Institute (Amsterdam, The Netherlands).

Drug treatments

Upon tumor outgrowth to approximately 200 mm³ (100%) the mice were either left untreated or received one of the following treatments: olaparib (50 mg/kg intraperitoneally, daily for 28 days),

topotecan (4 mg/kg intraperitoneally, day 0-4 and 14-18), doxorubicin (Amersham Pharmacia Netherlands, 5 mg/kg intravenously, day 0, 7 and 14), docetaxel (Aventis, 25 mg/kg intravenously, day 0, 7 and 14) or cisplatin (Mayne Pharma, 6 mg/kg intravenously, day 0). Mice with a relapsing tumor received another treatment cycle when the tumor was 100% of the original size at treatment start. For the re-sensitization experiment with tariquidar (Figure 4B) the mice received only one treatment cycle and tumor outgrowth was monitored. Tariquidar (Avaant, 10 mg/kg intraperitoneally) was administered 15 minutes prior to treatment with olaparib, docetaxel or doxorubicin. AZD2461³⁵ (100 mg/kg orally) was administered daily for 28 days.

Immunohistochemistry and fluorescence

Staining of E-cadherin and vimentin was performed on formalin-fixed paraffin-embedded (FFPE) tissue. Samples were boiled in Tris-EDTA pH9.0 to retrieve the antigens. Furthermore, we used 3% H₂O₂ in methanol to block endogenous peroxidase activity, and 10% milk (E-cadherin) or 4% bovine serum albumin (BSA) plus 5% normal goat serum in PBS (vimentin) as blocking buffer. Primary antibodies (mouse anti-E-cadherin, BD Transduction Laboratories 610182, 1:400; rabbit anti-vimentin, Cell Signalling 5741, 1:200) were diluted in 1.25% normal goat serum plus 1% bovine serum albumin (BSA) in PBS. For detection and visualisation labelled polymer-HRP anti-mouse and rabbit Envision (Dako K4007 and K4011), DAB (Sigma D5905) and hematoxylin counterstaining were applied.

CD31 staining was done on cryosections after acetone fixation for 10 minutes at -20 °C. Then we applied 0.3% H₂O₂ in methanol, avidin-biotin block (Dako X0590) and serum-free protein block (Dako X0909). The primary (rat anti-CD31, BD Bioscience 550274, 1:1000) and secondary antibody (biotinylated rabbit-anti-rat IgG, Dako E0468, 1:300) were diluted in 1% bovine serum albumin in PBS. For detection and visualisation, we used streptavidin-HRP (Dako K1016, 10 minutes incubation at room temperature), DAB (Dako K3468), and hematoxylin counterstaining.

For visualization of perfused blood vessels, biotinylated Lycopersicon Esculentum (Tomato) Lectin (B1175 Vector Laboratories) was added to streptavidin-AF633 (S21375 Invitrogen) in sterile PBS and injected in the tail vein 15 minutes before sacrificing the mouse. For visualisation of the Lectin-AF633 signal, FFPE slides were deparaffinised, rehydrated, incubated with DAPI for five minutes and mounted in Vectashield (H-1000 Vector Laboratories). Images were taken with a Leica TCS SP5 (Leica Microsystems) confocal system, equipped with a 405 nm Diode laser and 633 nm HeNe laser system.

Gene expression profiling

Total RNA was isolated with Trizol (Invitrogen) from snap-frozen tumor samples. The RNA was processed according to the manufacturer's instructions for single channel 45K MouseWG-6 v2.0 BeadChips (Illumina). Background correction was performed using the `bg.adjust` method from the Bioconductor `affy` package⁵⁴. For normalization between arrays the robust spline method was applied.

EMT signature and EMT score

A published EMT signature¹³ was converted from human to mouse, resulting in 239 epithelial genes (down after EMT) and 224 mesenchymal genes (up after EMT). Of these, 235 epithelial and 223 mesenchymal genes could be mapped to Ensembl gene identifiers using Ensembl Biomart⁵⁵.

Generation of gene expression data from *p53*^{-/-} and *Cdh1*^{-/-};*p53*^{-/-} mouse mammary tumors has been described (Klijn *et al.* PLoS One, *in press*). Gene expression profiles of mammary tumors derived from *K14cre;Brca1*^{E/F};*p53*^{E/F} (KB1P) and *K14cre;Brca1*^{E/F};*p53*^{E/F};*LSL-Met* (KB1P-MET) chimeric mice were determined by RNA sequencing. Total mRNA was converted into a library using the TruSeq RNA Sample Preparation Kit (Illumina) according to the manufacturer's protocol. Illumina HiSeq 2000 and TruSeq v3 kits and software were used to generate the sequence reads. The reads (10-16 million 51bp paired-end) were mapped to the mouse reference genome (mm9) using TopHat (Trapnell *et al* 2009, version 2.0.6), which was supplied with a known set of gene models (Ensembl version 66). The open-source tool HTSeq-Count (v.0.5.3p3) was used to obtain gene expression levels. This tool generates a list of the total number of uniquely mapped sequencing reads for each gene that is present in the provided Gene Transfer Format (GTF) file. Normalized log₂ gene expression levels were generated by normalizing all samples to 10 million reads per sample. Upon log₂ transformation we added 1 to all gene expression to avoid negative values. Gene expression data sets GSE3165³⁹, GSE23938⁴⁰ and GSE10885⁵⁶ were downloaded from the Gene Expression Omnibus.

Expression data were mean-centered per gene or probe for each data set. The EMT score of each tumor in all four data sets is calculated by subtracting the log₂ expression of the epithelial genes from the mean of the log₂ expression of the mesenchymal genes. Supplementary Table S1 summarizes the number of signature genes represented on each platform. As a result, tumors with a mesenchymal gene expression profile have a positive score and tumors with an epithelial profile have a negative EMT score. For the correlation between EMT score and *Abcb1a*, *Abcb1b* and *Abcg2* expression we used the Spearman correlation.

Array comparative genomic hybridization (aCGH)

aCGH data from *Brca2*^{Δ/Δ};*p53*^{Δ/Δ} mouse mammary tumors were downloaded from Array Express (E-NCMF-34 and E-NCMF-35). The phenotype was determined previously³⁰, with one exception: a tumor with unknown phenotype was later classified as carcinosarcoma. Unsupervised hierarchical clustering was performed using the Euclidean distance method with complete linkage.

RT-MLPA

Semi-quantitative levels of *Abcb1a*, *Abcb1b* and *Abcg2* mRNA were measured with RT-MLPA. Reverse transcription of total RNA, hybridization, ligation, PCR amplification and fragment analysis by capillary electrophoresis were performed as described⁵⁷. Gene expression levels were normalized to the internal reference *Actb* (beta-actin).

ACKNOWLEDGMENTS

We thank Arno Velds for analysing the aCGH data and generating Supplementary Figure S1 and Susan Bates from the NIH (Bethesda, MD) for providing tariquidar. This work was supported by grants from the Netherlands Organization for Scientific Research (NWO-Toptalent 021.002.104 to J.E. Jaspers, NWO-VIDI 91.711.302 to S. Rottenberg, and NWO-roadmap MCCA 184.032.303), Dutch Cancer Society (projects NKI 2007-3772, NKI 2009-4303 and NKI-2011-5220), the EU FP7 Project 260791-Eurocan-Platform, CTMM Breast Care, and the NKI-AVL Cancer Systems Biology Centre.

REFERENCES

1. Borst, P. Cancer drug pan-resistance: pumps, cancer stem cells, quiescence, epithelial to mesenchymal transition, blocked cell death pathways, persists or what? *Open Biol.* **2**, 120066 (2012).
2. Gorre, M. E. *et al.* Clinical resistance to STI-571 cancer therapy caused by BCR-ABL gene mutation or amplification. *Science* **293**, 876–880 (2001).
3. Burgess, D. J. *et al.* Topoisomerase levels determine chemotherapy response in vitro and in vivo. *Proc. Natl. Acad. Sci. U. S. A.* **105**, 9053–9058 (2008).
4. Foroni, C., Brogгинi, M., Generali, D. & Damia, G. Epithelial-mesenchymal transition and breast cancer: role, molecular mechanisms and clinical impact. *Cancer Treat. Rev.* **38**, 689–697 (2012).
5. Işeri, O. D. *et al.* Drug resistant MCF-7 cells exhibit epithelial-mesenchymal transition gene expression pattern. *Biomed. Pharmacother. Biomédecine Pharmacothérapie* **65**, 40–45 (2011).
6. Kajiyama, H. *et al.* Chemoresistance to paclitaxel induces epithelial-mesenchymal transition and enhances metastatic potential for epithelial ovarian carcinoma cells. *Int. J. Oncol.* **31**, 277–283 (2007).
7. McConkey, D. J. *et al.* Role of epithelial-to-mesenchymal transition (EMT) in drug sensitivity and metastasis in bladder cancer. *Cancer Metastasis Rev.* **28**, 335–344 (2009).
8. Shah, A. N. *et al.* Development and characterization of gemcitabine-resistant pancreatic tumor cells. *Ann. Surg. Oncol.* **14**, 3629–3637 (2007).
9. Yang, A. D. *et al.* Chronic oxaliplatin resistance induces epithelial-to-mesenchymal transition in colorectal cancer cell lines. *Clin. Cancer Res. Off. J. Am. Assoc. Cancer Res.* **12**, 4147–4153 (2006).
10. Chung, J.-H. *et al.* Clinical and molecular evidences of epithelial to mesenchymal transition in acquired resistance to EGFR-TKIs. *Lung Cancer Amst. Neth.* **73**, 176–182 (2011).
11. Konecny, G. E. *et al.* Activity of lapatinib a novel HER2 and EGFR dual kinase inhibitor in human endometrial cancer cells. *Br. J. Cancer* **98**, 1076–1084 (2008).
12. Li, Q.-Q. *et al.* Twist1-mediated adriamycin-induced epithelial-mesenchymal transition relates to multidrug resistance and invasive potential in breast cancer cells. *Clin. Cancer Res. Off. J. Am. Assoc. Cancer Res.* **15**, 2657–2665 (2009).
13. Huang, S. *et al.* MED12 controls the response to multiple cancer drugs through regulation of TGF- β receptor signaling. *Cell* **151**, 937–950 (2012).
14. Weigelt, B. *et al.* Refinement of breast cancer classification by molecular characterization of histological special types. *J. Pathol.* **216**, 141–150 (2008).
15. Geyer, F. C. *et al.* Molecular analysis reveals a genetic basis for the phenotypic diversity of metaplastic breast carcinomas. *J. Pathol.* **220**, 562–573 (2010).
16. Weigelt, B., Kreike, B. & Reis-Filho, J. S. Metaplastic breast carcinomas are basal-like breast cancers: a genomic profiling analysis. *Breast Cancer Res. Treat.* **117**, 273–280 (2009).
17. Lu, S. *et al.* Claudin expression in high-grade invasive ductal carcinoma of the breast: correlation with the molecular subtype. *Mod. Pathol. Off. J. United States Can. Acad. Pathol. Inc* **26**, 485–495 (2013).

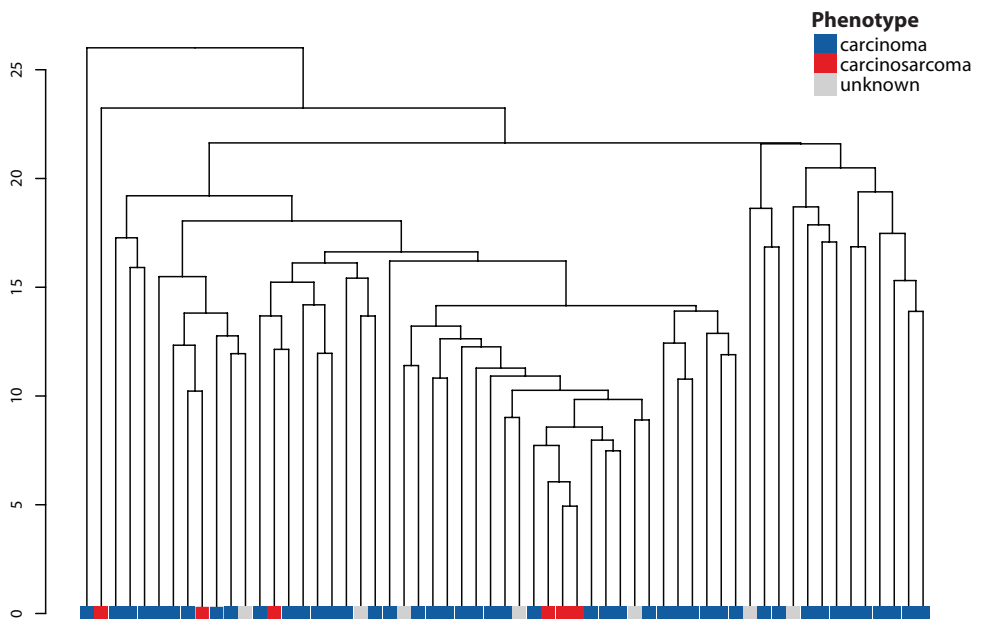
18. Prat, A. *et al.* Phenotypic and molecular characterization of the claudin-low intrinsic subtype of breast cancer. *Breast Cancer Res. BCR* **12**, R68 (2010).
19. Jonkers, J. *et al.* Synergistic tumor suppressor activity of BRCA2 and p53 in a conditional mouse model for breast cancer. *Nat. Genet.* **29**, 418–425 (2001).
20. Gillet, J.-P., Varma, S. & Gottesman, M. M. The clinical relevance of cancer cell lines. *J. Natl. Cancer Inst.* **105**, 452–458 (2013).
21. Hay, T. *et al.* Poly(ADP-ribose) polymerase-1 inhibitor treatment regresses autochthonous Brca2/p53-mutant mammary tumors in vivo and delays tumor relapse in combination with carboplatin. *Cancer Res.* **69**, 3850–3855 (2009).
22. Evers, B. *et al.* A high-throughput pharmaceutical screen identifies compounds with specific toxicity against BRCA2-deficient tumors. *Clin. Cancer Res. Off. J. Am. Assoc. Cancer Res.* **16**, 99–108 (2010).
23. Evers, B. *et al.* Selective inhibition of BRCA2-deficient mammary tumor cell growth by AZD2281 and cisplatin. *Clin. Cancer Res. Off. J. Am. Assoc. Cancer Res.* **14**, 3916–3925 (2008).
24. De Plater, L. *et al.* Establishment and characterisation of a new breast cancer xenograft obtained from a woman carrying a germline BRCA2 mutation. *Br. J. Cancer* **103**, 1192–1200 (2010).
25. Kortmann, U. *et al.* Tumor growth inhibition by olaparib in BRCA2 germline-mutated patient-derived ovarian cancer tissue xenografts. *Clin. Cancer Res. Off. J. Am. Assoc. Cancer Res.* **17**, 783–791 (2011).
26. Kriege, M. *et al.* Sensitivity to first-line chemotherapy for metastatic breast cancer in BRCA1 and BRCA2 mutation carriers. *J. Clin. Oncol. Off. J. Am. Soc. Clin. Oncol.* **27**, 3764–3771 (2009).
27. Lips, E. H. *et al.* Indicators of homologous recombination deficiency in breast cancer and association with response to neoadjuvant chemotherapy. *Ann. Oncol. Off. J. Eur. Soc. Med. Oncol. ESMO* **22**, 870–876 (2011).
28. Tutt, A. *et al.* Oral poly(ADP-ribose) polymerase inhibitor olaparib in patients with BRCA1 or BRCA2 mutations and advanced breast cancer: a proof-of-concept trial. *Lancet* **376**, 235–244 (2010).
29. Rottenberg, S. *et al.* High sensitivity of BRCA1-deficient mammary tumors to the PARP inhibitor AZD2281 alone and in combination with platinum drugs. *Proc. Natl. Acad. Sci. U. S. A.* **105**, 17079–17084 (2008).
30. Holstege, H. *et al.* Cross-species comparison of aCGH data from mouse and human BRCA1- and BRCA2-mutated breast cancers. *BMC Cancer* **10**, 455 (2010).
31. Olive, K. P. *et al.* Inhibition of Hedgehog signaling enhances delivery of chemotherapy in a mouse model of pancreatic cancer. *Science* **324**, 1457–1461 (2009).
32. Wils, P. *et al.* Polarized transport of docetaxel and vinblastine mediated by P-glycoprotein in human intestinal epithelial cell monolayers. *Biochem. Pharmacol.* **48**, 1528–1530 (1994).
33. Szakács, G., Paterson, J. K., Ludwig, J. A., Booth-Genthe, C. & Gottesman, M. M. Targeting multidrug resistance in cancer. *Nat. Rev. Drug Discov.* **5**, 219–234 (2006).
34. Maliepaard, M. *et al.* Overexpression of the BCRP/MXR/ABCP gene in a topotecan-selected ovarian tumor cell line. *Cancer Res.* **59**, 4559–4563 (1999).
35. Jaspers, J. E. *et al.* Loss of 53BP1 causes PARP inhibitor resistance in Brca1-mutated mouse mammary tumors. *Cancer Discov.* **3**, 68–81 (2013).
36. Liu, X. *et al.* Somatic loss of BRCA1 and p53 in mice induces mammary tumors with features of human BRCA1-mutated basal-like breast cancer. *Proc. Natl. Acad. Sci. U. S. A.* **104**, 12111–12116 (2007).
37. Derksen, P. W. B. *et al.* Mammary-specific inactivation of E-cadherin and p53 impairs functional gland development and leads to pleomorphic invasive lobular carcinoma in mice. *Dis. Model. Mech.* **4**, 347–358 (2011).
38. Derksen, P. W. B. *et al.* Somatic inactivation of E-cadherin and p53 in mice leads to metastatic lobular mammary carcinoma through induction of anoikis resistance and angiogenesis. *Cancer Cell* **10**, 437–449 (2006).
39. Herschkowitz, J. I. *et al.* Identification of conserved gene expression features between murine mammary carcinoma models and human breast tumors. *Genome Biol.* **8**, R76 (2007).

40. Zhu, M. *et al.* Integrated miRNA and mRNA expression profiling of mouse mammary tumor models identifies miRNA signatures associated with mammary tumor lineage. *Genome Biol.* **12**, R77 (2011).
41. Rottenberg, S. *et al.* Selective induction of chemotherapy resistance of mammary tumors in a conditional mouse model for hereditary breast cancer. *Proc. Natl. Acad. Sci. U. S. A.* **104**, 12117–12122 (2007).
42. Saxena, M., Stephens, M. A., Pathak, H. & Rangarajan, A. Transcription factors that mediate epithelial-mesenchymal transition lead to multidrug resistance by upregulating ABC transporters. *Cell Death Dis.* **2**, e179 (2011).
43. Li, W. *et al.* Overexpression of Snail accelerates adriamycin induction of multidrug resistance in breast cancer cells. *Asian Pac. J. Cancer Prev. APJCP* **12**, 2575–2580 (2011).
44. Chen, W.-J. *et al.* Multidrug resistance in breast cancer cells during epithelial-mesenchymal transition is modulated by breast cancer resistant protein. *Chin. J. Cancer* **29**, 151–157 (2010).
45. Zander, S. A. L. *et al.* Sensitivity and acquired resistance of BRCA1;p53-deficient mouse mammary tumors to the topoisomerase I inhibitor topotecan. *Cancer Res.* **70**, 1700–1710 (2010).
46. Amiri-Kordestani, L., Basseville, A., Kurdziel, K., Fojo, A. T. & Bates, S. E. Targeting MDR in breast and lung cancer: discriminating its potential importance from the failure of drug resistance reversal studies. *Drug Resist. Updat. Rev. Comment. Antimicrob. Anticancer Chemother.* **15**, 50–61 (2012).
47. Faneyte, I. F., Kristel, P. M. & van de Vijver, M. J. Determining MDR1/P-glycoprotein expression in breast cancer. *Int. J. Cancer J. Int. Cancer* **93**, 114–122 (2001).
48. Huff, L. M., Lee, J.-S., Robey, R. W. & Fojo, T. Characterization of gene rearrangements leading to activation of MDR-1. *J. Biol. Chem.* **281**, 36501–36509 (2006).
49. Taube, J. H. *et al.* Core epithelial-to-mesenchymal transition interactome gene-expression signature is associated with claudin-low and metaplastic breast cancer subtypes. *Proc. Natl. Acad. Sci. U. S. A.* **107**, 15449–15454 (2010).
50. Jung, S.-Y. *et al.* Worse prognosis of metaplastic breast cancer patients than other patients with triple-negative breast cancer. *Breast Cancer Res. Treat.* **120**, 627–637 (2010).
51. Iwatsuki, M. *et al.* Epithelial-mesenchymal transition in cancer development and its clinical significance. *Cancer Sci.* **101**, 293–299 (2010).
52. Moody, S. E. *et al.* The transcriptional repressor Snail promotes mammary tumor recurrence. *Cancer Cell* **8**, 197–209 (2005).
53. Van Nes, J. G. H. *et al.* Co-expression of SNAIL and TWIST determines prognosis in estrogen receptor-positive early breast cancer patients. *Breast Cancer Res. Treat.* **133**, 49–59 (2012).
54. Gautier, L., Cope, L., Bolstad, B. M. & Irizarry, R. A. affy--analysis of Affymetrix GeneChip data at the probe level. *Bioinforma. Oxf. Engl.* **20**, 307–315 (2004).
55. Kinsella, R. J. *et al.* Ensembl BioMarts: a hub for data retrieval across taxonomic space. *Database J. Biol. Databases Curation* **2011**, bar030 (2011).
56. Hennessy, B. T. *et al.* Characterization of a naturally occurring breast cancer subset enriched in epithelial-to-mesenchymal transition and stem cell characteristics. *Cancer Res.* **69**, 4116–4124 (2009).
57. Schouten, J. P. *et al.* Relative quantification of 40 nucleic acid sequences by multiplex ligation-dependent probe amplification. *Nucleic Acids Res.* **30**, e57 (2002).

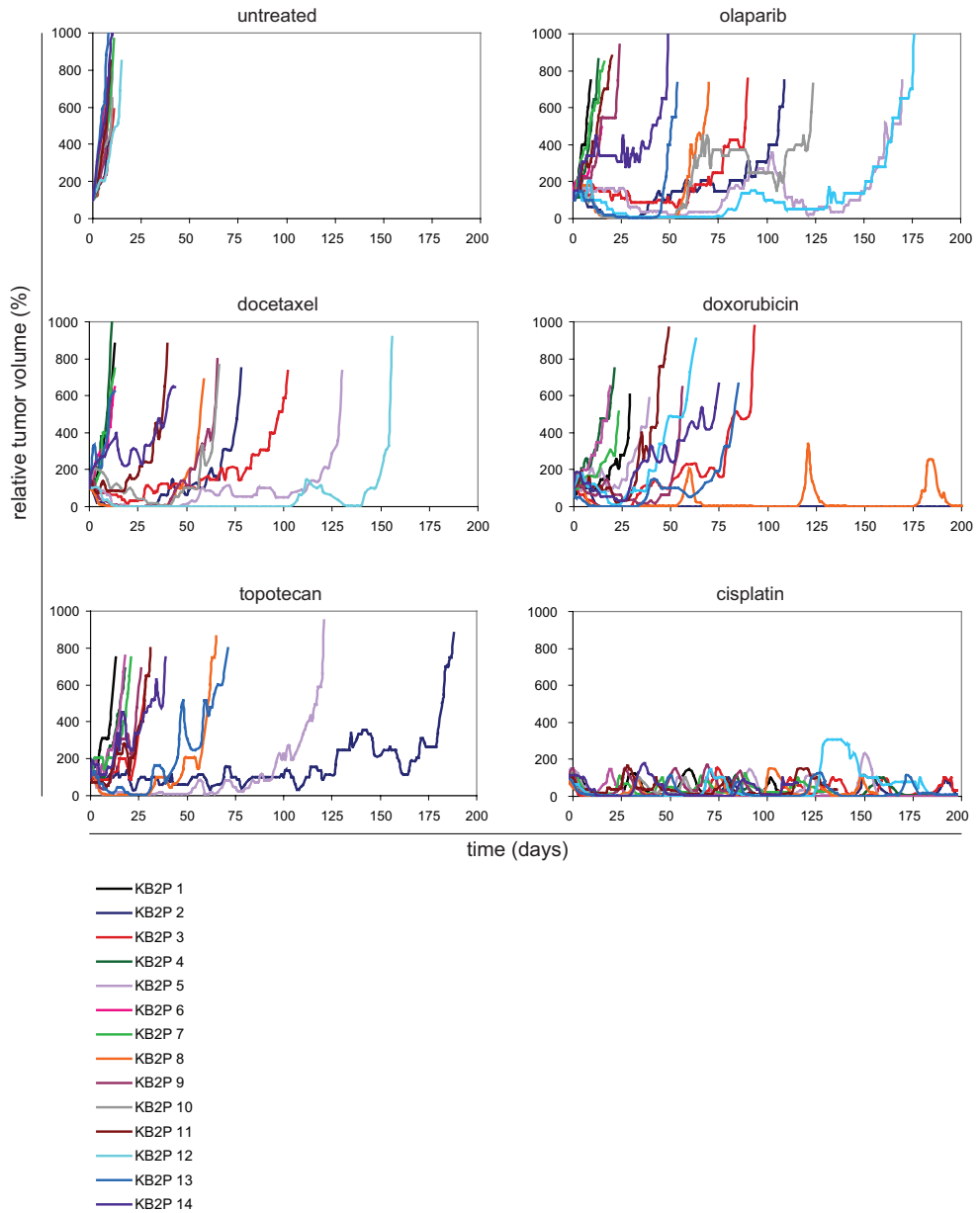
Supplementary Table S1

data set	total mouse signature	epithelial	mesenchymal
KB2P		239	224
<i>p53</i> ^{-/-} + <i>Cdh1</i> ^{-/-} ; <i>p53</i> ^{-/-}		235	222
KB1P-MET		197	192
GSE3165		211	199
GSE23938		183	176

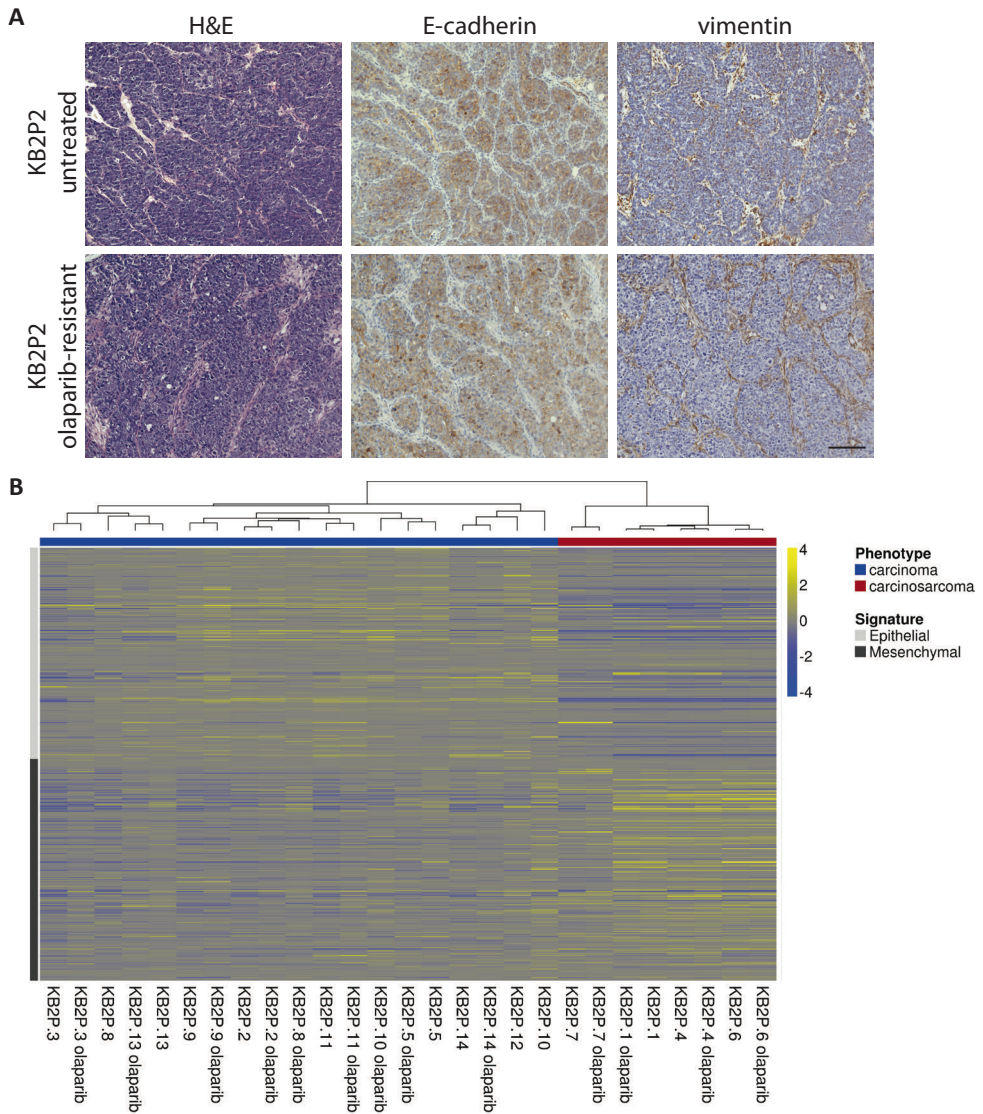
This table summarizes the number of EMT signature genes represented on each platform of the five gene expression data sets from genetically engineered mouse models of breast cancer.



Supplementary Figure S1. Unsupervised hierarchical clustering of array comparative genomic hybridization (aCGH) data from *Brca2*^{Δ/Δ}; *p53*^{Δ/Δ} tumors. The data were obtained from Holstege et al.³⁰: 46 carcinomas, 6 carcinosarcomas and 7 unknowns. Phenotypic classification was based on histology and E-cadherin and vimentin staining.

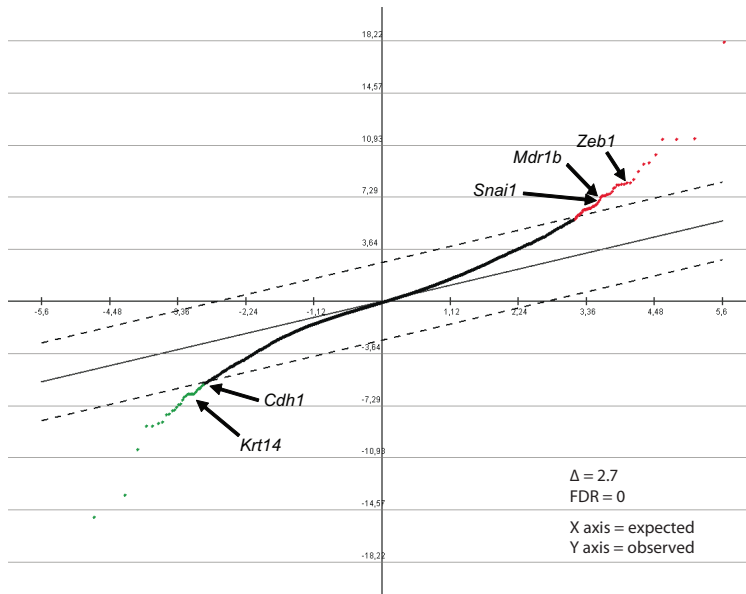


Supplementary Figure S2. Relative tumor volumes, corresponding to Figure 2. Response curves of untreated *Brca2^{Δ/Δ};p53^{Δ/Δ}* (KB2P) tumors, and tumors from mice treated with olaparib (50 mg/kg i.p., daily for 28 days), docetaxel (25 mg/kg i.v., day 0, 7 and 14), doxorubicin (5 mg/kg i.v., day 0, 7 and 14), topotecan (4 mg/kg i.p., day 0-4 and 14-18) or cisplatin (6 mg/kg i.v., day 0). Each treatment was repeated when the tumor relapsed and reached a size of 200 mm³ (100%).

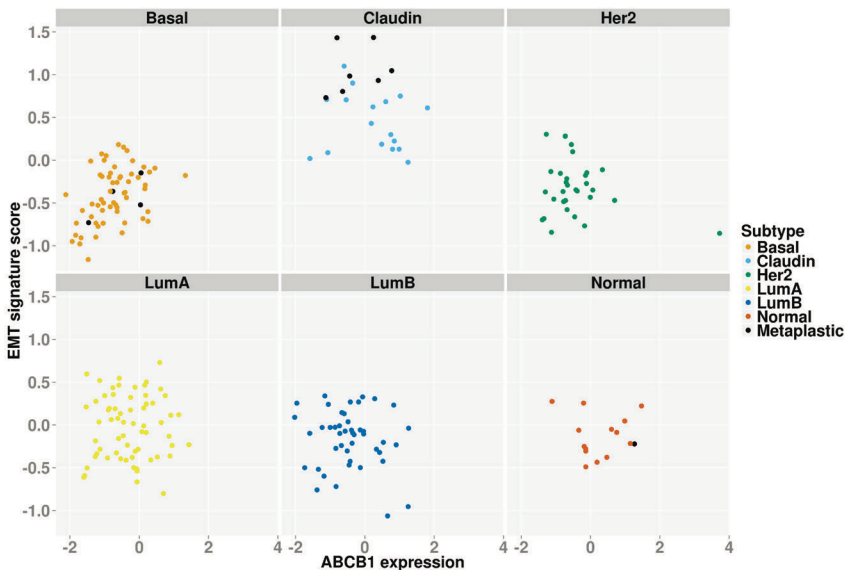


Supplementary Figure S3. Acquired resistant carcinomas retain their epithelial phenotype.

A, Histological characterization of a tumor from donor KB2P2 that has acquired resistance to olaparib and the corresponding untreated control. **B**, Unsupervised clustering of all untreated and olaparib-treated KB2P tumors with the EMT signature genes. The olaparib-treated carcinomas have acquired resistance and all olaparib-treated carcinosarcomas were resistant up-front. Tumors were harvested when they reached a size of 1500 mm³. The phenotype of all tumors was determined by histology (as in **A**). Most treated tumors cluster together with the untreated tumor from the same donor.



Supplementary Figure S4. SAM analysis of the four KB2P carcinosarcomas and 10 KB2P carcinomas ($\Delta = 2.7$; $FDR = 0$). Among the genes that are higher expressed in the carcinosarcomas are EMT-related transcription factors *Zeb1* and *Snai1* and the efflux transporter *Abcb1b* (encoding Pgp). Epithelial genes, such as *Krt14* and *Cdh1* (E-cadherin) are lower expressed in the carcinosarcomas.



Supplementary Figure S5. EMT score does not correlate with *ABCB1* levels in metaplastic breast cancer. The group of twelve metaplastic breast cancers⁵⁶ has tumors with a high or a low EMT score, indicating the heterogeneity of this subtype. No correlation between EMT score and *ABCB1* expression was detected in metaplastic breast cancers or in any of the molecular subtypes.

CHAPTER 5



The mammary stem cell markers CD24 and CD49f are less effective in identifying tumor-initiating cells in mesenchymal than in epithelial mouse mammary tumors

Janneke E. Jaspers^{1,2}, Ariena Kersbergen¹, Ute Boon², Wendy Sol¹, Frank van Diepen³,
Piet Borst¹, Jos Jonkers², Sven Rottenberg¹

¹ Divisions of Molecular Oncology and ² Molecular Pathology, ³ Flow Cytometry Facility, Netherlands Cancer Institute, Plesmanlaan 121, 1066 CX Amsterdam, The Netherlands

Manuscript in preparation

ABSTRACT

The cancer stem cell model was shown to be applicable to some cancer types. However, the high frequency of tumor-initiating cells (TICs) in other cancers, such as melanoma, suggests that the cancer stem cell model is not universally applicable. TICs have been characterized in human breast cancers and mouse mammary tumor models, but their frequency varies between studies. Moreover, epithelial-to-mesenchymal transition (EMT) has been shown to strongly increase the number of TICs in cultured cells. We used the mammary stem cell markers CD24 and CD49f to measure the tumorigenic potential of p53-deficient mouse mammary carcinomas with an epithelial phenotype or carcinosarcomas with a mesenchymal phenotype. Whereas the Lin⁻/CD24⁻/CD49f⁻ cells had the lowest tumor-initiating capacity in the carcinomas, this population was much more tumorigenic in the carcinosarcomas. Moreover, the increased tumor-initiating capacity of Lin⁻ cells in the carcinosarcomas was not accompanied by an increased Lin⁻/CD24⁺/CD49f⁺ cell population. This supports the idea that identification of TICs by the mammary stem cell markers CD24 and CD49f is context dependent.

INTRODUCTION

The cancer stem cell model describes the organization of hematological and solid tumors in which a rare subpopulation of undifferentiated cells drives tumorigenesis and is potentially more resistant to therapy¹⁻³. Cancer stem cells (CSCs) or tumor-initiating cells (TICs) have been characterized as Lineage⁻ (Lin⁻)/CD44⁺/CD24^{-/low} cells in human breast cancers⁴. In mammary gland repopulating unit (MRU) assays in mice, normal mammary stem cells have been identified as Lin⁻/CD24⁺/CD29^{high} (ref. 5) or Lin⁻/CD24^{med}/CD49f^{high} (ref. 6). Limiting dilution experiments with these and other stem cell markers have identified a low frequency of TICs in a distinctive subpopulation of various breast cancer models⁷⁻¹⁰. In contrast, Quintana *et al.*¹¹ showed that human melanomas have a very high frequency of tumorigenic cells, indicating that not all cancer types have this hierarchical organization or rare TIC frequency.

Epithelial-to-mesenchymal transition (EMT) is a normal developmental process that is also thought to contribute to invasiveness, metastatic potential and therapy resistance of breast cancer¹². In particular, it was reported that the induction of EMT in cell cultures leads to an increase in the TIC population¹³⁻¹⁶. In our study we used the stem cell markers CD24 and CD49f to identify TICs in p53-deficient mouse mammary tumors with either an epithelial phenotype (carcinomas), or an EMT-like mesenchymal morphology (carcinosarcomas). An advantage of mouse tumors is the availability of syngeneic, immunocompetent recipient mice for the transplantation of sorted cells. Using this transplantation approach, we show that in the carcinomas the Lin⁻/CD24⁺/CD49f⁺ fraction has the highest tumor-initiating capacity, but that all other fractions could also reconstitute the tumor heterogeneity. In the carcinosarcomas we did not find a larger population of Lin⁻/CD24⁺/CD49f⁺ cells, but in these tumors all Lin⁻ fractions had similar tumor-initiating capacity within the range of 100-1000 injected cells.

RESULTS

***P53*^{Δ/Δ} mouse mammary tumor models form carcinoma and carcinosarcoma tumors**

We have previously shown that our genetically engineered mouse mammary tumor models (*K14cre;p53^{F/F}*, *K14cre;Cdh1^{F/F};p53^{F/F}* and *WAPcre;Cdh1^{F/F};p53^{F/F}*) develop both solid *p53*^{Δ/Δ} carcinomas with epithelial morphology and *p53*^{Δ/Δ} carcinosarcomas with mesenchymal morphology¹⁷⁻¹⁹. The carcinosarcomas express the fibroblast marker vimentin (Figure 1A) and have a high EMT score (Jaspers *et al.* manuscript in preparation). The solid carcinomas have a low EMT score and express E-cadherin and keratin 8 (Figure 1A). For all subtypes the morphology is stable upon orthotopic transplantation into syngeneic, immunocompetent recipient mice (Figure 1B). The fact that E-cadherin-positive solid carcinomas are formed in the *K14cre;Cdh1^{F/F};p53^{F/F}* and *WAPcre;Cdh1^{F/F};p53^{F/F}* mammary tumor models shows that the floxed E-cadherin alleles are not always co-deleted by the *Cre* recombinase in these models.

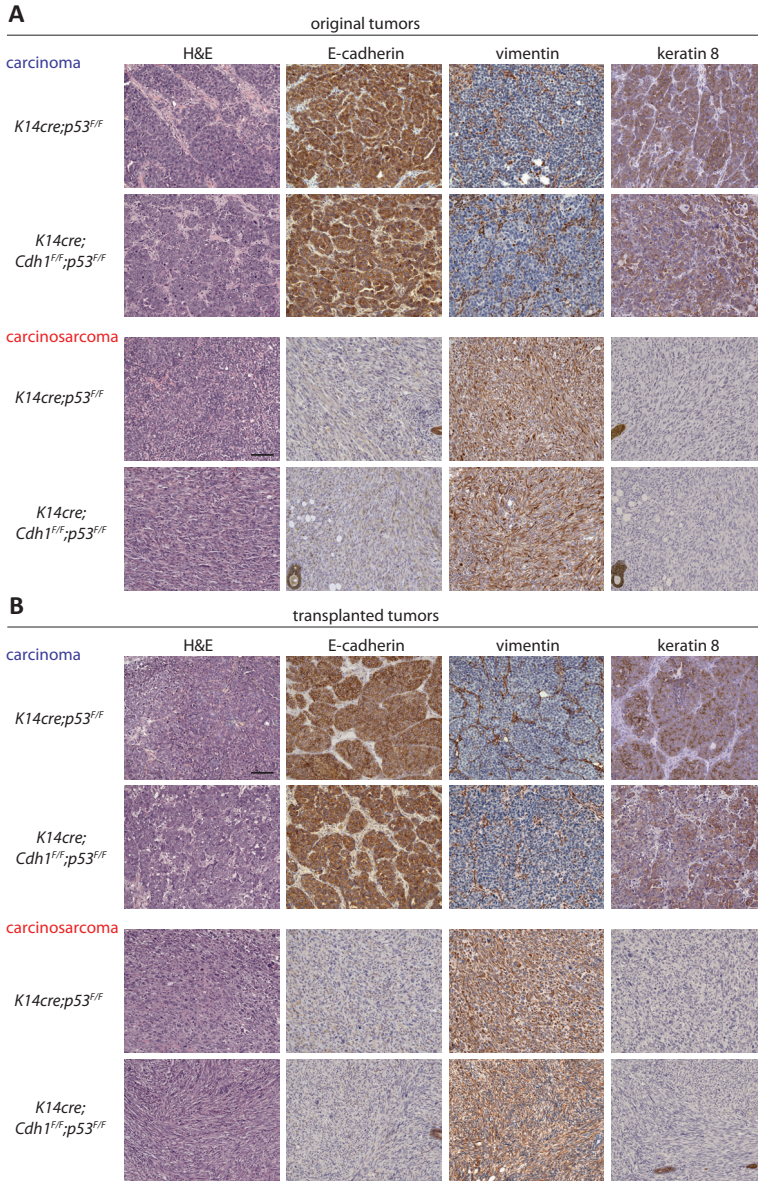


Figure 1. Phenotypic characterization of $p53^{\Delta/\Delta}$ mouse mammary carcinomas and carcinosarcomas. Representative examples of $p53^{\Delta/\Delta}$ carcinomas and carcinosarcomas from the *K14cre;p53^{F/F}* and *K14cre;Cdh1^{F/F};p53^{F/F}* mouse mammary tumor models (A). Immunohistochemical stainings show the presence of vimentin and absence of E-cadherin and keratin 8 in the carcinosarcomas. Carcinomas are positive for E-cadherin and keratin 8 and do not express vimentin. Tumors derived from small transplanted tumor fragments retain the original phenotype (B). The transplanted tumors in (B) are derived from the tumors shown in (A). Scale bar = 100 μ m and all pictures are taken with the same magnification.

***p53*^{Δ/Δ} carcinomas and carcinosarcomas have similar distributions of the Lin⁻ populations**

We have previously shown that selection for the CD24 and CD49f cell surface markers enriches for TICs in *Brca1*^{Δ/Δ};*p53*^{Δ/Δ} mammary carcinomas from *K14cre;Brca1*^{F/F};*p53*^{F/F} mice⁷. We therefore used these markers to investigate whether there is a difference in TIC frequencies between the epithelial and mesenchymal *p53*^{Δ/Δ} mammary tumors from our different mouse models. In freshly dissociated tumors, stromal cells (Lin⁺) were excluded using the CD45⁺, TER119⁺, CD31⁺ and CD140a⁺ markers and the remaining Lin⁻ cells were analyzed for expression of CD24 and CD49f by flow cytometry. The means of three of the four fractions (Lin⁻/CD24⁻/CD49f⁻, Lin⁻/CD24⁺/CD49f⁻, and Lin⁻/CD24⁺/CD49f⁺ cells) varied among the carcinomas (n=6) and also among the carcinosarcomas (n=7) within a range of 20-37% without significant differences ($p > 0.05$, ANOVA test (Figure 2)). Compared to the other Lin⁻ populations, the Lin⁻/CD24⁻/CD49f⁺ cells were present at a lower mean frequency in both the carcinomas and carcinosarcomas (5.7 and 15.6%, respectively), which is significant among the carcinomas ($p < 0.01$, ANOVA). Intriguingly, no significant difference between the carcinomas and carcinosarcomas was detected for any of the four cell surface marker combinations. This was somewhat surprising to us, as we expected to find more Lin⁻/CD24⁺/CD49f⁺ cells in the mesenchymal tumors on the basis of previous reports^{13-16,20}.

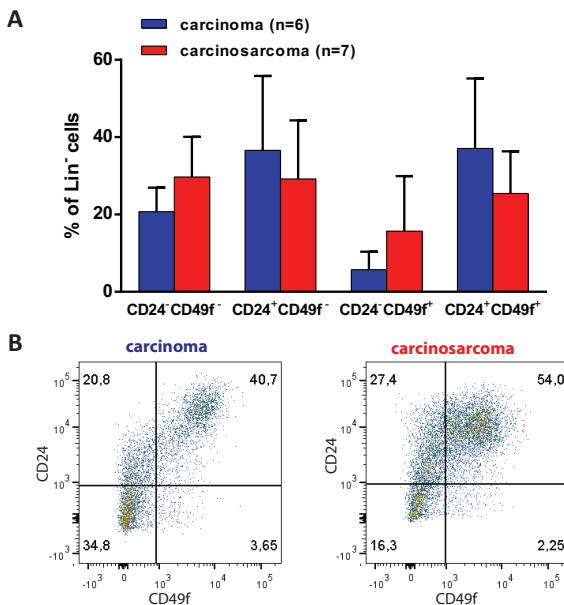


Figure 2. Mammary stem cell markers in *p53*^{Δ/Δ} carcinomas en carcinosarcomas. **A**, Analysis of the distribution of the four populations (CD24⁻/CD49f⁻, CD24⁺/CD49f⁻, CD24⁻/CD49f⁺, CD24⁺/CD49f⁺) of Lineage-negative (Lin⁻) cells in carcinomas and carcinosarcomas by flow cytometry. The mean plus standard deviation of all donors that have been used for sorting experiments is shown. **B**, Example of the CD24 and CD49f FACS profile of Lin⁻ cells from a representative *p53*^{Δ/Δ} carcinoma and carcinosarcoma.

Lin⁻/CD24⁻/CD49f⁻ and Lin⁻/CD24⁺/CD49f⁺ cells have higher tumor-initiating capacity in carcinosarcomas than in carcinomas

To test whether the Lin⁻/CD24⁺/CD49f⁺ cells are enriched for TICs in the *p53*^{Δ/Δ} mammary carcinomas and carcinosarcomas, as we observed in the *Brca1*^{Δ/Δ};*p53*^{Δ/Δ} mammary carcinomas⁷, we performed limiting dilution transplantation experiments. Re-analysis of FACS sorted cell fractions indicated >90% purity (Supplementary Figure S1). Per fraction and cell number three to five different donor tumors were used. In total, we performed all transplantations with cells derived from 6 different *p53*^{Δ/Δ} mammary carcinomas and 7 different *p53*^{Δ/Δ} mammary carcinosarcomas.

In carcinomas the Lin⁻/CD24⁻/CD49f⁻ fraction had clearly the lowest tumor-initiating capacity, with only 1 tumor growing out of 24 injections using 100 cells (Figure 3A and Table 1). The highest number of outgrowing tumors was seen for Lin⁻/CD24⁺/CD49f⁺ cells, which is consistent with our finding in *Brca1*^{Δ/Δ};*p53*^{Δ/Δ} carcinomas⁷. In the *p53*^{Δ/Δ} carcinosarcomas, however, all four subpopulations had similar outgrowth potential within the range of 100 to 1000 injected cells, and more than half of all injections with as few as 100 cells formed new tumors (Figure 3B and Table 1). Compared to carcinomas, the Lin⁻/CD24⁻/CD49f⁻ and Lin⁻/CD24⁺/CD49f⁺ subpopulations in carcinosarcomas have a higher tumor-initiating capacity. Together, this suggests that the utility of the CD24 and CD49f markers for identifying TICs is context dependent.

All cell fractions reconstitute the original tumor heterogeneity and phenotype

Despite our finding that within the *p53*^{Δ/Δ} carcinomas the Lin⁻/CD24⁻/CD49f⁻ and Lin⁻/CD24⁺/CD49f⁺ cells are less tumorigenic than the Lin⁻/CD24⁺/CD49f⁺ cells, they still form tumors, especially at higher cell numbers. It is possible that the Lin⁻/CD24⁻/CD49f⁻ fraction contains transit-amplifying cells that are not able to form CD24⁺ and CD49f⁺ cells. To examine this we analyzed the expression of CD24 and CD49f on Lin⁻ cells from tumor outgrowths by flow cytometry. Tumors that grew out of Lin⁻/CD24⁻/CD49f⁻ carcinoma cells contained all four Lin⁻ fractions (Figure 4A), indicating that these cells are not just transit-amplifying but are able to regenerate tumor outgrowths with the same heterogeneity as the donor tumor. Also the other three Lin⁻ fractions from *p53*^{Δ/Δ} carcinomas and carcinosarcomas gave rise to tumor outgrowths containing all Lin⁻ populations (Figure 4A and 4B), although the sorted population remained somewhat enriched in the tumor outgrowth compared with the original donor tumor. Importantly, all tumors derived from FACS sorted carcinoma or carcinosarcoma cells retained their epithelial or mesenchymal phenotype upon transplantation (Figure 4C and 4D). Taken together, these data indicate that there is a high degree of plasticity regarding the expression of CD24 and CD49f cell surface markers within the carcinomas and carcinosarcomas.

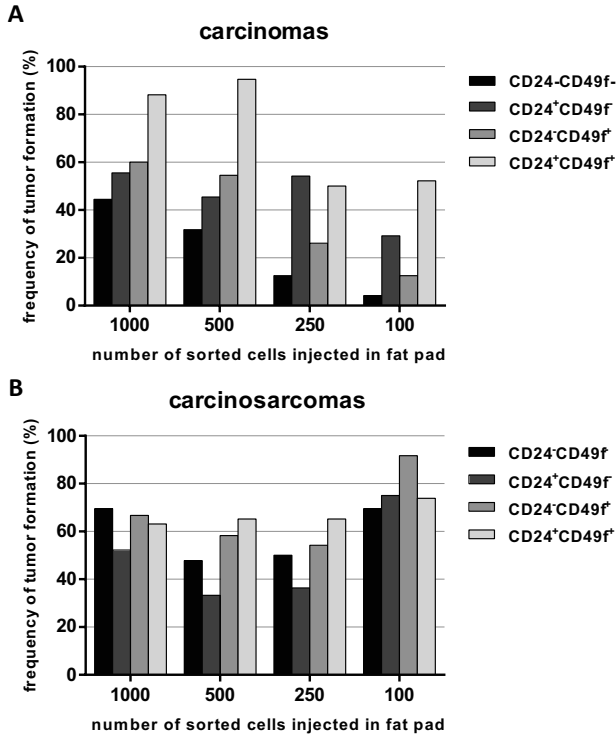


Figure 3. Tumorigenicity of $p53^{4/4}$ carcinoma and carcinosarcoma cell fractions. Frequency of tumor outgrowth after orthotopic transplantation in syngeneic mice of limiting dilutions of sorted Lin⁻ cells from carcinomas (A) or carcinosarcomas (B). The outgrowth frequencies are listed in Table 1.

Table 1

Carcinomas				
No. cells injected	Total tumor incidence (n)			
	Lin ⁻ /CD24 ⁻ /CD49f ⁻	Lin ⁻ /CD24 ⁺ /CD49f ⁻	Lin ⁻ /CD24 ⁻ /CD49f ⁺	Lin ⁻ /CD24 ⁺ /CD49f ⁺
1000	8/18 (3)	10/18 (4)	6/10 (3)	15/17 (4)
500	7/22 (5)	10/22 (5)	12/22 (5)	18/19 (5)
250	3/24 (5)	13/24 (5)	6/23 (5)	11/22 (5)
100	1/24 (5)	7/24 (5)	3/24 (5)	12/23 (5)
Carcinosarcomas				
No. cells injected	Total tumor incidence (n)			
	Lin ⁻ /CD24 ⁻ /CD49f ⁻	Lin ⁻ /CD24 ⁺ /CD49f ⁻	Lin ⁻ /CD24 ⁻ /CD49f ⁺	Lin ⁻ /CD24 ⁺ /CD49f ⁺
1000	16/23 (5)	12/23 (5)	14/21 (5)	12/19 (5)
500	11/23 (5)	8/24 (5)	14/24 (5)	15/23 (6)
250	11/22 (5)	8/22 (5)	13/24 (5)	15/23 (5)
100	16/23 (4)	18/24 (4)	22/24 (4)	17/23 (4)

Frequency of tumor outgrowth upon orthotopic transplantation of sorted cell fractions, as shown in Figure 3. (n) indicates the number of donor tumors used for the cell sorting and transplantations.

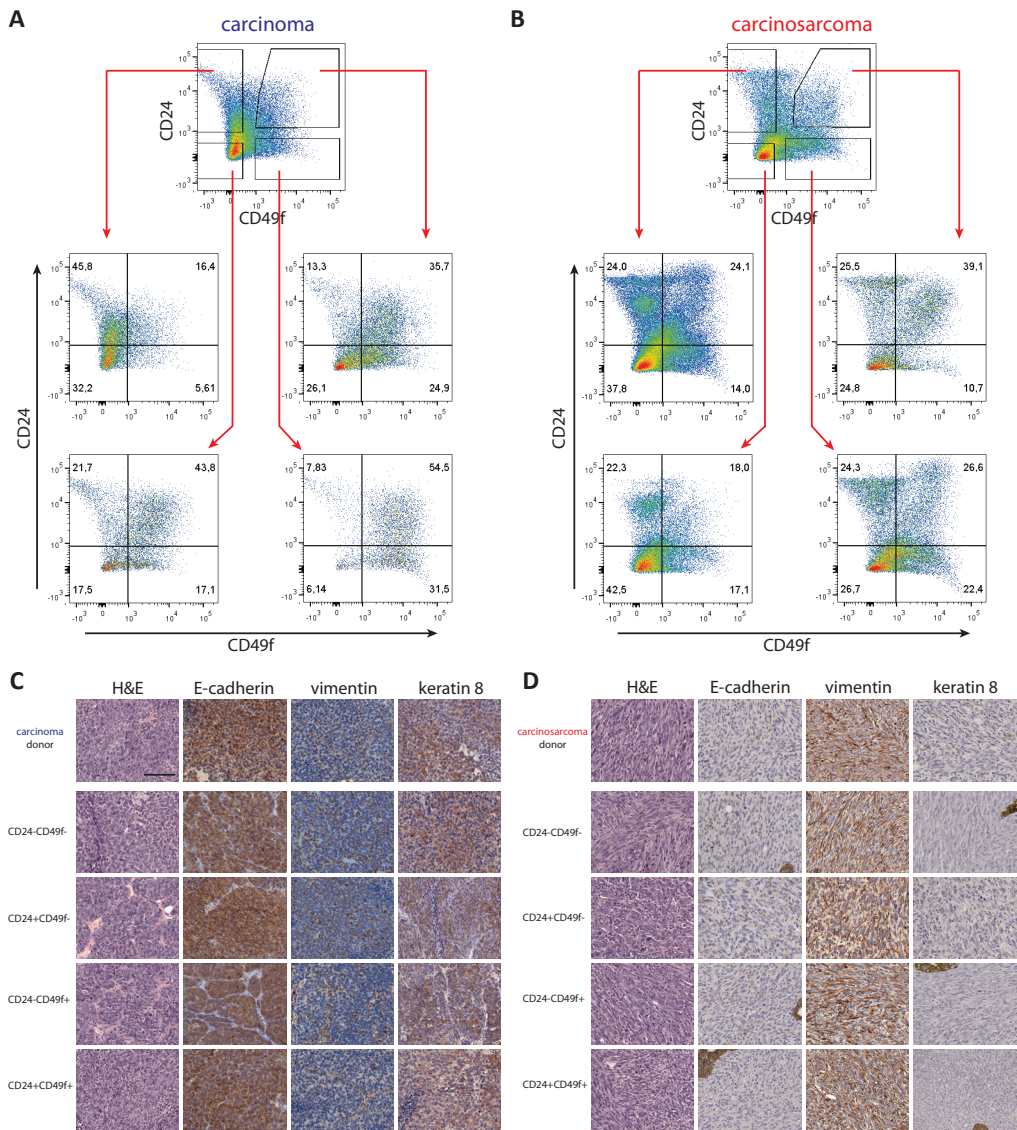


Figure 4. Characterization of tumors from sorted cells compared to the donor. FACS profiles of the carcinoma (A) and carcinosarcoma (B) donor tumor and tumors that grew out of each of the four fractions as indicated by the red arrows. Tumors arising from every subpopulation contain all four Lin⁺ fractions after tumor outgrowth. C-D, Representative histological characterization of a *p53^{Δ/Δ}* carcinoma and carcinosarcoma donor and tumor outgrowths from each of the four fractions. Scale bar = 100 μ m and all pictures are taken with the same magnification.

DISCUSSION

Here we show that tumor fractions of p53-deficient mouse mammary carcinomas and carcinosarcomas have different tumorigenic capacity when using the mammary stem cell markers CD24 and CD49f. In carcinosarcomas all Lin⁻ subpopulations appear to have equal tumorigenic capacity when 100 to 1000 cells are injected. In carcinomas, the Lin⁻/CD24⁻/CD49f⁻ population had the lowest tumor-initiating capacity, but still formed tumors at higher cell numbers. All Lin⁻ fractions of both tumor subtypes reconstituted the tumor heterogeneity and retained the original phenotype upon transplantation.

A link between EMT and TICs has been extensively studied by Mani *et al.*¹⁴, who showed that normal and neoplastic human CD44^{high}/CD24^{low} and mouse CD24^{med}/CD49f^{high} mammary stem cells have an EMT gene expression pattern. The induction of EMT in immortalized and transformed cultured human mammary epithelial (HMLE) cells by overexpression of the transcription factors Snail or Twist or treatment with TGFβ increased the number of CD44^{high}/CD24^{low} cells^{14–16}. More recently, Chaffer *et al.*²¹ demonstrated that non-tumorigenic CD44^{lo} breast cancer cells could become CD44^{hi} and tumorigenic through activation of the EMT transcription factor ZEB1, indicating plasticity of the non-TIC population.

In our p53-deficient carcinosarcomas that have an EMT phenotype and gene expression profile, we expected to find large populations of highly tumorigenic Lin⁻/CD24⁺/CD49f⁺ cells. However, we did not observe any significant differences in the relative abundance of the four Lin⁻ populations between mesenchymal and epithelial tumors. Moreover, we found that the tumor-initiating capacity of Lin⁻/CD24⁻/CD49f⁻ cells was much higher in the carcinosarcomas than in the carcinomas. Using HMLE cells, it would be interesting to test whether the remaining non-CD44^{high}/CD24^{low} cells after EMT induction are still non-tumorigenic or whether they have also acquired tumorigenic properties. The high tumorigenic capacity of our p53-deficient mammary carcinosarcomas is in line with Zhang *et al.*¹⁰ and Herschkowitz *et al.*²⁰, who used the stem cell markers CD24 and CD29 to characterize Lin⁻ cell populations in p53-deficient mouse mammary tumors. They found that all Lin⁻ subpopulations have a higher tumorigenic capacity in EMT-like claudin-low tumors compared to adenocarcinomas, in which the Lin⁻/CD24⁺/CD29⁺ subpopulation is most enriched for TICs. They also found, however, that the majority of cells in claudin-low tumors had a Lin⁻/CD24⁺/CD29⁺ phenotype, whereas we did not find any enrichment for Lin⁻/CD24⁺/CD49f⁺ cells in our carcinosarcomas.

Why do the subpopulations using the mammary stem cell markers CD24 and CD49f differ in tumor-initiating capacity between carcinomas and carcinosarcomas? One possibility is that these markers identify cells with increased survival properties rather than cells with unique tumor-initiating properties. In this respect it is noteworthy that the currently used mouse mammary stem cell markers are all components of the integrin pathway, which plays a key role in cell survival. CD29 is also known as β1 integrin, CD49f is known as α6 integrin,

and CD24 is required for stabilizing CD29²². The presence of CD24 in combination with CD29 or CD49f might therefore enhance the survival of carcinoma cells through interaction with integrin ligands present in the matrigel or the mammary fat pad stroma. Survival of sarcomatoid tumor cells in carcinosarcomas might be less dependent on integrin-mediated interactions with the extracellular matrix because they may have invoked other anti-apoptotic mechanisms. In support of this notion, the EMT transcription factor Twist was shown to inhibit apoptosis through suppression of Myc-induced apoptosis²³. Twist was also shown to be a critical mediator of NFκB-controlled protection against apoptosis²⁴. Survival signaling via integrins or EMT factors could have a strong impact on the TIC frequencies as determined by transplantation experiments, in which enzymatic dissociation, single-cell preparation, cell sorting and transplantation impose substantial stress on tumor cells. As a result of this, the TIC frequencies that are found in transplantation assays might actually be an underestimation². Indeed, Quintana *et al.*¹¹ have shown that the measured frequency in human melanomas can vary a lot depending on dissociation, sorting and transplantation procedures and the recipient mice.

The cancer stem cell model was originally described for hematopoietic malignancies and later also applied to solid cancers. It is still unclear which cancer types, or perhaps subtypes, have this hierarchical organization with relatively rare cancer-initiating cells. Several reports show a high frequency of TICs in human melanoma¹¹ and mouse models of leukemia and lymphomas^{25,26}, whereas others reported that in spite of improvements in the tumorigenesis assays the TIC frequency remained low in AML²⁷ and several solid tumors²⁸. Recently Kurpios *et al.*²⁹ demonstrated a high TIC frequency in unsorted mammary tumors of three MMTV-driven models.

How reliable CSC markers are and whether they are equally useful in different human cancer (sub)types or mouse tumor models remains unclear, as the plasticity in the expression of these markers remains to be investigated. Induction of EMT has been shown to induce expression of stem cell markers¹⁴, but the EMT-like carcinosarcomas from our mouse models still show heterogeneous expression of CD24 and CD49f. Moreover, in our carcinomas each of the four sorted populations reconstituted all other populations without undergoing EMT, indicating that expression of these markers is dynamic. Attempts to specifically target CSCs³⁰, which are thought to be drug resistant, might thus be hampered by the context specificity and cellular plasticity of TICs.

In summary, our results suggest that CD24 and CD49f may not universally distinguish tumorigenic from non-tumorigenic cells in mouse mammary tumors. This indicates that markers for characterization of TICs in mouse tumors or patients may be context dependent and need to be functionally validated before they can be applied to other tumor (sub)types or patients.

METHODS

Mice and mammary tumors

For the generation of carcinoma and carcinosarcoma mammary tumors we used *K14cre;p53^{f/f}* (ref. ¹⁷), *WAPcre;Cdh1^{f/f};p53^{f/f}* (ref. ¹⁸) and *K14cre;Cdh1^{f/f};p53^{f/f}* (ref. ¹⁹) mice, that were generated and genotyped as described. When harvested, part of the tumor was cut in pieces and cryopreserved in DMSO and part was taken for histology. Orthotopic transplantations were performed as described³¹. Starting from two weeks after transplantation, tumor growth was monitored at least three times a week. Tumor growth was measured by caliper and tumors were used for FACS analysis and sorting at a size of 200-500 mm³. After opening the skin, limiting dilutions of sorted cell fractions were injected in the fourth right and left mammary gland, without clearing the fat pad first. When only one of the two grew out, a mastectomy was performed. Mice were monitored for tumor outgrowth for at least four months. All experiments with animals were approved by the Animal Ethics Committee of the Netherlands Cancer Institute.

Preparation and flow cytometry of single-cell suspensions

Tumors were digested and processed as previously described⁷. In brief, minced pieces were sequentially incubated with collagenase/hyaluronidase (StemCell Technologies), red blood cell lysis buffer (Sigma) and dispase (StemCell Technologies) supplemented with DNase I (Sigma). Antibodies used are CD24-FITC (BD Biosciences) and CD49f-PE (BD Biosciences). To remove lymphocytes, erythrocytes, endothelial cells and fibroblasts (collectively designated Lineage⁺) we used biotinylated CD45, TER119, CD31, CD140a (BD Biosciences) and Streptavidin-Cy5 (Invitrogen). Dead cells were excluded in the gating strategy using propidium iodide (PI) or 4',6-diamidino-2-phenylindole (DAPI). From each tumor all single-color controls were taken along for optimal gating. All analyses and sorts were performed on a Cyan analyzer (Beckman Coulter) and FACS Aria (Becton Dickinson), respectively.

For transplantation of sorted fractions viable cells were counted with Trypan Blue under the microscope. Cells were re-suspended in a 1:1 mix of Hanks' Balanced Salt Solution (HBSS, StemCell Technologies) and matrigel (growth factor-reduced, BD Biosciences) and injected in 20 µl per fat pad.

Immunohistochemical analysis

For immunohistochemical staining slides were boiled in Tris-EDTA pH9.0 (E-cadherin and vimentin) or citrate buffer (BioGenex, keratin 8) to retrieve antigens. Primary antibodies (mouse anti-E-cadherin, BD Transduction Laboratories 610182, 1:400; rabbit anti-vimentin, Cell Signalling 5741, 1:200; rat anti-keratin 8, University of Iowa, TROMA-1, 1:600) were diluted in 1.25% normal goat serum plus 1% bovine serum albumin (BSA) in PBS. For keratin 8 slides were incubated with a biotinylated secondary goat-anti-rat antibody (SantaCruz) and Streptavidin-HRP (DAKO). For E-cadherin and vimentin detection labelled polymer-HRP anti-mouse and rabbit Envision (Dako K4007 and K4011) were used. For visualization DAB (Sigma D5905) and hematoxylin counterstaining were applied.

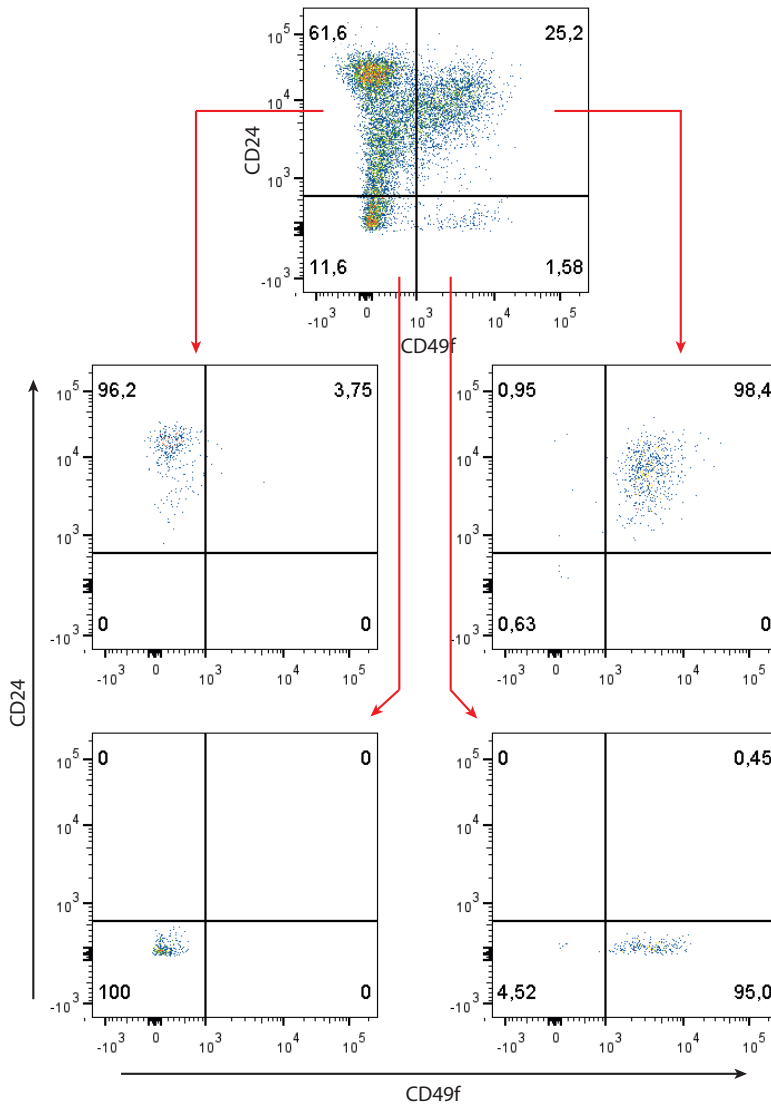
ACKNOWLEDGMENTS

This work was supported by grants from the Netherlands Organization for Scientific Research (NWO-Toptalent 021.002.104 to J.E. Jaspers, NWO-VIDI 91.711.302 to S. Rottenberg, and NWO-roadmap MCCA 184.032.303), Dutch Cancer Society (projects NKI 2007-3772, NKI 2009-4303 and NKI-2011-5220), the EU FP7 Project 260791-Eurocan-Platform, CTMM Breast Care, and the NKI-AVL Cancer Systems Biology Centre.

REFERENCES

1. Reya, T., Morrison, S. J., Clarke, M. F. & Weissman, I. L. Stem cells, cancer, and cancer stem cells. *Nature* **414**, 105–111 (2001).
2. Magee, J. A., Piskounova, E. & Morrison, S. J. Cancer stem cells: impact, heterogeneity, and uncertainty. *Cancer Cell* **21**, 283–296 (2012).
3. Clevers, H. The cancer stem cell: premises, promises and challenges. *Nat. Med.* **17**, 313–319 (2011).
4. Al-Hajj, M., Wicha, M. S., Benito-Hernandez, A., Morrison, S. J. & Clarke, M. F. Prospective identification of tumorigenic breast cancer cells. *Proc. Natl. Acad. Sci. U. S. A.* **100**, 3983–3988 (2003).
5. Shackleton, M. *et al.* Generation of a functional mammary gland from a single stem cell. *Nature* **439**, 84–88 (2006).
6. Stingl, J. *et al.* Purification and unique properties of mammary epithelial stem cells. *Nature* **439**, 993–997 (2006).
7. Pajic, M. *et al.* Tumor-initiating cells are not enriched in cisplatin-surviving BRCA1;p53-deficient mammary tumor cells in vivo. *Cell Cycle Georget. Tex* **9**, 3780–3791 (2010).
8. Cho, R. W. *et al.* Isolation and molecular characterization of cancer stem cells in MMTV-Wnt-1 murine breast tumors. *Stem Cells Dayt. Ohio* **26**, 364–371 (2008).
9. Shafee, N. *et al.* Cancer stem cells contribute to cisplatin resistance in Brca1/p53-mediated mouse mammary tumors. *Cancer Res.* **68**, 3243–3250 (2008).
10. Zhang, M. *et al.* Identification of tumor-initiating cells in a p53-null mouse model of breast cancer. *Cancer Res.* **68**, 4674–4682 (2008).
11. Quintana, E. *et al.* Efficient tumour formation by single human melanoma cells. *Nature* **456**, 593–598 (2008).
12. Foroni, C., Brogгинi, M., Generali, D. & Damia, G. Epithelial-mesenchymal transition and breast cancer: role, molecular mechanisms and clinical impact. *Cancer Treat. Rev.* **38**, 689–697 (2012).
13. Lim, S. *et al.* SNAI1-Mediated Epithelial-Mesenchymal Transition Confers Chemoresistance and Cellular Plasticity by Regulating Genes Involved in Cell Death and Stem Cell Maintenance. *Plos One* **8**, e66558 (2013).
14. Mani, S. A. *et al.* The epithelial-mesenchymal transition generates cells with properties of stem cells. *Cell* **133**, 704–715 (2008).
15. Morel, A.-P. *et al.* Generation of breast cancer stem cells through epithelial-mesenchymal transition. *Plos One* **3**, e2888 (2008).
16. Scheel, C. *et al.* Paracrine and autocrine signals induce and maintain mesenchymal and stem cell states in the breast. *Cell* **145**, 926–940 (2011).
17. Liu, X. *et al.* Somatic loss of BRCA1 and p53 in mice induces mammary tumors with features of human BRCA1-mutated basal-like breast cancer. *Proc. Natl. Acad. Sci. U. S. A.* **104**, 12111–12116 (2007).

18. Derksen, P. W. B. *et al.* Mammary-specific inactivation of E-cadherin and p53 impairs functional gland development and leads to pleomorphic invasive lobular carcinoma in mice. *Dis. Model. Mech.* **4**, 347–358 (2011).
19. Derksen, P. W. B. *et al.* Somatic inactivation of E-cadherin and p53 in mice leads to metastatic lobular mammary carcinoma through induction of anoikis resistance and angiogenesis. *Cancer Cell* **10**, 437–449 (2006).
20. Herschkowitz, J. I. *et al.* Comparative oncogenomics identifies breast tumors enriched in functional tumor-initiating cells. *Proc. Natl. Acad. Sci. U. S. A.* **109**, 2778–2783 (2012).
21. Chaffer, C. L. *et al.* Poised Chromatin at the ZEB1 Promoter Enables Breast Cancer Cell Plasticity and Enhances Tumorigenicity. *Cell* **154**, 61–74 (2013).
22. Lee, K. *et al.* CD24 regulates cell proliferation and transforming growth factor β -induced epithelial to mesenchymal transition through modulation of integrin $\beta 1$ stability. *Cell. Signal.* **24**, 2132–2142 (2012).
23. Valsesia-Wittmann, S. *et al.* Oncogenic cooperation between H-Twist and N-Myc overrides failsafe programs in cancer cells. *Cancer Cell* **6**, 625–630 (2004).
24. Pham, C. G. *et al.* Upregulation of Twist-1 by NF-kappaB blocks cytotoxicity induced by chemotherapeutic drugs. *Mol. Cell. Biol.* **27**, 3920–3935 (2007).
25. Kelly, P. N., Dakic, A., Adams, J. M., Nutt, S. L. & Strasser, A. Tumor growth need not be driven by rare cancer stem cells. *Science* **317**, 337 (2007).
26. Williams, R. T., den Besten, W. & Sherr, C. J. Cytokine-dependent imatinib resistance in mouse BCR-ABL+, Arf-null lymphoblastic leukemia. *Genes Dev.* **21**, 2283–2287 (2007).
27. Eppert, K. *et al.* Stem cell gene expression programs influence clinical outcome in human leukemia. *Nat. Med.* **17**, 1086–1093 (2011).
28. Ishizawa, K. *et al.* Tumor-initiating cells are rare in many human tumors. *Cell Stem Cell* **7**, 279–282 (2010).
29. Kurpios, N. A. *et al.* Single unpurified breast tumor-initiating cells from multiple mouse models efficiently elicit tumors in immune-competent hosts. *Plos One* **8**, e58151 (2013).
30. Gupta, P. B. *et al.* Identification of selective inhibitors of cancer stem cells by high-throughput screening. *Cell* **138**, 645–659 (2009).
31. Rottenberg, S. *et al.* Selective induction of chemotherapy resistance of mammary tumors in a conditional mouse model for hereditary breast cancer. *Proc. Natl. Acad. Sci. U. S. A.* **104**, 12117–12122 (2007).



Supplementary Figure S1. Re-analysis of the FACS sorted fractions to verify the purity.

CHAPTER 6



Proteomics of mouse BRCA1-deficient mammary tumors identifies DNA repair proteins with potential diagnostic and prognostic value in human breast cancer

Marc Warmoes¹, Janneke E. Jaspers², Thang V. Pham¹, Sander R. Piersma¹,
Gideon Oudgenoeg¹, Maarten P.G. Massink³, Quinten Waisfisz³, Sven Rottenberg²,
Epie Boven¹, Jos Jonkers², Connie R. Jimenez¹

¹ Oncoproteomics Laboratory, Department of Medical Oncology and ³ Department of Clinical Genetics, VU Medical Center, De Boelelaan 1117, 1081 HV Amsterdam, The Netherlands; ² Division of Molecular Biology, Netherlands Cancer Institute, Plesmanlaan 121, 1066 CX Amsterdam, The Netherlands

*This research was originally published in **Molecular and Cellular Proteomics**, 2012; 11(7):M111.013334. © the American Society for Biochemistry and Molecular Biology*

ABSTRACT

Breast cancer 1, early onset (BRCA1) hereditary breast cancer, a type of cancer with defects in the homology-directed DNA repair pathway, would benefit from the identification of proteins for diagnosis, which might also be of potential use as screening, prognostic or predictive markers. Sporadic breast cancers with defects in the BRCA1 pathway might also be diagnosed. We employed proteomics based on one-dimensional gel electrophoresis in combination with nano-LC-MS/MS and spectral counting to compare the protein profiles of mammary tumor tissues of genetic mouse models either deficient or proficient in BRCA1. We identified a total of 3545 proteins, of which 801 were significantly differentially regulated between the BRCA1-deficient and -proficient breast tumors. Pathway and protein complex analysis identified DNA repair and related functions as the major processes associated with the up-regulated proteins in the BRCA1-deficient tumors. In addition, by selecting highly connected nodes, we identified a BRCA1 deficiency signature of 45 proteins that enriches for homology-directed DNA repair deficiency in human gene expression breast cancer data sets. This signature also exhibits prognostic power across multiple data sets, with optimal performance in a data set enriched in tumors deficient in homology-directed DNA repair. In conclusion, by comparing mouse proteomes from BRCA1-proficient and -deficient mammary tumors, we were able to identify several markers associated with BRCA1 deficiency and a prognostic signature for human breast cancer deficient in homology-directed DNA repair.

INTRODUCTION

Breast cancer associated with BRCA1 mutations accounts for 1-2 % of breast cancer cases in the Western world. BRCA1 hereditary breast cancer falls into the molecular subtype of basal-like breast cancer that has a poor prognosis¹. Sporadic basal-like breast tumors represent ≈10-15 % of all breast carcinomas and comprise many tumors that share key features of BRCA1-associated tumors². A major function of BRCA1 is its role in homology-directed double-strand break repair, a DNA repair mechanism that uses the sister chromatid as a template and therefore repairs double-strand breaks in an error-free manner. Deficiencies in homology-directed DNA repair cause high levels of genomic instability that increase the risk of tumorigenesis^{3,4}. Nevertheless, BRCA1 pathway dysfunction may provide an opportunity for therapeutic intervention: preclinical models suggest an increased sensitivity to ionizing radiation and DNA (repair)-targeting agents³. In particular, the use of poly(ADP-ribose) polymerase (PARP) inhibitors holds great promise for clinical application. First results from clinical trials support this therapeutic approach for breast cancer⁵. A major clinical challenge remains the identification of patients that are likely to benefit from DNA (repair)-targeting therapy. Global analyses of molecular alterations in sporadic or hereditary breast cancer have mainly used genome and transcriptome profiling methods. These studies yielded a molecular classification of breast cancer⁶. In addition, genomics and transcriptomics studies yielded a number of gene signatures that were prognostic for survival, time to distant metastasis and response to treatment^{1,6-15}. Two prognostic signatures, Oncotype DX^{®11} and MammaPrint^{®,7;16} have currently been registered for clinical use. Recently, Vollebergh *et al.*¹³ have found in a retrospective study that a comparative genomic hybridization BRCA1-like classifier predicts the response to intensive platinum-based chemotherapy in patients with high risk breast cancer. The classifier also identifies patients with BRCA1 loss conferred by causes other than mutations. However, the underlying gene products, which would allow for a better understanding of tumor biology and a more practical diagnostic test, remain unknown. To identify patients with BRCA1-like breast cancer, the analysis of tumor proteins may also be useful in selecting patients that might benefit from tailored therapies. Mass-spectrometry based proteomics technologies have matured to the extent that they can now identify and quantify thousands of proteins. Applying these approaches to cancer tissues provides a complementary insight in breast cancer biology and may identify novel diagnostic and prognostic protein profiles and candidate biomarkers. Protein based biomarkers may be of particular advantage in comparison with transcript-based and genomic markers, because they can be measured in routine assays, *e.g.* by antibody-based methods such as immunohistochemistry and ELISA, of which the latter allows for non-invasive testing. In addition, targeted multiplex mass spectrometry is emerging as a novel quantitative strategy for measuring protein signatures in tumor tissues or blood. Proteomic studies of

breast cancer cells and tissues have already shown the potential for candidate biomarkers discovery¹⁷⁻²². In a promising pilot study using SELDI-TOF-MS, serum peptide profiles could distinguish women with BRCA1 mutations who developed breast cancer from those who did not (carrier), normal volunteers, and women with sporadic breast cancer with good sensitivity and specificity²³. To date, no studies employing in depth nano-LC-MS/MS-based proteomics have focused on BRCA1/2-deficient tumor tissues.

In this study, we employed state of the art mass spectrometry-based proteomics to identify proteins associated with BRCA1-deficient breast tumors. To this end, we made use of inbred mouse models that display a minimal amount of genetic variability. As a model for human breast cancers deficient in BRCA1, we analyzed mouse mammary tumors harboring conditional tissue-specific mutations in BRCA1 and p53²⁴. The majority of these tumors is highly similar to their human counterpart with respect to histological and molecular characteristics and shows a high level of genomic instability. For comparison, we analyzed two BRCA1-proficient reference tumor models that are genomically stable²⁵. We report a BRCA1 deficiency signature based on 45 proteins with DNA repair(-associated) functions that can enrich for homology-directed DNA repair-deficient tumors and identify breast cancer patients with a poor prognosis in various publicly available breast cancer gene expression data sets.

RESULTS

Protein regulations in BRCA1-deficient versus -proficient mouse mammary tumors

For comparative protein profiling, we employed a label-free workflow based on protein fractionation by gel electrophoresis coupled to nano-LC-MS/MS of in-gel digested proteins and spectral counting. Before embarking on a differential analysis, we assessed the reproducibility of our discovery workflow by analyzing three aliquots of a pooled mammary tumor lysate by gel LC-MS/MS (see Supplementary Figure S1A for gel images). In this analysis, 2220 of 2473 proteins (90%, see Supplementary Figure S1B for Venn diagram) were identified in all three replicates with an average CV of 24 % of the normalized spectral counts, indicating a very good reproducibility of the entire discovery workflow.

To identify proteins associated with BRCA1-deficient mammary tumors, we compared the protein expression profiles in five BRCA1-deficient mammary tumors (*Brca1*^{-/-};*p53*^{-/-}, carcinoma histology) with five BRCA1-proficient tumors (two *p53*^{-/-} and three *p53*^{-/-};*Cdh1*^{-/-} tumors, all carcinosarcomas). Whereas the carcinomas have an epithelial phenotype, the carcinosarcomas have a mesenchymal phenotype characterized by spindle cell morphology. The protein band patterns obtained after gel electrophoresis of the 10 tumor lysates and Coomassie staining were similar in terms of overall pattern and intensity (Supplementary Figure S2A). A total of 3545 proteins were identified across all 10 samples (Supplementary

Table S1 for all identifications and spectral count data). The number of proteins identified in the BRCA1-deficient tumor samples was 3409, with 1894 proteins identified in all five mammary tumors (Supplementary Figure S2B), indicating acceptable reproducibility of protein identification and quantification across different biological samples. Similar values were obtained for the five BRCA1-proficient tumors (Supplementary Figure S2C)

To obtain a global overview of the data set, we performed unsupervised hierarchical clustering using the normalized spectral count data from all 3545 identified proteins. The BRCA1-deficient and -proficient tumors clustered in separate groups (Figure 1A). The two different BRCA1-proficient tumor types (*p53*^{-/-} and *p53*^{-/-};*Cdh1*^{-/-}) did not form two separate groups, but were intermingled, indicating that BRCA1 status and/or histology type were the predominant factors separating the samples. Overlap analysis showed that 338 proteins were uniquely identified in the BRCA1-deficient samples and 136 were uniquely identified in the BRCA1-proficient tumors. Statistical testing³⁰ revealed 801 proteins with significantly altered abundance in the BRCA1-deficient and -proficient groups ($p < 0.05$) of which 417 were up-regulated in the BRCA1-deficient tumors, whereas 384 were down-regulated. As expected, supervised hierarchical clustering using the 801 differential proteins (Figure 1B) clearly showed two different groups that clustered according to BRCA1/cell type status. See Supplementary Table S2 for all differential proteins. For integration with transcriptomics, we employed the data set of Liu *et al.*²⁴ containing gene expression data for the same BRCA1-proficient and -deficient mouse models as used in this study, with the exception that most of the tumors in the discovery set were mammary carcinomas. Of the 801 differential proteins, we were able to retrieve mRNA expression data for 565 proteins, of which 429 (76%) had the same direction of differential expression with 201 of these mRNAs (36%) being significantly differentially expressed (Supplementary Table S2).

In summary, a large proportion (23 %) of the mammary tumor tissue proteome is regulated in BRCA1-deficient tumors as compared with proficient tumors. Because a large fraction of proteins showed co-regulation with a transcriptomics data set that only used BRCA1-deficient carcinomas *versus* BRCA1-proficient carcinomas, we conclude that the differential proteins are related mainly to BRCA1 status and only partially to cell type.

Identification of known markers of human BRCA1-deficient breast cancer

Because BRCA1-deficient breast tumors often belong to the highly proliferative basal-like subtype, we examined the abundance of protein markers known in basal-like breast cancer in our data set. In addition, we looked for known markers of human BRCA1 deficiency. Two basal cytokeratin markers (Krt14 and Krt6b) were significantly up-regulated in the BRCA1-deficient mouse tumors (Table 1). The third cytokeratin (Krt5) was up-regulated ($p = 0.066$) with a fold-change of 3.2. ALDH1, a cancer stem cell marker, was exclusively detected in BRCA1-deficient mouse tumors, in accordance with previous findings³⁵. PCNA and Ki67,

two well-known proliferation markers³⁶, were also significantly up-regulated in the BRCA1-deficient mouse tumors. These confirmatory findings underscore the value of these genetic mouse tumor models and the validity of our proteomics approach to identify proteins associated with BRCA1-related or basal-like breast cancers in patients.

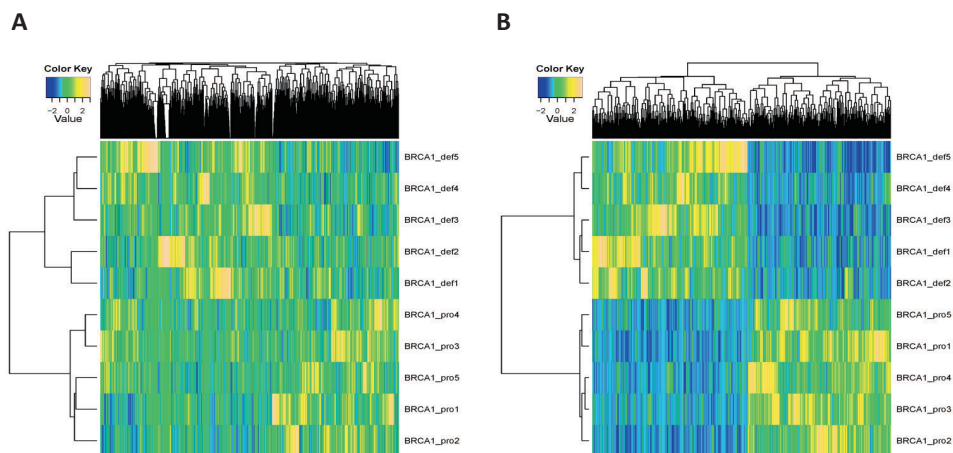


Figure 1. Heat map and cluster analysis using protein expression data from breast tumors of genetic mouse models. **A**, BRCA1-deficient and -proficient tumors are clustered in separate groups using unsupervised clustering. **B**, supervised clustering clearly separates the BRCA1-deficient tumors from the proficient ones and shows a distinct heat map pattern for up- and down-regulated proteins.

Table 1. Known BRCA1/basal-like and proliferation markers associated with BRCA1 deficiency

Gene name	Basal, proliferation and stem cell markers	Fold change *	<i>p</i> value	Marker type
Aldh1a1	Retinal dehydrogenase 1	^a	0.000471	Stem cell
Krt14	Keratin, type I cytoskeletal 14	6.5	0.023115	Basal
Krt5	Keratin, type II cytoskeletal 5	3.7	0.065672	Basal
Krt6b	Keratin, type II cytoskeletal 6B	^a	0.016174	Basal
Pcna	Proliferating cell nuclear antigen	1.8	0.001747	Proliferation
Mki67	Ki-67 protein	79.8	1.18E-05	Proliferation

^a Unique detection in BRCA1-deficient tumors

DNA repair pathways and protein complexes are associated with proteins up-regulated in BRCA1-deficient mammary tumors

To associate biological functions with the differentially expressed BRCA1 deficiency proteins of the mouse mammary tumors, we used the software tool Ingenuity Pathway Analysis. The molecular and cellular functions associated with the up-regulated proteins in BRCA1-

deficient mammary tumors are listed in Table 2, with the number one function identified as DNA Replication, Recombination, and Repair (61 proteins). See Figure 2 for a visualization of the protein network using Ingenuity. The network contains a number of highly connected nodes (*i.e.*, proteins), among which several are well established drug targets (*i.e.*, TOP1, TOP2A, PARP1, and SRC). The top molecular and cellular function associated with the down-regulated proteins was cellular movement (Table 2). The 61 DNA repair proteins up-regulated in BRCA1-deficient mammary tumors were involved in sub-functions like excision repair, chromatin remodeling and modification, double-strand DNA repair and DNA damage response, amongst others. Moreover, canonical pathways associated with the up-regulated proteins in BRCA1-deficient tumors were involved in DNA repair, including ATM signaling, p53 signaling, and role of BRCA1 in DNA damage response (data not shown).

Table 2. Molecular and cellular functions associated with proteins regulated in BRCA1-deficient mammary tumors

Name	p value	No. of proteins
Up-regulated proteins		
DNA Replication, Recombination, and Repair	1.07E-10 – 1.08E-02	61
Cell Cycle	1.19E-09 – 1.08E-02	73
Gene Expression	8.25E-07 – 1.08E-02	73
Cellular Growth and Proliferation	1.90E-06 – 1.08E-02	115
Cellular Development	3.77E-06 – 1.05E-02	39
Down-regulated proteins		
Cellular Movement	4.49E-21 – 1.63E-03	104
Cell Morphology	3.92E-20 – 1.63E-03	85
Cell-To-Cell Signaling and Interaction	6.47E-15 – 1.63E-03	82
Cellular Development	2.26E-13 – 1.70E-03	88
Cellular Function and Maintenance	2.43E-12 – 1.63E-03	69

IPA was used to associate functions to the up- and down-regulated proteins of the BRCA1-deficient mouse tumors. IPA analysis of the up-regulated proteins identified DNA replication, recombination, and repair as the most significant up-regulated molecular and cellular function. Pathway analysis of the down-regulated proteins identified cellular movement as the most significant up-regulated molecular and cellular function.

To identify protein complexes underlying the differential proteins and to further dissect the DNA repair pathways, we employed the COFECO tool³². The up-regulated proteins were linked to 53 significant protein complexes (corrected $p < 0.05$, Supplementary Table S3A), of which 44 have a DNA repair(-associated) function (Supplementary Table S3A, highlighted rows). After removing the redundant protein complexes where all members were present in one of the other significant complexes, 29 DNA repair(-associated) complexes were obtained (Supplementary Table S3B).

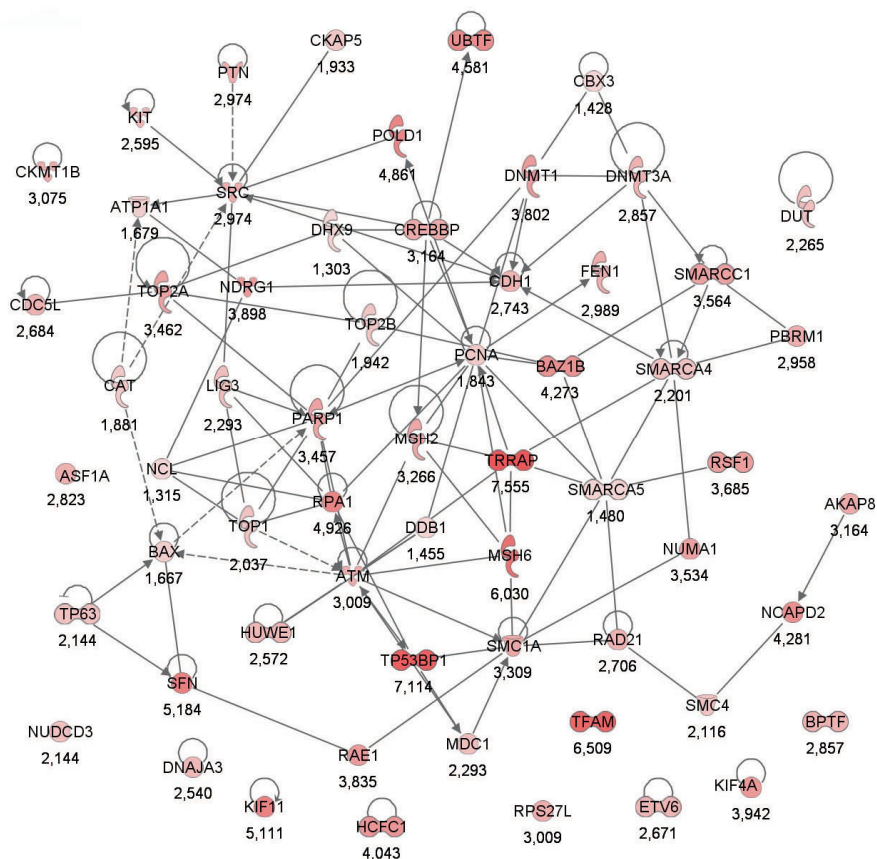


Figure 2. Protein network of significantly up-regulated proteins in BRCA1-deficient tumors that are associated with the top molecular and cellular function DNA replication, recombination, and repair. The nodes represent proteins and the lines between them represent interactions. The dashed lines represent indirect interactions. Color intensity indicates fold change, which is also stated below the nodes.

The DNA repair complexes were involved in chromosome condensation, chromosome cohesion, chromosome remodeling, RNA processing, histone methylation, histone acetylation and the topoisomerase complex, among others. We identified also five complexes which we could not readily link to a physiological process involved in DNA repair. These non-nuclear complexes were involved in integrin cell surface interactions with laminins and collagens. Although these complexes have been implicated in evading apoptosis after DNA damage³⁷, we did not consider these non-nuclear complexes for further analysis. The down-regulated proteins in BRCA1-deficient tumors were not associated with any DNA repair protein complex in a COFECO analysis, but instead revealed complexes involved in integrin signaling, cytoskeleton regulation and extracellular matrix signaling amongst others (Supplementary Table S3C).

We focused in subsequent analyses on the proteins up-regulated in BRCA1-deficient tumors with a link to DNA repair because we hypothesized that the up-regulation of DNA repair proteins and pathways is linked to BRCA1 status and reflects a compensatory response to the loss of BRCA1 DNA repair function. The 29 nonredundant DNA repair protein complexes associated with the up-regulated proteins in the BRCA1-deficient tumors are visualized in Figure 3 using Cytoscape. It is apparent that many protein complexes have multiple up-regulated members. Examples of DNA repair(-associated) complexes included the BRCA1-associated complex (BASC), involved in double-stranded DNA repair³⁸, and the condensin I-PARP1-XRCC1 complex with established functions in single-strand DNA repair³⁹. In addition, five of seven members of the toposome complex including the drug targets TOP1 and TOP2A were significantly up-regulated⁴⁰. Moreover, many chromatin remodeling complexes, with a wide involvement in different types of DNA repair processes⁴¹, were highly prevalent in our data set. Examples included the WINAC complex, the PBAF complex, the SWI/SNF complex, the GCN5-TRRAP histone acetyl-transferase complex and the DNMT3B histone methylation complex (Supplementary Table S3). Together, the analyses pinpoint a major up-regulation of a broad range of DNA repair/chromatin remodeling pathways and protein complexes in BRCA1-deficient mammary tumors.

Identification of a BRCA1 deficiency DNA repair signature

To identify a protein signature with biological relevance for BRCA1-deficient breast tumors, we reasoned this signature should represent the range of up-regulated DNA repair processes in these tumors and therefore contain selected up-regulated members of each of the 29 nonredundant protein complexes described above. To this end, we selected the most connected up-regulated node in each of the 29 DNA repair protein complexes (Figure 3). This strategy may yield multiple proteins per protein complex, because some nodes show the same level of connectivity. Using this strategy a BRCA1 deficiency signature of 45 proteins was obtained (Table 3). The signature includes PARP1, involved in single-strand base repair; TRRAP, a large adaptor protein involved in histone acetylation; TOP2A, a topoisomerase; SMC1A and SMC4, involved in chromatid cohesion and condensation; BAZ1B and ATM, involved in phosphorylation of H2AX upon DNA damage; and MSH2 and MSH6, involved in mismatch repair.

Up-regulated proteins mapped to human transcripts identify human BRCA1/2-deficient tumors

To investigate the power of the 45 protein BRCA1 deficiency signature in separating BRCA1-deficient and -proficient breast cancers in humans in comparison with all up-regulated proteins, we performed *in silico* analysis using publicly available gene expression data sets (Table 4).

Table 3. List of 45 proteins in BRCA1 deficiency signature

Protein description	Mouse IPI identifier	Human gene symbol	Fold change	p value	Regulation comparison mRNA and protein ^a
Transformation/transcription domain-associated protein	IPI00330902	TRRAP	8,4	<0.001	c
Bromodomain adjacent to zinc finger domain protein 1B	IPI00130597	BAZ1B	4,0	<0.001	d
Structural maintenance of chromosomes protein 3	IPI00132122	SMC3	2,4	<0.001	c
Isoform 2 of Condensin complex subunit 1	IPI00172226	NCAPD2	4,5	<0.001	d
Replication protein A 70 kDa DNA-binding subunit	IPI00124520	RPA1	6,3	<0.001	c
Isoform 1 of Paired amphipathic helix protein Sin3a	IPI00117932	SIN3A	20,0	<0.001	d
Pold1 DNA polymerase	IPI00313515	POLD1	8,5	<0.001	c
Activating signal cointegrator 1 complex subunit 3-like 1	IPI00420329	SNRNP200	1,6	0,001	n/a
Structural maintenance of chromosomes protein 1A	IPI00123870	SMC1A	3,2	0,001	c
DNA topoisomerase 2-alpha	IPI00122223	TOP2A	4,0	0,001	n/a
SWI/SNF-related matrix-associated actin-dependent regulator of chromatin subfamily C member 1	IPI00125662	SMARCC1	3,0	0,001	e
DNA topoisomerase 2-beta	IPI00135443	TOP2B	2,1	0,001	d
Host cell factor C1	IPI00828490	HCFC1	3,5	0,002	c
Proliferating cell nuclear antigen	IPI00113870	PCNA	1,8	0,002	d
Raf1 hepatitis B virus x associated protein	IPI00122845	RSF1	^b	0,002	c
Casein kinase II alpha subunit	IPI00408176	C5NK2A1	2,4	0,002	n/a
Cell division cycle 5-related protein	IPI00284444	CDC5L	3,1	0,002	n/a
DNA topoisomerase 1	IPI00109764	TOP1	2,2	0,003	c
Isoform 1 of UDP-N-acetylglucosamine-peptide N-acetylglucosaminyltransferase 110 kDa subunit	IPI00420870	OGT	3,8	0,004	d
Isoform 2 of E1A-binding protein p400	IPI00229659	EP400	9,7	0,004	d
MutS homolog 6	IPI00310173	MSH6	7,1	0,006	d
Isoform 1 of Transcription intermediary factor 1-beta	IPI00312128	TRIM28	1,9	0,008	c
Isoform 1 of Splicing factor, arginine/serine-rich 1	IPI00420807	SFRS1	1,4	0,008	n/a
Snf2-related CBP activator protein	IPI00620743	SRCAP	^b	0,008	n/a
Poly (ADP-ribose) polymerase 1	IPI00139168	PARP1	3,1	0,008	c
SWI/SNF related, matrix associated, actin dependent regulator of chromatin, subfamily a, member 4	IPI00460668	SMARCA4	2,3	0,009	c
CREB binding protein	IPI00463549	CREBBP	5,5	0,010	d
Serine-protein kinase ATM	IPI00124810	ATM	6,0	0,010	c
Double-strand-break repair protein rad21 homolog	IPI00329840	RAD21	3,1	0,014	d

Pre-mRNA-processing-splicing factor 8	IP100121596	PRPF8	1,5	0,014	c
MRG (MORF4-related gene)-binding protein	IP100720110	C20ORF20	b	0,019	d
Cleavage stimulation factor 50 kDa subunit	IP100116747	CSTF1	b	0,020	c
Metastasis associated 1	IP100776055	MTA1	b	0,020	c
DEAD (Asp-Glu-Ala-Asp) box polypeptide 21	IP100652987	DDX21	2,3	0,020	c
Isoform 1 of Heterogeneous nuclear ribonucleoprotein F	IP1002226073	HNRNPF	1,4	0,022	n/a
Nuclear cap-binding protein subunit 1	IP100458056	NCBP1	1,9	0,028	n/a
SWI/SNF-related matrix-associated actin-dependent regulator of chromatin subfamily A member 5	IP100396739	SMARCA5	1,4	0,030	c
DNA mismatch repair protein Msh2	IP100118158	MSH2	3,0	0,031	d
Isoform Long of Splicing factor, arginine/serine-rich 3	IP100129323	SFRS3	1,4	0,035	d
DEAH (Asp-Glu-Ala-His) box polypeptide 9	IP100339468	DHX9	1,3	0,037	c
FACT complex subunit SPT16	IP100120344	SUPT16H	2,1	0,045	d
Cleavage stimulation factor 77 kDa subunit	IP100116929	CSTF3	6,4	0,046	d
Isoform 2 of FACT complex subunit SSRP1	IP100407571	SSRP1	3,1	0,047	d
Structural maintenance of chromosomes protein 4	IP100229397	SMC4	2,4	0,049	d
AT rich interactive domain 1A	IP100648459	ARID1A	3,8	0,049	d

^a For mRNA regulation

^b Unique detection in BRCA1-deficient tumors

^c Significantly up-regulated mRNA

^d No significant regulation mRNA

^e Significant opposite regulation mRNA

n/a = no mRNA probe on microarray

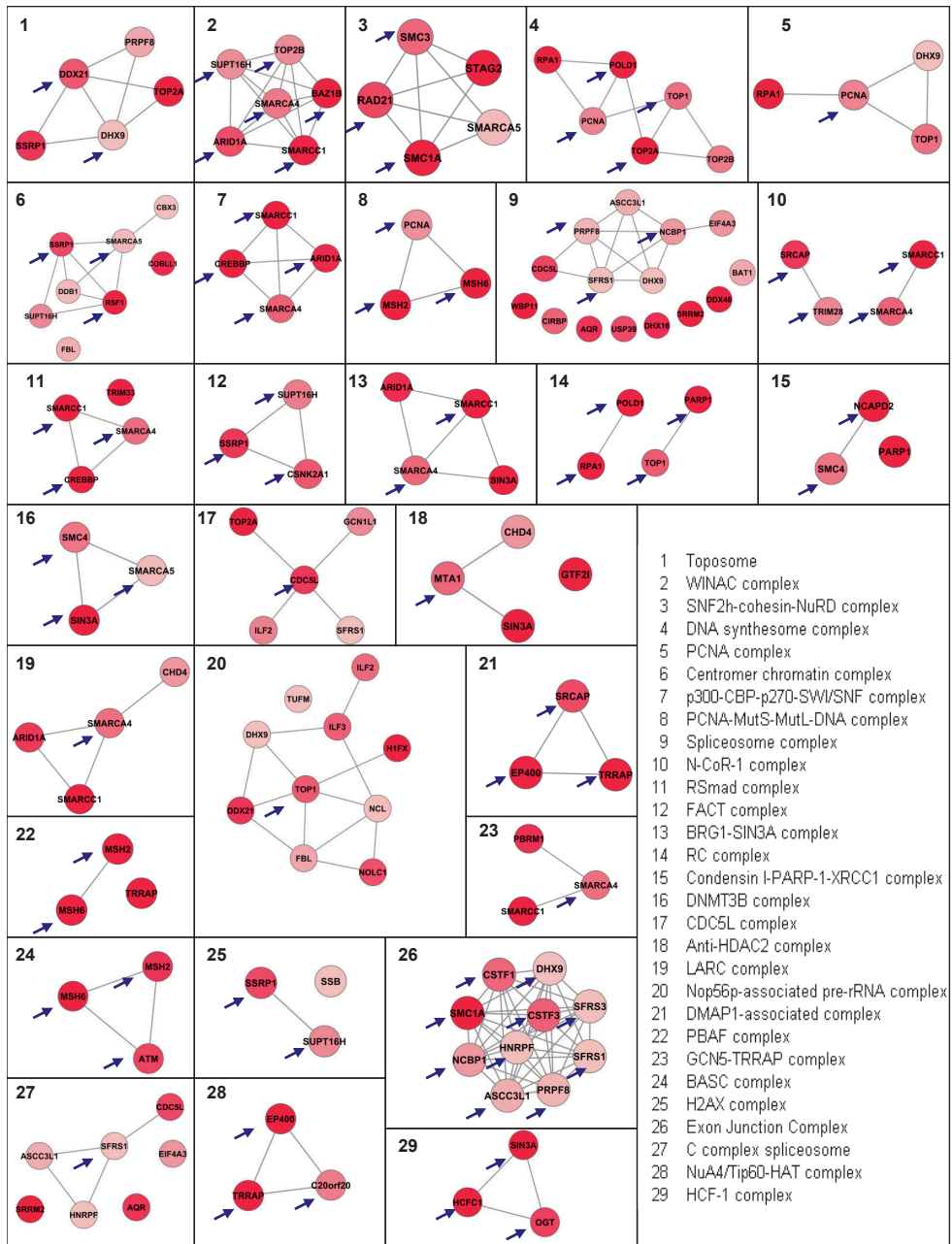


Figure 3. Nonredundant up-regulated DNA repair protein complexes identified by COFECO and visualized using STRING in Cytoscape. The nodes represent proteins and the lines indicate their association as identified in the STRING database. Color intensity is representative of the degree of up-regulation in BRCA1-deficient proteins. Arrows indicate most connected nodes.

We also evaluated the specificity for BRCA2, a gene involved in the same pathway as BRCA1, to examine the ability to identify deficiency in homology-directed DNA repair in general⁴². This is important because of the recent availability of drugs targeting this particular deficiency⁴³.

We first focused on the Jönsson data set containing 22 *BRCA1*- and 32 *BRCA2*-mutated tumors and other familial and sporadic tumors (Table 4), because this whole genome gene expression data set contained the largest number of *BRCA1/2*-mutated tumors. Hierarchical clustering using all up-regulated proteins showed that the majority of *BRCA1*-mutated tumors were clustered within one branch of the dendrogram, which coincides, as expected, with the basal-like tumors (Figure 4A). The *BRCA2* samples were also clustered largely together within the middle branch of the dendrogram. Figure 4B depicts a clustering using the *BRCA1* deficiency signature. Here, a large proportion of the *BRCA1* and *BRCA2* falls within one branch of the dendrogram, making up approximately one-third of the tumors. Thus, the cluster analysis indicates that the 45-protein *BRCA1* deficiency signature shows specificity, not only for *BRCA1*-mutated tumors, but also for *BRCA2*-mutated tumors.

Table 4. Description of relevant information of human breast cancer gene expression data sets used for *in silico* validation

	No. of patients	Patient characteristics	Clinical end point	Source
Van de Vijver <i>et al.</i>	315	295 sporadic patients	Survival	http://www.rii.com/publications
Van 't Veer <i>et al.</i>	20	18 <i>BRCA1</i> and 2 <i>BRCA2</i> mutation carriers	n/a	http://www.rii.com/publications
Wang <i>et al.</i>	286	286 sporadic patients	Time to distant metastasis	GEO accession GSE2034
Naderi <i>et al.</i>	134	134 sporadic patients (120 with survival data)	Survival	Array express accession E-UCON-1
Jönsson <i>et al.</i>	359	22 <i>BRCA1</i> , 32 <i>BRCA2</i> , 173 sporadic and 132 non- <i>BRCA1/2</i> familial patients	Survival	GEO accession GSE22133
Waddell <i>et al.</i>	75	19 <i>BRCA1</i> , 30 <i>BRCA2</i> , 1 unknown, and 25 non- <i>BRCA1/2</i> familial patients	n/a	GEO accession GSE19177

The nearest centroid classification method was employed to characterize more precisely the sensitivity and specificity of the mouse *BRCA1* deficiency signature for *BRCA1*- and *BRCA2*-mutated tumors, as well as for the list of all up-regulated proteins. Table 5A reports the classification results on the Jönsson data set with leave-one-out cross-validation. The sensitivities for *BRCA1*-mutated tumors were 77 % and 82 % for the 417 up-regulated proteins and the *BRCA1* deficiency signature, respectively. Classification for the combination of *BRCA1*- and *BRCA2*-mutated tumors yielded a similar performance: 83 % sensitivity for all up-regulated proteins and 81 % for the *BRCA1* deficiency signature.

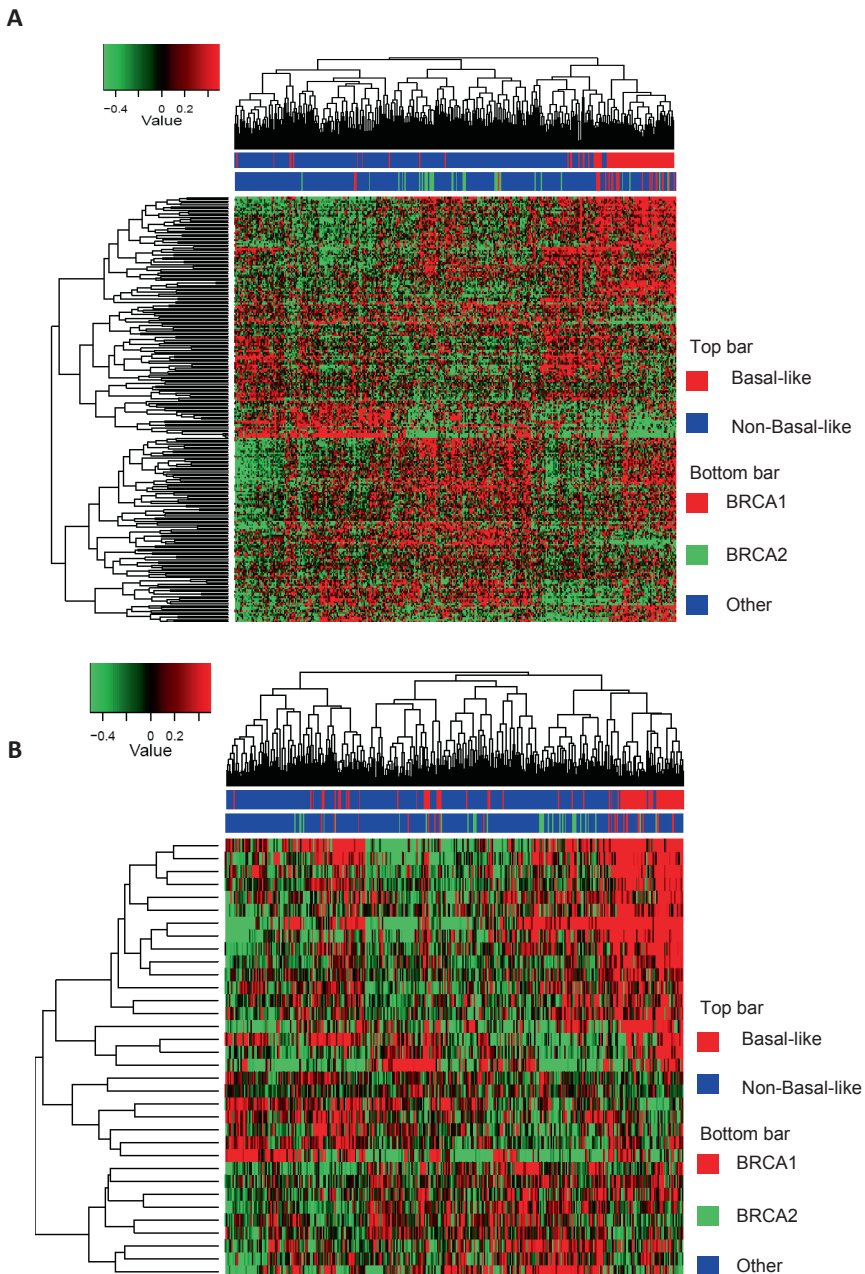


Figure 4. Hierarchical clustering of proteins mapped to gene transcripts for the Jönsson data set. **A**, Cluster analysis using the 417 up-regulated mapped proteins. The majority of the BRCA1 patients cluster together within the basal cluster in one branch of the dendrogram. The adjacent cluster contains the majority of the BRCA2 patients. **B**, Cluster analysis using the 45-protein BRCA1-deficiency signature. The BRCA1 and BRCA2 samples are now adjacent to each other in one cluster containing approximately one third of all patients.

We also assessed the performance of 1000 sets of genes randomly sampled from the whole genome and, in a more stringent approach, from the list of DNA replication, recombination and repair genes as defined by IPA (Table 5). Although both all up-regulated proteins and the BRCA1 deficiency signature achieved similar sensitivities in classifying *BRCA1/2*-mutated tumors, this was only significantly better compared to random gene lists, when using all up-regulated proteins. Nevertheless, the BRCA1 deficiency signature compared favorably to both random gene lists sampled from all genes and from random DNA repair lists, showing confidence that the classification accuracies were not obtained by chance.

In addition to leave-one-out cross-validation, we performed completely independent validation using the two other data sets containing samples with *BRCA1/2* mutation status (the combined Van de Vijver and Van 't Veer cohorts and the Waddell cohort; Table 4). The centroids constructed from the Jönsson *et al.* data set can classify *BRCA1/2* samples in the Van de Vijver/Van 't Veer cohorts with a very high sensitivity of 95 % for both the up-regulated proteins and the BRCA1 deficiency signature (Table 5). A large portion of sporadic samples were assigned to the *BRCA1/2* class. Because the sporadic samples were not tested for *BRCA1/2* dysfunction or inactivation of other components of the homologous recombination (HR) pathway, part of these mismatching predictions reported here might reflect a true deficiency in the *BRCA1/2* pathway, *i.e.*, a BRCAness phenotype⁴⁴. For the Waddell cohort, we obtained sensitivity of 79 % and 68 % for *BRCA1* patients by the up-regulated proteins and *BRCA1* deficiency signature respectively (Table 5), which is comparable with the result of 74 % sensitivity reported by the authors of the data set. Our result is significant, given that the test data is completely independent from the training data, whereas internal validation was used in Waddell *et al.*¹⁴.

These data show that the 417 up-regulated proteins in *BRCA1*-deficient mouse tumors, as well as the *BRCA1* deficiency signature of 45 proteins can classify human *BRCA1*-deficient breast tumors when mapped to human transcriptomics data sets. Importantly, the classification results for the mapped mouse *BRCA1* deficiency protein signature were better than the results that we obtained with the published mouse transcriptome data²⁴ from which we also constructed a signature using the same network-based *in silico* approach (data not shown). For example sensitivities of the protein signature for selecting *BRCA1*-deficient tumors were 81.8, 94.4, and 68.4 % in the Jönsson data set, the combined Van de Vijver/Van 't Veer data set and the Waddell data set, whereas these values were 63.6, 50.0 and 57.9% for the transcriptome signature (data not shown). The set of all up-regulated proteins achieved the best performance for diagnosing *BRCA1* mutations in comparison to random (DNA repair) genes. *BRCA2*-deficient tumors were also classified, implying enrichment for homology-directed repair-deficient tumors in general. Moreover, the 45 protein signature and all up-regulated proteins also classify a number of familial tumors without *BRCA1/2*

mutation and sporadic patients as BRCA1/2-like, suggesting that these tumors might be deficient in homology-directed DNA repair.

BRCA1 deficiency signature proteins show prognostic power when mapped to human breast cancer gene expression data sets

To investigate whether the BRCA1 deficiency proteins and signature have prognostic power, we used the mapped mRNAs of the up-regulated proteins in the four public breast cancer gene expression data sets that have associated clinical end point data (Van de Vijver, Wang, Naderi and Jönsson^{8;10;12;34}, Table 4) to perform a Kaplan-Meier survival analysis. The Jönsson data set was the only cohort that has an enrichment of familial (BRCA1/2-related) patients. For comparison, we also performed a Kaplan-Meier analysis using two commercially available prognostic gene signatures (MammaPrint[®] and Oncotype DX[®]). In a third comparison, we used the Naderi signature (discovered in the Naderi cohort), which has been shown to also have prognostic power in both the Van de Vijver and Wang cohorts¹⁰.

The mapped list of all 417 up-regulated proteins in BRCA1-deficient tumors yielded highly significant *p* values for survival analysis across all data sets, but these were only significantly better than random gene lists in the Van de Vijver data set. When sampling from a DNA repair gene background, no significant *p* values for the permutation analysis were obtained (Table 6). It is of note here that the external (commercial) gene expression-based signatures in some instances showed a similar level of underperformance when compared with random DNA repair gene lists in the sporadic data sets and were performing nonsignificantly in all permutation settings in the Jönsson cohort. Not surprisingly, the two mRNA signatures identified within their discovery cohort, (MammaPrint[®] in the Van de Vijver cohort^{1;12}, and Naderi signature in the Naderi Cohort¹⁰), outperformed all other signatures within their cohort.

The mapped BRCA1 deficiency signature has highly significant prognostic value. The Kaplan-Meier plots of the BRCA1 deficiency signature in the four breast cancer data sets is shown in Figure 5. Performance was comparable to the gene expression-based signatures in the three sporadic cohorts (the Van de Vijver, Wang and Caldas data sets).

Importantly, in the data set with an over-representation of familial (BRCA1/2) tumors (the Jönsson cohort), the mapped mouse BRCA1 deficiency signature outperformed all human gene expression-based signatures, and performance was still significant when compared with random (DNA-repair) gene lists. In summary, these data demonstrate that the mouse BRCA1 deficiency protein signature, when mapped to human gene expression data has prognostic value and outperforms (commercial) gene expression-based signatures in a cohort enriched for breast cancer with defects in the homology-directed DNA repair pathway.

Table 5. Performance of all 417 up-regulated proteins and the 45-protein BRCA1 deficiency signature in human gene expression data sets

True/ predicted	BRCA1	BRCA2	Familial	Sporadic	Total	Sensitivity	Specificity	All genes ^a	DNA repair background ^d
Jönsson <i>et al.</i> data set									
All 417 up-regulated proteins									
BRCA1	17	0	1	4	22	77,3%	84,7%	0,016	0,017
BRCA2	4	24	3	1	32	75,0%	85,9%	0,286	0,315
BRCA1/2	45	45	4	5	54	83,3%	69,5%	0,040	0,012
Familial	15	26	63	28	132	47,7%	78,4%		
Sporadic	32	20	45	76	173	43,9%	82,3%		
BRCA1 deficiency signature									
BRCA1	18	0	1	3	22	81,8%	81,3%	0,329	0,243
BRCA2	5	16	8	3	32	50,0%	86,5%	0,184	0,217
BRCA1/2	39	39	9	6	54	72,2%	66,6%	0,245	0,178
Familial	16	25	65	26	132	49,2%	72,7%		
Sporadic	42	19	53	59	173	34,1%	85,6%		
Combined Van de Vijver <i>et al.</i> and Van 't Veer <i>et al.</i> data sets									
All 417 up-regulated proteins									
BRCA1	17	0		1	18	94,4%	75,8%		
BRCA2	0	2		0	2	100,0%	57,2%		
BRCA1/2	19	19		1	20	95,0%	30,2%		
Sporadic	72	134		89	295	30,2%	95,0%		
BRCA1 deficiency signature									
BRCA1	17	0		1	18	94,4%	80,3%		
BRCA2	0	2		0	2	100,0%	71,1%		
BRCA1/2	19	19		1	20	95,0%	32,2%		
Sporadic	73	127		95	295	32,2%	95,0%		
Waddell <i>et al.</i> data set									
All 417 up-regulated proteins									
BRCA1	15	1	3		19	78,9%	78,6%		
BRCA2	7	12	11		30	40,0%	91,7%		
BRCA1/2	35	35	14		49	71,4%	56,0%		
Familial	8	3	14		25	56,0%	71,4%		
BRCA1 deficiency signature									
BRCA1	13	3	3		19	68,4%	77,5%		
BRCA2	8	8	14		30	26,7%	86,3%		
BRCA1/2	32	32	17		49	65,3%	52,0%		
Familial	8	4	13		25	54,0%	65,3%		

^a *p* value of permutation analysis using random gene lists (the fraction of 1000 random gene lists of the same length performing better than the 417 up-regulated proteins or the BRCA1 deficiency signature). In the case of "All genes" sampling was done from all genes present in the human genome that had an official gene symbol. Genes from a DNA repair background were sampled from a list generated by IPA.

Poor outcome human breast tumors identified by BRCA1 deficiency signature show enrichment in p53 mutations

p53 mutations have the capacity to disrupt the signaling between accumulated DNA damage and the induction of apoptosis. Moreover, loss of functional p53 is often associated

with BRCA1-related hereditary breast cancer in humans^{45;46}. For this reason, we investigated whether the poor prognosis patients identified in the survival analysis showed a significant enrichment for p53 mutations. For the Van de Vijver cohort, we were able to retrieve p53 mutational status for 204 of the 295 tumors (data not shown). Enrichment of p53 mutation in the poor prognosis patients was assessed using Fisher's exact test. Both the total list of 417 up-regulated proteins and the BRCA1 deficiency signature showed a highly significant enrichment for p53 mutations in poor prognosis patients (both p values were $< 10^{-10}$; Table 7). These data highlight the finding that the BRCA1 deficiency proteins and signature associate with p53 mutation as well as with survival.

Protein quantitation by targeted mass spectrometry

We have selected several proteins for follow-up at the protein level: four genes/proteins that showed discordant regulations: significantly up-regulated protein levels and down-regulated mRNA expression levels (NCAPD2, SIN3A, BAZ1B, TOP2B) in the BRCA1-deficient breast tumors of the mouse model. We also included one gene for which no probe was available on the microarray (TOP2A) and one protein for which protein and mRNA regulation was concordant (PARP1) in the mouse model. Of these gene products, SIN3A and TOP2B had also down-regulated mRNAs in the human data set of Jönsson, whereas PARP1 was not regulated, TOP2A was up-regulated, and for NCAPD2 and BAZ1B no probes were available. First, we confirmed the protein regulations as revealed by the spectral count data in the discovery samples using an independent measure of label-free protein quantitation, *i.e.*, the area under the curve of the extracted ion chromatograms. Second, we performed targeted mass spectrometry by SRM-MS in 10 independent mouse mammary tumors, all carcinomas.

The regulation of SIN3A, NCAPD2, TOP2A, TOP2B and PARP1 was confirmed by SRM-MS in independent tumors, with all peptides being significantly up-regulated in BRCA1-deficient breast tumors, whereas only BAZ1B was not significantly up-regulated (Supplementary Figure S3). Hierarchical clustering using all peptides from the discordant proteins clearly separated this pilot validation set according BRCA1 status (Supplementary Figure S4). In conclusion, the SRM validation of protein expression levels for which the RNA levels were discordant, underscores the fact that RNA expression levels can not always be simply translated to protein expression levels, as well as the importance of analysis of the end products of genes by proteomics.

DISCUSSION

In the present study, we aimed to identify proteins that are associated with the loss of expression of BRCA1, which is involved in homology-directed DNA repair. These proteins could potentially find use as screening, prognostic or predictive biomarkers.

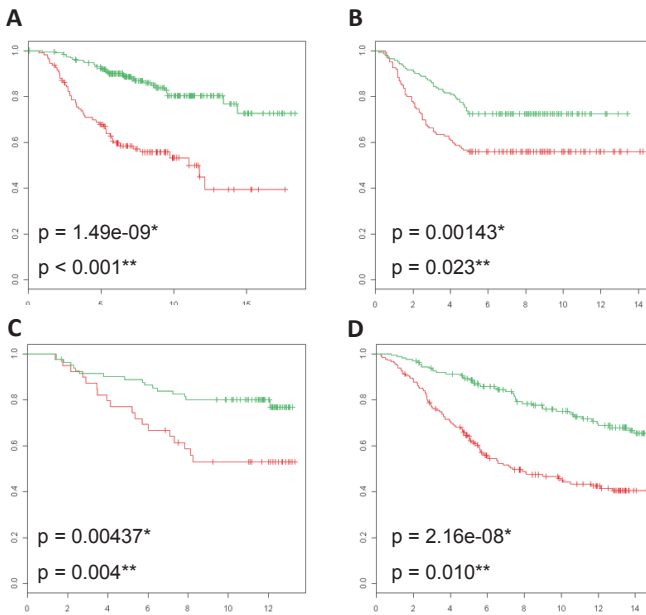


Figure 5. Survival analysis displaying Kaplan-Meier curves on a diverse set of public human gene expression breast cancer data using the BRCA1-deficiency signature. Red curves represent patients with poor prognosis and green curves are patients with good prognosis. Overall survival was used as clinical end point, unless specified otherwise. **A**, Van de Vijver data set of 295 patients. **B**, Wang cohort with 286 tumors using metastasis free

survival as clinical end point. **C**, Naderi data set with 120 early stage tumors. **D**, Jönsson data set containing 359 tumors, which includes 186 familial tumors, of which 54 were confirmed BRCA1/2 carriers. * p value from Kaplan-Meier survival analysis. ** p value from permutation analysis (the fraction of a 1000 random gene lists of the same length performing better than the BRCA1 deficiency signature).

To this end, we analyzed protein profiles in BRCA1-proficient and -deficient mouse mammary tumors using a high resolution tandem mass spectrometry-based proteomics approach. We identified 3545 proteins, of which 801 were significantly differentially regulated. A BRCA1 deficiency 45-protein signature was defined through the use of pathway and protein complex analysis, with good performance in human gene expression data sets enriched for BRCA1 deficiency. To our knowledge, this is the first comprehensive in depth proteomics analysis in genetic breast cancer. An overview of the discovery and data mining strategies is given in Figure 6.

Up-regulated proteins in BRCA1-deficient mouse mammary tumors contain basal-like markers, multiple drug targets and DNA repair(-associated) proteins

As expected, we found significant up-regulation of basal-like markers that are known to occur in breast cancer of the basal-like subtype. This is in line with the fact that human *BRCA1*-mutated tumors belong predominantly to the basal-like breast cancer subtype.

Table 6. Overview of Kaplan-Meier survival analysis in four breast cancer gene expression data sets that have associated clinical end point data

	Van de Vijver cohort				Wang cohort	
	p value ^a	# of mapped genes or proteins ^b	All genes ^c	DNA repair background ^c	p value	# of mapped genes or proteins ^b
Mouse BRCA1 deficiency proteins						
All 417 up-regulated proteins	6,12E-9	326/417	<0,001	>0,5	0,000	309/417
BRCA1 deficiency proteins	1,49E-9	43/45	<0,001	0,207	0,001	43/45
Gene expression-based signatures						
Naderi signature	1,01E-8	50/70	<0,001	0,355	6,30E-4	48/70
Oncotype DX (commercial signature)	2,22E-10	16/16	<0,001	0,029	2,07E-5	14/16
MammaPrint (commercial signature)	1,60E-14	60/61	<0,001	<0,001	0,001	47/61

^a p value from Kaplan-Meier survival analysis

^b number of proteins or genes from a signature or protein list that could be mapped to one or multiple probes on the microarray (mapped genes or proteins/all genes or proteins in the list).

^c p value of permutation analysis using random (DNA repair) gene lists (the fraction of 1000 random gene lists of the same length performing better than the gene/protein list used in survival analysis). In the case of "All genes" sampling was done from all genes present in the human genome that had an official gene symbol. For this reason, genes from a DNA repair background were sampled from a list generated by IPA.

This table contains data on the Van de Vijver, Wang, Naderi and Jönsson cohorts. The top two rows represent the performance of all up-regulated BRCA1 deficiency proteins and the 45-protein BRCA1 deficiency signature mapped to matching gene symbols. The bottom three rows contain the performance of gene expression-derived signatures, as a means of comparison with the protein-based signature.

Therefore these confirmatory findings underscore the human relevance of the BRCA1-deficient mouse tumor models. BRCA1 has recently, through its function as a transcription factor, been linked to the basal transcription machinery, whereby functional BRCA1 represses transcription of basal keratins⁴⁷. In addition, we identified a number of up-regulated proliferative markers, a feature that is more prevalent in human basal-like breast cancer.

Pathway and protein complex analysis identified DNA repair and associated processes as the most important biological function associated with the up-regulated proteins of the BRCA1-deficient tumors. This is in line with previous reports that loss of functional homology-directed DNA repair through knock-out of BRCA1 might be partially compensated for by other DNA repair mechanisms^{42,48}. Importantly, we found a number of therapeutic targets to be up-regulated in the BRCA1-deficient tumors, including PARP1, TOP1, TOP2A and TOP2B.

PARP1 has been shown to be a *bona fide* drug target for human *BRCA1*-mutated tumors⁴³. Up-regulation of the PARP1 protein may be a marker for the loss of functional homology-directed DNA repair in general, and might therefore be a predictive marker for the efficacy of PARP1 inhibition.

Wang cohort		Naderi cohort				Jönsson cohort			
All genes ^c	DNA repair background ^c	p value ^a	# of mapped genes or proteins ^b	All genes ^c	DNA repair background ^c	p value ^a	# of mapped genes or proteins ^b	All genes ^c	DNA repair background ^c
0,247	>0,5	0,023	262/417	0,133	0,309	9,80E-6	227/417	0,248	0,277
0,023	0,440	0,004	32/45	0,004	0,044	2,16E-8	33/45	0,010	0,008
0,008	>0,5	0,000	60/70	<0,001	0,005	1,44E-6	33/70	0,090	0,088
<0,001	0,024	0,000	13/15	<0,001	0,005	6,40E-4	13/16	0,435	0,359
0,013	>0,5	0,009	41/61	0,004	0,056	1,16E-5	35/61	0,250	0,233

Table 7. Overview and statistical analysis of enrichment for p53 mutations in poor prognosis patients versus good prognosis patients using Fisher's exact test in the Van de Vijver *et al.* data set

	Poor prognosis	Good prognosis	Sum
All 417 up-regulated proteins: p value = $2,20E-16^a$			
p53 mutation	55 (79%)	15 (21)	70
Wild-type p53	25 (19%)	109 (81%)	134
Sum	80	124	204
BRCA1 deficiency signature (45 proteins): p value = $2,55E-12^a$			
p53 mutation	49 (70%)	21 (30%)	70
Wild-type p53	26 (19%)	108 (81%)	134
Sum	75	129	204

^a p value from Fisher's exact test

In line with this, the tumors of the BRCA1-deficient mice used in this study responded well to the PARP inhibitor olaparib, whereas the BRCA1-proficient mouse tumor models did not⁴⁹. Moreover, we also found up-regulation of the topoisomerases TOP1, TOP2A and TOP2B drug targets for topotecan (TOP1 inhibitor) and doxorubicin (TOP2A and TOP2B inhibitor). These drugs inhibit the religation step of topoisomerases and therefore also induce indirectly DNA breaks. Higher levels of these proteins might have predictive value, since the BRCA1-deficient mouse tumors used in our experiments have been shown to be sensitive to topotecan⁵⁰ and doxorubicin⁵¹. We detected a number of other potential drug targets. HDAC1 and HDAC2, two proteins involved in chromatin remodeling by histone acetylation, were also up-regulated, although this was not significant ($p = 0.07$ and $p = 0.14$, respectively). At least 11 kinases were significantly up-regulated of which established drug targets included KIT and SRC (Supplementary Table S2, IPA drug targets). Novel kinase candidate drug targets included MAPK14, CDK9 and CSFR1. Multiple proteins

up-regulated in the BRCA1-deficient mice tumors act upstream of BRCA1 function in the homology-directed DNA repair pathway (ATM, BAZ1B, and TP53BP1), which may indicate an accumulation of these proteins in response to BRCA1 loss. In a previous study, Liu *et al.*²⁴ used gene expression analysis in the same mouse models as used in this study. Using gene set enrichment analysis, they reported a number of processes that were induced after BRCA1 loss, including recombinatorial repair, mitotic recombination, telomere maintenance and transcriptional regulation (e.g. chromatin remodeling).

Mouse BRCA1 deficiency protein signature with diagnostic and prognostic value in human gene expression data sets

We used an *in silico* validation approach to show that mouse proteins up-regulated in BRCA1-deficient tumors, including a BRCA1 deficiency signature, could classify human BRCA1 and BRCA2 tumors in cohorts that contained both sporadic and hereditary breast cancers. Using the BRCA1 deficiency signature, high sensitivities were achieved for classifying homology-directed DNA repair-deficient tumors in data sets known to be enriched for these patients¹⁴. The BRCA1 deficiency signature also classified a considerable number of sporadic and familial tumors as BRCA1/2-like. This result may be explained by the possibility that a number of sporadic and familial tumors lacking mutations in the *BRCA* genes might still harbor undetected deficiencies in homology-directed DNA repair and might therefore benefit from DNA-damaging agents. There is growing evidence that the majority of sporadic basal-like breast cancer have BRCA1 dysfunctionality other than a mutation in BRCA1 itself^{9;13}.

Approximately 25 % of BRCA1 tumors were not picked up by our classifier. This might be explained by the fact that our mouse BRCA1 classifier is not able to capture the full heterogeneity of all *BRCA1*-mutated breast carcinomas. In addition, a number of *BRCA1*-mutated breast carcinomas might escape detection due to restoration of homology-directed DSB repair via loss of TP53BP1^{52;53} or equivalent factors.

The BRCA1 deficiency DNA repair signature showed prognostic power across a wide variety of breast cancer data sets. Moreover, our mouse protein signature outperformed two commercially available prognostic RNA-based signatures (MammaPrint® and Oncotype DX®) in a data set enriched for homology repair-deficient tumors. Finally, in breast cancer, proteins with prognostic power may have predictive value as well. Examples are the hormone receptor ESR1 and the receptor tyrosine kinase ERBB2, the expression of which predicts response to targeted therapy as well as prognosis⁵⁴.

Furthermore, patients with sporadic breast cancer identified as poor outcome by our BRCA1 deficiency signature were highly enriched for p53 mutations. Although both mouse models used to develop the BRCA1 deficiency signature were p53 deficient, this result is explained by the clinical observation that BRCA1-deficient breast cancers frequently comprise p53 mutations, and both BRCA1 and p53 alterations are enriched in triple-

negative breast cancer^{45;46}. The up-regulation of drug targets involved in DNA repair (PARP1, TOP1, TOP2A and HDAC1), may indicate the predictive potential of our BRCA1 deficiency DNA repair candidates. We were not able to verify the predictive potential of our BRCA1 deficiency protein signature in large cohorts of treated breast cancers, since the therapeutic agents (PARP1 and TOP inhibition, cisplatin treatment, HDAC inhibition) are still in clinical trial phase, so no large-scale publicly available gene-expression data sets exist to date.

Several breast cancer proteomic studies have been reported to date. Biological materials used ranged from mouse tissue^{21;55}, human breast cancer cell lines and tissues^{18;20;21;56-58}. A few studies yielded a number of markers with potential for treatment prediction. Umar *et al.*¹⁹ have recently identified a protein profile in microdissected breast tumor cells putatively predictive for the efficacy of tamoxifen. Moreover, the differential up-regulation and activity of a number of kinases across a panel of breast cancer cell lines correlated with differential responsiveness to small molecule inhibitors in these cancer cell lines⁵⁹.

Concluding remarks

Our study demonstrates that in-depth high resolution proteomics of tumor tissue from different mouse models is a successful strategy to discover candidate protein biomarkers with screening, prognostic and possibly also predictive potential for human BRCA1 and homology-directed double-strand break repair-deficient breast tumors. The proteins up-regulated in mammary tumors from mouse models with a deficiency in BRCA1 are enriched in DNA repair(-associated) proteins, which points towards a potential rescue mechanism for the loss of homology-directed DNA repair. In addition, a pathway in conjunction with protein complex analysis has proven to be a promising strategy to construct a signature that has diagnostic and prognostic potential across multiple human breast cancer gene expression data sets. This signature shows specificity for BRCA1 and homology-directed DNA repair deficiency and has high prognostic potential in breast cancer data sets enriched with homology-directed repair-deficient tumors. Several up-regulated DNA repair proteins within this signature have been shown to be drug targets in homology-directed DNA repair-deficient tumors, suggesting that they may have predictive power for tailored therapies. Because multiple drug targets are up-regulated, these tumors might also benefit from combination therapy.

Finally, we point out that the BRCA1 deficiency transcriptome signature that we obtained by mapping mouse BRCA1 deficiency-associated breast tumor proteins is novel and could not be obtained by using the published mouse transcriptome data²⁴ as a starting point. To date, there is only one BRCAness gene expression signature reported for ovarian cancer⁶⁰. However, this signature was developed using a publicly available ovarium cancer transcriptomics data set and with a pilot study for predictiveness based on only 10 BRCA mutated/reverted samples originating from 6 patients and this signature was not externally

evaluated in multiple large (BRCA1/2-deficient) breast cancer data sets. Together, these results underscore the novelty of our BRCAness transcriptome signature that we obtained by mapping mouse BRCA1 deficiency-associated breast tumor proteins.

Future studies should address the value of our BRCA1 deficiency signature both at the transcriptome and proteome level for patient selection for treatment in breast cancer and other tumors types with potential homology repair deficiencies. With the advent of targeted mass spectrometry methods like SRM-MS, the signature proteins may be analyzed in pretreatment biopsies in one multiplex analysis, without the need for antibodies. Targeted multiplex analysis in aspirate fluid and plasma may highlight their potential use for non-invasive testing.

METHODS

Materials

All chemicals, unless otherwise specified, were obtained from Sigma (Sigma Aldrich, Zwijndrecht, The Netherlands). HPLC solvents, LC-MS grade water, acetonitrile and formic acid, were obtained from Biosolve (Biosolve B.V., Valkenswaard, The Netherlands). Porcine sequence-grade modified trypsin was obtained from Promega (Promega Benelux B.V., Leiden, The Netherlands).

Mouse strains and tumors

Generation of conditional mutants and K14*cre* transgenic mice has been described previously^{24,25}. All animal experiments were approved by the Animal Ethics Committee of the Netherlands Cancer Institute (NKI). When grown to a size of approximately 500 mm³, tumors were dissected, snap frozen and stored at -80 °C until use.

Tissue homogenization and fractionation using gel electrophoresis

For homogenization, we cut a piece of ~20 mg in a bath of liquid nitrogen in smaller parts. The proteins in the mammary tumors tissue samples were solubilised in 800 µL 1x reducing sodium dodecyl sulfate (SDS) sample buffer (containing 62.5 mM Tris-HCl, 2 % w/v SDS, 10 % v/v glycerol, and 0.0025 % bromophenol blue, 100 mM DTT, pH 6.8) using a Pellet Pestles microgrinder system (Kontes glassware, Vineland, NJ). Subsequently the proteins were denatured by heating at 100 °C for 10 min. Any insoluble debris was removed by centrifuging for 15 min at maximum speed (16.1 rcf) in a benchtop centrifuge.

The proteins were fractionated using one-dimensional SDS-polyacrylamide gel electrophoresis (SDS-PAGE). 25 µL of each homogenized sample (containing about 50 µg protein) was loaded on a well of a pre-cast NuPAGE 4–12 % w/v Bis-Tris 1.5-mm minigel (Invitrogen). The stacking gel contained 4 % w/v acrylamide/Bis-Tris. Electrophoresis was carried out at 200 V in NuPAGE MES SDS running buffer (50 mM Tris base, 50 mM MES, 0.1 % w/v SDS, 1 mM EDTA, pH 7.3) until the dye front reached the end of the gel. Following electrophoresis, gels were fixed with a solution of 50 % ethanol and 3 %

phosphoric acid. Staining was carried out in a solution of 34 % methanol, 3 % phosphoric acid, 15 % ammonium sulfate and 0.1 % Coomassie Blue G-250 (Bio-Rad) with subsequent destaining in MilliQ water.

In-gel digestion and nanoLC-FTMS

For in-gel digestion, gel lanes were cut in 10 bands and each band was processed according to the method of Shevchenko *et al.*²⁶. Briefly, the bands were washed and dehydrated three times in 50 mM ammonium bicarbonate (ABC, pH 7.9) / 50 mM ABC + 50% acetonitrile (ACN). Subsequently, cysteine bonds were reduced with 10 mM DTT (dithiothreitol) for 1 h at 56°C and alkylated with 50 mM iodoacetamide for 45 minutes at room temperature in the dark. After two subsequent wash/dehydration cycles the bands were dried 10 min in a vacuum centrifuge and incubated overnight with 0.06 µg/µl trypsin at 25 °C. Peptides were extracted once in 1% formic acid and subsequently twice in 50% ACN in 5% formic acid. The volume was reduced to 50 µl in a vacuum centrifuge prior to LC-MS analysis.

Peptides were separated by an Ultimate 3000 nanoLC system (Dionex LC-Packings, Amsterdam, The Netherlands) equipped with a 20-cm x 75-µm inner diameter fused silica column custom packed with 3-µm 100 Å ReproSil Pur C18 aqua (Dr Maisch GMBH, Ammerbuch-Entringen, Germany) as described before²⁷. After injection, the peptides were trapped at 30 µl/min on a 0.5-cm x 300-µm inner diameter Pepmap C18 cartridge (Dionex LC-Packings, Amsterdam, The Netherlands) at 2% buffer B (buffer A: 0.05% formic acid in MQ; buffer B: 80 % ACN + 0.05% formic acid in MQ) and separated at 300 nl/min in a 10-40 % buffer B gradient in 60 min. Eluting peptides were ionized at 1.7 kV in a Nanomate Triversa Chip-based nanospray source using a Triversa LC coupler (Advion, Ithaca, NJ). Intact peptide mass spectra and fragmentation spectra were acquired on a LTQ-FT hybrid mass spectrometer (Thermo Fisher, Bremen, Germany). Intact masses were measured at resolution 50.000 in the ICR cell using a target value of 1×10^6 charges. In parallel, following an FT prescan, the top five peptide signals (charge states 2+ and higher) were submitted to MS/MS in the linear ion trap (3-atomic mass unit isolation width, 30-ms activation, 35 % normalized activation energy, Q value of 0.25, and a threshold of 5000 counts). Dynamic exclusion was applied with a repeat count of 1 and an exclusion time of 30 s.

LC-SRM-analyses

Independent BRCA1-deficient and -proficient mouse breast tumors (n = 5 in each group) were analysed in triplicate on an Ultimate 3000 RSCL Nanosystem (Dionex) that was hyphenated to an QTRAP® 5500 instrument (AB SCIEX, Foster City, CA) operated in positive SRM mode and equipped with a nano-electrospray source with applied voltage of 2.404 kV and a capillary heater temperature of 225 °C. The Nanoflow LC system and QTRAP® 5500 system were both controlled using Analyst 1.5.1 Software. The combined information from each SRM information dependent acquisition (IDA) experiment was used to perform Mascot searches against the international protein index (IPI) mouse database v3.65 and MultiQuant™ software version 2.1 (AB SCIEX).

The scheduled SRM mode comprised the following parameters: SRM detection window of 420 s, target scan time of 3.0 s, curtain gas of 15, ion source gas 1 of 15, declustering potential of 80, and entrance potential of 10. Q1 resolution was set to unit and Q3 resolution was set to unit. Pause between mass ranges was set to 1 ms. Collision cell exit potentials (CXP) was set to 36 for all transitions. Peak integration was performed using MultiQuant™ software version 2.1 (AB SCIEX) software and manually reviewed.

Chromatographic separation of peptides was performed by a 68-min gradient at 300 nl/min. Solvent A (0.05 % formic acid water) and solvent B (0.05 % formic acid, 80% acetonitrile) were mixed at 2 % B from 0 to 3 min, 15 % B at 4 min, 36 % B at 49 min, 99 % B from 50 to 54 min, and 2 % B at 55 to 68 min. The nano-LC columns were made in house and consisted of 20-cm x 75- μ m inner diameter fused silica custom packed with 3- μ m 100 Å ReproSil Pur C18 aqua (Dr Maisch GMBH, Ammerbuch-Entringen, Germany) as described before²⁷. After injection, peptides were trapped at 6 μ l/min at 2 % buffer B.

An SRM assay for the target proteins (NCAPD2, SIN3A, BAZ1B, TOP2A, TOP2B, PARP1) was developed using the MRMPilot™ software version 2.1 from AB SCIEX. The software requires an amino acid sequence of the protein of interest, a starter method containing the LC conditions, and an empty SRM-IDA experiment. The software performs an *in silico* digest of the protein and creates a set of peptides that would result after full tryptic digestion. For each of these peptides, it will generate an SRM transition for the calculated m/z of the precursor ion and an appropriate fragment ion. Assay development subsequently entails verification of the peptides and CE optimisation of the transitions, both in multiplexed LC-SRM analyses. During verification, the highest responding peptides/transitions at a theoretically calculated optimum CE energy are determined, as well as the identity of the peptide via SRM triggered MS/MS. During CE optimisation the transitions selected after verification are optimised during the chromatographic elution of the peptide.

For verification, a mixture of samples previously analysed using FTMS and indicating abundance of the target candidates was analysed in 10 unscheduled SRM analyses to find the highest responding tryptic peptides from the target proteins, as well as their elution time during the chromatographic run. For each peptide 10 theoretically predicted transitions were assessed for detection response and identity. Identity was confirmed using MIDAS (MRM Initiated Detection and Sequencing) with a threshold of 500 counts for an SRM transition response to trigger two MS/MS spectra of the peptide to be acquired at rolling collision energy. Each of the 10 verification analyses was set up to detect 289 of all theoretically predicted transitions and their theoretically predicted optimum collision energy for all theoretically predicted peptides that can result after tryptic digestion of the candidate proteins. The total scan time for each cycle of the instrument during verification was 3.757 s, resulting in a dwell time of 10 ms for each transition in the unscheduled verification analyses.

For CD optimization, all data of unscheduled analyses were uploaded to the MRMPilot, which was set to select the five best detected transitions for each peptide and assign a chromatographic retention time to each peptide. Subsequently collision energy for each transition was optimised in 13 LC-SRM

analyses, with each analysis set-up to detect 104 scheduled transitions that resulted from verification, at nine different collision energies, centred at 3 V intervals around the theoretically predicted optimum with a dwell time of 25 ms. All data of CE optimisation cycles were uploaded to the MRMPilot and for each peptide three transitions at the experimentally found optimum and the experimentally found retention time were included in the final assay. The final assay contained 129 scheduled transitions, three for each peptide, with one to five peptides for each of the seven candidate proteins.

Data analysis

Protein identification – MS/MS spectra were searched against the mouse IPI database (56,555 entries) using Sequest (version 27, revision 12), which is part of the BioWorks 3.3 data analysis package (Thermo Fisher, San Jose, CA). MS/MS spectra were searched with a maximum allowed deviation of 10 ppm for the precursor mass and 1 atomic mass unit for fragment masses. Methionine oxidation and cysteine carbamidomethylation were allowed modifications, two missed cleavages were allowed and the minimum number of tryptic termini was 1. After database searching, the DTA and OUT files were imported into Scaffold 1.07 (Proteome software, Portland, OR). Scaffold was used to organize the gel-band data and to validate peptide identifications using the Peptide Prophet algorithm^{28;29}. Only identifications with a probability of >95 % were retained. Subsequently, the Protein Prophet algorithm was applied and protein identifications with a probability of >99 % with two peptides or more in at least sample were retained. The false discovery rate for the detected proteins using this workflow is on average around 0.5 %, and was not calculated again. Proteins that contained similar peptides and could not be differentiated based on MS/MS analysis alone were grouped to satisfy the principles of parsimony. For each protein identified, the total number of MS/MS spectra detected for each protein identified (spectral counts) was exported to Excel 2003 (Microsoft, Redmond, USA).

Spectral count normalization and statistics – Normalization was performed as described previously^{30;31}. The spectral counts of each protein were divided by the total spectral counts of all proteins within a sample. This number was multiplied with a constant equal to the average of total spectral counts of all samples to obtain a normalized spectral count value in the same range as the non-normalized spectral counts. The beta-binomial test³⁰ was applied to find proteins that show significant differences in spectral count numbers between the tumor group and the reference group. Proteins with a *p* value less than 0.05 were designated as being significant. Hierarchical clustering was carried out using R. For analysis of reproducibility, we calculated the average coefficient of variation (CV) of the normalized spectral counts from overlapping proteins for three technical replicates.

SRM data analysis – Technical replicates were removed until CV of all triplicate analysis was <20 %. Subsequently, in each remaining analysis, the ratio of the AUC of Transition1/Transition2, Transition 2/Transition3 and Transition1/Transition3 was calculated. The two transitions resulting in the lowest CV percentage over all analyses were selected for further calculations; the sum of the AUC of these two transitions was determined in each sample, and a fold change for each peptide between the groups was determined by the ratio of the summed AUC in each group. The average of the fold changes of

peptides belonging to one protein was determined for each protein. When the CV percentage of the average of the fold changes of the peptides of one protein was >10 %, the transitions of these peptides were visually inspected and excluded when co-eluting false positive responses were observed that had not been detected by Multiquant smoothing and peak splitting algorithms or in-house developed R-script processing. The calculated levels for each approved peptide were normalised on the level of Tuba1b in each sample.

Pathway analysis – The list of identified proteins was uploaded into the Ingenuity Pathways Analysis (IPA) software (Ingenuity Systems, Redwood City, CA) as a tab-delimited text file containing IPI accession numbers, *p* values, and fold changes calculated with a correction factor (adding 0.5 to the spectral counts of all proteins before normalization). The proteins were uploaded and mapped to the corresponding “gene objects” in the Ingenuity Pathways knowledge base. Functional analysis was performed to identify the high level biological functions that were most significantly associated to the differentially regulated proteins in the data set. Significantly regulated proteins within the high level functions are displayed graphically as nodes (proteins/gene objects) and edges (the biological relationships between the nodes). All edges are supported by at least one reference from the literature, textbook or canonical information stored in the Ingenuity knowledge base. Ingenuity Pathways Analysis computes one or more *p* values for each specific function within a high level function according to the fit of the user’s set of significant proteins. The significance of functional enrichment is computed by a Fisher’s exact test. Finally, the Path Designer feature was used to create graphically rich network images. In addition, we used the COFECO tool for the mapping of significantly differentially regulated proteins to protein complexes³². The obtained complexes were further visualized using STRING³³ and Cytoscape, respectively.

Human gene expression data sets

To explore the diagnostic and prognostic value of the protein expression data from the mouse models, we made use of publicly available human gene expression data sets. To map the up-regulated mouse BRCA1 deficiency proteins to public data sets of human arrays, we first matched mouse gene symbols to human gene symbols using the BioMart website (<http://www.biomart.org>). We used layout documentation files for the various microarray platforms from Gene Expression Omnibus (<http://www.ncbi.nlm.nih.gov/geo>), MIAMExpress (<http://www.ebi.ac.uk/miamexpress/>) or Rosetta Inpharmatics (<http://www.rii.com/publications/default.html/>) to retrieve the matching gene symbols on each platform. The following human breast cancer data sets were used: (i) Van de Vijver data set¹². A validation study of a prognostic gene expression signature (MammaPrint®), which included 295 young patients with early stage breast cancer, of which 151 were lymph node negative, 226 were estrogen receptor-positive, and 110 had received adjuvant chemotherapy. We were also able to retrieve p53 mutational status for 204 tumors in this data set (data not shown). (ii) Van’t Veer data set¹. In this discovery study for a prognostic signature (MammaPrint®), the authors also analyzed 18 BRCA1 and 2 BRCA2 samples on the same platform used for the Van de Vijver data set¹². (iii) E-UCON-1

data set¹⁰ (subsequently referred to as the Naderi data set). This data set was used for discovery of a prognosis profile in a set of women with early stage breast cancer representative of breast cancer demographics. Of the 132 breast cancer tissues, we used a subset of 120 patients for survival analysis that had the same orientation in dye labeling concerning the reference and tumor samples and that also had associated survival data. (iv) GSE2034 data set³⁴ (subsequently referred to as Wang data set). This was a discovery and validation analysis of a gene signature for the prediction of breast cancer patient outcomes. It consists of 286 lymph node-negative breast cancer patients who never received adjuvant chemotherapy and of which 209 were estrogen receptor-positive. We logged the normalized intensity values and performed zero mean and unit variance normalization. (v) GSE22133 data set⁸ (subsequently referred to as the Jönsson data set). This discovery data set consists of 359 breast tumors including 186 familial, of which 22 were BRCA1-mutated and 32 were BRCA2 mutated. (vi) GSE19177 data set¹⁴ (subsequently referred to as the Waddell data set). This data set contains familial tumors only. Nineteen had a BRCA1 mutation, 30 had a BRCA2 mutation, whereas 25 did not have an identifiable mutation. One tumor was excluded from analysis because it had unknown mutational status. For all data sets, we used the normalized log ratios in the analyses, unless specified otherwise above.

Centroid classification and survival analysis

We used a nearest centroid classifier to test the diagnostic and prognostic power of the mapped protein/gene signature on the public human gene expression data sets in combination with leave-one-out-cross-validation. First, the signature proteins/genes in the validation sets were identified. We used a centroid classification scheme to assess BRCA1 and homology-directed DNA repair deficiency, whereby centroids were built by taking the average expression value for each signature gene in the diagnostic groups, excluding the leave-out sample. The leave-out samples were then classified into different diagnostic groups using the nearest correlation criterion. For classification with a centroid on external data sets, genes were collapsed by taking the median across all probes. This centroid classification scheme was also used for classifications in the Kaplan-Meier survival analysis. In all data sets, patients who survived 5 years or more constituted the good prognosis group (centroid), while patients who survived less than 5 years were used for the poor prognosis group (centroid)^{10;12;34}. The average expression value for each signature gene in the good and poor prognosis centroid was computed without the leave-out sample. The leave-out samples were then classified into good or poor prognostic groups using the nearest correlation criterion. To see if a gene list performed better than random, both in the diagnostic and in the survival analysis, we also ran analysis with 1000 random gene lists of the same size using the same scheme. We only included probes on the arrays which were annotated with a gene symbol. The same scheme was applied for the prognostics mRNA based signatures used as a comparison.

ACKNOWLEDGMENTS

We would like to acknowledge Anne-Lise Borresen, Anita Langerod and Hugo Horlings for generation and access to p53 mutation data from the Van de Vijver cohort and Davide Chiasserini for generating the protein complex images using Cytoscape. We also acknowledge Piet Borst for careful reading and adjusting this manuscript. This research was supported by the CenE/Van Lanschot (MW) and the VUmc-Cancer Center Amsterdam (CRJ, TVP and proteomics infrastructure), the Dutch Cancer Society (project grants to SR and JJ) and the Netherlands Organization for Scientific Research (NWO-Vidi grant to SR and NWO Cancer Systems Biology Center (CSBC) grant to JJ). JEJ was supported by a Toptalent fellowship from the Netherlands Organization for Scientific Research (NWO).

REFERENCES

1. Van 't Veer, L. J., Dai, H., van, d., V, He, Y. D., Hart, A. A., Mao, M., Peterse, H. L., van der, K. K., Marton, M. J., Witteveen, A. T., Schreiber, G. J., Kerkhoven, R. M., Roberts, C., Linsley, P. S., Bernards, R., and Friend, S. H. (2002) Gene expression profiling predicts clinical outcome of breast cancer. *Nature* 415, 530-536.
2. Turner, N. C., Reis-Filho, J. S. (2006) Basal-like breast cancer and the BRCA1 phenotype. *Oncogene* 25, 5846-5853.
3. Jaspers, J. E., Rottenberg, S., and Jonkers, J. (2009) Therapeutic options for triple-negative breast cancers with defective homologous recombination. *Biochim. Biophys. Acta* 1796, 266-280.
4. Gudmundsdottir, K., Ashworth, A. (2006) The roles of BRCA1 and BRCA2 and associated proteins in the maintenance of genomic stability. *Oncogene* 25, 5864-5874.
5. Tutt A., Robson M., Garber J.E., Domchek S.M., Audeh M.W., Weitzel J.N., Friedlander M., Arun B., Loman N., Schmutzler R.K., Wardley A., Mitchell G., Earl H., Wickens M., Carmichael J. (2010) Oral poly(ADP-ribose) polymerase inhibitor olaparib in patients with BRCA1 or BRCA2 mutations and advanced breast cancer: a proof-of-concept trial. *Lancet* 376, 235-244.
6. Sorlie, T., Perou, C. M., Tibshirani, R., Aas, T., Geisler, S., Johnsen, H., Hastie, T., Eisen, M. B., van de, R. M., Jeffrey, S. S., Thorsen, T., Quist, H., Matese, J. C., Brown, P. O., Botstein, D., Eystein, L. P., and Borresen-Dale, A. L. (2001) Gene expression patterns of breast carcinomas distinguish tumor subclasses with clinical implications. *Proc. Natl. Acad. Sci. USA* 98, 10869-10874.
7. Glas, A. M., Floore, A., Delahaye, L. J., Witteveen, A. T., Pover, R. C., Bakx, N., Lahti-Domenici, J. S., Bruinsma, T. J., Warmoes, M. O., Bernards, R., Wessels, L. F., and Van't Veer, L. J. (2006) Converting a breast cancer microarray signature into a high-throughput diagnostic test. *BMC Genomics* 7, 278.
8. Jonsson, G., Staaf, J., Vallon-Christersson, J., Ringner, M., Holm, K., Hegardt, C., Gunnarsson, H., Fagerholm, R., Strand, C., Agnarsson, B. A., Kilpivaara, O., Luts, L., Heikkila, P., Aittomaki, K., Blomqvist, C., Loman, N., Malmstrom, P., Olsson, H., Johannsson, O. T., Arason, A., Nevanlinna, H., Barkardottir, R. B., and Borg, A. (2010) Genomic subtypes of breast cancer identified by array-comparative genomic hybridization display distinct molecular and clinical characteristics. *Breast Cancer Res.* 12, R42.
9. Joosse, S. A., Brandwijk, K. I., Mulder, L., Wesseling, J., Hannemann, J., and Nederlof, P. M. (2011) Genomic signature of BRCA1 deficiency in sporadic basal-like breast tumors. *Genes Chromosomes Cancer* 50, 71-81.
10. Naderi, A., Teschendorff, A. E., Barbosa-Morais, N. L., Pinder, S. E., Green, A. R., Powe, D. G., Robertson, J. F., Aparicio, S., Ellis, I. O., Brenton, J. D., and Caldas, C. (2007) A gene-expression signature to predict survival in breast cancer across independent data sets. *Oncogene* 26, 1507-1516.

11. Paik, S., Shak, S., Tang, G., Kim, C., Baker, J., Cronin, M., Baehner, F. L., Walker, M. G., Watson, D., Park, T., Hiller, W., Fisher, E. R., Wickerham, D. L., Bryant, J., and Wolmark, N. (2004) A multigene assay to predict recurrence of tamoxifen-treated, node-negative breast cancer. *N. Engl. J. Med.* 351, 2817-2826.
12. van de Vijver, M., He, Y. D., Van 't Veer, L. J., Dai, H., Hart, A. A., Voskuil, D. W., Schreiber, G. J., Peterse, J. L., Roberts, C., Marton, M. J., Parrish, M., Atsma, D., Witteveen, A., Glas, A., Delahaye, L., van, d., V, Bartelink, H., Rodenhuis, S., Rutgers, E. T., Friend, S. H., and Bernards, R. (2002) A gene-expression signature as a predictor of survival in breast cancer. *N. Engl. J. Med.* 347, 1999-2009.
13. Vollebbergh, M. A., Lips, E. H., Nederlof, P. M., Wessels, L. F., Schmidt, M. K., van Beers, E. H., Cornelissen, S., Holtkamp, M., Froklage, F. E., de Vries, E. G., Schrama, J. G., Wesseling, J., van, d., V, van, T. H., de, B. M., Hauptmann, M., Rodenhuis, S., and Linn, S. C. (2010) An aCGH classifier derived from BRCA1-mutated breast cancer and benefit of high-dose platinum-based chemotherapy in HER2-negative breast cancer patients. *Ann. Oncol.* Advance Access.
14. Waddell, N., Arnold, J., Cocciardi, S., da, S. L., Marsh, A., Riley, J., Johnstone, C. N., Orloff, M., Assie, G., Eng, C., Reid, L., Keith, P., Yan, M., Fox, S., Devilee, P., Godwin, A. K., Hogervorst, F. B., Couch, F., Grimmond, S., Flanagan, J. M., Khanna, K., Simpson, P. T., Lakhani, S. R., and Chenevix-Trench, G. (2010) Subtypes of familial breast tumours revealed by expression and copy number profiling. *Breast Cancer Res. Treat.* 123, 661-677.
15. Straver, M. E., Glas, A. M., Hannemann, J., Wesseling, J., van, d., V, Rutgers, E. J., Vrancken Peeters, M. J., van, T. H., Van't Veer, L. J., and Rodenhuis, S. (2010) The 70-gene signature as a response predictor for neoadjuvant chemotherapy in breast cancer. *Breast Cancer Res. Treat.* 119, 551-558.
16. Cardoso, F., Piccart-Gebhart, M., Van't, V. L., and Rutgers, E. (2007) The MINDACT trial: the first prospective clinical validation of a genomic tool. *Mol. Oncol.* 1, 246-251.
17. Pavlou, M. P., Kulasingham, V., Sauter, E. R., Kliethermes, B., and Diamandis, E. P. (2010) Nipple aspirate fluid proteome of healthy females and patients with breast cancer. *Clin. Chem.* 56, 848-855.
18. Xu, X., Qiao, M., Zhang, Y., Jiang, Y., Wei, P., Yao, J., Gu, B., Wang, Y., Lu, J., Wang, Z., Tang, Z., Sun, Y., Wu, W., and Shi, Q. (2010) Quantitative proteomics study of breast cancer cell lines isolated from a single patient: discovery of TIMM17A as a marker for breast cancer. *Proteomics* 10, 1374-1390.
19. Umar, A., Kang, H., Timmermans, A. M., Look, M. P., Meijer-van Gelder, M. E., den Bakker, M. A., Jaitly, N., Martens, J. W., Luijck, T. M., Foekens, J. A., and Pasa-Tolic, L. (2009) Identification of a putative protein profile associated with tamoxifen therapy resistance in breast cancer. *Mol. Cell Proteomics* 8, 1278-1294.
20. Lai, T. C., Chou, H. C., Chen, Y. W., Lee, T. R., Chan, H. T., Shen, H. H., Lee, W. T., Lin, S. T., Lu, Y. C., Wu, C. L., and Chan, H. L. (2010) Secretomic and proteomic analysis of potential breast cancer markers by two-dimensional differential gel electrophoresis. *J. Proteome Res.* 9, 1302-1322.
21. Celis, J. E., Gromov, P., Cabezon, T., Moreira, J. M., Ambartsumian, N., Sandelin, K., Rank, F., and Gromova, I. (2004) Proteomic characterization of the interstitial fluid perfusing the breast tumor microenvironment: a novel resource for biomarker and therapeutic target discovery. *Mol. Cell Proteomics* 3, 327-344.
22. Geiger, T., Cox, J., Ostasiewicz, P., Wisniewski, J. R., and Mann, M. (2010) Super-SILAC mix for quantitative proteomics of human tumor tissue. *Nat. Methods* 7, 383-385.
23. Becker, S., Cazares, L. H., Watson, P., Lynch, H., Semmes, O. J., Drake, R. R., and Laronga, C. (2004) Surfaced-enhanced laser desorption/ionization time-of-flight (SELDI-TOF) differentiation of serum protein profiles of BRCA-1 and sporadic breast cancer. *Ann. Surg. Oncol.* 11, 907-914.
24. Liu, X., Holstege, H., van der, G. H., Treur-Mulder, M., Zevenhoven, J., Velds, A., Kerkhoven, R. M., van Vliet, M. H., Wessels, L. F., Peterse, J. L., Berns, A., and Jonkers, J. (2007) Somatic loss of BRCA1 and p53 in mice induces mammary tumors with features of human BRCA1-mutated basal-like breast cancer. *Proc. Natl. Acad. Sci. USA* 104, 12111-12116.
25. Derksen, P. W., Liu, X., Saridin, F., van der, G. H., Zevenhoven, J., Evers, B., van, B., Jr., Griffioen, A. W., Vink, J., Krimpenfort, P., Peterse, J. L., Cardiff, R. D., Berns, A., and Jonkers, J. (2006) Somatic

- inactivation of E-cadherin and p53 in mice leads to metastatic lobular mammary carcinoma through induction of anoikis resistance and angiogenesis. *Cancer Cell* 10, 437-449.
26. Shevchenko, A., Wilm, M., Vorm, O., and Mann, M. (1996) Mass spectrometric sequencing of proteins silver-stained polyacrylamide gels. *Anal. Chem.* 68, 850-858.
 27. Piersma, S. R., Fiedler, U., Span, S., Lingnau, A., Pham, T. V., Hoffmann, S., Kubbutat, M. H., and Jimenez, C. R. (2010) Workflow comparison for label-free, quantitative secretome proteomics for cancer biomarker discovery: method evaluation, differential analysis, and verification in serum. *J. Proteome Res.* 9, 1913-1922.
 28. Nesvizhskii, A. I., Keller, A., Kolker, E., and Aebersold, R. (2003) A statistical model for identifying proteins by tandem mass spectrometry. *Anal. Chem.* 75, 4646-4658.
 29. Keller, A., Nesvizhskii, A. I., Kolker, E., and Aebersold, R. (2002) Empirical statistical model to estimate the accuracy of peptide identifications made by MS/MS and database search. *Anal. Chem.* 74, 5383-5392.
 30. Pham, T. V., Piersma, S. R., Warmoes, M., and Jimenez, C. R. (2010) On the beta-binomial model for analysis of spectral count data in label-free tandem mass spectrometry-based proteomics. *Bioinformatics* 26, 363-369.
 31. Albrethsen, J., Knol, J. C., Piersma, S. R., Pham, T. V., de, W. M., Mongera, S., Carvalho, B., Verheul, H. M., Fijneman, R. J., Meijer, G. A., and Jimenez, C. R. (2010) Subnuclear proteomics in colorectal cancer: identification of proteins enriched in the nuclear matrix fraction and regulation in adenoma to carcinoma progression. *Mol. Cell Proteomics* 9, 988-1005.
 32. Sun, C. H., Kim, M. S., Han, Y., and Yi, G. S. (2009) COFECO: composite function annotation enriched by protein complex data. *Nucleic Acids Res.* 37, W350-W355.
 33. Jensen, L. J., Kuhn, M., Stark, M., Chaffron, S., Creevey, C., Muller, J., Doerks, T., Julien, P., Roth, A., Simonovic, M., Bork, P., and von, M. C. (2009) STRING 8--a global view on proteins and their functional interactions in 630 organisms. *Nucleic Acids Res.* 37, D412-D416.
 34. Wang, Y., Klijn, J. G., Zhang, Y., Sieuwerts, A. M., Look, M. P., Yang, F., Talantov, D., Timmermans, M., Meijer-van Gelder, M. E., Yu, J., Jatke, T., Berns, E. M., Atkins, D., and Foekens, J. A. (2005) Gene-expression profiles to predict distant metastasis of lymph-node-negative primary breast cancer. *Lancet* 365, 671-679.
 35. Wright, M. H., Calcagno, A. M., Salcido, C. D., Carlson, M. D., Ambudkar, S. V., and Varticovski, L. (2008) Brca1 breast tumors contain distinct CD44+/. *Breast Cancer Res.* 10, R10.
 36. Stuart-Harris, R., Caldas, C., Pinder, S. E., and Pharoah, P. (2008) Proliferation markers and survival in early breast cancer: a systematic review and meta-analysis of 85 studies in 32,825 patients. *Breast* 17, 323-334.
 37. Cordes, N. (2006) Integrin-mediated cell-matrix interactions for prosurvival and antiapoptotic signaling after genotoxic injury. *Cancer Lett.* 242, 11-19.
 38. Wang, Y., Cortez, D., Yazdi, P., Neff, N., Elledge, S. J., and Qin, J. (2000) BASC, a super complex of BRCA1-associated proteins involved in the recognition and repair of aberrant DNA structures. *Genes Dev.* 14, 927-939.
 39. Heale, J. T., Ball, A. R., Jr., Schmiesing, J. A., Kim, J. S., Kong, X., Zhou, S., Hudson, D. F., Earnshaw, W. C., and Yokomori, K. (2006) Condensin I interacts with the PARP-1-XRCC1 complex and functions in DNA single-strand break repair. *Mol. Cell* 21, 837-848.
 40. Lee, C. G., Hague, L. K., Li, H., and Donnelly, R. (2004) Identification of toposome, a novel multisubunit complex containing topoisomerase IIalpha. *Cell Cycle* 3, 638-647.
 41. Osley, M. A., Tsukuda, T., and Nickoloff, J. A. (2007) ATP-dependent chromatin remodeling factors and DNA damage repair. *Mutat. Res.* 618, 65-80.
 42. Gudmundsdottir, K., Ashworth, A. (2006) The roles of BRCA1 and BRCA2 and associated proteins in the maintenance of genomic stability. *Oncogene* 25, 5864-5874.
 43. Fong, P. C., Boss, D. S., Yap, T. A., Tutt, A., Wu, P., Mergui-Roelvink, M., Mortimer, P., Swaisland, H., Lau, A., O'Connor, M. J., Ashworth, A., Carmichael, J., Kaye, S. B., Schellens, J. H., and de Bono, J. S. (2009) Inhibition of poly(ADP-ribose) polymerase in tumors from BRCA mutation carriers. *N. Engl. J. Med.* 361, 123-134.
 44. Turner, N., Tutt, A., and Ashworth, A. (2004) Hallmarks of 'BRCAness' in sporadic cancers. *Nat. Rev. Cancer* 4, 814-819.

45. Manie, E., Vincent-Salomon, A., Lehmann-Che, J., Pierron, G., Turpin, E., Warcoin, M., Gruel, N., Lebigoit, I., Sastre-Garau, X., Lidereau, R., Remenieras, A., Feunteun, J., Delattre, O., de, T. H., Stoppa-Lyonnet, D., and Stern, M. H. (2009) High frequency of TP53 mutation in BRCA1 and sporadic basal-like carcinomas but not in BRCA1 luminal breast tumors. *Cancer Res.* 69, 663-671.
46. Holstege, H., Joosse, S. A., van Oostrom, C. T., Nederlof, P. M., de, V. A., and Jonkers, J. (2009) High incidence of protein-truncating TP53 mutations in BRCA1-related breast cancer. *Cancer Res.* 69, 3625-3633.
47. Gorski, J. J., James, C. R., Quinn, J. E., Stewart, G. E., Staunton, K. C., Buckley, N. E., McDyer, F. A., Kennedy, R. D., Wilson, R. H., Mullan, P. B., and Harkin, D. P. (2010) BRCA1 transcriptionally regulates genes associated with the basal-like phenotype in breast cancer. *Breast Cancer Res. Treat.* 122, 721-731.
48. Helleday, T., Petermann, E., Lundin, C., Hodgson, B., and Sharma, R. A. (2008) DNA repair pathways as targets for cancer therapy. *Nat. Rev. Cancer* 8, 193-204.
49. Rottenberg, S., Jaspers, J. E., Kersbergen, A., van der, B. E., Nygren, A. O., Zander, S. A., Derksen, P. W., de, B. M., Zevenhoven, J., Lau, A., Boulter, R., Cranston, A., O'Connor, M. J., Martin, N. M., Borst, P., and Jonkers, J. (2008) High sensitivity of BRCA1-deficient mammary tumors to the PARP inhibitor AZD2281 alone and in combination with platinum drugs. *Proc. Natl. Acad. Sci. USA* 105, 17079-17084.
50. Zander, S. A., Kersbergen, A., van der, B. E., de, W. N., van, T. O., Gunnarsdottir, S., Jaspers, J. E., Pajic, M., Nygren, A. O., Jonkers, J., Borst, P., and Rottenberg, S. (2010) Sensitivity and acquired resistance of BRCA1;p53-deficient mouse mammary tumors to the topoisomerase I inhibitor topotecan. *Cancer Res.* 70, 1700-1710.
51. Rottenberg, S., Nygren, A. O., Pajic, M., van Leeuwen, F. W., van, d. H., I, van de, W. K., Liu, X., de Visser, K. E., Gilhuijs, K. G., van, T. O., Schouten, J. P., Jonkers, J., and Borst, P. (2007) Selective induction of chemotherapy resistance of mammary tumors in a conditional mouse model for hereditary breast cancer. *Proc. Natl. Acad. Sci. USA* 104, 12117-12122.
52. Bouwman, P., Aly, A., Escandell, J. M., Pieterse, M., Bartkova, J., van der, G. H., Hiddingh, S., Thanasoula, M., Kulkarni, A., Yang, Q., Haffty, B. G., Tommiska, J., Blomqvist, C., Drapkin, R., Adams, D. J., Nevanlinna, H., Bartek, J., Tarsounas, M., Ganesan, S., and Jonkers, J. (2010) 53BP1 loss rescues BRCA1 deficiency and is associated with triple-negative and BRCA-mutated breast cancers. *Nat. Struct. Mol. Biol.* 17, 688-695.
53. Bunting, S. F., Callen, E., Wong, N., Chen, H. T., Polato, F., Gunn, A., Bothmer, A., Feldhahn, N., Fernandez-Capetillo, O., Cao, L., Xu, X., Deng, C. X., Finkel, T., Nussenzweig, M., Stark, J. M., and Nussenzweig, A. (2010) 53BP1 inhibits homologous recombination in Brca1-deficient cells by blocking resection of DNA breaks. *Cell* 141, 243-254.
54. Cianfrocca, M., Goldstein, L. J. (2004) Prognostic and predictive factors in early-stage breast cancer. *Oncologist* 9, 606-616.
55. Sun, B., Zhang, S., Zhang, D., Li, Y., Zhao, X., Luo, Y., and Guo, Y. (2008) Identification of metastasis-related proteins and their clinical relevance to triple-negative human breast cancer. *Clin. Cancer Res.* 14, 7050-7059.
56. Cha, S., Imielinski, M. B., Rejtár, T., Richardson, E. A., Thakur, D., Sgroi, D. C., and Karger, B. L. (2010) In situ proteomic analysis of human breast cancer epithelial cells using laser capture microdissection: annotation by protein set enrichment analysis and gene ontology. *Mol. Cell Proteomics* 9, 2529-2544.
57. Mbeunkui, F., Metge, B. J., Shevde, L. A., and Pannell, L. K. (2007) Identification of differentially secreted biomarkers using LC-MS/MS in isogenic cell lines representing a progression of breast cancer. *J. Proteome Res.* 6, 2993-3002.
58. Ou, K., Yu, K., Kesuma, D., Hooi, M., Huang, N., Chen, W., Lee, S. Y., Goh, X. P., Tan, L. K., Liu, J., Soon, S. Y., Bin Abdul, R. S., Putti, T. C., Jikuya, H., Ichikawa, T., Nishimura, O., Salto-Tellez, M., and Tan, P. (2008) Novel breast cancer biomarkers identified by integrative proteomic and gene expression mapping. *J. Proteome Res.* 7, 1518-1528.
59. Hochgrafe, F., Zhang, L., O'Toole, S. A., Browne, B. C., Pinese, M., Porta, C. A., Lehrbach, G. M., Croucher, D. R., Rickwood, D., Boulghourjian, A., Shearer, R., Nair, R., Swarbrick, A., Faratian, D., Mullen, P., Harrison, D. J., Biankin, A. V., Sutherland, R. L., Raftery, M. J., and Daly, R. J. (2010)

- Tyrosine phosphorylation profiling reveals the signaling network characteristics of Basal breast cancer cells. *Cancer Res.* 70, 9391-9401.
60. Konstantinopoulos, P. A., Spentzos, D., Karlan, B. Y., Taniguchi, T., Fountzilas, E., Francoeur, N., Levine, D. A., and Cannistra, S. A. (2010) Gene expression profile of BRCAness that correlates with responsiveness to chemotherapy and with outcome in patients with epithelial ovarian cancer. *J. Clin. Oncol.* 28, 3555-3561.

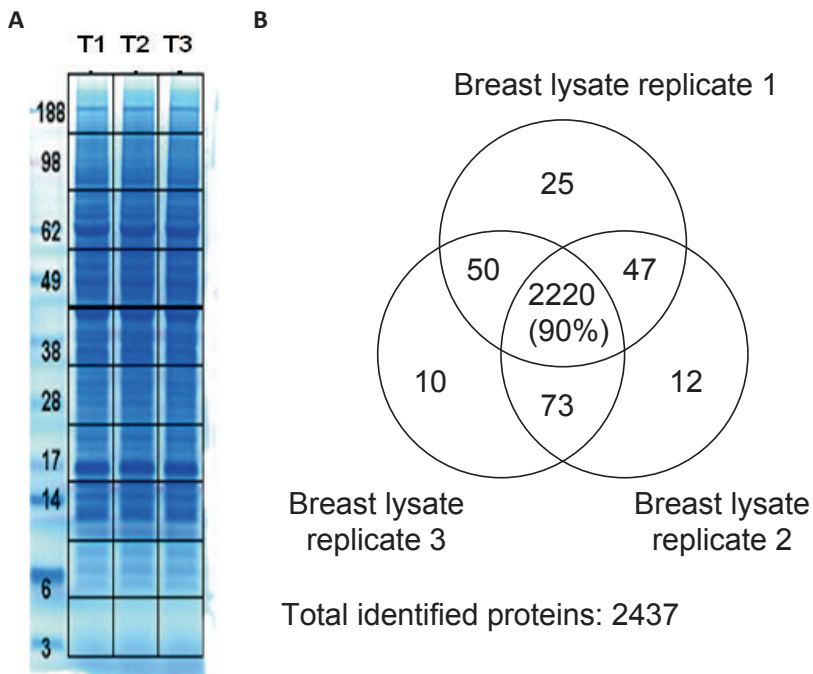
Supplementary Tables

The Supplementary Tables S1-3 can be requested via j.jaspers@nki.nl or janneke_jaspers@hotmail.com.

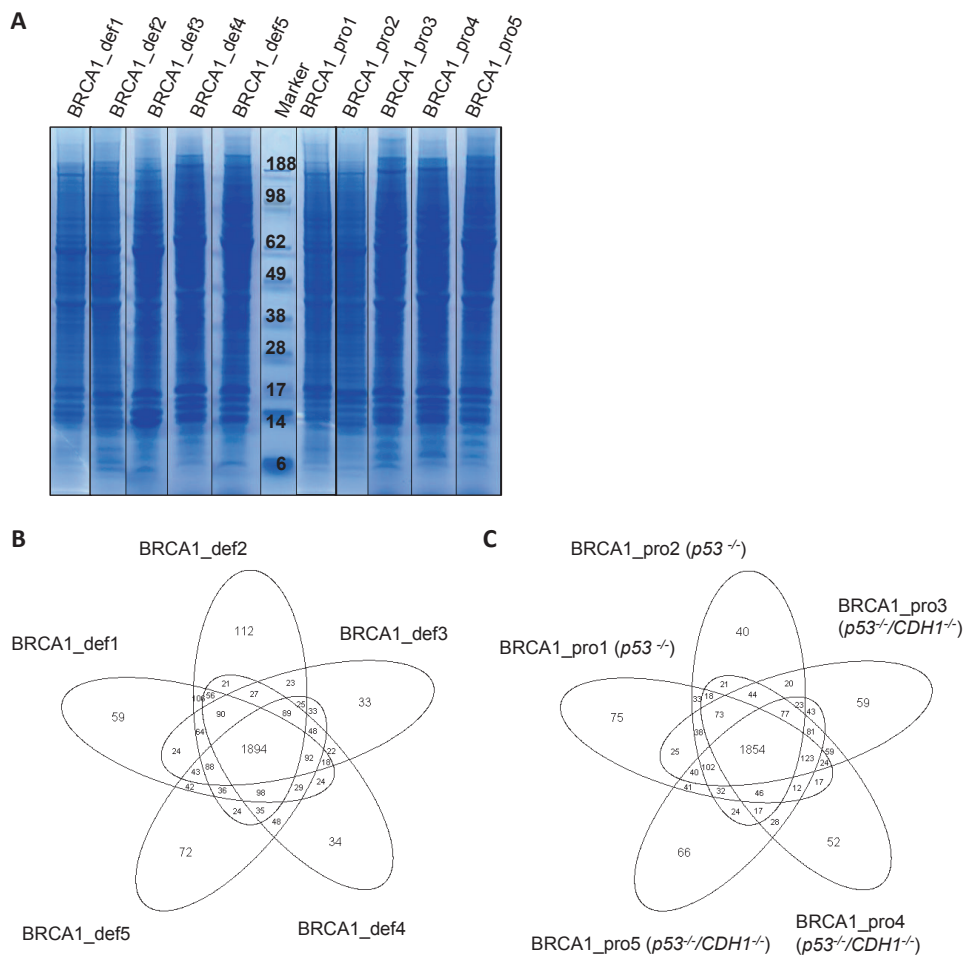
Supplementary Table S1. List of proteins detected in BRCA1-deficient and -proficient mouse tumor tissue lysates and associated spectral count quantification data

Supplementary Table S2. List of significantly differential proteins between BRCA1-deficient and -proficient mouse tumor tissue lysates and associated spectral count quantification data

Supplementary Table S3. List of significantly enriched protein complexes in significantly regulated proteins from BRCA1 deficient mouse tumor tissue lysates



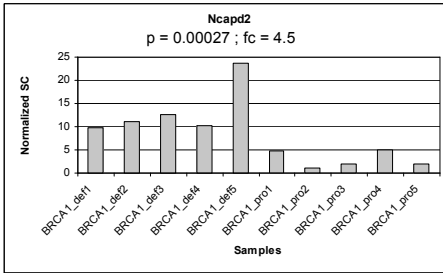
Supplementary Figure S1. Replicate analysis of pooled mammary tumor lysates. **A**, Coomassie stained gel displaying protein fractionation of three samples from a pooled mammary tumor tissue lysate. **B**, Summary of protein identification by nano-LC-MS/MS. The average CV of the normalized spectral counts is 24 % for the 2220 proteins present in all replicates (90 % of all proteins are overlapping). The total data set contained 2437 proteins.



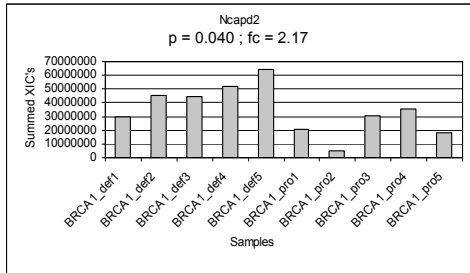
Supplementary Figure S2. Analysis of biological reproducibility. **A**, Protein fractionation of 10 samples from BRCA1-proficient and -deficient tumor tissue lysates. **B**, Five-way Venn diagram showing the distribution of the protein identifications within the five BRCA1-deficient samples. **C**, Five-way Venn diagram showing the distribution of all 3270 protein identifications within the five BRCA1-proficient samples. 1856 (56 %) proteins were present in all five samples and had an average CV of 36 %.

A

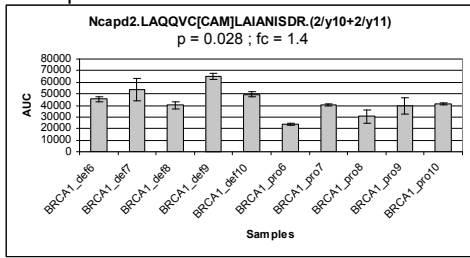
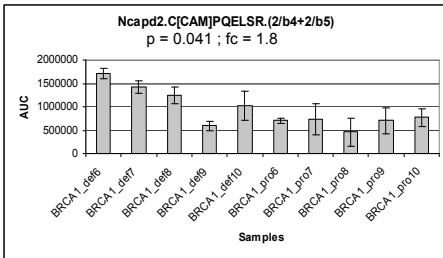
SC discovery samples



XIC discovery samples

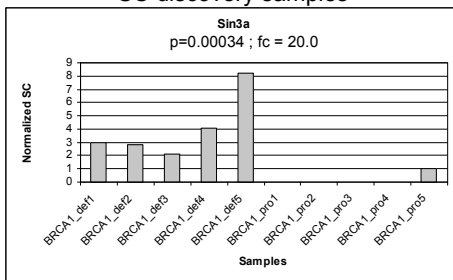


SRM validation samples

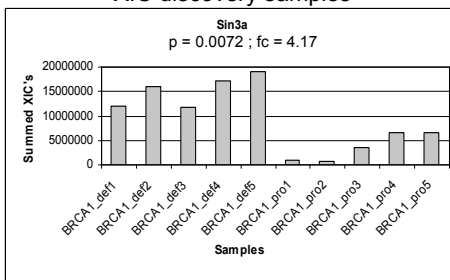


B

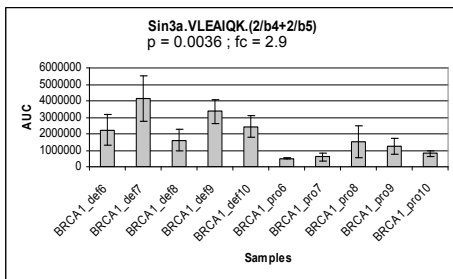
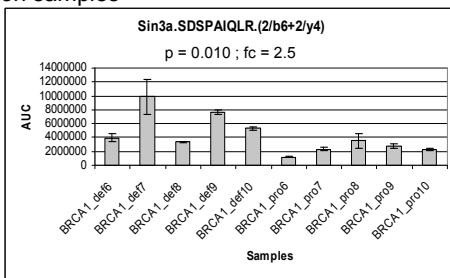
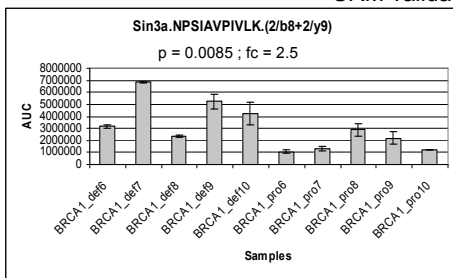
SC discovery samples



XIC discovery samples

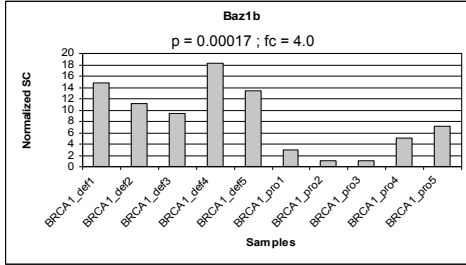


SRM validation samples

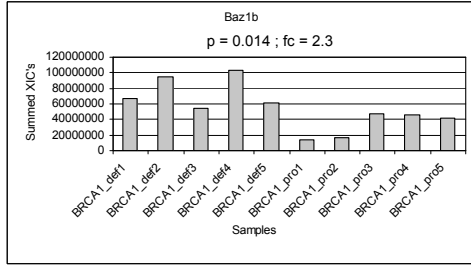


C

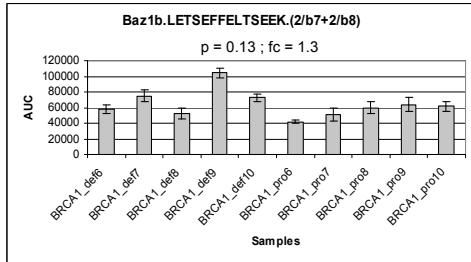
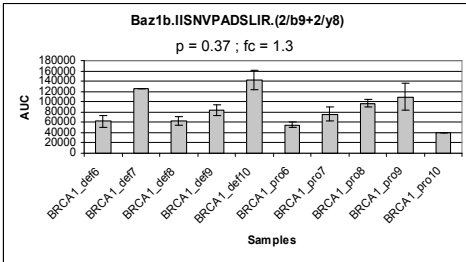
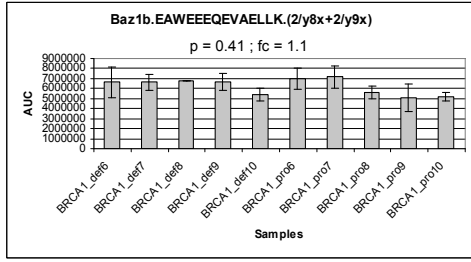
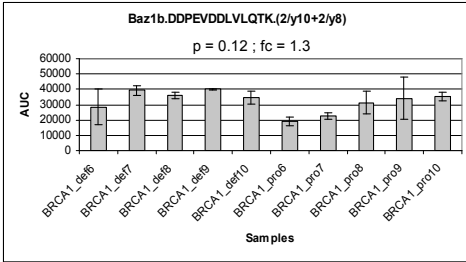
SC discovery samples



XIC discovery samples

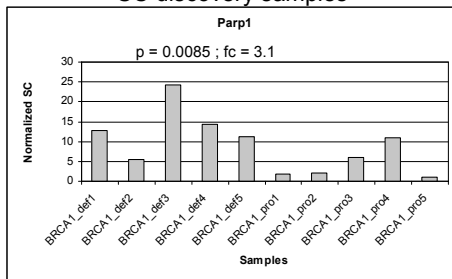


SRM validation samples

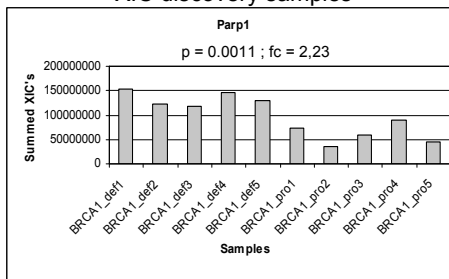


D

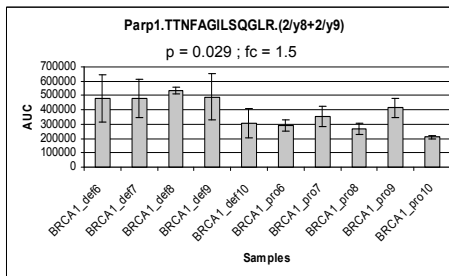
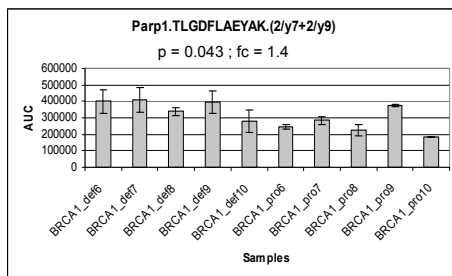
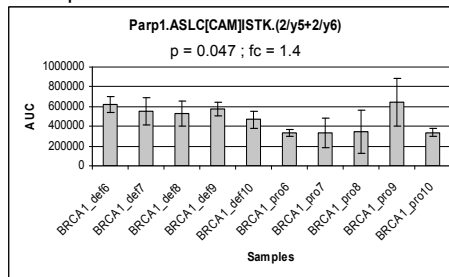
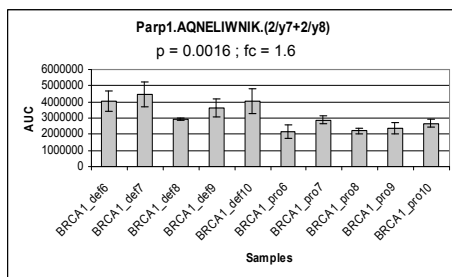
SC discovery samples



XIC discovery samples

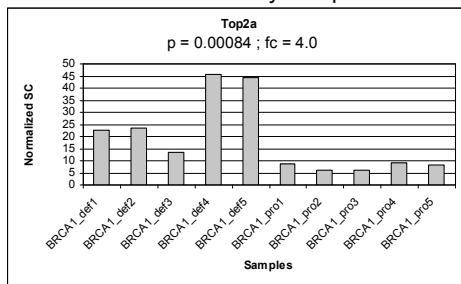


SRM validation samples

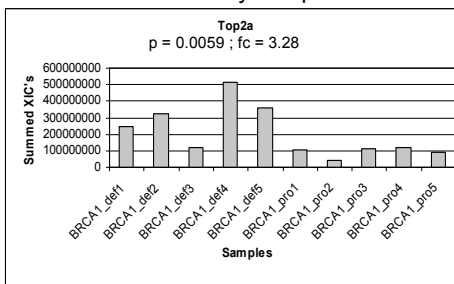


E

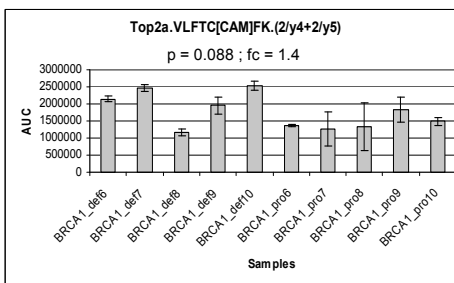
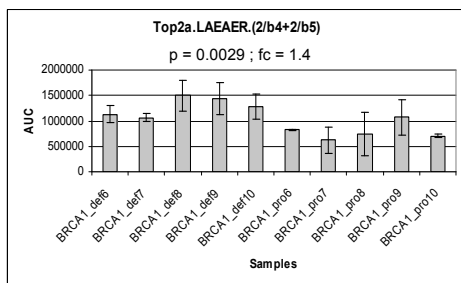
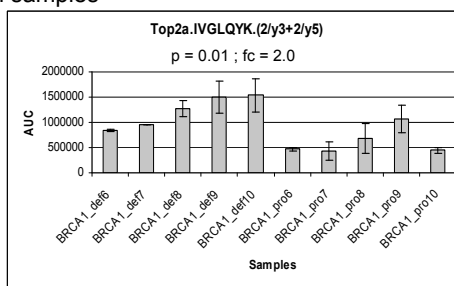
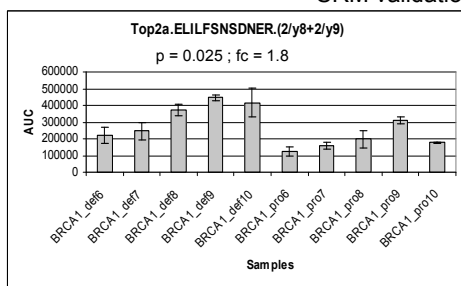
SC discovery samples



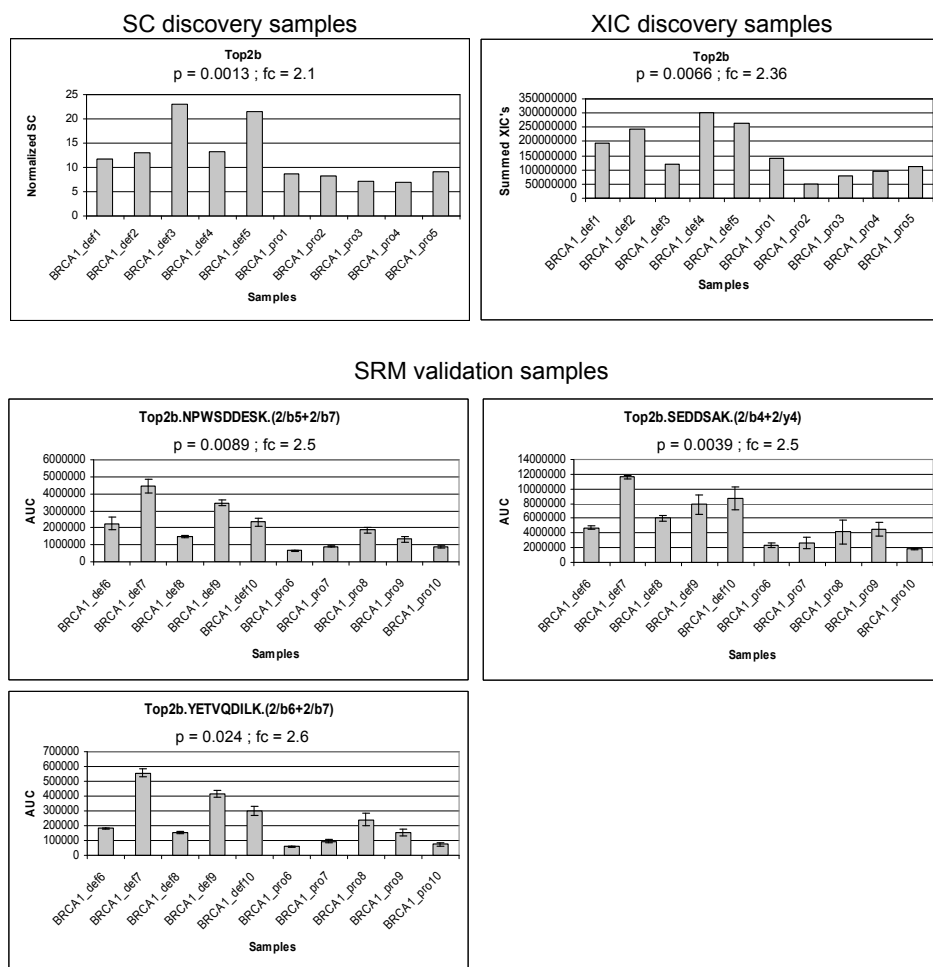
XIC discovery samples



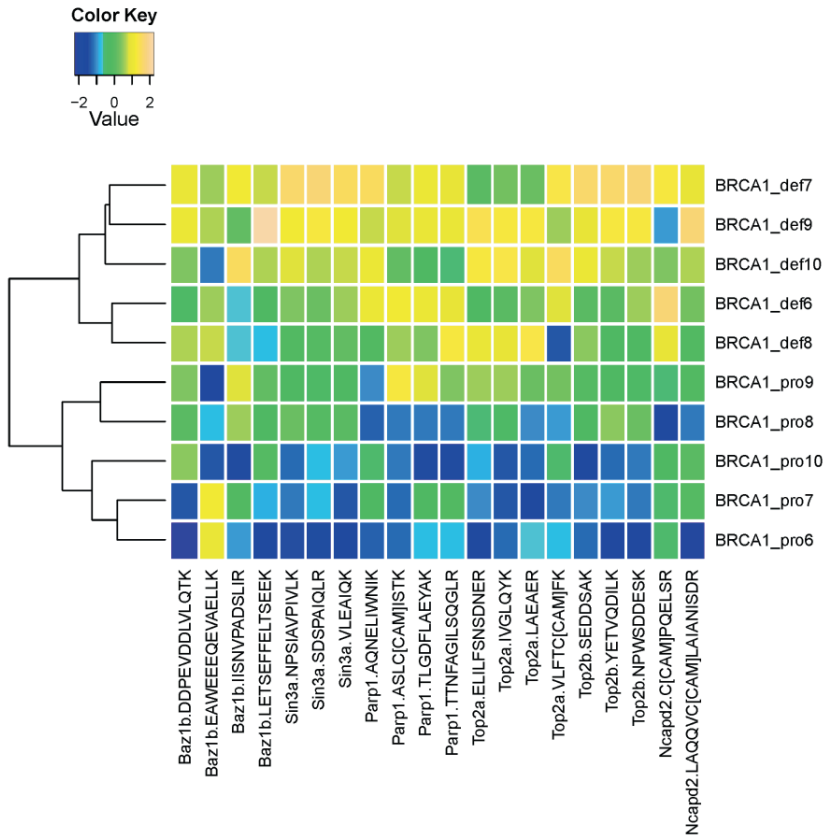
SRM validation samples



F



Supplementary Figure S3. Bar graphs representing the normalized area under the curve (AUC) from SRM analysis on four proteins that showed discordant behaviour between protein expression and mRNA expression (NCAPD2, SIN3A, BAZ1B and TOP2B), one protein of which the mRNA level could not be measured because there was no probe on the array (TOP2A), and one positive control that was up-regulated in both the proteomics and transcriptomics measurements (PARP1). Error bars represent the standard deviation of triplicate analysis. **A**, Measurements for NCAPD2; **B**, for SIN3A; **C**, for BAZ1B; **D**, for PARP1; **E**, for TOP2A; **F**, and for TOP2B.



Supplementary Figure S4. Heat map and cluster analysis using peptide intensities in an independent validation set of ten samples (five BRCA1-deficient and five BRCA1-proficient carcinomas). Peptides were derived from proteins that showed discordant behaviour between the protein and mRNA expression. This multiplexed analysis and visualization clearly delineates two groups based on BRCA1 status.

CHAPTER 7



Proteomics of genetically engineered mouse mammary tumors identifies fatty acid metabolism members as potential predictive markers for cisplatin resistance

Marc Warmoes^{1*}, Janneke E. Jaspers^{2,3*}, Guotai Xu², Barath K. Sampadi^{1,2}, Thang V. Pham¹, Jaco C. Knol¹, Sander R. Piersma¹, Epie Boven¹, Jos Jonkers³, Sven Rottenberg², Connie R. Jimenez¹

* contributed equally

¹Oncoproteomics Laboratory, Department of Medical Oncology, VU Medical Center, De Boelelaan 1117, 1081 HV Amsterdam, The Netherlands; ²Divisions of Molecular Oncology and ³Molecular Pathology, Netherlands Cancer Institute, Plesmanlaan 121, 1066 CX Amsterdam, The Netherlands

This research was originally published in *Molecular and Cellular Proteomics*, 2013; 11(5): 1319-34. © the American Society for Biochemistry and Molecular Biology

ABSTRACT

In contrast to various signatures that predict prognosis of breast cancer patients, markers that predict chemotherapy response are still elusive. To detect such predictive biomarkers, we investigated early changes in protein expression using two mouse models for distinct breast cancer subtypes who have a differential knock-out status for the breast cancer 1, early onset (*Brca1*) gene. The proteome of cisplatin-sensitive BRCA1-deficient mammary tumors was compared to that of cisplatin-resistant mammary tumors resembling pleomorphic invasive lobular carcinoma. The analyses were performed 24 h after administration of the maximum tolerable dose of cisplatin. At this time point, drug-sensitive BRCA1-deficient tumors showed DNA damage, but cells were largely viable. By applying paired statistics and quantitative filtering we identified highly discriminatory markers for the sensitive and resistant model. Proteins up-regulated in the sensitive model are involved in centrosome organization, chromosome condensation, homology-directed DNA repair, and nucleotide metabolism. Major discriminatory markers that were up-regulated in the resistant model were predominantly involved in fatty acid metabolism, such as fatty acid synthase. Specific inhibition of fatty acid synthase sensitized resistant cells to cisplatin. Our data suggest that exploring the functional link between the DNA damage response and cancer metabolism shortly after the initial treatment may be a useful strategy to predict the efficacy of cisplatin.

INTRODUCTION

Breast cancer is a heterogeneous disease consisting of a variety of subtypes that need different treatment strategies. In contrast to several prognostic signatures for clinical outcome, markers that predict treatment efficacy have been difficult to define. Reasons to explain this failure have been discussed elsewhere¹. A shortcoming of previous attempts to identify such markers may be that tumors were usually not challenged by drugs when sampled for analysis, or treatment was given a few weeks before sampling (neoadjuvant trials). Moreover, most previous studies focused on the analysis of gene expression to identify useful markers. However, differential expression of relevant factors, such as those involved in the DNA damage response, may be easier to detect shortly after chemotherapy-induced stress and protein level readouts may provide a more direct way of assessing drug response.

In this study, we aimed at detecting predictive biomarkers at the protein level by comparing the short-term treatment response of platinum-sensitive *versus* platinum-resistant mouse mammary tumors that represent different breast cancer subtypes. As a sensitive model we used the *K14cre;Brca1^{F/F};p53^{F/F}* mouse model² for BRCA1-deficient breast cancer. The *Brca1^{-/-};p53^{-/-}* tumors that arise in this model include a large intragenic deletion of *Brca1*, and we have previously shown that these tumors are highly sensitive to cisplatin treatment³. The response that we observed in this mouse model is consistent with the sensitivity of BRCA1-like breast cancer to intensive platinum-based chemotherapy in the clinic⁴. Moreover, it was recently shown that triple-negative breast cancer patients frequently respond to cisplatin treatment, especially in patients with lower BRCA1 expression⁵.

As resistant model we chose *WAPcre;Cdh1^{F/F};p53^{F/F}* mice. The cadherin-1 (CDH1)- and p53-deficient mammary tumors generated in these animals resemble human pleomorphic invasive lobular carcinomas⁶. We show here that the tumors of this model hardly respond to cisplatin. This is also consistent with the nature of invasive lobular carcinoma (ILC) cancers in patients, which usually have only a modest benefit of chemotherapy as compared to invasive ductal carcinoma⁷.

Platinum agents induce DNA damage by forming inter- and intrastrand DNA cross-links. The repair of DNA-platinum adducts involves several repair pathways including the Fanconi anemia pathway, nucleotide excision repair, and homologous recombination (HR)⁸. Because BRCA1 is an important player in the HR pathway, which results in error-free repair of double strand breaks, it is not unexpected that BRCA1-deficient tumors respond to platinum. Multiple cisplatin resistance mechanisms have been put forward⁹, of which reactivation of the HR pathway by genetic restoration of BRCA1 function is found to be a clinically relevant cisplatin resistance mechanism¹⁰.

Unfortunately, the precise BRCA1 status or HR activity of tumor cells is frequently not known for breast cancer patients. Early treatment resistance and response proteins that assess HR competence, both in familial and sporadic breast cancers, could therefore aid in selecting patients for platinum-based chemotherapy. In addition, identification of (druggable) predictive markers of resistant tumors might help to identify patients that need an alternative treatment.

In this study we found that major discriminatory proteins after treatment with cisplatin are involved in fatty acid metabolism and signaling. These proteins include the following: FASN, which is known as a central player in *de novo* fatty acid synthesis; fatty acid binding protein 4 (FABP4), a major transporter of fatty acids; and γ -synuclein (SNCG), a protein that has hypothesized lipid-binding properties. Our data suggest that the analysis of fatty acid metabolism may be a useful readout to predict platinum resistance early after initial treatment.

RESULTS

BRCA1-proficient/CDH1-deficient mammary tumors respond poorly to cisplatin

We have previously shown that BRCA1-deficient mammary tumors, which contain large intragenic deletions of the *Brca1* and *p53* genes, are highly sensitive to the maximum tolerable dose of cisplatin³. When we treated CDH1-deficient tumors, however, we found that these hardly responded to the same regimen (Figure 1A). This difference in cisplatin response between the models is not unexpected, because CDH1-deficient tumors are still capable of repairing cisplatin-induced DNA damage by homologous recombination (HR), in contrast to BRCA1-deficient tumors. In line with this, we previously observed that the CDH1-deficient tumors do not respond to treatment with the PARP inhibitor olaparib, which targets HR deficiency²³. These contrary drug responses therefore provide an opportunity to investigate differential treatment-induced protein expression in two mouse models, which carry mammary tumors that resemble specific breast cancer subtypes.

To measure proteins of viable tumor cells after treatment, we aimed at a time point at which sufficient DNA damage was induced, but at which most drug-sensitive tumor cells had not yet entered apoptosis. Moreover, the percentage of stromal cells that eventually replace viable tumor tissue should be small. As presented in Figure 1B, we found that 24 h after cisplatin administration most BRCA1-deficient tumor cells showed DNA damage foci (pH2AX), but only few tumor cells showed morphologic signs of cell death (*e.g.* pyknosis, nuclear fragmentation, or hypereosinophilic cytoplasm) or activation of caspase 3. In contrast, 48 h or 96 h after treatment, the number of dying BRCA1-deficient tumor cells increased and was replaced by reactive stroma. In cisplatin-resistant (*Cdh1*^{-/-};*p53*^{-/-}) tumors, the number of apoptotic or necrotic tumor cells was also low after 24 h of treatment as expected by the poor response (data not shown). Hence, the 24-h time-point is appropriate

to investigate differential induction of protein expression in cisplatin-sensitive *versus* cisplatin-resistant tumors.

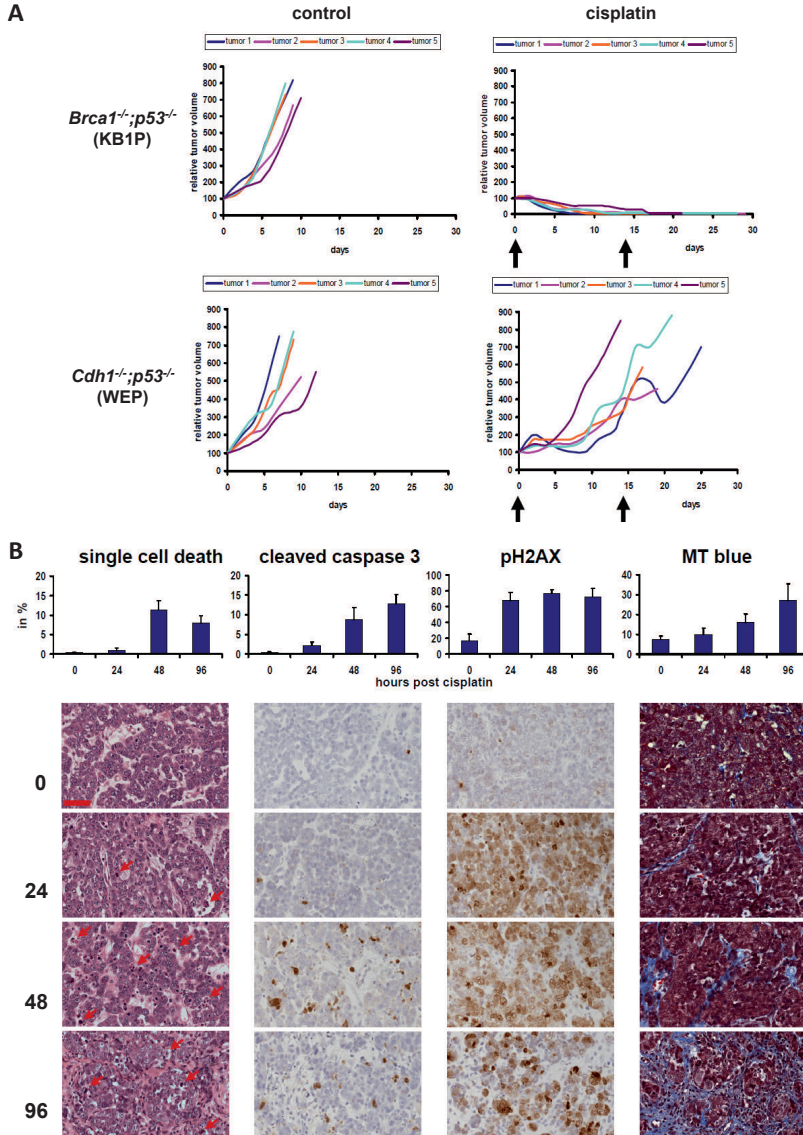


Figure 1. Responses of *Brca1*^{-/-};*p53*^{-/-} (KB1P) or *Cdh1*^{-/-};*p53*^{-/-} (WEP) mammary tumors to cisplatin. **A**, Five individual KB1P or WEP tumors were transplanted orthotopically into syngeneic mice. Once tumors reached a volume of 200 mm³, they were left untreated or treated with the maximum tolerable dose of cisplatin (6 mpk i.v. on days 0 and 14). **B**, Analyses of drug-sensitive KB1P tumors using H&E staining (arrows indicate examples of cells with morphologic characteristics of single cell death such as fragmented or pyknotic nuclei and hyper eosinophilic cytoplasm), cleaved caspase 3, pH2AX, and Masson's trichrome stain (MT). Scale bar = 50 μm.

Proteome differences between cisplatin-sensitive and -resistant mouse mammary tumors shortly after cisplatin treatment

To identify early response biomarkers, we used three individual cisplatin-sensitive tumors (*Brca1^{-/-};p53^{-/-}*) and three cisplatin-resistant tumors (*Cdh1^{-/-};p53^{-/-}*) that were either treated with cisplatin or left untreated (see Figure 2 for experimental setup). Comparative proteomics based on SDS-PAGE (see Supplementary Figure S1A for gel images) in combination with nanoLC-MS/MS identified a total of 3486 proteins in the 12 mammary tumor samples using stringent protein identification criteria (only protein identifications with a probability of >99 % identified with at least two peptides of >95 % in one of the samples were retained). The whole data set of identified proteins is provided in Supplementary Table S1, and Supplementary Table S2 contains the peptide identifications. The number of identified proteins in each biological group was comparable and ranged from 3104 to 3206 with good reproducibility of protein identification in the four groups: 66-75 % of the proteins were identified in all three biological replicates (for Venn diagrams see Supplementary Figure S1B).

Unsupervised cluster analysis using all 3486 proteins (Supplementary Figure S2) showed that CDH1-deficient tumors were clearly separated from the BRCA1-deficient ones. Within these groups, however, treated tumors were not separated from untreated controls. Instead, tumors derived from the same donor tumor clustered together. This result demonstrates that proteome differences between the three different tumors are larger than those induced by short-term cisplatin treatment. This is consistent with previous gene expression analyses of matched tumor samples before and after acquiring drug resistance³. Statistical analysis¹⁸ of the cisplatin-treated *versus* -untreated samples in the sensitive model identified 167 differentially expressed proteins ($p < 0.05$). Of these, 105 were up-regulated and 62 were down-regulated (see Supplementary Table S1). In the cisplatin-resistant model, we found 98 proteins differentially expressed between the control tumor and the cisplatin-treated tumor, with 68 up- and 30 down-regulated. Supplementary Table S3 contains the combined lists of the 254 proteins regulated after cisplatin treatment in the sensitive and resistant models. Importantly, supervised cluster analysis using subsets of the significantly regulated proteins that showed highly divergent properties in the two models (Figure 3 and see below) clearly showed that the treatment and control groups are in different sub-clusters of the branches containing each model (Figure 5 and Supplementary Figures S2B and S2C), thereby underscoring the potential of a proteomics readout for assessing drug response. For a study overview that includes the different comparisons, analyses, and marker selections, see Figure 3 and below.

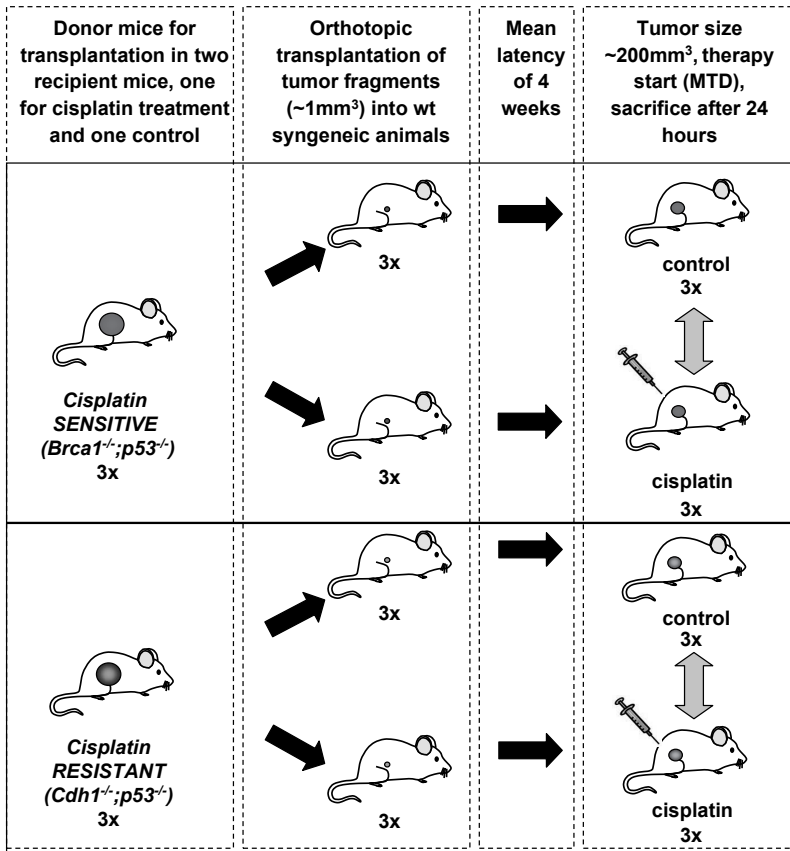


Figure 2. Experimental setup for the high-throughput proteomics experiment using KB1P or WEP mouse models with and without cisplatin treatment.

Protein interactions in cisplatin-sensitive BRCA1-deficient mammary mouse tumors after cisplatin treatment

To visualize interactions of the differentially expressed proteins in the sensitive BRCA1-deficient tumors before and after cisplatin treatment, we employed the STRING protein network analysis tool¹⁹ together with graphic-rich graphs generated in Cytoscape²⁰. Network analysis using the Cluster ONE software²¹ and BiNGO gene ontology analysis²² was used to associate subsets of proteins with biological information.

To this end, we annotated the three most significant groups of well-connected proteins (with a *p* value < 0.05 generated by Cluster ONE). Within the network of the 105 up-regulated proteins by cisplatin, Figure 4A shows significant groups of highly connected nodes that were identified.

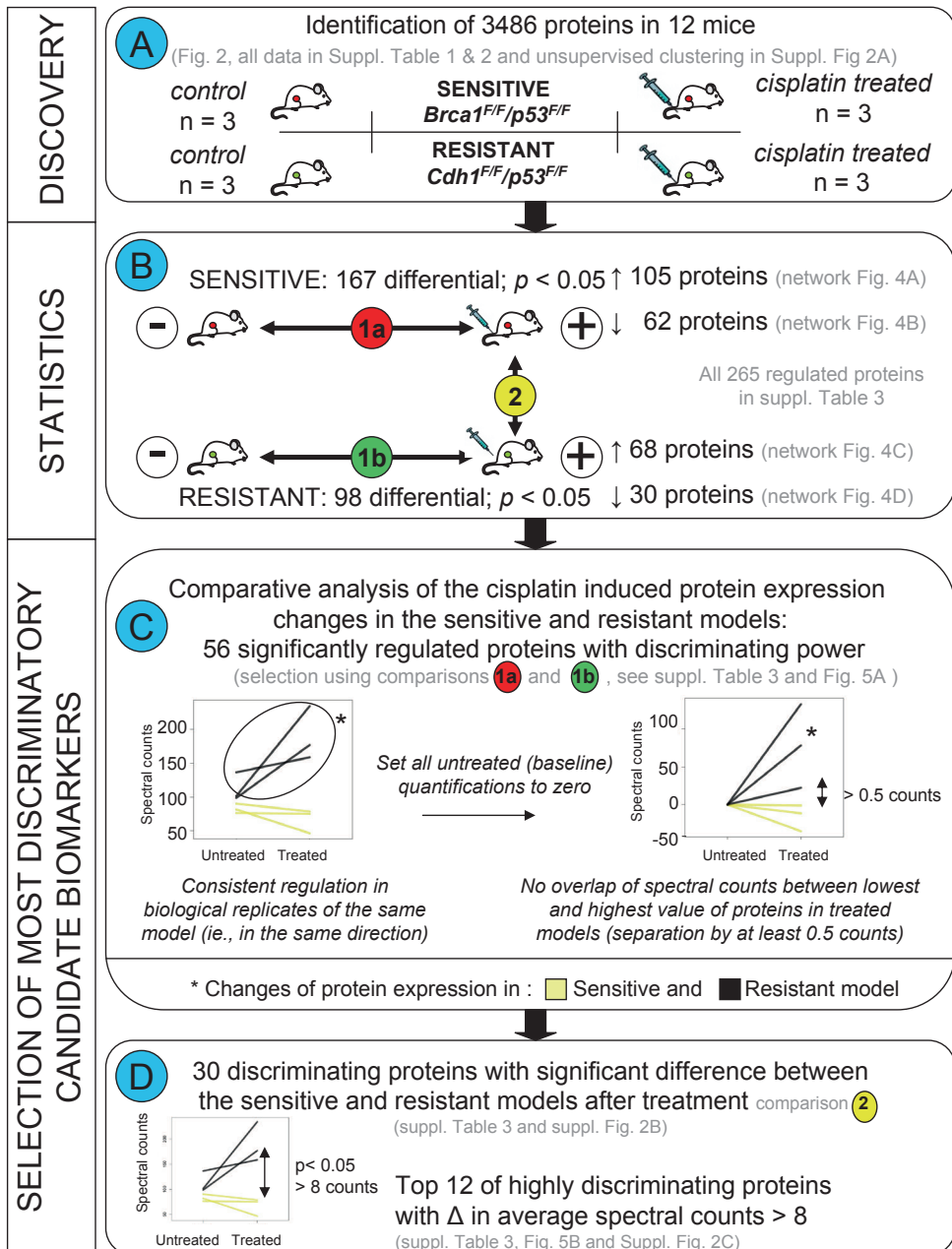


Figure 3. Flowchart depicting the different comparisons and criteria for selection of the most discriminatory biomarkers. (A) describes the discovery experiment including four groups consisting of cisplatin-sensitive and -resistant models with the control and cisplatin treatment groups for each model, with three animals in each group. (B) displays the statistical comparisons. All statistical analyses

were performed using R as described previously^{17,18}. To select the most discriminatory markers we applied quantitative filtering in Excel. To this end, protein spectral count data of the 3486 proteins were exported from Scaffold to Excel. Paired statistical testing¹⁸ in R identifies differentially expressed proteins between the treated and untreated tumors in each tumor type separately (comparisons 1a and 1b). **C**, Criteria to select for proteins with divergent regulation in the sensitive and resistant model. To this end, baseline transformation was applied to each protein. Furthermore, only proteins were retained that displayed a minimum separation of 0.5 counts between the lowest and the highest value in the two models after cisplatin treatment. This led to a selection of 56 discriminatory candidate markers. Left graph: example of untransformed spectral counts for the sensitive and resistant paired sets. Right graph: example using the same protein, with untreated tumors brought to a baseline of zero counts. **D**, Further selection was made to pinpoint the most discriminatory proteins. Using β -binomial statistics¹⁷ on the list of 56 proteins, we selected 30 proteins that were significantly different between the sensitive and resistant models after cisplatin treatment (comparison 2 in B). From these 30 proteins, the top 12 was selected with highly divergent regulation patterns in the two models, *i.e.* proteins displaying on average at least 8 counts separation between the average values in both models after treatment (before baseline transformation).

The largest group of well-connected proteins, containing 25 members, was associated with GO terms involving chromosome segregation during mitosis (*e.g.* “M-phase” and “chromosome segregation”) and “DNA metabolic process/deoxyribonucleotide metabolic process”. See Figure 4E and Supplementary Table S4A for BiNGO analysis results on the regulated proteins and the significant groups of well-connected proteins. Well known examples of chromosome segregation proteins include multiple kinesins (KIF11, KIF23, and KIF4B) as well as centrosome-related proteins (INCENP, CENPE, KNTC1, and AURKB). Also chromosome condensation proteins were up-regulated (NCAPG and NCAPH). In the GO category “nucleic acid metabolic process” we detected proteins such as TOP2A, RRM1 and DTYMK. In addition, this cluster comprises DNA repair proteins such as MRE1A, poly(ADP-ribose) polymerase 1 (PARP1), FEN1, and LIG1. The second group contained eight proteins (Figure 4A) involved in “multi-organism process” and “response to biotic stimulus”. The third group consisted of five members (Figure 4A) that are mainly involved in RNA splicing with GO terms like “RNA splicing” and “RNA metabolic process” (Figure 4E and Supplementary Table S4A). FXR1, an RNA-binding protein that is not a member of this group, was also up-regulated. Other proteins of interest but not included in the top three groups are CHD4, a modulator of homologous repair²⁴, the DNA-associated protein NCOR2, a chromatin remodeler and the histone binding protein NASP.

When visualizing the down-regulated proteins in BRCA1-deficient tumors after cisplatin treatment as a protein-protein interaction network using the STRING tool (see Figure 4B), we identified two large groups of well connected proteins of 14 and 9 proteins related to inflammatory response as indicated by GO-terms like “response to wounding” and “inflammatory response” (Figure 4E and Supplementary Table S4B).

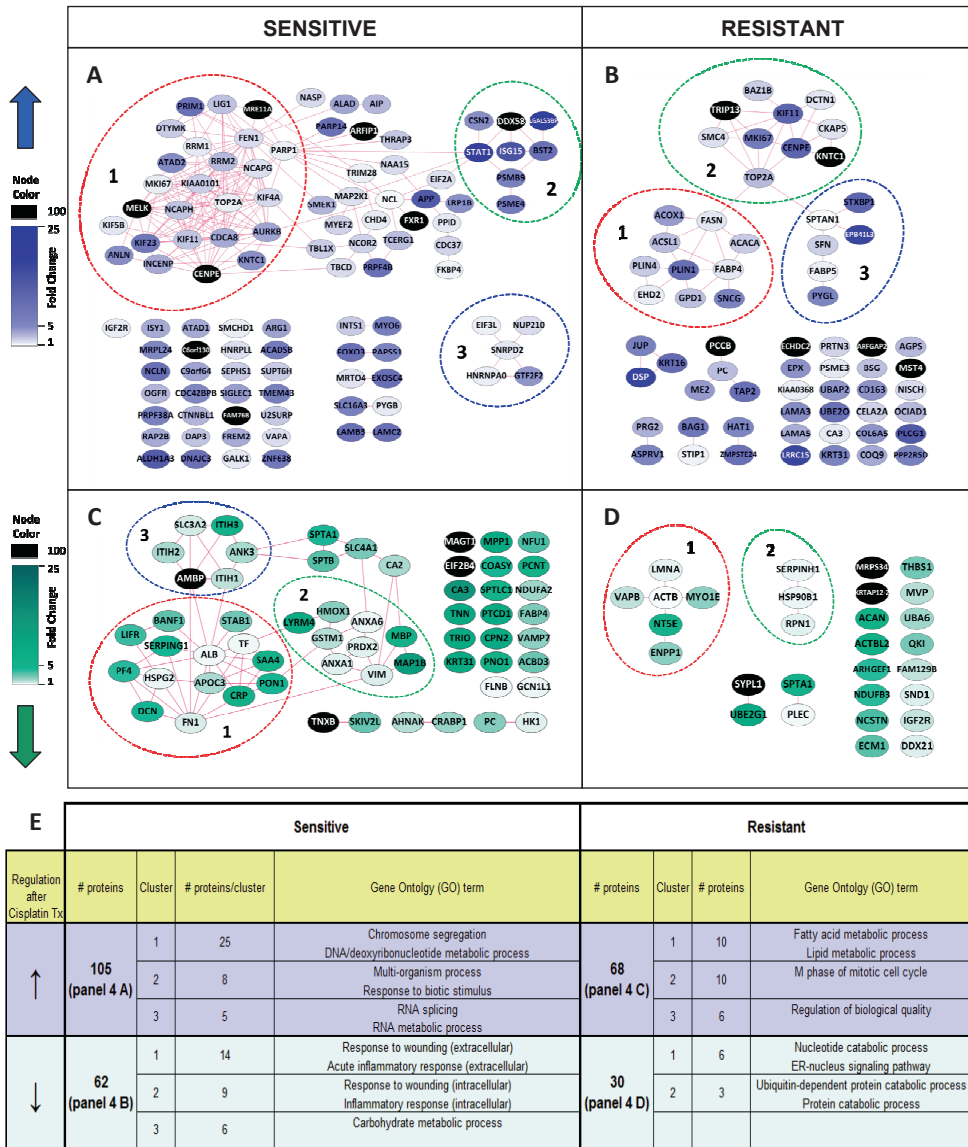


Figure 4. Protein-protein networks of the regulated proteins selected using a paired statistical analysis between treated and untreated conditions. The networks were generated using default settings in STRING and visualized using Cytoscape. Dashed lines indicate the top three most significant clusters identified by Cluster ONE cluster analysis. Nodes represent proteins, and the edges represent interactions that include direct (physical) and indirect (functional) associations. See Szklarczyk *et al.*¹⁹ for more details on edge generation. **A**, Up-regulated proteins in the cisplatin-sensitive tumors. **B**, Down regulated proteins in the cisplatin-resistant tumors. **C**, Up-regulated proteins in the cisplatin-resistant tumors. **D**, Down-regulated proteins in the cisplatin-resistant tumors. **E**, Representative GO terms identified by BiNGO analysis for the top three clusters within in the regulated proteins.

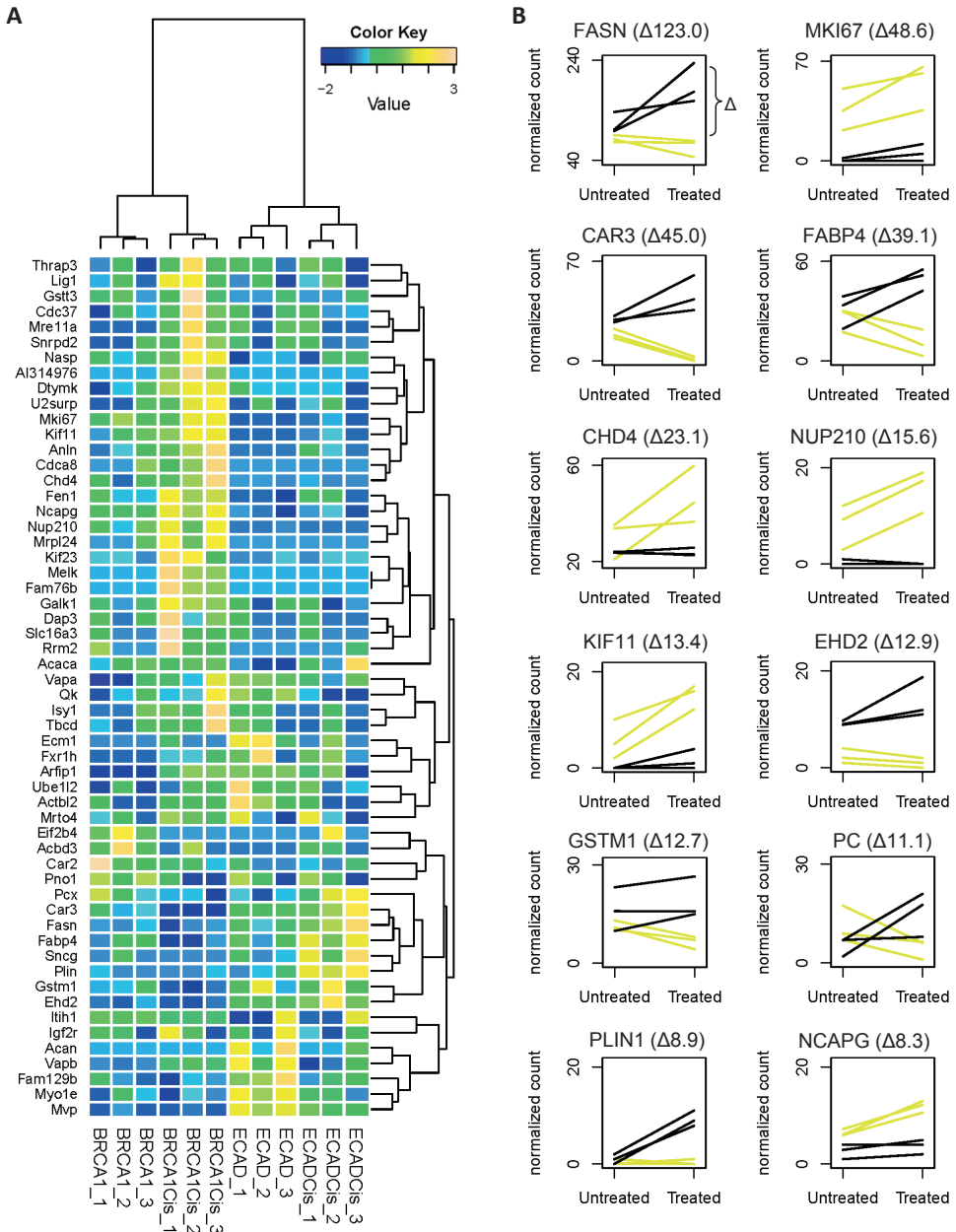


Figure 5. **A**, Hierarchical cluster analysis of the top 56 discriminatory proteins, showing complete separation of all four control and treatment conditions of the cisplatin-sensitive (KB1P) and -resistant (WEP) tumors. **B**, Expression profiles using spectral counting of the 12 significant proteins with at least 8 spectral counts difference between the two treated tumor types. Expression profiles were constructed using normalized spectral count. Lines connect paired samples before and after treatment. Yellow lines represent the three sensitive tumors before and after treatment, and black lines represent the resistant tumors.

The main difference between the two groups is that proteins in group 1 are mainly localized in the extracellular space, while the smaller group 2 contains predominantly intracellular proteins that are also implicated in regulation of vesicle-mediated transport, response to oxidative stress and anti-apoptosis. The majority of proteins in the third group are associated with “carbohydrate metabolic process” with ITIH1, ITIH2, and ITIH3 involved in the transport of the carbohydrate polymer hyaluronan. Other proteins outside this group (*e.g.* PC, MAGT1, and HK1) are also implicated in carbohydrate metabolism. A total of 34 proteins within the 62 down-regulated proteins fell within the GO term called “metabolic process” suggesting major down-regulation of metabolic proteins.

In conclusion, the proteomics and gene ontology data of early cisplatin response show that DNA segregation/metabolism/repair and inflammatory response are the major biological processes altered in the sensitive *Brca1*^{-/-};*p53*^{-/-} tumors after cisplatin treatment.

Protein interactions in cisplatin-resistant mammary mouse tumors after cisplatin treatment

Protein network analysis in the cisplatin-resistant model using the 68 up-regulated proteins after cisplatin treatment revealed two main groups of well-connected proteins with functions involved in fatty acid synthesis and chromosome/centrosome regulation as identified in Cluster ONE/BiNGO analysis (Figure 4C). The first sub-network is associated with fatty acid synthesis, as indicated by the GO terms “fatty acid metabolic process” and “lipid metabolic process” (Figure 4E and Supplementary Table S4C). Some of these proteins are known to be involved mainly in *de novo* fatty acid synthesis and/or fatty acid degradation (*e.g.* FASN, ACACA, ACOX1, and ACSL1), while others function in mechanisms related to lipid storage or transport (*e.g.* FABP4 and PLIN1). In addition, γ -synuclein (SNCG), a known interactor of FABP4 (ref. ²⁵) with a hypothesized lipid binding domain, was up-regulated.

The second group contained mostly chromosome/centromere proteins that function during cell division (*e.g.* GO term “M phase of mitotic cell cycle”). Members include TRIP13, involved in chromosome recombination and chromosome structure development during meiosis and also KNTC1, an essential component of the mitotic checkpoint. The third group is involved in “regulation of biological quality” with a diverse set of sub-functions within this GO term (Supplementary Table S4C). STXBP1 functions as a vesicle-membrane regulating protein, whereas SPTAN1 is responsible for cytoskeleton movement near the membrane, but is also implicated in DNA repair and the cell cycle. PYGL, an enzyme functioning within the carbohydrate metabolism, was also present in this group. Moreover, outside the three main clusters, a number of other proteins are involved in metabolism, including PC, CAR3, ME2, and PCCB.

The protein network of the down-regulated proteins (Figure 4D) contained two groups of well connected proteins: the first and main group is associated with the GO terms

“nucleotide catabolic process” (NT5E and ENPP1) and “ER-nucleus signaling pathway” (VAPB and LMNA, also see Figure 4E and Supplementary Table S4D), and the second, smaller group includes proteins associated mostly to “ubiquitin-dependent protein catabolic process” and “protein catabolic process” (HSP90B1 and RPN1). Overall, seven out of the 30 proteins in Figure 4D are involved in “cellular catabolic process”, and included for example UBA6 and UBE2G1, two enzymes functioning as ubiquitination proteins.

In summary, fatty acid metabolism and the M phase of the cell cycle are the major processes associated with the up-regulated proteins after short-term cisplatin treatment in resistant tumors, whereas several proteins involved in catabolic processes are down-regulated.

Selection of FASN for functional follow up

To identify cisplatin response markers showing the most diverging pattern between sensitive and resistant models, we selected proteins with optimal separating properties by applying a number of filtering criteria on the differential proteins identified using the paired statistics (Figure 3 and Supplementary Table S3 for all relevant criteria used for inclusion). First, we reasoned that the more robust markers are those proteins whose regulation is consistent in all biological replicates (*i.e.* in the same direction) and that have an average fold change of minimally 1.5. Next, we selected proteins with divergent regulation in the cisplatin sensitive and resistant models (Figure 3C). To this end, we brought all protein quantifications of the untreated tumors to a baseline of zero counts, whereby the protein quantifications of the matching treated tumors were adjusted in the same way for each protein separately. After this baseline transformation, we selected proteins whose normalized spectral counts in the treated tumors did not overlap between the sensitive and the resistant models. See Figure 3C for a graphical example. This resulted in 56 top discriminatory candidates that are described in Table 1 (also see Supplementary Table S3 for detailed quantitative information). These top 56 discriminatory proteins showed an optimal clustering pattern that could separate the 4 groups in a supervised clustering (Figure 5A). For a further selection of proteins with optimal separation power, we selected proteins that were significantly differential between the two cisplatin treated groups ($p < 0.05$, using the unpaired β -binomial test¹⁷), yielding 30 proteins (Figure 3D). Of these, 12 proteins displayed strong opposite regulations as revealed by applying a cutoff of eight spectral counts between the averaged spectral counts of the two treated groups (Figure 3D) (both criteria were implemented before baseline transformation). Both top lists also displayed optimal clustering patterns. See Supplementary Figures S2B and S2C for the supervised hierarchical clustering results of the 30 and 12 most discriminatory proteins, respectively. Figure 5B displays expression profiles for the 12 proteins. We chose FASN for targeted follow up because it showed the largest quantitative difference (123 spectral counts) between the two models after treatment and because of its involvement in one of the major discriminatory pathways, namely fatty acid metabolism.

Table 1. Top discriminating proteins between BRCA1-deficient and -proficient mammary tumors after short term cisplatin treatment

Description	International Protein Index	Gene Ontology
Fatty acid synthase	IPI00113223	Lipid metabolic process
Ki-67 protein	IPI00124959	M phase
Carbonic anhydrase 3	IPI00221890	Small molecule metabolic process
Fatty acid-binding protein, adipocyte	IPI00116705	Lipid metabolic process
Chromodomain-helicase-DNA-binding protein 4	IPI00396802	Chromosome organization
Nuclear pore membrane glycoprotein 210 precursor	IPI00342158	Establishment of protein localization
Kinesin-like protein KIF11	IPI00130218	Mitotic spindle organization
EH DOMAIN-CONTAINING PROTEIN-2 homolog	IPI00402968	Organelle organization
Glutathione S-transferase Mu 1	IPI00230212	Metabolic process
pyruvate carboxylase, full insert sequence	IPI00114710	Lipid metabolic process
Perilipin	IPI00223783	Lipid metabolic process
Condensation protein G isoform 1	IPI00122202	M phase
Major vault protein	IPI00111258	mRNA transport
Small nuclear ribonucleoprotein Sm D2	IPI00119220	Nucleic acid metabolic process
γ -Synuclein	IPI00271440	Regulation of neurotransmitter secretion
thymidylate kinase, full insert sequence	IPI00831272	Deoxyribonucleotide biosynthetic process
Galactokinase 1	IPI00265025	Monosaccharide metabolic process
Isoform 1 of Nuclear autoantigenic sperm protein	IPI00130959	Chromosome organization
Kinesin family member 23	IPI00407864	Mitotic spindle organization
flap structure specific endonuclease 1, full insert sequence	IPI00410836	Nucleic acid metabolic process
Tubulin-specific chaperone D	IPI00461857	Macromolecule metabolic process
Actin-binding protein anillin	IPI00172197	Nuclear division
Ribonucleoside-diphosphate reductase M2 subunit	IPI00112645	Deoxyribonucleotide biosynthetic process
Isoform 1 of Mitochondrial 28S ribosomal protein S29	IPI00275050	Cellular component organization
Isoform 1 of Borealin	IPI00621765	M phase
Pre-mRNA-splicing factor ISY1 homolog	IPI00469994	Nucleic acid metabolic process
39S ribosomal protein L24, mitochondrial precursor	IPI00162769	Macromolecule biosynthetic process
Uncharacterized protein C6orf130 homolog	IPI00154005	Purine nucleoside binding
Isoform 1 of Protein FAM76B	IPI00330763	n/a
Maternal embryonic leucine zipper kinase	IPI00323045	Cellular macromolecule metabolic process
ligase I, DNA, ATP-dependent	IPI00473314	Nucleic acid metabolic process
Cation-independent mannose-6-phosphate receptor precursor	IPI00308971	Positive regulation of apoptosis
Glutathione S-transferase, theta 3	IPI00116236	Glutathione metabolic process
Hsp90 co-chaperone Cdc37	IPI00117087	M phase
Thyroid hormone receptor-associated protein 3	IPI00556768	Nucleic acid metabolic process
Isoform E of Fragile X mental retardation syndrome-related protein 1	IPI00122521	Regulation of translation
Isoform 2 of U2-associated protein SR140	IPI00467507	RNA processing
Aggrecan core protein precursor	IPI00119035	Proteolysis
mRNA turnover protein 4 homolog	IPI00132578	Ribosome biogenesis
Isoform 7 of Protein quaking	IPI00130483	mRNA transport
Monocarboxylate transporter 4	IPI00118910	Monocarboxylic acid transport
Carbonic anhydrase 2	IPI00121534	Metabolic process
Myosin IE	IPI00330649	Vasculogenesis
Niban-like protein	IPI00330695	Negative regulation of apoptotic process
Vesicle-associated membrane protein-associated protein B	IPI00135655	Nucleotide catabolic process
Isoform 1 of Double-strand break repair protein MRE11A	IPI00118853	Nucleic acid metabolic process
Vesicle-associated membrane protein-associated protein A	IPI00125267	Cellular membrane fusion
Isoform 2 of Acetyl-CoA carboxylase 1	IPI00848443	Lipid metabolic process
ADP-ribosylation factor interacting protein 1	IPI00466057	Establishment of localization in cell
Actin, cytoplasmic type5 homolog	IPI00221528	Nucleotide and ATP binding
Isoform 1 of Translation initiation factor eIF-2B subunit delta	IPI00124879	Metabolic process
Pno1 RNA-binding protein PNO1	IPI00131909	RNA binding
Isoform Long of Extracellular matrix protein 1 precursor	IPI00122272	System development
Itih1 protein	IPI00322867	Metabolic process
Ubiquitin-activating enzyme E1-like protein 2	IPI00226815	Proteolysis involved in cellular protein catabolic process
Golgi resident protein GCP60	IPI00129907	Metabolic process

Human Gene Names	Significant regulation in sensitive model ^a	Fold change in sensitive model ^a	p value in sensitive tumors ^a	Significant regulation in resistant model ^a	Fold change in resistant model ^a	p value in resistant tumors ^a	Top 30 proteins ^b	Top 12 proteins ^c
<i>FASN</i>		-1,3	0,070	↑	1,7	0,017	x	x
<i>MKI67</i>	↑	1,5	0,012	↑	7,1	0,006	x	x
<i>CA3</i>	↓	-13,9	0,000	↑	1,6	0,009	x	x
<i>FABP4</i>	↓	-2,6	0,010	↑	1,6	0,007	x	x
<i>CHD4</i>	↑	1,6	0,022		-1,0	0,488	x	x
<i>NUP210</i>	↑	1,9	0,011		-2,0	0,282	x	x
<i>KIF11</i>	↑	2,6	0,011	↑	11,1	0,028	x	x
<i>EHD2</i>		-2,3	0,100	↑	1,5	0,047	x	x
<i>GSTM1</i>	↓	-1,8	0,025		1,2	0,206	x	x
<i>PC</i>	↓	-2,5	0,014	↑	2,8	0,026	x	x
<i>PLIN1</i>		-1,1	0,385	↓	-1,6	0,033	x	x
<i>Ncapg</i>	↑	1,9	0,017		1,4	0,240	x	x
<i>MVP</i>		2,0	0,281	↓	-3,3	0,038	x	
<i>LIG1</i>	↑	1,7	0,032		-1,1	0,407	x	
<i>IGF2R</i>		-3,8	0,113	↑	5,7	0,004	x	
<i>SNRPD2</i>	↑	2,4	0,019		-1,3	0,272	x	
<i>SNCG</i>	↑	1,6	0,043		-1,2	0,265	x	
<i>DTYMK</i>	↑	2,0	0,024		1,4	0,246	x	
<i>GALK1</i>	↑	7,7	0,003		1,7	0,303	x	
<i>NASP</i>	↑	1,9	0,035		2,0	0,094	x	
<i>KIF23</i>	↑	1,9	0,045		-1,5	0,189	x	
<i>FEN1</i>	↑	4,7	0,008		7,0	0,060	x	
<i>TBCD</i>	↑	3,0	0,025		2,0	0,278	x	
<i>ANLN</i>	↑	2,6	0,033		-1,0	0,498	x	
<i>RRM2</i>	↑	3,5	0,042		1,0	1,000	x	
<i>DAP3</i>	↑	3,5	0,043		-1,7	0,310	x	
<i>Gstt3</i>	↑	5,0	0,044		1,0	1,000	x	
<i>CDC37</i>	↑	100,0	0,011		1,0	1,000	x	
<i>THRAP3</i>	↑	100,0	0,011		1,0	1,000	x	
<i>CDCA8</i>	↑	100,0	0,011		1,0	1,000	x	
<i>FXR1</i>	↑	2,7	0,010		1,5	0,185		
<i>U2SURP</i>	↑	1,5	0,050	↓	-1,6	0,035		
<i>ISY1</i>	↑	2,9	0,036		1,0	0,497		
<i>Acan</i>	↑	2,1	0,020		1,0	0,492		
<i>MRTO4</i>	↑	2,5	0,014		1,0	0,493		
<i>QKI</i>	↑	100,0	0,002		-1,3	0,247		
<i>SLC16A3</i>	↑	2,4	0,040		1,2	0,375		
<i>MRPL24</i>		1,0	1,000	↓	-6,1	0,005		
<i>CA2</i>	↑	1,7	0,046		1,2	0,304		
<i>MYO1E</i>		-1,0	0,498	↑	9,4	0,000		
<i>FAM129B</i>	↑	6,0	0,027		-1,0	0,499		
<i>C6orf130</i>	↓	-1,9	0,035		1,1	0,431		
<i>FAM76B</i>		1,3	0,230	↓	-1,7	0,050		
<i>MELK</i>		-1,4	0,343	↓	-1,8	0,021		
<i>VAPB</i>		3,0	0,151	↓	-6,0	0,026		
<i>MRE11A</i>	↑	100,0	0,011		-1,7	0,308		
<i>VAPA</i>	↑	1,9	0,033		-1,3	0,171		
<i>ACACA</i>		1,5	0,212	↓	-2,7	0,034		
<i>ARFIP1</i>	↑	100,0	0,006		-2,0	0,160		
<i>ACTBL2</i>		1,1	0,237	↑	2,4	0,020		
<i>EIF2B4</i>	↓	-100,0	0,012		3,0	0,151		
<i>PNO1</i>	↓	-5,0	0,044		1,0	0,499		
<i>ECM1</i>		-1,3	0,264	↓	-2,4	0,011		
<i>ITIH1</i>	↓	-1,7	0,013		1,1	0,289		
<i>UBA6</i>		2,8	0,056	↓	-2,1	0,036		
<i>ACBD3</i>	↓	-2,9	0,044		7,0	0,060		

^a Fold change and one-sided p-value calculated between protein levels in control and treated tumors.

^b Top proteins with on average 8 spectral counts difference between treated tumors.

^c Proteins with significant (P > 0.05, two sided) difference between treated tumors.

n/a = not applicable

FASN knock-down sensitizes resistant cells for cisplatin treatment

In a proof-of-concept experiment, we determined whether inhibition of the fatty acid metabolism sensitizes *Cdh1^{-/-};p53^{-/-}* tumor cells to cisplatin. For this purpose, we transduced KEP11 cells with two *Fasn*-targeting shRNA constructs. These resulted in target inhibition of about 60 % for mRNA and protein expression levels (Figure 6A and B). There was no alteration of cell proliferation for the transduced cells (Figure 6C). When we tested the cells expressing these hairpins for cisplatin sensitivity, we found that cells with a lower *Fasn* gene expression were more sensitive to cisplatin (Figure 6D). We obtained the same result when we transduced another *Cdh1^{-/-};p53^{-/-}* cell line (called KEP23) with the indicated control or sh*Fasn* constructs (data not shown). These data suggest that targeting fatty acid metabolism may be a useful therapeutic strategy to sensitize the cisplatin-resistant tumors and further emphasizes the validity of our approach for finding candidate biomarkers that are predictive of cisplatin treatment.

DISCUSSION

In this study, we generated proteome signatures after a short pulse of cisplatin treatment using two mouse models for specific breast cancer subtypes that display a marked difference in drug response. We report a comprehensive data set of about 3400 proteins with 167 and 98 proteins differentially expressed in the sensitive and resistant model, respectively. To our knowledge, this study provides the first and largest proteomic screen to date to identify cisplatin-responsive candidate markers shortly after treatment. Most notably, we identified highly discriminatory protein subsets of 56, 30 and 12 proteins that showed diverging patterns in the two models and could separate all four conditions using hierarchical clustering (see flowchart in Figure 3 for selection of different discriminatory subsets).

To predict chemotherapy response, the additional use of tumor samples taken shortly after the first treatment may be advantageous over the common practice to find predictive markers only by using unchallenged tumors. This approach is encouraged by the recent finding that low scores of RAD51 foci, assessed 24h after the first chemotherapy cycle, help to find patients with breast cancers that are defective in DNA repair by HR²⁶. Future clinical trials will show whether the predictive value of RAD51 scores is sufficient to identify patients who may benefit from DNA repair-targeting therapy, such as PARP inhibition.

In our study we used cisplatin, because platinum drugs are frequently applied in the clinic to treat cancer patients. In particular, platinum drugs may be helpful to treat breast cancer patients with HR-defective tumors^{4,5}. This is consistent with our previous finding that mammary tumors generated in our mouse model for BRCA1-deficient tumors are highly sensitive to cisplatin³. In these tumors, we found that up-regulated proteins after cisplatin treatment were mostly involved in DNA repair, DNA metabolism and chromosome segregation.

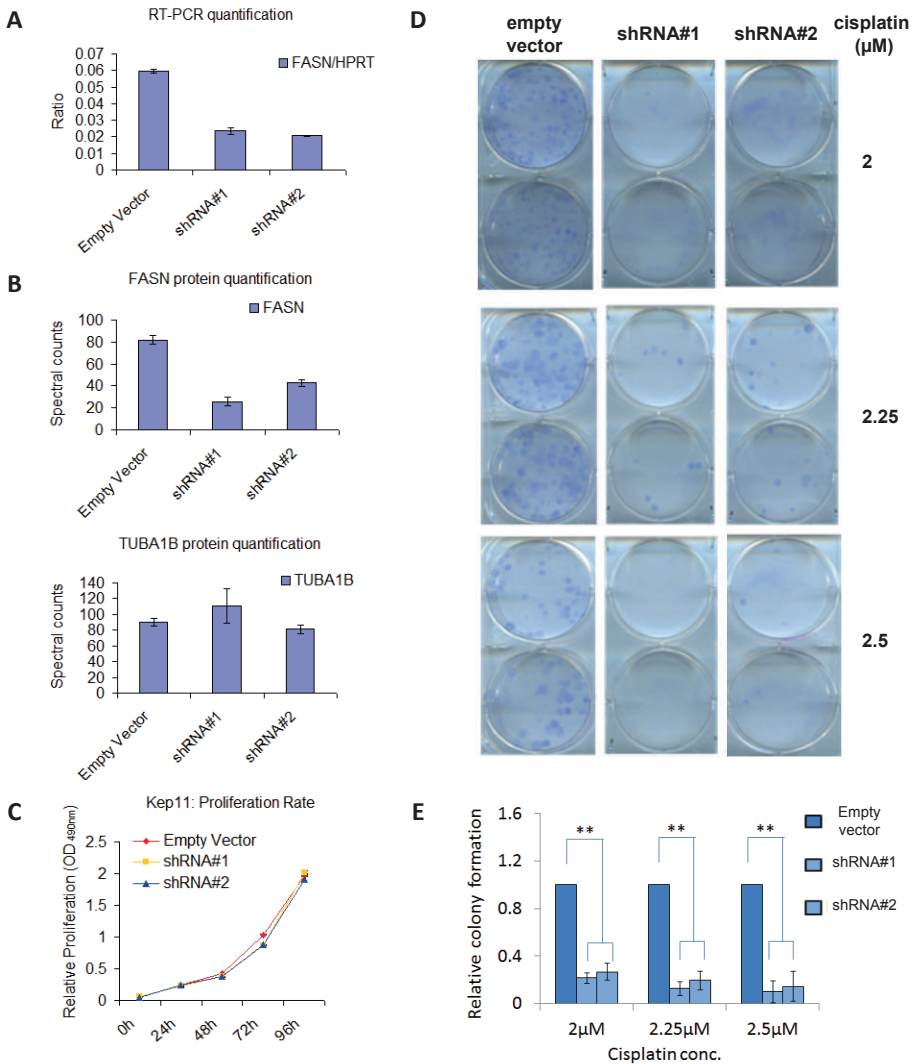


Figure 6. *Fasn* knock-down and clonogenic survival after cisplatin treatment in *Cdh1*^{-/-};*p53*^{-/-} (KEP11) cells. **A**, Knock-down efficacy of two shRNA hairpins targeting *Fasn* and an empty vector as determined by quantitative RT-PCR. *Hprt* gene expression was used as reference. All experiments were performed in triplicate, and the error bars indicate the standard deviation (also for B and C). **B**, Knock-down efficacy of the same two shRNA hairpins targeting and empty vector at the protein level as determined by mass spectrometry. TUBA1B expression is shown as a reference. **C**, Proliferation rate of the cell lines transduced with the two *Fasn*-targeting shRNAs and empty vector. **D**, Clonogenic survival of the cell lines transduced with the two *Fasn*-targeting shRNAs and empty vector after cisplatin treatment. Six, eight or nine days after treatment with 2, 2.25 or 2.5 μM cisplatin, respectively, the surviving colonies were stained. This experiment was carried out in triplicate and a representative result is shown. **E**, Quantification of (D) Average colony numbers of cells with the *Fasn*-targeting shRNAs are presented relative to the number of colonies of the control cells. The error bars indicate the standard deviation, and ** indicates a $p < 0.001$ (Student's *t* test).

Of these, only three (TOP2A, KIF11, and KNTC1) were also significantly up-regulated in the cisplatin-resistant tumors. Previously, we already showed major up-regulation of DNA repair proteins in drug-naive BRCA1-deficient mouse tumors¹². Consistent with the important role that BRCA1 plays in the DNA damage response²⁷, we illustrate that DNA damage repair is further challenged in response to treatment with the DNA damaging agent cisplatin. In the absence of a proper homology-directed DNA repair, more pressure appears to be put on other DNA repair mechanisms. This is indicated by the increased levels of enzymes involved in single-strand DNA break repair such as PARP1, FEN1, and LIG1. Moreover, up-regulated MRE11A suggests that more error-prone non-homologous end joining may occur to repair double-strand DNA breaks.

One of the down-regulated proteins in the BRCA1 model that is part of the top 12 proteins, GSTM1, is involved in glutathione metabolism and acts as detoxification protein. GSTM1 and other glutathione-S-transferases have been linked with differences in cisplatin response²⁸.

In the cisplatin-resistant model, a remarkable finding was that fatty acid metabolism proteins were the most significant up-regulated cluster. Some of these proteins (FABP4, CA3, and PC) were also significantly down-regulated in the sensitive (BRCA1-deficient) model. This indicates a good resolving power to distinguish the two models in a short-term treatment setting and suggests the potential usefulness of such markers for cisplatin resistance.

Among the top 56 discriminatory proteins, FASN and ACACA are two core proteins involved in *de novo* fatty acids synthesis, of which FASN showed the largest quantitative difference between the two models after cisplatin treatment. Proliferating cancer cells have a highly up-regulated *de novo* fatty acid synthesis to provide sufficient lipids for membrane components, β -oxidation and lipid modification of proteins. In human breast cancer cell lines, vector-induced FASN overexpression has been shown to increase resistance to cisplatin as well as inducing overexpression of ERBB2, a receptor tyrosine kinase that induces cell proliferation²⁹. In CDH1-deficient cells derived from our mouse model we do not find a change in proliferation after FASN inhibition. FASN inhibition has also been described as a sensitizer for cisplatin treatment in mice xenografted with human ovarian cancer cells³⁰. In fact, FASN is highly expressed across a wide range of (human) tumor types where its inhibition either induces apoptosis and/or synergizes with cytotoxic agents³¹⁻³⁸. Consistent with these data, we show that inhibition of FASN with short hairpin RNAs also sensitized our CDH1-deficient cells to cisplatin treatment. In contrast to previous FASN inhibitors that displayed off-target effects and induced weight loss, novel FASN inhibitors are currently being developed that specifically target only FASN and have shown encouraging *in vitro* and *in vivo* anti-cancer activity in human breast cancer³⁹⁻⁴¹.

Another, more complex functional link between fatty acids and cisplatin resistance has recently been described in xenotransplantation models. Specific unsaturated platinum-

induced fatty acids (PIFAs) secreted from circulating mesenchymal stem cells cause cisplatin resistance⁴². The precise mechanism by which these PIFAs induce resistance still remains to be elucidated, and we are currently investigating whether there is an effect of PIFAs on our BRCA1-defective tumors.

In this study, we did not only identify proteins involved in *de novo* fatty acid synthesis (e.g. FASN and ACACA), but also in fatty acid signaling, transport and storage. Two of our top discriminatory proteins, FABP4 and γ -synuclein, have lipid binding potential, while PLIN is involved in lipid droplet storage. Lipid droplet accumulation has been correlated with malignancy and chemotherapy treatment. FABP4 is thought to bind primarily palmitic acid, although the majority of FAPB-family, including FABP4, have a more broader binding affinity for different fatty acid structures⁴³. FABP4 can activate the PPAR γ signaling when translocated to the nucleus. PPAR γ regulates fatty acid storage and glucose metabolism. FABP4 has also been described as a PTEN interactor, whose loss has been described as an activator of cancer-specific metabolic activity. Also, PTEN loss has been shown to increase FABP4 expression. Recently FABP4 was implicated as an important mediator for metastasis to fat-rich tissues⁴⁴, whereby FABP4 was used to transport fatty acids from fat cell to cancer cells. Furthermore, activated AMP kinase, a known inhibitor of FASN and ACACA, two of our top discriminatory proteins, has been shown to inhibit PPAR γ . AMP kinase, a major metabolic sensor, is frequently inactivated in a wide range of cancers. Recently, CA3, also a major discriminatory enzyme, has been described to be functionally involved with PPAR γ in adipose tissue⁴⁵. Moreover, proteins with established roles in double-strand DNA repair (e.g. BRCA1 and DNA-PK) have been implemented as regulators of fatty acid metabolism^{46,47}. Combined, our data points towards an intricate cooperation between metabolic and DNA repair proteins when tumors with differential BRCA1 status are treated with cisplatin.

In summary, we showed the feasibility of proteomic profiling in mouse tumor models to assess treatment outcome for cisplatin treatment. Early treatment profiling to predict therapy outcome might also be useful for less toxic treatments such as PARP inhibitors, which specifically target HR-deficient tumors. Our proteomic screen identified proteins involved in DNA repair and cancer (fatty acid) metabolism as the major discriminators between sensitive and resistant tumors shortly after cisplatin treatment. These proteins may contribute to functionally test whether tumors respond to anti-cancer therapy. Because finding markers that distinguish drug-resistant from drug-sensitive tumors before treatment starts, has proven to be difficult, the analysis of protein changes shortly after initial treatment may facilitate clinical decision making and help to optimize personalized treatments.

METHODS

Materials

All chemicals, unless otherwise specified, were obtained from Sigma-Aldrich. HPLC solvents, LC-MS grade water, acetonitrile, and formic acid, were obtained from Biosolve (Biosolve B.V., Valkenswaard, The Netherlands). Porcine sequence-grade modified trypsin was obtained from Promega (Promega Benelux B.V., Leiden, The Netherlands).

Mouse tumors

The generation of *Cdh1*^{-/-};*p53*^{-/-}(WEP) or *Brca1*^{-/-};*p53*^{-/-}(KB1P) mammary tumors has been described previously^{2,6,11}. Orthotopic transplantation of tumors into syngeneic mice and treatment with cisplatin were performed as reported previously³. Tumor samples for the proteomic analysis were snap-frozen and stored at -80 °C until use. All animal experiments were approved by The Netherlands Cancer Institute ethical review committee.

Cell culture and RNA interference

The *Cdh1*^{-/-};*p53*^{-/-} cell line (KEP11) was derived from a primary tumor that arose in a *K14cre*;*Cdh1*^{F/F};*Trp53*^{F/F} mouse, and the cells were cultured as described¹¹. KEP11 cells were transduced with pLKO-puro short hairpin RNA (shRNA) lentiviruses obtained from Mission library clones (Sigma-Aldrich). To target *Fasn*, we used TRCN0000075704 (shRNA#1) and TRCN0000075707 (shRNA#2). After selection with 3µg/ml puromycin, 8000 cells per well were seeded in 6-well plates and assayed for clonal growth in the presence of cisplatin. One day after seeding, cells were incubated for 24 h with 2, 2.25, or 2.5 µM cisplatin. Surviving colonies were visualized using Leishman stain 6, 8, or 9 days after treatment start.

The efficacy of *Fasn* inhibition was determined by quantitative RT-PCR using the LightCycler® 480 SYBR Green I Master reagents according to the manufacturer's protocol (Roche Applied Science, catalogue number 4707516001). To amplify mouse hypoxanthine guanine phosphoribosyl transferase *Hprt* or *Fasn* cDNA the following primers were used (5'-3'): *Hprt_for* (CTGGTGAAAAGGACCTCTCG) and *Hprt_rev* (TGAAGTACTCATTATAGTCAAGGGCA); *Fasn_for* (ATTGTCGCTCTGAGGCTGTTG) and *Fasn_rev* (TTGTCCTTGCTGCCATCTG). To measure cell proliferation, 2000 KEP11-derived cells were seeded into 96-well plates. At the indicated time points, each well was refreshed by 150 µl fresh medium containing MTT (0.5 mg/ml, Sigma-Aldrich) and incubated for another 4 h at 37 °C. Then the medium was removed and 150 µl of DMSO was added into each well to dissolve the resultant formazan crystals. Cell growth was determined by the absorbance detected at 490 nm using a microplate reader (Tecan, Infinite M200PRO).

Tissue homogenization and fractionation using gel electrophoresis

For homogenization, we cut a piece of approximately 20 mg of tumor tissue in a bath of liquid nitrogen in smaller parts. The proteins in the breast tumor tissue samples were solubilized in 800 μ L 1x reducing Sodium Dodecyl Sulfate (SDS) sample buffer (containing 62.5 mM Tris-HCl, 2 % w/v SDS, 10 % v/v glycerol, and 0.0025 % bromophenol blue, 100 mM DDT, pH 6.8) using a Pellet Pestles micro-grinder system (Kontes glassware, Vineland, NJ). Subsequently, the proteins were denatured by heating at 100 °C for 10 min. Any insoluble debris was removed by centrifugation for 15 min at maximum speed (16.1 rcf) in a benchtop centrifuge.

Proteins were fractionated using one-dimensional SDS-PAGE. 25 μ L of each homogenized sample (containing about 50 μ g of protein) was loaded in a well of a pre-cast 4–12 % NuPAGE w/v Bis-Tris 1.5-mm minigel (Invitrogen). The stacking gel contained 4 % w/v acrylamide/Bis-Tris. Electrophoresis was carried out at 200 V in NuPAGE MES SDS running buffer (50 mM Tris base, 50 mM MES, 0.1 % w/v SDS, 1 mM EDTA, pH 7.3) until the dye front reached the end of the gel. Following electrophoresis, gels were fixed with a solution of 50 % ethanol and 3 % phosphoric acid. Staining was carried out in a solution of 34 % methanol, 3 % phosphoric acid, 15 % ammonium sulfate, and 0.1 % Coomassie Blue G-250 (Bio-Rad, Hercules, CA) with subsequent destaining in MilliQ water.

In-gel digestion and nano-Liquid chromatography-Fourier transformation-Mass spectrometry (nanoLC-FT-MS)

In-gel digestion and nanoLC-FT-MS for the 12 tumors from the discovery experiment were performed as described previously¹². In short, processed gel lanes were cut in 10 equal bands, after which they were in-gel digested with trypsin. Extracted peptides from each band were separated on a C18 column for subsequent MS/MS analysis.

In-gel digestion and nano-Liquid chromatography-Q Exactive-Mass spectrometry

Cell lysates from the FASN knock-down and control experiments were applied to a one-dimensional SDS-polyacrylamide gel. Proteins were allowed to enter the stacking gel and the voltage was switched-off when the proteins were just in the running gel. The samples on gel were processed as a single gel-band and were in-gel digested with trypsin. After vacuum centrifugation, the peptide extract was filtered through a 0.45- μ m low protein-binding PVDF membrane (Millipore) to remove particles. Extracted peptides were separated on a 75- μ m x 20-cm custom-packed Reprosil C18 aqua column (1.9 μ m, 120 Å) in a 150-min gradient (5–32 % Acetonitrile + 0.5 % Acetic acid at 300 nl/min) using a U3000 RSLC high pressure nanoLC (Dionex). Eluting peptides were measured on line by a Q Exactive mass spectrometer (ThermoFisher Scientific) operating in data-dependent acquisition mode. Peptides were ionized using a stainless steel emitter at a potential of +2 kV (ThermoScientific). Intact peptide ions were detected at a resolution of 35000 and fragment ions at a resolution of 17500; the MS mass range was 350–1500 Da. AGC Target settings for MS were 3E6 charges and for MS/MS 2E5 charges. Peptides were selected for higher-energy C-trap dissociation fragmentation at an underfill ratio of 1 % and a

quadrupole isolation window of 1.5 Da, peptides were fragmented at a normalized collision energy (NCE) of 30. QE raw files were searched against the International Protein Index mouse 3.68 database (56729 entries, released December 18, 2009) using MaxQuant 1.2.2.5 (ref. ¹³). Data was filtered at 1 % FDR at both the peptide and protein level.

Data analysis

Protein identification – MS/MS spectra were searched against the mouse International Protein Index database 3.31 (56555 entries, released August 17, 2007) using Sequest (version 27, revision 12), which is part of the BioWorks 3.3 data analysis package (Thermo Fisher, San Jose, CA). MS/MS spectra were searched with a maximum allowed deviation of 10 ppm for the precursor mass and 1 atomic mass unit for fragment masses. Methionine oxidation and cysteine carboxamidomethylation were allowed modifications, two missed cleavages were allowed and the minimum number of tryptic termini was one. After database searching the DTA and OUT files were imported into Scaffold version 1.07 (Proteome software, Portland, OR). Scaffold was used to organize the gel band data and to validate peptide identifications using the Peptide Prophet algorithm^{14,15}. Only identifications with a probability >95 % were retained. Subsequently, the Protein Prophet algorithm was applied and protein identifications with a probability of >99 % with two peptides or more were retained. The false discovery rate for the detected proteins using this workflow is on average around 0.5 %, and was not calculated again¹⁶. For each protein identified, the total number of MS/MS spectra detected for each protein identified (spectral counts) was exported to Excel 2003 (Microsoft, Redmond, WA).

Spectral count normalization and statistics – Normalization was performed as described previously^{12,17}. A one-sided paired β -binomial test¹⁸ was applied to find proteins that showed statistically significant differences in spectral count numbers between the untreated control tumors and the cisplatin-treated tumors, and it was applied both to the BRCA1-deficient and -proficient model. Statistical testing between the two different treated tumor models was performed using an unpaired two-sided β -binomial test¹⁷. Proteins with a p value of less than 0.05 were designated as being significant. Hierarchical clustering was carried out using R statistical software. For protein clustering, the abundances were normalized to zero mean and unit variance for each individual protein. Subsequently, the Euclidean distance measure was used. For sample clustering, a divergence measure between two Poisson distributions was used, preventing highly abundant proteins from dominating others in contribution to the total sample difference, as described by Albrethsen *et al.*¹⁶. The Ward linkage was used. For analysis of reproducibility, we calculated the average coefficient of variation of the spectral counts from overlapping proteins of each set of three biological replicates.

Data mining for functional analyses – For STRING (Search Tool for the Retrieval of Interacting Genes/Proteins) pathway analysis (version 9.0)¹⁹, International Protein Index identifiers were mapped to human gene symbols, after which networks were generated and downloaded. Graphic-rich networks with color intensities indicating protein fold changes were made using the Cytoscape software²⁰ after which groups of well connected proteins were identified²¹. Gene ontology analysis was performed

using the BiNGO (Biological Networks Gene Ontology, Gent, Belgium) software²² on the top three most significant groups of well connected proteins identified by Cluster ONE (Cluster with Overlapping Neighborhood Expansion, Egham, UK).

ACKNOWLEDGMENTS

We thank Piet Borst for critical reading of the manuscript. This research was supported by the CenE/Van Lanschot (MW) and the VUmc-Cancer Center Amsterdam (CRJ, TVP and proteomics infrastructure), CTMM BreastCare (SR and JJ), the Dutch Cancer Society (project grants to SR and JJ) and the Netherlands Organization for Scientific Research (NWO-Vidi grant to SR and WO Cancer Systems Biology Center (CSBC) grant to JJ). JEJ was supported by a Toptalent fellowship from the Netherlands Organization for Scientific Research (NWO).

REFERENCES

1. Borst, P., and Wessels, L. (2010) Do predictive signatures really predict response to cancer chemotherapy? *Cell Cycle* 9, 4836-4840
2. Liu, X., Holstege, H., van der, G. H., Treur-Mulder, M., Zevenhoven, J., Velds, A., Kerkhoven, R. M., van Vliet, M. H., Wessels, L. F., Peterse, J. L., Berns, A., and Jonkers, J. (2007) Somatic loss of BRCA1 and p53 in mice induces mammary tumors with features of human BRCA1-mutated basal-like breast cancer. *Proc. Natl. Acad. Sci. USA* 104, 12111-12116
3. Rottenberg, S., Nygren, A. O., Pajic, M., van Leeuwen, F. W., van, d. H., I, van de, W. K., Liu, X., de Visser, K. E., Gilhuijs, K. G., van, T. O., Schouten, J. P., Jonkers, J., and Borst, P. (2007) Selective induction of chemotherapy resistance of mammary tumors in a conditional mouse model for hereditary breast cancer. *Proc. Natl. Acad. Sci. USA* 104, 12117-12122
4. Vollebergh, M. A., Lips, E. H., Nederlof, P. M., Wessels, L. F., Schmidt, M. K., van Beers, E. H., Cornelissen, S., Holtkamp, M., Froklage, F. E., de Vries, E. G., Schrama, J. G., Wesseling, J., van, d., V, van, T. H., de, B. M., Hauptmann, M., Rodenhuis, S., and Linn, S. C. (2010) An aCGH classifier derived from BRCA1-mutated breast cancer and benefit of high-dose platinum-based chemotherapy in HER2-negative breast cancer patients. *Ann. Oncol.*, Advance Access
5. Silver, D. P., Richardson, A. L., Eklund, A. C., Wang, Z. C., Szallasi, Z., Li, Q., Juul, N., Leong, C. O., Calogrias, D., Buraimoh, A., Fatima, A., Gelman, R. S., Ryan, P. D., Tung, N. M., De, N. A., Ganesan, S., Miron, A., Colin, C., Sgroi, D. C., Ellisen, L. W., Winer, E. P., and Garber, J. E. (2010) Efficacy of neoadjuvant Cisplatin in triple-negative breast cancer. *J. Clin. Oncol.* 28, 1145-1153
6. Derksen, P. W., Braumuller, T. M., van der, B. E., Hornsveld, M., Mesman, E., Wesseling, J., Krimpenfort, P., and Jonkers, J. (2011) Mammary-specific inactivation of E-cadherin and p53 impairs functional gland development and leads to pleomorphic invasive lobular carcinoma in mice. *Dis. Model. Mech.* 4, 347-358
7. Cristofanilli, M., Gonzalez-Angulo, A., Sneige, N., Kau, S. W., Broglio, K., Theriault, R. L., Valero, V., Buzdar, A. U., Kuerer, H., Buccholz, T. A., and Hortobagyi, G. N. (2005) Invasive lobular carcinoma classic type: response to primary chemotherapy and survival outcomes. *J. Clin. Oncol.* 23, 41-48
8. Deans, A. J., and West, S. C. (2011) DNA interstrand crosslink repair and cancer. *Nat. Rev. Cancer* 11, 467-480
9. Galluzzi, L., Senovilla, L., Vitale, I., Michels, J., Martins, I., Kepp, O., Castedo, M., and Kroemer, G. (2012) Molecular mechanisms of cisplatin resistance. *Oncogene* 31, 1869-1883
10. Borst, P., Rottenberg, S., and Jonkers, J. (2008) How do real tumors become resistant to cisplatin? *Cell Cycle* 7, 1353-1359

11. Derksen, P. W., Liu, X., Saridin, F., van der, G. H., Zevenhoven, J., Evers, B., van, B., Jr., Griffioen, A. W., Vink, J., Krimpenfort, P., Peterse, J. L., Cardiff, R. D., Berns, A., and Jonkers, J. (2006) Somatic inactivation of E-cadherin and p53 in mice leads to metastatic lobular mammary carcinoma through induction of anoikis resistance and angiogenesis. *Cancer Cell* 10, 437-449
12. Warmoes, M., Jaspers, J. E., Pham, T. V., Piersma, S. R., Oudgenoeg, G., Massink, M. P., Waisfisz, Q., Rottenberg, S., Boven, E., Jonkers, J., and Jimenez, C. R. (2012) Proteomics of mouse BRCA1-deficient mammary tumors identifies DNA repair proteins with diagnostic and prognostic value in human breast cancer. *Mol. Cell Proteomics*
13. Cox, J., and Mann, M. (2008) MaxQuant enables high peptide identification rates, individualized p.p.b.-range mass accuracies and proteome-wide protein quantification. *Nat. Biotechnol.* 26, 1367-1372
14. Nesvizhskii, A. I., Keller, A., Kolker, E., and Aebersold, R. (2003) A statistical model for identifying proteins by tandem mass spectrometry. *Anal. Chem.* 75, 4646-4658
15. Keller, A., Nesvizhskii, A. I., Kolker, E., and Aebersold, R. (2002) Empirical statistical model to estimate the accuracy of peptide identifications made by MS/MS and database search. *Anal. Chem.* 74, 5383-5392
16. Albrethsen, J., Knol, J. C., Piersma, S. R., Pham, T. V., de, W. M., Mongera, S., Carvalho, B., Verheul, H. M., Fijneman, R. J., Meijer, G. A., and Jimenez, C. R. (2010) Subnuclear proteomics in colorectal cancer: identification of proteins enriched in the nuclear matrix fraction and regulation in adenoma to carcinoma progression. *Mol. Cell Proteomics.* 9, 988-1005
17. Pham, T. V., Piersma, S. R., Warmoes, M., and Jimenez, C. R. (2010) On the beta-binomial model for analysis of spectral count data in label-free tandem mass spectrometry-based proteomics. *Bioinformatics* 26, 363-369
18. Pham, T. V., and Jimenez, C. R. (2012) An accurate paired sample test for count data. *Bioinformatics.* 28, i596-i602
19. Szklarczyk, D., Franceschini, A., Kuhn, M., Simonovic, M., Roth, A., Minguéz, P., Doerks, T., Stark, M., Muller, J., Bork, P., Jensen, L. J., and von, M. C. (2011) The STRING database in 2011: functional interaction networks of proteins, globally integrated and scored. *Nucleic Acids Res.* 39, D561-D568
20. Shannon, P., Markiel, A., Ozier, O., Baliga, N. S., Wang, J. T., Ramage, D., Amin, N., Schwikowski, B., and Ideker, T. (2003) Cytoscape: a software environment for integrated models of biomolecular interaction networks. *Genome Res.* 13, 2498-2504
21. Nepusz, T., Yu, H., and Paccanaro, A. (2012) Detecting overlapping protein complexes in protein-protein interaction networks. *Nat. Methods* 9, 471-472
22. Maere, S., Heymans, K., and Kuiper, M. (2005) BiNGO: a Cytoscape plugin to assess overrepresentation of gene ontology categories in biological networks. *Bioinformatics* 21, 3448-3449
23. Rottenberg, S., Jaspers, J. E., Kersbergen, A., van der, B. E., Nygren, A. O., Zander, S. A., Derksen, P. W., de, B. M., Zevenhoven, J., Lau, A., Boulter, R., Cranston, A., O'Connor, M. J., Martin, N. M., Borst, P., and Jonkers, J. (2008) High sensitivity of BRCA1-deficient mammary tumors to the PARP inhibitor AZD2281 alone and in combination with platinum drugs. *Proc. Natl. Acad. Sci. USA* 105, 17079-17084
24. Pan, M. R., Hsieh, H. J., Dai, H., Hung, W. C., Li, K., Peng, G., and Lin, S. Y. (2012) Chromodomain helicase DNA-binding protein 4 (CHD4) regulates homologous recombination DNA repair and its deficiency sensitizes cells to poly (ADP-ribose) polymerase (PARP) inhibitor treatment. *J. Biol. Chem.*
25. Ewing, R. M., Chu, P., Elisma, F., Li, H., Taylor, P., Climie, S., Broom-Cerajewski, L., Robinson, M. D., O'Connor, L., Li, M., Taylor, R., Dharsee, M., Ho, Y., Heilbut, A., Moore, L., Zhang, S., Ornatsky, O., Bukhman, Y. V., Ethier, M., Sheng, Y., Vasilescu, J., bu-Farha, M., Lambert, J. P., Duewel, H. S., Stewart, I. I., Kuehl, B., Hogue, K., Colwill, K., Gladwish, K., Muskat, B., Kinach, R., Adams, S. L., Moran, M. F., Morin, G. B., Topaloglou, T., and Figey, D. (2007) Large-scale mapping of human protein-protein interactions by mass spectrometry. *Mol. Syst. Biol.* 3, 89
26. Graeser, M., McCarthy, A., Lord, C. J., Savage, K., Hills, M., Salter, J., Orr, N., Parton, M., Smith, I. E., Reis-Filho, J. S., Dowsett, M., Ashworth, A., and Turner, N. C. (2010) A marker of homologous

- recombination predicts pathologic complete response to neoadjuvant chemotherapy in primary breast cancer. *Clin. Cancer Res.* 16, 6159-6168
27. Roy, R., Chun, J., and Powell, S. N. (2012) BRCA1 and BRCA2: different roles in a common pathway of genome protection. *Nat. Rev. Cancer* 12, 68-78
 28. Wang, C. H., Wu, H. T., Cheng, H. M., Yen, T. J., Lu, I. H., Chang, H. C., Jao, S. C., Shing, T. K., and Li, W. S. (2011) Inhibition of glutathione S-transferase M1 by new gabosine analogues is essential for overcoming cisplatin resistance in lung cancer cells. *J. Med. Chem.* 54, 8574-8581
 29. Vazquez-Martin, A., Colomer, R., Brunet, J., Lupu, R., and Menendez, J. A. (2008) Overexpression of fatty acid synthase gene activates HER1/HER2 tyrosine kinase receptors in human breast epithelial cells. *Cell Prolif.* 41, 59-85
 30. Uddin, S., Jehan, Z., Ahmed, M., Alyan, A., Al-Dayel, F., Hussain, A., Bavi, P., and Al-Kuraya, K. S. (2011) Over Expression of Fatty Acid Synthase in Middle Eastern Epithelial Ovarian Carcinoma Activates AKT and its Inhibition Potentiates Cisplatin Induced Apoptosis. *Mol. Med.*
 31. Carvalho, M. A., Zecchin, K. G., Seguin, F., Bastos, D. C., Agostini, M., Rangel, A. L., Veiga, S. S., Raposo, H. F., Oliveira, H. C., Loda, M., Coletta, R. D., and Graner, E. (2008) Fatty acid synthase inhibition with Orlistat promotes apoptosis and reduces cell growth and lymph node metastasis in a mouse melanoma model. *Int. J. Cancer* 123, 2557-2565
 32. Flavin, R., Peluso, S., Nguyen, P. L., and Loda, M. (2010) Fatty acid synthase as a potential therapeutic target in cancer. *Future. Oncol.* 6, 551-562
 33. Mansour, M., Schwartz, D., Judd, R., Akingbemi, B., Braden, T., Morrison, E., Dennis, J., Bartol, F., Hazi, A., Napier, I., and bdel-Mageed, A. B. (2011) Thiazolidinediones/PPARGgamma agonists and fatty acid synthase inhibitors as an experimental combination therapy for prostate cancer. *Int. J. Oncol.* 38, 537-546
 34. Olsen, A. M., Eisenberg, B. L., Kuemmerle, N. B., Flanagan, A. J., Morganelli, P. M., Lombardo, P. S., Swinnen, J. V., and Kinlaw, W. B. (2010) Fatty acid synthesis is a therapeutic target in human liposarcoma. *Int. J. Oncol.* 36, 1309-1314
 35. Uddin, S., Siraj, A. K., Al-Rasheed, M., Ahmed, M., Bu, R., Myers, J. N., Al-Nuaim, A., Al-Sobhi, S., Al-Dayel, F., Bavi, P., Hussain, A. R., and Al-Kuraya, K. S. (2008) Fatty acid synthase and AKT pathway signaling in a subset of papillary thyroid cancers. *J. Clin. Endocrinol. Metab* 93, 4088-4097
 36. Uddin, S., Hussain, A. R., Ahmed, M., Bu, R., Ahmed, S. O., Ajarim, D., Al-Dayel, F., Bavi, P., and Al-Kuraya, K. S. (2010) Inhibition of fatty acid synthase suppresses c-Met receptor kinase and induces apoptosis in diffuse large B-cell lymphoma. *Mol. Cancer Ther.* 9, 1244-1255
 37. Vazquez-Martin, A., Ropero, S., Brunet, J., Colomer, R., and Menendez, J. A. (2007) Inhibition of Fatty Acid Synthase (FASN) synergistically enhances the efficacy of 5-fluorouracil in breast carcinoma cells. *Oncol. Rep.* 18, 973-980
 38. Zecchin, K. G., Rossato, F. A., Raposo, H. F., Melo, D. R., Alberici, L. C., Oliveira, H. C., Castilho, R. F., Coletta, R. D., Vercesi, A. E., and Graner, E. (2011) Inhibition of fatty acid synthase in melanoma cells activates the intrinsic pathway of apoptosis. *Lab Invest* 91, 232-240
 39. Turrado, C., Puig, T., Garcia-Carceles, J., Artola, M., Benhamu, B., Ortega-Gutierrez, S., Relat, J., Oliveras, G., Blancafort, A., Haro, D., Marrero, P. F., Colomer, R., and Lopez-Rodriguez, M. L. (2012) New synthetic inhibitors of fatty acid synthase with anticancer activity. *J. Med. Chem.* 55, 5013-5023
 40. Puig, T., Aguilar, H., Cufi, S., Oliveras, G., Turrado, C., Ortega-Gutierrez, S., Benhamu, B., Lopez-Rodriguez, M. L., Urruticochea, A., and Colomer, R. (2011) A novel inhibitor of fatty acid synthase shows activity against HER2+ breast cancer xenografts and is active in anti-HER2 drug-resistant cell lines. *Breast Cancer Res.* 13, R131
 41. Puig, T., Turrado, C., Benhamu, B., Aguilar, H., Relat, J., Ortega-Gutierrez, S., Casals, G., Marrero, P. F., Urruticochea, A., Haro, D., Lopez-Rodriguez, M. L., and Colomer, R. (2009) Novel Inhibitors of Fatty Acid Synthase with Anticancer Activity. *Clin. Cancer Res.* 15, 7608-7615
 42. Roodhart, J. M., Daenen, L. G., Stigter, E. C., Prins, H. J., Gerrits, J., Houthuijzen, J. M., Gerritsen, M. G., Schipper, H. S., Backer, M. J., van, A. M., Vermaat, J. S., Moerer, P., Ishihara, K., Kalkhoven, E., Beijnen, J. H., Derksen, P. W., Medema, R. H., Martens, A. C., Brenkman, A. B., and Voest, E. E. (2011) Mesenchymal stem cells induce resistance to chemotherapy through the release of platinum-induced fatty acids. *Cancer Cell* 20, 370-383

43. Furuhashi, M., and Hotamisligil, G. S. (2008) Fatty acid-binding proteins: role in metabolic diseases and potential as drug targets. *Nat. Rev. Drug Discov.* 7, 489-503
44. Nieman, K. M., Kenny, H. A., Penicka, C. V., Ladanyi, A., Buell-Gutbrod, R., Zillhardt, M. R., Romero, I. L., Carey, M. S., Mills, G. B., Hotamisligil, G. S., Yamada, S. D., Peter, M. E., Gwin, K., and Lengyel, E. (2011) Adipocytes promote ovarian cancer metastasis and provide energy for rapid tumor growth. *Nat. Med.* 17, 1498-1503
45. Mitterberger, M. C., Kim, G., Rostek, U., Levine, R. L., and Zwerschke, W. (2012) Carbonic anhydrase III regulates peroxisome proliferator-activated receptor-gamma2. *Exp. Cell Res.* 318, 877-886
46. Brunet, J., Vazquez-Martin, A., Colomer, R., Grana-Suarez, B., Martin-Castillo, B., and Menendez, J. A. (2008) BRCA1 and acetyl-CoA carboxylase: the metabolic syndrome of breast cancer. *Mol. Carcinog.* 47, 157-163
47. Wong, R. H., Chang, I., Hudak, C. S., Hyun, S., Kwan, H. Y., and Sul, H. S. (2009) A role of DNA-PK for the metabolic gene regulation in response to insulin. *Cell* 136, 1056-1072

Supplementary Tables

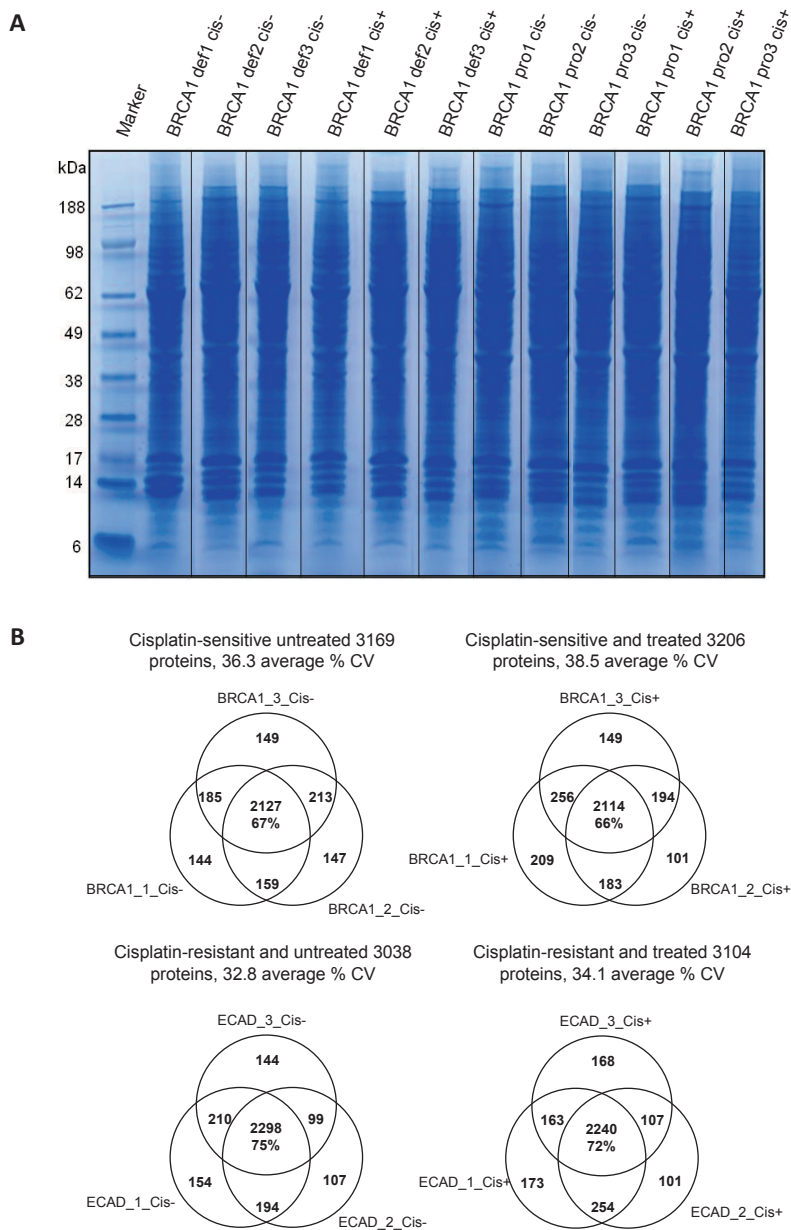
The Supplementary Tables S1-4 can be requested via j.jaspers@nki.nl or janneke_jaspers@hotmail.com.

Supplementary Table S1. Information on identification and quantitative data of the proteins identified in BRCA1-proficient and -deficient mouse mammary tumors, both with and without cisplatin treatment, including peptide counts and protein identification probability.

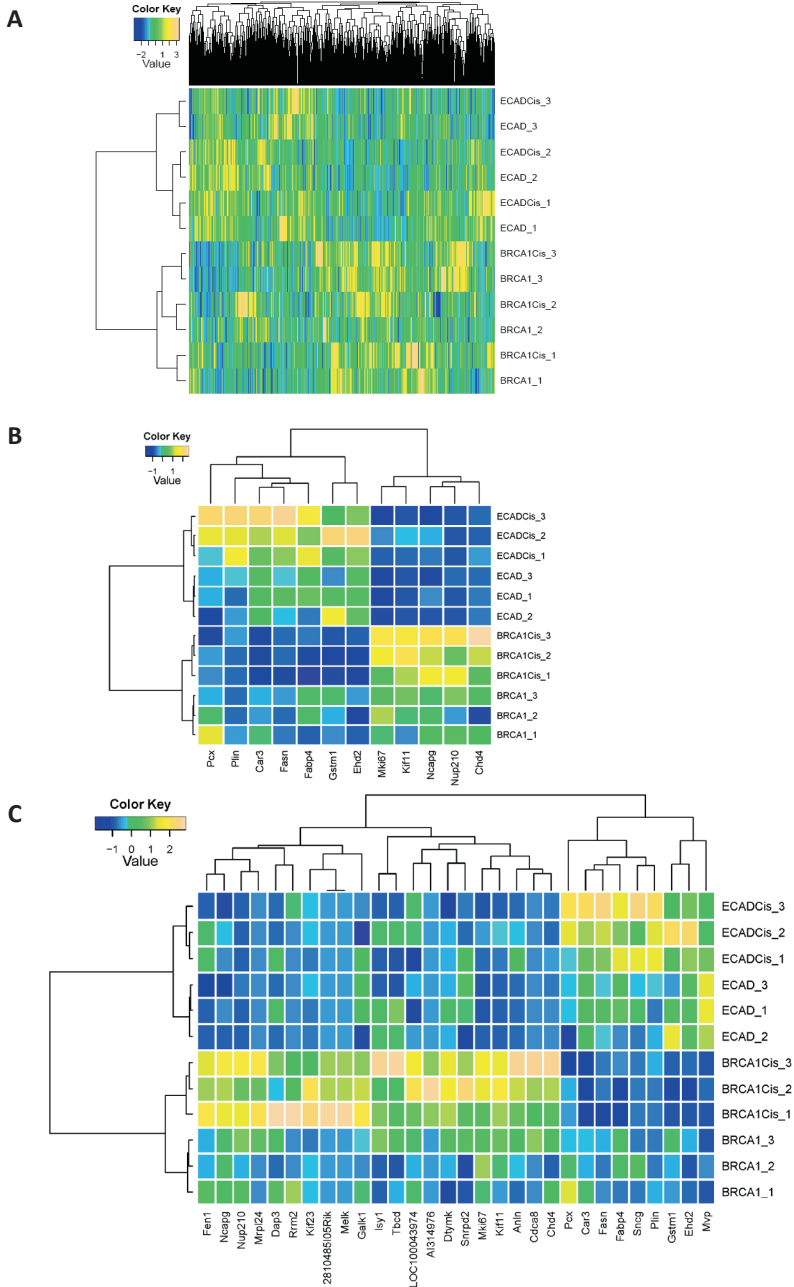
Supplementary Table S2. Information on all peptides identified in the 12 samples.

Supplementary Table S3. Information on identification and quantitative data of the differential proteins identified in BRCA1-proficient and -deficient mouse mammary tumors, both with and without cisplatin treatment. Also additional quantitative characterises and additional statistical data to select proteins with highly discriminative markers that can separate the four conditions is provided.

Supplementary Table S4. BiNGO gene ontology analysis on significant groups of densely connected proteins after sort-term cisplatin treatment for the top three sub-clusters of Figure 4A-D (only the top 20 most significant terms are shown) together with BiNGO analysis on all proteins.

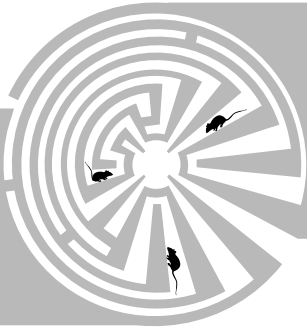


Supplementary Figure S1. A, Coomassie-stained gel displaying protein fractionation the 12 samples from BRCA1-proficient and -deficient tumor tissue lysates. **B**, three-way Venn diagrams showing the distributions of the protein identifications within the triplicate analysis of all four conditions.



Supplemental Figure S2. A, Unsupervised clustering using protein expression data of all 3486 identified proteins. Protein spectral count data of the 3486 proteins was exported from Scaffold to Excel. Unsupervised clustering in R shows co-clustering of treated and untreated tumors. **B**, Supervised clustering using the subset of 30 highly discriminatory proteins. **C**, Supervised clustering using the subset of 12 highly discriminatory proteins.

CHAPTER 8



General discussion

Most cancer patients die from disseminated cancers that do not respond to systemic anti-cancer therapy. Such systemic therapy comprises cytotoxic chemotherapy, as well as signal transduction inhibitors and antibodies that are more targeted towards tumor cells. Despite the benefits of chemotherapy for patient survival, one of the biggest challenges remains the development of resistance to these therapies. In general, two types of resistance can be distinguished: intrinsic, or primary, resistance, when the tumor does not respond well to treatment upfront; and acquired, or secondary, resistance, when the tumor is initially sensitive to the therapy, but later becomes resistant. Even though it is an ongoing debate whether a mechanism of acquired resistance is truly acquired (i.e. drug-induced), or a pre-existing resistant subpopulation is selected and grows out as a resistant tumor¹, I use the terms intrinsic and acquired to distinguish between primary and secondary resistance. In this thesis we have studied both types of resistance to PARP inhibitors in mouse models of BRCA1/2-associated hereditary breast cancer. For this purpose, we used mammary tumors that were generated in genetically engineered mouse models. The use of such defined mouse models for the study of drug resistance has a number of advantages compared with xenograft models (reviewed by Rottenberg and Borst²): (1) GEMM tumors are derived from an isogenic genetic background of the tumor cohort; (2) GEMM tumors can be transplanted orthotopically into syngeneic mice that have an intact immune system; (3) the effects of single drugs and drug/combinations can be studied using the same tumor; (4) genes identified to cause resistance can be genetically targeted.

The mechanism by which a tumor acquires resistance to a drug is often related to the drug's mechanism of action. Possible mechanisms include alteration or down regulation of the drug target^{3,4}, circumvention of the inhibited pathway through activation of by-pass mechanisms⁵, and alternative DNA repair⁶ (Chapter 3). It is however still unknown what causes "pan-resistance"⁷, which is frequently observed in metastatic disease: resistance to different classes of drugs and radiotherapy. Epithelial-to-mesenchymal transition (EMT) and the presence of cancer stem cells (CSCs) have been linked to pan-resistance and will be discussed here. The high sensitivity of BRCA1/2-deficient tumors to PARP inhibitors and the subsequent development of resistance will also be discussed.

8.1 PARP inhibition in BRCA-deficient breast cancer

BRCA1 and BRCA2

Hereditary breast cancer is frequently caused by an inactivating mutation in the breast and ovarian cancer susceptibility genes *BRCA1* or *BRCA2*. Women with heterozygous germ-line mutations in *BRCA1* or *BRCA2* have a life-time risk of 50-80% to develop breast cancer and of 30-50% to develop ovarian cancer. For both cancer types, a higher risk is associated with *BRCA1* mutations than with *BRCA2* mutations. *BRCA1*-related breast cancers are associated with a triple-negative phenotype, which means that they are hormone receptor negative

and do not have a HER2 amplification. Currently no specific therapies are available for triple-negative breast cancers (TNBCs). The Cancer Genome Atlas (TCGA) network has identified germline or somatic variants in *BRCA1* and *BRCA2* in 20% of basal-like breast cancers, which are mostly TNBCs⁸. In addition to mutations in *BRCA1* or *BRCA2*, other breast cancers show properties of “BRCAness”⁹, evidenced by typical histopathological features¹⁰, *BRCA1* promoter methylation and characteristic DNA copy number variations¹¹.

BRCA1 and *BRCA2* are both important for the maintenance of genomic integrity. *BRCA1* is involved in many cellular processes, such as G2-M checkpoint control, DNA replication, homologous recombination (HR), and inter-strand cross link (ICL) repair^{12,13}. *BRCA2* is thought to be primarily important for HR. In addition, both proteins were recently shown to be involved in replication fork stability^{14,15}. HR is the error-free pathway to repair DNA double strand breaks (DSBs) by using the sister chromosome as template for repair. *BRCA1* and *BRCA2* each function at different stages in the pathway. *BRCA1* binds shortly after damage detection to the DSB via RAP80^{16,17} and abraxas^{18–20} and promotes end-resection through binding to CtIP²¹. *BRCA2* promotes RAD51 loading on the single-strand DNA (ssDNA) after strand resection^{22,23}, but also on ssDNA of stalled replication forks to prevent MRE11-mediated degradation¹⁴. RAD51 foci formation is often used as marker for HR and with a DR-GFP reporter construct HR specific repair of an I-SceI endonuclease-induced DSB can be measured *in vitro*²⁴. HR deficiency (HRD) promotes the formation of genomically unstable tumors^{25,26}, but also renders tumors more sensitive to DNA damage. Patients with *BRCA1*-like breast cancer specifically benefited from high-dose DSB-inducing chemotherapy²⁷. In 2005, a less harmful therapeutic strategy to target HR-deficient cancer was introduced: inhibition of poly(ADP-ribose) polymerase (PARP).

Poly(ADP-ribose) polymerase (PARP) 1

By regulating transcription, chromatin remodeling and the DNA damage response (DDR), PARP1 is another important protein for maintenance of genomic integrity. It uses the substrate NAD⁺ for transferring poly(ADP-ribose) groups to itself and other proteins, a process called PARYlation. Thus far the PARP superfamily consists of 17 members, but not all PARPs are enzymatically active (reviewed by Schreiber *et al.*²⁸). PARP1, PARP2 and PARP3 play a role in the DDR. Through its zinc finger domains, PARP1 is activated by structural DNA aberrations such as single- and double-strand breaks²⁹. DNA binding of PARP1 leads to auto-PARYlation and PARYlation of multiple target proteins such as histone H1 and H2B (for the relaxation of chromatin³⁰), XRCC1³¹ (activating the single-strand break (SSB) repair machinery³²) and other PAR-binding SSB repair proteins. Interestingly, PARP1 is important in direct SSB repair, but dispensable for base excision repair (BER), a process that removes a damaged base followed by SSB repair³³.

Several small molecule inhibitors of PARP activity have been developed (reviewed by Curtin and Szabo³⁴). In contrast to genetic inactivation of PARP1, chemical PARP1 inhibition blocks efficient damage repair by trapping PARP on the DNA^{33,35}. Indeed, PARP inhibitors (PARPi) that have the strongest potency of trapping PARP on the DNA are more toxic than PARP inhibitors with less potency and than unrepaired SSBs because of PARP deficiency³⁶. The activity of PARP1 in the DDR is not limited to SSB repair, as PARP1 is also involved in DSB repair via non-homologous end joining (NHEJ)^{37–41} and re-activation of stalled replication forks⁴².

Synthetic lethality: PARP inhibition in HR-deficient breast cancer

The inhibition of PARP leads to DSBs and HR, as measured by γ H2AX and RAD51 foci respectively. Two groups showed that PARP inhibition is highly toxic to BRCA1/2-deficient cells^{43,44}; an instructive example of synthetic lethality that was brought from bench to bedside. Two genes are synthetic lethal when deficiency of one of them is viable, but disruption of both leads to cell death⁴⁵, for example when one is mutated (*BRCA1* or *BRCA2*) and the other one is chemically inhibited (PARP1). Also deficiencies in other HR proteins, such as RAD51, ATM and RPA1, sensitize cells to PARP inhibition⁴⁶. Preclinical studies in BRCA1/2-deficient mouse mammary tumor models demonstrated clear anti-tumor efficacy of the PARP inhibitor olaparib^{6,47–50} (Chapter 2 and 3). Importantly, this was also observed in patients with BRCA1/2-related breast and ovarian cancer in phase I and II clinical trials with olaparib, while only moderate side effects were reported^{51–54}. A phase I trial with niraparib also showed anti-tumor efficacy of this novel PARP inhibitor⁵⁵. The PARP inhibitor veliparib is less potent as single agent, but potentiates other drugs in combination studies⁵⁶. The difference in anti-tumor activity of these PARP inhibitors can be explained by differences in their ability to trap PARP on the DNA³⁶.

In addition to BRCA1/2-mutated and BRCA-like breast cancer, there may be more cancers with a defect in HR that may benefit from PARP inhibitor treatment. Interestingly, contradictory changes in the phosphatidylinositol 3' kinase (PI3K) pathway were found to influence HR. Loss of the tumor suppressor PTEN, which is frequently mutated in human cancer and is a suppressor of the PI3K pathway, has been linked to HR deficiency and sensitivity to PARP inhibition⁵⁷, which is dependent on the SUMOylation of PTEN⁵⁸. Also inhibition of PI3K was suggested to induce HR deficiency via down regulation of *BRCA1/2* expression⁵⁹ and thereby sensitizing breast cancer cells to PARP inhibition^{59,60}. Other processes that have been shown to inhibit RAD51 and HR include local mild hyperthermia resulting in *BRCA2* degradation⁶¹, hypoxia⁶², targeting of the *BRCA1*-BRCT domain⁶³, CDK inhibition⁶⁴, cyclin D1 inhibition⁶⁵, *HER2* overexpression⁶⁶, proteasome inhibition⁶⁷, Hsp90 inhibition⁶⁸, inhibition of DDR pathways by curcumin⁶⁹ and targeting *BRCA1* localization⁷⁰. It will be interesting to test PARP inhibition in combination with these treatments in BRCA-

proficient mouse mammary tumors, although due to the loss of tumor-specific synthetic lethality, such combination therapies may have a narrow therapeutic window. The central role for HR deficiency in determining the sensitivity to PARP inhibitors emphasizes the importance of biomarkers for HR deficiency (see paragraph 8.5).

8.2 Resistance to PARP inhibition in BRCA1/2-related breast cancer

In spite of the promising results from clinical trials with PARP inhibitors, not all patients responded well initially or they acquired resistance later on. Patients from the phase I and II clinical trials were often pre-treated with various drugs, which could have triggered cross-resistance to PARP inhibition (*e.g.* by HR restoration). But also when PARP inhibitors are given as first-line therapy, I expect intrinsic or acquired resistance to occur. Preclinical work has uncovered several mechanisms by which BRCA1/2-deficient tumors can become resistant to PARP inhibition, and I will discuss them in this section.

Homologous recombination activity

Genetic reversion

Deficiency in homologous recombination appears to be the most important sensitizer for PARP inhibition. HR restoration would, therefore, annihilate the synthetic lethality effect and result in PARP inhibitor resistance. The first identified mechanism to restore HR was the re-expression of truncated but functional BRCA1 or BRCA2 proteins in therapy-resistant cells that had acquired a secondary *BRCA1/2* mutation. As a result of this secondary mutation, the open-reading frame is restored, leading to a crippled, but still functional BRCA1/2 protein. Therapy resistance caused by genetic reversion was identified in cell lines and subsequently confirmed in some platinum-resistant ovarian cancers^{71–73}. More recently protein-restoring secondary mutations in *BRCA2* have been found in olaparib-resistant metastases from two patients⁷⁴. It is unclear whether all *BRCA1/2* mutations can be reversed by secondary mutations and how frequent this mechanism is. Norquist *et al.*⁷⁵ showed that in about half of the platinum-resistant recurrences of BRCA1/2-related ovarian carcinomas a secondary mutation was present.

Hypomorphic BRCA1 alleles

Mutations in different domains of *BRCA1* have a different effect on protein function, stability and therefore on HR activity and drug sensitivity. Missense mutations in *BRCA1* that are predicted to be pathogenic based on *in vitro* assays are only present in the RING and BRCT domain⁷⁶. However, not all deleterious and pathogenic mutations lead to complete HR deficiency. Whereas introduction of the pathogenic *BRCA1*^{C61G} mutation in mice resulted in the formation of genomically unstable mammary tumors, these BRCA1-C61G expressing tumors could still form RAD51 foci and responded only moderately to PARP inhibition and cisplatin⁷⁷. So it seems that a pathogenic *BRCA1* mutation does not predict PARP inhibitor

sensitivity per se, but that additional assays are required, for example measuring RAD51 foci formation (see also paragraph 8.5).

Loss of 53BP1

The group of André Nussenzweig and our group have demonstrated for the first time that HR can also take place in BRCA1-deficient cells through the loss of p53 binding protein 1 (53BP1)^{78–80}. Together with BRCA1, 53BP1 is a key protein for deciding whether DSBs are repaired by HR or by NHEJ. 53BP1 blocks end resection which is required for HR, and thereby promotes NHEJ^{78,81}. When 53BP1 is absent, end resection and HR can again take place in BRCA1-deficient cells. Due to the more downstream activity of BRCA2 in the HR pathway, loss of 53BP1 could not rescue HR in BRCA2-deficient cells⁷⁹. We have shown that loss of 53BP1 causes PARP inhibitor resistance *in vivo* and occurs spontaneously in BRCA1-deficient mammary tumors that have acquired resistance to PARP inhibition⁶ (Chapter 4). In four of six 53BP1-negative tumors we found genetic aberrations that could explain the lack of 53BP1 protein. Interestingly, low expression or absence of 53BP1 protein is associated with TNBC and BRCA-associated breast cancer⁷⁹, suggesting that this could be a relevant mechanism in human breast cancer.

53BP1 is recruited to the chromatin at DSBs where it binds to H4K20me2, methylated by MMSET⁸², and to H2AK15ub, ubiquitinated by RNF168 E3 ubiquitin ligase^{83,84}. In addition, the balance between binding of 53BP1 to H4K20me2 and binding of BRCA1 to the chromatin at DSBs is regulated by H4 acetylation⁸⁵. Together this illustrates that the balance between 53BP1 and BRCA1 chromatin binding, and thus between NHEJ and HR, is tightly controlled by epigenetic processes. This makes it less likely that a mutation in one of the factors upstream of 53BP1, such as RNF8 or RNF168, could cause a complete block in recruitment of 53BP1 and thereby restore HR in BRCA1-deficient tumors. In line with this notion, we have not found genetic aberrations in these upstream factors in our panel of BRCA1-deficient tumors that acquired PARPi resistance.

Cathepsin L has been shown to promote degradation of 53BP1, which could be inhibited by vitamin D, adding yet another layer to 53BP1 regulation⁸⁶. BRCA1 loss activates the cathepsin L-mediated degradation of 53BP1, again emphasizing the tightly controlled balance between BRCA1 and 53BP1. Whereas cathepsin L was found to inversely correlate with 53BP1 in triple-negative breast cancer, we did not find such a correlation in our PARPi-resistant mouse mammary tumor panel (data not shown).

Recently, two effector proteins of 53BP1 were identified: RIF1^{87–91} and PTIP⁹². Both act upon ATM-dependent 53BP1 phosphorylation, albeit via distinct phosphorylation sites, and inhibit end resection. BRCA1 and RIF1 inhibit each other's accumulation at damaged sites in a cell cycle dependent manner^{87,89}. RIF1 loss only partially restores RAD51 foci formation and PARPi sensitivity^{87,88}, while abrogation of the binding between PTIP and 53BP1 completely restores RAD51 foci formation and PARPi sensitivity⁹². This makes losing PTIP, but also RIF1,

good candidates for causing PARP inhibitor resistance in BRCA1-deficient tumors. In high-throughput sequencing data from our PARPi-resistant mouse mammary tumor panel no aberrations in *Paxip1* (encoding PTIP) or *Rif1* were identified (unpublished data of J. de Ruiter), but it would be interesting to test both proteins by immunohistochemistry and validate PARPi resistance by knock-down of *Paxip1* and *Rif1* in BRCA1-deficient mammary tumor cell lines.

P-glycoprotein and other drug efflux pumps

Lowering intra-cellular drug concentrations by pumping compounds out of the cell is an effective way to avoid drug-induced toxicity. ATP-binding cassette (ABC) efflux transporters, which are expressed in physiological barriers such as liver, kidney, gut and the blood-brain-barrier, were shown to have many anti-cancer agents as their substrates, both classical chemotherapeutics and targeted inhibitors⁹³. When the ATP-binding cassette (ABC) transporters were discovered, they were thought to have a major impact on anti-cancer drug resistance. Several ABC transporter inhibitors were developed to re-sensitize tumors to chemotherapeutic drugs. In cancer cell lines up-regulation of especially P-glycoprotein (Pgp) and also breast cancer resistance protein (BCRP) leads to multi-drug resistance^{94,95}. In the *K14cre;Brca1^{F/F};p53^{F/F}* mouse model of BRCA1-related breast cancer, we have seen that even moderate up-regulation of Pgp or BCRP can cause drug resistance to the taxane docetaxel, the anthracyclin doxorubicin and topotecan^{96–98}. In the same tumor model we found that resistance to the PARP inhibitor olaparib could frequently be explained by up-regulation of Pgp⁴⁹ (Chapter 2). In line with this, a prolonged response to PARP inhibition was observed when Pgp-deficient tumors were treated with olaparib or when Pgp-proficient tumors were treated with AZD2461, a novel PARP inhibitor that is a poor substrate for Pgp⁶ (Chapter 3). Hay and colleagues⁴⁸ found a higher expression of BCRP in olaparib-resistant BRCA2-deficient mammary tumors, but this is not likely causing the resistance. Olaparib is not transported by BCRP in a competitive vesicular uptake assay and we did not find high *Bcrp* expression in our BRCA1- or BRCA2-deficient tumors, even not in those that also lack Pgp (data not shown).

Despite the clear effect of Pgp on preclinical anti-cancer drug resistance, the influence of efflux transporters in the clinic is controversial. None of the transporters has repeatedly been linked to a poor treatment response. Clinical studies with transporter inhibitors have largely failed for various reasons (reviewed by Szakács *et al.*⁹³). In breast cancers, Pgp and BCRP levels are reported to be very low, even after treatment^{99,100}. Even though Pgp-mediated clinical resistance is rare, a few cases have been reported in which it does play role. Pusztai *et al.*¹⁰¹ report that in one of 17 breast cancer patients studied, the tumor not only stained positive for Pgp on IHC, but also showed increased uptake of ^{99m}T-Sestamibi after tariquidar administration. This patient benefited from the combination of chemotherapy plus tariquidar.

It remains a mystery why such an efficient resistance mechanism is hardly used in human tumors. One possible explanation is the very low promoter activity of *MDR1* (which encodes Pgp). Gene rearrangements that link a constitutively active promoter to *MDR1* have been reported in treated cancer cell lines and two patients with refractory acute lymphoblastic leukemia (ALL) with high *MDR1* expression^{102,103}. One would expect this mechanism to occur more frequently in genomically unstable tumors, such as BRCA1-related breast cancers. Gene rearrangements at the *BRCA1* locus – leading to re-expression of *BRCA1* from a heterologous promoter – do occur in a patient-derived xenograft (PDX) model of BRCA1-methylated breast cancer. For *MDR1*, however, no rearrangements have been observed thus far in therapy-resistant tumors from three independent PDX models for BRCA1-deficient breast cancer (Peter Brugge, manuscript in preparation).

Other resistance mechanisms

In addition to the above-mentioned resistance mechanisms, one could envision other ways to acquire resistance to PARPi-induced damage in BRCA1-deficient tumors. First, the repair of SSBs. In theory, an increase in PARP-independent repair of SSBs (long-patch repair¹⁰⁴) could prevent the accumulation of lethal double-strand breaks in BRCA-deficient cells. However, the finding that PARP inhibitors not only prevent SSB repair, but also induce the formation of toxic PARP-DNA complexes, suggests that alternative SSB repair is only effective when simultaneously PARP levels are down-regulated and thereby the PARP-DNA complexes are not formed, or the repair of the PARP-DNA complexes is increased. Several of these repair factors have been identified³⁶. Inactivating mutations in *Parp1* or down-regulation of PARP1 expression to prevent harmful trapping on the DNA has been observed as a resistance mechanism to the PARP inhibitor olaparib in BRCA-proficient mouse embryonic stem cells¹⁰⁵, but not in our BRCA-deficient tumors.

Second, chromatin-mediated drug-tolerance. Sharma *et al.*¹⁰⁶ identified a subpopulation of non-small cell lung cancer cells that had a >100-fold reduced sensitivity to tyrosine-kinase inhibitors (TKIs). This was mediated by IGF-1 receptor signaling and an altered chromatin state, which required the histone demethylase KDM5A/Jarid1A. These ‘drug-tolerant persisters’ were cross-resistant to cisplatin, indicating a general drug resistance mechanism. Further studies are required to test the presence of this altered chromatin state in PARP inhibitor treated cells, as PARP1 is a regulator of chromatin structure (reviewed by Lovato *et al.*¹⁰⁷).

Third, epithelial-to-mesenchymal transition (EMT). EMT has frequently been linked to resistance in different cancer cell types and for various types of drugs. We have shown an association between EMT and resistance to olaparib in BRCA2-deficient mouse mammary tumors (Chapter 4). The role of EMT in drug resistance is discussed below.

8.3 Epithelial-to-mesenchymal transition

In a set of BRCA2-deficient mouse mammary tumors we observed in some tumors intrinsic resistance to several chemotherapy drugs and to the PARP inhibitor olaparib (Chapter 4). This multi-drug resistance phenotype was only observed in tumors with an EMT phenotype (called carcinosarcomas), which also showed high expression of the drug efflux transporters Pgp and BCRP. By combining the Pgp-inhibitor tariquidar and chemotherapy we showed that Pgp contributes to the multi-drug resistance in BRCA2-deficient carcinosarcomas, but does not explain it entirely. This suggests that EMT itself causes multi-drug resistance. EMT leads to reversible reprogramming of epithelial cancer cells that have gained mesenchymal properties, involving EMT transcription factors, epigenetic modifications and non-coding RNAs¹⁰⁸. Some hallmarks of EMT are the loss of cell adhesion molecules, such as E-cadherin and claudins, expression of fibroblast marker vimentin and a spindle cell morphology. A role of EMT in pan-resistance is supported by a number of *in vitro* studies that observed for various classes of chemotherapy and different targeted agents an EMT phenotype in the resistant cancer cell lines^{109–117}. The frequency of EMT in human tumors differs per cancer type. In contrast to, for example, colorectal cancer¹¹⁸, EMT is not frequently observed in breast cancer. The rare subtype of metaplastic breast cancers is characterized by different morphological phenotypes, including spindle-shaped tumors with EMT characteristics^{119–121}. Patients with metaplastic breast cancer are often refractory to treatment and have a poor prognosis¹²². The molecular subtype claudin-low is associated with metaplastic breast cancer and is characterized by the expression of EMT-associated genes^{123,124}. In one study claudin-low tumors had a poorer response than the basal-like breast cancers, but not than the luminal breast cancer subtypes¹²³. In addition to gene expression signatures, single EMT-related markers, such as E-cadherin, claudin, vimentin and N-cadherin, were shown to predict the prognosis of patients with various cancer types¹²⁵. In breast cancer a shorter relapse-free survival is predicted by high levels of SNAIL alone¹²⁶ or of both SNAIL and TWIST¹²⁷.

To further elucidate the role of EMT on drug sensitivity, mouse models with inducible overexpression of EMT transcription factors, such as Twist, Snail or Zeb1, will be very helpful. This can be done in chimeric mice from existing genetically engineered mouse tumor models¹²⁸, preferably on a Pgp-deficient background. While patients usually receive a combination of different drugs to maximize the anti-cancer effect, with these mouse models one can address the effect of EMT on individual drugs. For example, we found that multi-drug resistant BRCA2-deficient carcinosarcomas are still highly sensitive to cisplatin.

Data from *in vitro* studies support a role of EMT in acquired drug resistance in various cancer types. We did not observe EMT in our BRCA2-deficient carcinomas that acquired resistance to olaparib, topotecan, docetaxel or doxorubicin. We also did not succeed in inducing EMT in cell lines derived from BRCA-deficient carcinomas, indicating low plasticity

of this model. The presence of EMT in human tumors with acquired resistance is difficult to study as not many samples are available. In two studies with EGFR inhibitor-resistant lung cancer samples an EMT phenotype was observed in some of the resistant samples, but not in the corresponding pre-treatment samples, suggesting that EMT may induce therapy resistance in this setting^{129,130}. Whether EMT is also involved in acquired resistance in breast cancer and if so, for which drugs, remains to be examined.

Altogether, there is substantial preclinical evidence that EMT is associated with resistance to a wide range of chemotherapeutic and targeting agents. But how EMT exactly causes the wide-spread drug resistance is currently not known. As a clear EMT phenotype or gene expression profile in breast cancer is rare, an in-depth analysis of the available data is required to demonstrate whether an EMT profile is associated with poor treatment response (Chapter 4).

8.4 Cancer stem cells

The cancer stem cell concept postulates that there is a tumor hierarchy in which a small subpopulation of cancer stem cells (CSCs) is able to self-renew and give rise to the differentiated bulk of the tumor. The CSCs would have tumor-initiating capacity in contrast to the differentiated cells and would be more resistant to therapy. As a consequence CSCs may be responsible for tumor relapse and metastases and should get high priority to target^{131,132}. Tumor-initiating cells (TICs) were first identified in acute myeloid leukemia (AML)¹³³ and later also in solid carcinomas¹³⁴ with the help of cell surface markers. But the concept has been challenged by studies that demonstrate a high frequency of tumor-initiation by unsorted tumor cells^{135,136}. Because they lack phenotypic and functional heterogeneity, some tumor types may not follow the cancer stem cell model.

In humans, breast cancer stem cells have been identified as CD44⁺/CD24^{-/low} cells¹³⁷. In mice, normal mammary stem cells and also TICs have been characterized as Lin⁻/CD24⁺/CD29⁺ or Lin⁻/CD24⁺/CD49f⁺ cells^{138–142}. But also the identification of TICs appears to be context dependent. We (Chapter 5) and others¹⁴³ demonstrated that in one mouse model with epithelial and mesenchymal tumors, the latter ones show less functional heterogeneity of the subpopulations. In epithelial *BRCA1*^{-/-};*p53*^{-/-} and *p53*^{-/-} carcinomas Lin⁻/CD24⁺/CD49f⁺ cells have the highest outgrowth frequency¹⁴¹, but in EMT-like carcinosarcomas also the Lin⁻/CD24⁺/CD49f⁺ fraction is highly tumorigenic (Chapter 5). The induction of EMT in human mammary epithelial cells increases the CSC population of CD44⁺/CD24^{-/low} cells^{144–147}. In line with this, Herschkowitz *et al.*¹⁴³ found in a *p53*^{-/-} mouse mammary tumor model that EMT-like tumors have a large population of Lin⁻/CD24⁺/CD29⁺ cells, whereas carcinomas do not. Using the stem cell markers CD24 and CD49f, we did not find this difference in populations between carcinomas and carcinosarcomas from our mouse models (Chapter 5), suggesting that these stem cell markers may not be useful to identify TICs in EMT-like tumors.

What would be the implications of TICs on therapy response? In breast cancer Lin⁻/CD44⁺/CD24^{-/low} cells are more resistant to chemotherapy¹⁴⁸ and ionizing radiation¹⁴⁹ than other cells. The underlying mechanism of resistance is currently unknown. An attempt to inhibit breast cancer stem cells with a γ -secretase inhibitor in combination with docetaxel gave varying results¹⁵⁰. Our group did not observe any benefit of combining a γ -secretase inhibitor with cisplatin, compared to cisplatin single treatment in a BRCA1-deficient mouse mammary tumor model (R. Drost *et al.*, unpublished observations). To be able to correlate TIC markers with therapy response, more studies are required.

While many studies use breast TIC markers, it is still possible that the identification of TICs is in fact an artifact of the transplantation assays and measures integrin-mediated survival, rather than tumorigenic capacity. A mesenchymal cellular state is indeed associated with anchorage-independent growth and the EMT transcription factor TWIST mediates inhibition of apoptosis^{151,152}. Also unclear is the plasticity of the TIC markers. If tumor cells could easily switch TIC markers on and off, there is no point in targeting specifically the TIC subpopulation.

8.5 Biomarkers for homologous recombination-deficient breast cancer

Because of the therapeutic opportunities for patients with HRD cancers, it is of utmost importance to be able to identify this group. Robust HRD biomarkers are not only important to identify sporadic cancer patients with BRCA-like tumors for treatment with PARP inhibitors, but also to offer alternative therapies to patients who do not have HRD cancer (anymore) (see also paragraph 8.6). A key feature of BRCA1-deficient tumors is high genomic instability, which has been exploited with array comparative genomic hybridization (aCGH) for the development of BRCA1-like signatures^{153–156}.

Others developed measures for allelic imbalance at telomere ends¹⁵⁷, genomic patterns of loss of heterozygosity (LOH)¹⁵⁸ and single-nucleotide polymorphism (SNP)-based ploidy and large-scale chromosomal aberrations¹⁵⁹ for the identification of HRD cancers. With these methods some sporadic basal-like breast cancers or TNBCs could be classified as BRCA1-like. In chapter 7 I present a proteomic approach that we performed to identify a DNA repair-related signature for the prediction of BRCA1-deficiency, based on a comparison of BRCA1-proficient and -deficient mouse mammary tumors¹⁶⁰. Sporadic tumors that are classified as “BRCA1” may represent non-BRCA1-mutated HR deficient cancers and should be validated by another classification method, for example an aCGH signature. Recent data with *Brca1*^{G61G}-mutated mouse mammary tumors suggest, however, that a BRCA1-like aCGH pattern does not always predict HR deficiency⁷⁷. This is also expected in *BRCA1/2*-mutated tumors that have become HR proficient by genetic reversion, as these BRCA-like signatures reflect the HRD history of the tumor rather than the actual state. This limitation could be overcome by employing functional assays for HR. In tumors this has been explored by

several labs by detecting RAD51 foci as a surrogate HR marker. Graeser *et al.*¹⁶¹ and Asakawa *et al.*¹⁶² measured RAD51 in core biopsies taken 24 hours after the first chemotherapy cycle. In both studies a low RAD51 score correlated with better therapy response. Mukhopadhyay *et al.*¹⁶³ took pre-treatment ascitic fluid in culture and found that a low number of RAD51 foci correlated with PARP inhibitor sensitivity *in vitro*, higher sensitivity to cisplatin and improved survival. Thus, testing the formation of RAD51 foci shortly after DNA damaging chemotherapy seems to be a promising assay for HR activity and for selection of patients for PARP inhibitor treatment. In search of biomarkers for cisplatin response we also studied changes in tumors 24 hours after treatment in mice and found an increase in fatty acid metabolism specifically in BRCA1-proficient, cisplatin-resistant mammary tumors (Chapter 7). Fatty acid metabolism may be involved in cisplatin resistance and may even be regulated by BRCA1¹⁶⁴. A potential link between DNA damage repair and fatty acid metabolism requires further investigations.

8.6 Perspectives

Studying anti-cancer drug resistance

Cell lines derived from patient tumors have been widely used to study drug resistance *in vitro*. Classically, *in vivo* validation of the findings is done by transplantation of tumor cell lines in immune deficient mice. On the one hand this has provided valuable insight in the molecular pathways and potential resistance mechanisms. On the other hand there are often discrepancies between *in vitro* results and the outcome of clinical studies. One major difference is the lack of the immune system in xenograft models, which prevents natural tumor-host interactions. Moreover, cell lines are heavily selected to grow under culture conditions and may have acquired mutations over time. The transplantation of small tumor fragments from patients directly into mice has yielded a number of transplantable models that recapitulate the morphology and genomic profile of the original tumor¹⁶⁵⁻¹⁶⁷ and that show comparable drug responses (P. ter Brugge, manuscript in preparation). These patient-derived tumor xenograft (PDX) models provide a heterogeneous cohort of 'xenopatients' to study drug sensitivity and resistance of tumors with specific genetic aberrations. One of the drawbacks is that the take rate of primary breast cancers is very low and established lines need to be maintained by serial transplantation. The majority of the breast cancer PDX models are triple-negative because this breast cancer subtype has a higher take rate than other subtypes. Also, PDX models do not permit manipulation of individual genes to study their effect on drug sensitivity in an *in vivo* setting. Genetically engineered mouse models (GEMMs) do provide this opportunity and many human cancer (sub)types have been effectively modeled in GEMMs by introducing (combinations of) cancer driver mutations that are also recurrently found in the cognate human tumors^{2,168}. Following the induction of the genetically engineered driver mutations, tumorigenesis is driven by accumulation of

mutations in additional cancer genes. These additional mutations vary between individual tumors and give rise to a heterogeneous cohort. Nevertheless, inter-tumor heterogeneity in GEMMs is still relatively limited compared to the enormous heterogeneity in human tumors. Recently new methods have been developed for accelerated production of GEMMs carrying multiple mutations without the need for time-consuming crossing schemes. *Ex vivo* introduction of genetic elements in GEMM-derived embryonic stem cells (ESCs) results in the production of chimeric mice that can directly be used to study tumor development and therapy response^{128,169}. Another approach is the CRISPR/Cas technique with which multiple mutations can be introduced in mouse ESCs at the same time¹⁷⁰. These novel approaches will speed up the validation of candidate genes in a realistic *in vivo* setting.

It will be important to carefully validate the preclinical findings in PARP inhibitor resistant tumors of patients. These can be patients that responded poorly up-front or patients that initially showed a response but later progressed on treatment. The latter would enable a comparison of matched pairs of untreated and resistant tumors. Unfortunately, such paired samples are rare, because samples are usually not taken from patients with relapsing tumors that progress under treatment. Recently, patients with metastatic disease had an olaparib-resistant metastatic lesion surgically removed, which might enable us to study the underlying mechanisms (J. Schellens, personal communication). Next-generation sequencing of the resistant and sensitive tumors would shed light on genetic changes that are potentially causal to PARP inhibitor resistance. The data from human tumors could be compared with results from functional genetic screens with PARP inhibitors, which are currently being done in *Brca1*^{-/-};*p53*^{-/-} and *Brca2*^{-/-};*p53*^{-/-} cell lines, and with genetic aberrations that we find specifically in PARPi-resistant BRCA1-deficient mouse tumors. We have collected whole-exome and RNA sequencing data from 44 PARPi-resistant BRCA1-deficient tumors and the corresponding sensitive control tumors that are being analyzed for resistance-specific mutations.

Optimizing treatment strategies with PARP inhibitors

PARP inhibitors have shown great promise for the treatment of patients with BRCA1/2-related breast or ovarian cancer. But, as described above, resistance has been observed in heavily pre-treated patients in clinical trials and is also expected in patients that are treated with PARP inhibitors as first-line therapy. Several strategies could be exploited to prevent or overcome resistance to PARP inhibition in order to maximize the treatment benefit for patients.

Chronic PARP inhibitor treatment suppresses the development of resistance. We found a prolonged relapse-free and overall survival when mice bearing BRCA1-deficient mammary tumors were treated with PARP inhibitors for 100 consecutive days, compared to 28 days^{6,49} (Chapter 2 and 3). Clinical studies also use continuous daily treatment with a PARP

inhibitor until disease progression or until dose-limiting toxicity forces discontinuation^{51,53}. Additional side effects due to long-term treatment should be carefully monitored. PARP1 is important for DNA repair and chronic treatment with PARP inhibitors may therefore lead to accumulation of genomic aberrations and development of secondary cancers. PARP1 also regulates chromatin remodeling and stimulates transcription¹⁰⁷, raising the possibility that PARP inhibition may promote tumorigenesis by suppressing transcription of tumor-suppressor genes.

Combining PARP inhibitors with chemotherapy may enhance the treatment effect and minimize the risk of developing resistance in patients with BRCA1/2-related cancer. In BRCA1-deficient mouse mammary tumors we observed a prolonged relapse-free and overall survival when olaparib was combined with platinum drugs⁴⁹ (Chapter 2). Inducing additional damage may, however, also increase the toxicity. The topotecan dose in mice had to be lowered eight-fold, when it was combined with olaparib⁹⁷. In a Phase I study of the combination of olaparib with cisplatin and gemcitabine dose-limiting toxicities were observed at relatively low doses¹⁷¹. PARP inhibition in combination with other targeted inhibitors, for example EGFR inhibitors, may be less toxic. Sequential use of chemotherapy and PARP inhibition may also avoid dose-limiting toxicity. The use of olaparib maintenance therapy prolonged progression-free survival in patients with platinum-sensitive, relapsed, high-grade serous ovarian cancer¹⁷². Further benefit may be achieved when olaparib treatment is started shortly after platinum-based chemotherapy rather than after disease relapse.

Depending on the underlying mechanism of resistance, strategies to reverse this resistance may be exploited. Olaparib resistance caused by Pgp-mediated drug efflux could be reversed by co-administration of the Pgp inhibitor tariquidar⁴⁹ (Chapter 2). Even though Pgp-mediated resistance has not been demonstrated in breast cancer patients, an optimized PARP inhibitor that has poor substrate specificity for Pgp, such as AZD2461, can be used to prevent Pgp-mediated resistance⁶ (Chapter 3). Reduction or abrogation of HR deficiency by 53BP1 loss or genetic reversion mutations is more complex to target, but mechanistic studies have provided interesting new opportunities. Partial restoration of HR by the loss of 53BP1 in BRCA1-deficient cells was shown to be ATM dependent⁷⁸. Combination therapy of a PARP inhibitor and an ATM inhibitor is likely to have a small therapeutic window, but this could be tested in mouse models with BRCA1-deficient mammary tumors that have lost 53BP1⁶ (Chapter 3). The loss of 53BP1 does not rescue the role of BRCA1 in replication fork stability¹⁵, involved in inter-strand crosslink repair (ICL), indicating that BRCA1-deficient tumors with 53BP1 loss are still sensitive to platinum drugs^{6,12} (Chapter 3). Even tumors with hypomorphic BRCA1 or re-expression of partly functional BRCA1 due to secondary mutations are still responsive to the bifunctional alkylator nimustine⁷⁷ or 6-thioguanine¹⁷³. The presence of different resistance mechanisms in one tumor (intra-tumor heterogeneity),

such as loss of 53BP1 in only part of the tumor⁶ (Chapter 3), may complicate strategies to re-sensitize tumors by alternative therapies (reviewed by Fisher *et al.*¹⁷⁴).

In conclusion, others and we have identified several mechanisms of PARP inhibitor resistance in preclinical models of BRCA1/2-deficient breast cancer. Characterization of PARP inhibitor-resistant tumors from BRCA1/2-mutation carriers will be crucial to determine which of these resistance mechanisms are also clinically relevant. This will be important for determining up-front which patients are eligible for PARP inhibition therapy. To further tackle the hurdle of resistance to novel targeted drugs and to optimize their clinical use, GEMMs are instrumental in testing alternative strategies to prevent or overcome therapy escape.

REFERENCES

1. Turner, N. C. & Reis-Filho, J. S. Genetic heterogeneity and cancer drug resistance. *Lancet Oncol.* **13**, e178–185 (2012).
2. Rottenberg, S. & Borst, P. Drug resistance in the mouse cancer clinic. *Drug Resist. Updat. Rev. Comment. Antimicrob. Anticancer Chemother.* **15**, 81–89 (2012).
3. Burgess, D. J. *et al.* Topoisomerase levels determine chemotherapy response in vitro and in vivo. *Proc. Natl. Acad. Sci. U. S. A.* **105**, 9053–9058 (2008).
4. Gorre, M. E. *et al.* Clinical resistance to STI-571 cancer therapy caused by BCR-ABL gene mutation or amplification. *Science* **293**, 876–880 (2001).
5. Prahallad, A. *et al.* Unresponsiveness of colon cancer to BRAF(V600E) inhibition through feedback activation of EGFR. *Nature* **483**, 100–103 (2012).
6. Jaspers, J. E. *et al.* Loss of 53BP1 causes PARP inhibitor resistance in Brca1-mutated mouse mammary tumors. *Cancer Discov.* **3**, 68–81 (2013).
7. Borst, P. Cancer drug pan-resistance: pumps, cancer stem cells, quiescence, epithelial to mesenchymal transition, blocked cell death pathways, persists or what? *Open Biol.* **2**, 120066 (2012).
8. Network, T. C. G. A. Comprehensive molecular portraits of human breast tumours. *Nature* **490**, 61–70 (2012).
9. Turner, N., Tutt, A. & Ashworth, A. Hallmarks of ‘BRCAness’ in sporadic cancers. *Nat. Rev. Cancer* **4**, 814–819 (2004).
10. Da Silva, L. & Lakhani, S. R. Pathology of hereditary breast cancer. *Mod. Pathol. Off. J. United States Can. Acad. Pathol. Inc* **23 Suppl 2**, S46–51 (2010).
11. Lips, E. H. *et al.* Indicators of homologous recombination deficiency in breast cancer and association with response to neoadjuvant chemotherapy. *Ann. Oncol. Off. J. Eur. Soc. Med. Oncol. ESMO* **22**, 870–876 (2011).
12. Bunting, S. F. *et al.* BRCA1 functions independently of homologous recombination in DNA interstrand crosslink repair. *Mol. Cell* **46**, 125–135 (2012).
13. Huen, M. S. Y., Sy, S. M. H. & Chen, J. BRCA1 and its toolbox for the maintenance of genome integrity. *Nat. Rev. Mol. Cell Biol.* **11**, 138–148 (2010).
14. Schlacher, K. *et al.* Double-strand break repair-independent role for BRCA2 in blocking stalled replication fork degradation by MRE11. *Cell* **145**, 529–542 (2011).
15. Schlacher, K., Wu, H. & Jasin, M. A distinct replication fork protection pathway connects Fanconi anemia tumor suppressors to RAD51-BRCA1/2. *Cancer Cell* **22**, 106–116 (2012).
16. Kim, H., Chen, J. & Yu, X. Ubiquitin-binding protein RAP80 mediates BRCA1-dependent DNA damage response. *Science* **316**, 1202–1205 (2007).

17. Sobhian, B. *et al.* RAP80 targets BRCA1 to specific ubiquitin structures at DNA damage sites. *Science* **316**, 1198–1202 (2007).
18. Kim, H., Huang, J. & Chen, J. CCDC98 is a BRCA1-BRCT domain-binding protein involved in the DNA damage response. *Nat. Struct. Mol. Biol.* **14**, 710–715 (2007).
19. Wang, B. *et al.* Abraxas and RAP80 form a BRCA1 protein complex required for the DNA damage response. *Science* **316**, 1194–1198 (2007).
20. Liu, Z., Wu, J. & Yu, X. CCDC98 targets BRCA1 to DNA damage sites. *Nat. Struct. Mol. Biol.* **14**, 716–720 (2007).
21. Yun, M. H. & Hiom, K. CtIP-BRCA1 modulates the choice of DNA double-strand-break repair pathway throughout the cell cycle. *Nature* **459**, 460–463 (2009).
22. Liu, J., Doty, T., Gibson, B. & Heyer, W.-D. Human BRCA2 protein promotes RAD51 filament formation on RPA-covered single-stranded DNA. *Nat. Struct. Mol. Biol.* **17**, 1260–1262 (2010).
23. Thorslund, T. *et al.* The breast cancer tumor suppressor BRCA2 promotes the specific targeting of RAD51 to single-stranded DNA. *Nat. Struct. Mol. Biol.* **17**, 1263–1265 (2010).
24. Pierce, A. J., Johnson, R. D., Thompson, L. H. & Jasin, M. XRCC3 promotes homology-directed repair of DNA damage in mammalian cells. *Genes Dev.* **13**, 2633–2638 (1999).
25. Wessels, L. F. A. *et al.* Molecular classification of breast carcinomas by comparative genomic hybridization: a specific somatic genetic profile for BRCA1 tumors. *Cancer Res.* **62**, 7110–7117 (2002).
26. Van Beers, E. H. *et al.* Comparative genomic hybridization profiles in human BRCA1 and BRCA2 breast tumors highlight differential sets of genomic aberrations. *Cancer Res.* **65**, 822–827 (2005).
27. Vollebergh, M. A. *et al.* An aCGH classifier derived from BRCA1-mutated breast cancer and benefit of high-dose platinum-based chemotherapy in HER2-negative breast cancer patients. *Ann. Oncol. Off. J. Eur. Soc. Med. Oncol. ESMO* **22**, 1561–1570 (2011).
28. Schreiber, V., Dantzer, F., Ame, J.-C. & de Murcia, G. Poly(ADP-ribose): novel functions for an old molecule. *Nat. Rev. Mol. Cell Biol.* **7**, 517–528 (2006).
29. Langelier, M.-F., Planck, J. L., Roy, S. & Pascal, J. M. Crystal structures of poly(ADP-ribose) polymerase-1 (PARP-1) zinc fingers bound to DNA: structural and functional insights into DNA-dependent PARP-1 activity. *J. Biol. Chem.* **286**, 10690–10701 (2011).
30. Poirier, G. G., de Murcia, G., Jongstra-Bilen, J., Niedergang, C. & Mandel, P. Poly(ADP-ribosylation) of polynucleosomes causes relaxation of chromatin structure. *Proc. Natl. Acad. Sci. U. S. A.* **79**, 3423–3427 (1982).
31. Okano, S., Lan, L., Caldecott, K. W., Mori, T. & Yasui, A. Spatial and temporal cellular responses to single-strand breaks in human cells. *Mol. Cell. Biol.* **23**, 3974–3981 (2003).
32. Caldecott, K. W. XRCC1 and DNA strand break repair. *DNA Repair* **2**, 955–969 (2003).
33. Ström, C. E. *et al.* Poly (ADP-ribose) polymerase (PARP) is not involved in base excision repair but PARP inhibition traps a single-strand intermediate. *Nucleic Acids Res.* **39**, 3166–3175 (2011).
34. Curtin, N. J. & Szabo, C. Therapeutic applications of PARP inhibitors: Anticancer therapy and beyond. *Mol. Aspects Med.* (2013). doi:10.1016/j.mam.2013.01.006
35. Godon, C. *et al.* PARP inhibition versus PARP-1 silencing: different outcomes in terms of single-strand break repair and radiation susceptibility. *Nucleic Acids Res.* **36**, 4454–4464 (2008).
36. Murai, J. *et al.* Trapping of PARP1 and PARP2 by Clinical PARP Inhibitors. *Cancer Res.* **72**, 5588–5599 (2012).
37. Audebert, M., Salles, B. & Calsou, P. Involvement of poly(ADP-ribose) polymerase-1 and XRCC1/DNA ligase III in an alternative route for DNA double-strand breaks rejoining. *J. Biol. Chem.* **279**, 55117–55126 (2004).
38. Patel, A. G., Sarkaria, J. N. & Kaufmann, S. H. Nonhomologous end joining drives poly(ADP-ribose) polymerase (PARP) inhibitor lethality in homologous recombination-deficient cells. *Proc. Natl. Acad. Sci. U. S. A.* **108**, 3406–3411 (2011).
39. Wang, M. *et al.* PARP-1 and Ku compete for repair of DNA double strand breaks by distinct NHEJ pathways. *Nucleic Acids Res.* **34**, 6170–6182 (2006).
40. Mansour, W. Y., Rhein, T. & Dahm-Daphi, J. The alternative end-joining pathway for repair of DNA double-strand breaks requires PARP1 but is not dependent upon microhomologies. *Nucleic Acids Res.* **38**, 6065–6077 (2010).

41. Robert, I., Dantzer, F. & Reina-San-Martin, B. Parp1 facilitates alternative NHEJ, whereas Parp2 suppresses IgH/c-myc translocations during immunoglobulin class switch recombination. *J. Exp. Med.* **206**, 1047–1056 (2009).
42. Yang, Y.-G., Cortes, U., Patnaik, S., Jasin, M. & Wang, Z.-Q. Ablation of PARP-1 does not interfere with the repair of DNA double-strand breaks, but compromises the reactivation of stalled replication forks. *Oncogene* **23**, 3872–3882 (2004).
43. Bryant, H. E. *et al.* Specific killing of BRCA2-deficient tumours with inhibitors of poly(ADP-ribose) polymerase. *Nature* **434**, 913–917 (2005).
44. Farmer, H. *et al.* Targeting the DNA repair defect in BRCA mutant cells as a therapeutic strategy. *Nature* **434**, 917–921 (2005).
45. Kaelin, W. G., Jr. The concept of synthetic lethality in the context of anticancer therapy. *Nat. Rev. Cancer* **5**, 689–698 (2005).
46. McCabe, N. *et al.* Deficiency in the repair of DNA damage by homologous recombination and sensitivity to poly(ADP-ribose) polymerase inhibition. *Cancer Res.* **66**, 8109–8115 (2006).
47. Evers, B. *et al.* A high-throughput pharmaceutical screen identifies compounds with specific toxicity against BRCA2-deficient tumors. *Clin. Cancer Res. Off. J. Am. Assoc. Cancer Res.* **16**, 99–108 (2010).
48. Hay, T. *et al.* Poly(ADP-ribose) polymerase-1 inhibitor treatment regresses autochthonous Brca2/p53-mutant mammary tumors in vivo and delays tumor relapse in combination with carboplatin. *Cancer Res.* **69**, 3850–3855 (2009).
49. Rottenberg, S. *et al.* High sensitivity of BRCA1-deficient mammary tumors to the PARP inhibitor AZD2281 alone and in combination with platinum drugs. *Proc. Natl. Acad. Sci. U. S. A.* **105**, 17079–17084 (2008).
50. Menear, K. A. *et al.* 4-[3-(4-cyclopropanecarbonylpiperazine-1-carbonyl)-4-fluorobenzyl]-2H-phthalazin-1-one: a novel bioavailable inhibitor of poly(ADP-ribose) polymerase-1. *J. Med. Chem.* **51**, 6581–6591 (2008).
51. Audeh, M. W. *et al.* Oral poly(ADP-ribose) polymerase inhibitor olaparib in patients with BRCA1 or BRCA2 mutations and recurrent ovarian cancer: a proof-of-concept trial. *Lancet* **376**, 245–251 (2010).
52. Fong, P. C. *et al.* Inhibition of poly(ADP-ribose) polymerase in tumors from BRCA mutation carriers. *N. Engl. J. Med.* **361**, 123–134 (2009).
53. Tutt, A. *et al.* Oral poly(ADP-ribose) polymerase inhibitor olaparib in patients with BRCA1 or BRCA2 mutations and advanced breast cancer: a proof-of-concept trial. *Lancet* **376**, 235–244 (2010).
54. Gelmon, K. A. *et al.* Olaparib in patients with recurrent high-grade serous or poorly differentiated ovarian carcinoma or triple-negative breast cancer: a phase 2, multicentre, open-label, non-randomised study. *Lancet Oncol.* **12**, 852–861 (2011).
55. Sandhu, S. K. *et al.* The poly(ADP-ribose) polymerase inhibitor niraparib (MK4827) in BRCA mutation carriers and patients with sporadic cancer: a phase 1 dose-escalation trial. *Lancet Oncol.* (2013). doi:10.1016/S1470-2045(13)70240-7
56. Kummar, S. *et al.* A phase I study of veliparib in combination with metronomic cyclophosphamide in adults with refractory solid tumors and lymphomas. *Clin. Cancer Res. Off. J. Am. Assoc. Cancer Res.* **18**, 1726–1734 (2012).
57. Mendes-Pereira, A. M. *et al.* Synthetic lethal targeting of PTEN mutant cells with PARP inhibitors. *EMBO Mol. Med.* **1**, 315–322 (2009).
58. Bassi, C. *et al.* Nuclear PTEN controls DNA repair and sensitivity to genotoxic stress. *Science* **341**, 395–399 (2013).
59. Ibrahim, Y. H. *et al.* PI3K inhibition impairs BRCA1/2 expression and sensitizes BRCA-proficient triple-negative breast cancer to PARP inhibition. *Cancer Discov.* **2**, 1036–1047 (2012).
60. Juvekar, A. *et al.* Combining a PI3K inhibitor with a PARP inhibitor provides an effective therapy for BRCA1-related breast cancer. *Cancer Discov.* **2**, 1048–1063 (2012).
61. Krawczyk, P. M. *et al.* Mild hyperthermia inhibits homologous recombination, induces BRCA2 degradation, and sensitizes cancer cells to poly (ADP-ribose) polymerase-1 inhibition. *Proc. Natl. Acad. Sci. U. S. A.* **108**, 9851–9856 (2011).

62. Chan, N. *et al.* Contextual synthetic lethality of cancer cell kill based on the tumor microenvironment. *Cancer Res.* **70**, 8045–8054 (2010).
63. Pessetto, Z. Y., Yan, Y., Besho, T. & Natarajan, A. Inhibition of BRCT(BRCA1)-phosphoprotein interaction enhances the cytotoxic effect of olaparib in breast cancer cells: a proof of concept study for synthetic lethal therapeutic option. *Breast Cancer Res. Treat.* **134**, 511–517 (2012).
64. Deans, A. J. *et al.* Cyclin-dependent kinase 2 functions in normal DNA repair and is a therapeutic target in BRCA1-deficient cancers. *Cancer Res.* **66**, 8219–8226 (2006).
65. Jirawatnotai, S. *et al.* A function for cyclin D1 in DNA repair uncovered by protein interactome analyses in human cancers. *Nature* **474**, 230–234 (2011).
66. Nowsheen, S., Cooper, T., Bonner, J. A., LoBuglio, A. F. & Yang, E. S. HER2 overexpression renders human breast cancers sensitive to PARP inhibition independently of any defect in homologous recombination DNA repair. *Cancer Res.* **72**, 4796–4806 (2012).
67. Jacquemont, C. & Taniguchi, T. Proteasome function is required for DNA damage response and fanconi anemia pathway activation. *Cancer Res.* **67**, 7395–7405 (2007).
68. Noguchi, M. *et al.* Inhibition of homologous recombination repair in irradiated tumor cells pretreated with Hsp90 inhibitor 17-allylamino-17-demethoxygeldanamycin. *Biochem. Biophys. Res. Commun.* **351**, 658–663 (2006).
69. Ogiwara, H. *et al.* Curcumin suppresses multiple DNA damage response pathways and has potency as a sensitizer to PARP inhibitor. *Carcinogenesis* (2013). doi:10.1093/carcin/bgt240
70. Yang, E. S., Nowsheen, S., Rahman, M. A., Cook, R. S. & Xia, F. Targeting BRCA1 Localization to Augment Breast Tumor Sensitivity to Poly(ADP-Ribose) Polymerase Inhibition. *Cancer Res.* **72**, 5547–5555 (2012).
71. Edwards, S. L. *et al.* Resistance to therapy caused by intragenic deletion in BRCA2. *Nature* **451**, 1111–1115 (2008).
72. Sakai, W. *et al.* Secondary mutations as a mechanism of cisplatin resistance in BRCA2-mutated cancers. *Nature* **451**, 1116–1120 (2008).
73. Swisher, E. M. *et al.* Secondary BRCA1 mutations in BRCA1-mutated ovarian carcinomas with platinum resistance. *Cancer Res.* **68**, 2581–2586 (2008).
74. Barber, L. J. *et al.* Secondary mutations in BRCA2 associated with clinical resistance to a PARP inhibitor. *J. Pathol.* **229**, 422–429 (2013).
75. Norquist, B. *et al.* Secondary somatic mutations restoring BRCA1/2 predict chemotherapy resistance in hereditary ovarian carcinomas. *J. Clin. Oncol. Off. J. Am. Soc. Clin. Oncol.* **29**, 3008–3015 (2011).
76. Bouwman, P. *et al.* A high-throughput functional complementation assay for classification of BRCA1 missense variants. *Cancer Discov.* (2013). doi:10.1158/2159-8290.CD-13-0094
77. Drost, R. *et al.* BRCA1 RING Function Is Essential for Tumor Suppression but Dispensable for Therapy Resistance. *Cancer Cell* **20**, 797–809 (2011).
78. Bunting, S. F. *et al.* 53BP1 inhibits homologous recombination in Brca1-deficient cells by blocking resection of DNA breaks. *Cell* **141**, 243–254 (2010).
79. Bouwman, P. *et al.* 53BP1 loss rescues BRCA1 deficiency and is associated with triple-negative and BRCA-mutated breast cancers. *Nat. Struct. Mol. Biol.* **17**, 688–695 (2010).
80. Cao, L. *et al.* A selective requirement for 53BP1 in the biological response to genomic instability induced by Brca1 deficiency. *Mol. Cell* **35**, 534–541 (2009).
81. Bothmer, A. *et al.* 53BP1 regulates DNA resection and the choice between classical and alternative end joining during class switch recombination. *J. Exp. Med.* **207**, 855–865 (2010).
82. Pei, H. *et al.* MMSET regulates histone H4K20 methylation and 53BP1 accumulation at DNA damage sites. *Nature* **470**, 124–128 (2011).
83. Doil, C. *et al.* RNF168 binds and amplifies ubiquitin conjugates on damaged chromosomes to allow accumulation of repair proteins. *Cell* **136**, 435–446 (2009).
84. Fradet-Turcotte, A. *et al.* 53BP1 is a reader of the DNA-damage-induced H2A Lys 15 ubiquitin mark. *Nature* **499**, 50–54 (2013).
85. Tang, J. *et al.* Acetylation limits 53BP1 association with damaged chromatin to promote homologous recombination. *Nat. Struct. Mol. Biol.* **20**, 317–325 (2013).

86. Gonzalez-Suarez, I. *et al.* A new pathway that regulates 53BP1 stability implicates cathepsin L and vitamin D in DNA repair. *EMBO J.* **30**, 3383–3396 (2011).
87. Feng, L., Fong, K.-W., Wang, J., Wang, W. & Chen, J. RIF1 counteracts BRCA1-mediated end resection during DNA repair. *J. Biol. Chem.* **288**, 11135–11143 (2013).
88. Escribano-Díaz, C. *et al.* A cell cycle-dependent regulatory circuit composed of 53BP1-RIF1 and BRCA1-CtIP controls DNA repair pathway choice. *Mol. Cell* **49**, 872–883 (2013).
89. Chapman, J. R. *et al.* RIF1 is essential for 53BP1-dependent nonhomologous end joining and suppression of DNA double-strand break resection. *Mol. Cell* **49**, 858–871 (2013).
90. Zimmermann, M., Lottersberger, F., Buonomo, S. B., Sfeir, A. & de Lange, T. 53BP1 regulates DSB repair using Rif1 to control 5' end resection. *Science* **339**, 700–704 (2013).
91. Di Virgilio, M. *et al.* Rif1 prevents resection of DNA breaks and promotes immunoglobulin class switching. *Science* **339**, 711–715 (2013).
92. Callen, E. *et al.* 53BP1 Mediates Productive and Mutagenic DNA Repair through Distinct Phosphoprotein Interactions. *Cell* **153**, 1266–1280 (2013).
93. Szakács, G., Paterson, J. K., Ludwig, J. A., Booth-Genthe, C. & Gottesman, M. M. Targeting multidrug resistance in cancer. *Nat. Rev. Drug Discov.* **5**, 219–234 (2006).
94. Doyle, L. A. *et al.* A multidrug resistance transporter from human MCF-7 breast cancer cells. *Proc. Natl. Acad. Sci. U. S. A.* **95**, 15665–15670 (1998).
95. Juliano, R. L. & Ling, V. A surface glycoprotein modulating drug permeability in Chinese hamster ovary cell mutants. *Biochim. Biophys. Acta* **455**, 152–162 (1976).
96. Rottenberg, S. *et al.* Selective induction of chemotherapy resistance of mammary tumors in a conditional mouse model for hereditary breast cancer. *Proc. Natl. Acad. Sci. U. S. A.* **104**, 12117–12122 (2007).
97. Zander, S. A. L. *et al.* Sensitivity and acquired resistance of BRCA1;p53-deficient mouse mammary tumors to the topoisomerase I inhibitor topotecan. *Cancer Res.* **70**, 1700–1710 (2010).
98. Pajic, M. *et al.* Moderate increase in Mdr1a/1b expression causes in vivo resistance to doxorubicin in a mouse model for hereditary breast cancer. *Cancer Res.* **69**, 6396–6404 (2009).
99. Faneyte, I. F., Kristel, P. M. & van de Vijver, M. J. Determining MDR1/P-glycoprotein expression in breast cancer. *Int. J. Cancer J. Int. Cancer* **93**, 114–122 (2001).
100. Faneyte, I. F. *et al.* Expression of the breast cancer resistance protein in breast cancer. *Clin. Cancer Res. Off. J. Am. Assoc. Cancer Res.* **8**, 1068–1074 (2002).
101. Pusztai, L. *et al.* Phase II study of tariquidar, a selective P-glycoprotein inhibitor, in patients with chemotherapy-resistant, advanced breast carcinoma. *Cancer* **104**, 682–691 (2005).
102. Huff, L. M., Lee, J.-S., Robey, R. W. & Fojo, T. Characterization of gene rearrangements leading to activation of MDR-1. *J. Biol. Chem.* **281**, 36501–36509 (2006).
103. Mickley, L. A. *et al.* Genetic polymorphism in MDR-1: a tool for examining allelic expression in normal cells, unselected and drug-selected cell lines, and human tumors. *Blood* **91**, 1749–1756 (1998).
104. Mégnin-Chanet, F., Bollet, M. A. & Hall, J. Targeting poly(ADP-ribose) polymerase activity for cancer therapy. *Cell. Mol. Life Sci. CMLS* **67**, 3649–3662 (2010).
105. Pettitt, S. J. *et al.* A genetic screen using the PiggyBac transposon in haploid cells identifies Parp1 as a mediator of olaparib toxicity. *PLoS One* **8**, e61520 (2013).
106. Sharma, S. V. *et al.* A chromatin-mediated reversible drug-tolerant state in cancer cell subpopulations. *Cell* **141**, 69–80 (2010).
107. Lovato, A., Panasci, L. & Witcher, M. Is there an epigenetic component underlying the resistance of triple-negative breast cancers to parp inhibitors? *Front. Pharmacol.* **3**, 202 (2012).
108. De Craene, B. & Berx, G. Regulatory networks defining EMT during cancer initiation and progression. *Nat. Rev. Cancer* **13**, 97–110 (2013).
109. Işeri, O. D. *et al.* Drug resistant MCF-7 cells exhibit epithelial-mesenchymal transition gene expression pattern. *Biomed. Pharmacother. Biomédecine Pharmacothérapie* **65**, 40–45 (2011).
110. Kajiyama, H. *et al.* Chemoresistance to paclitaxel induces epithelial-mesenchymal transition and enhances metastatic potential for epithelial ovarian carcinoma cells. *Int. J. Oncol.* **31**, 277–283 (2007).

111. McConkey, D. J. *et al.* Role of epithelial-to-mesenchymal transition (EMT) in drug sensitivity and metastasis in bladder cancer. *Cancer Metastasis Rev.* **28**, 335–344 (2009).
112. Li, Q.-Q. *et al.* Twist1-mediated adriamycin-induced epithelial-mesenchymal transition relates to multidrug resistance and invasive potential in breast cancer cells. *Clin. Cancer Res. Off. J. Am. Assoc. Cancer Res.* **15**, 2657–2665 (2009).
113. Shah, A. N. *et al.* Development and characterization of gemcitabine-resistant pancreatic tumor cells. *Ann. Surg. Oncol.* **14**, 3629–3637 (2007).
114. Yang, A. D. *et al.* Chronic oxaliplatin resistance induces epithelial-to-mesenchymal transition in colorectal cancer cell lines. *Clin. Cancer Res. Off. J. Am. Assoc. Cancer Res.* **12**, 4147–4153 (2006).
115. Konecny, G. E. *et al.* Activity of lapatinib a novel HER2 and EGFR dual kinase inhibitor in human endometrial cancer cells. *Br. J. Cancer* **98**, 1076–1084 (2008).
116. Chung, J.-H. *et al.* Clinical and molecular evidences of epithelial to mesenchymal transition in acquired resistance to EGFR-TKIs. *Lung Cancer Amst. Neth.* **73**, 176–182 (2011).
117. Huang, S. *et al.* MED12 controls the response to multiple cancer drugs through regulation of TGF- β receptor signaling. *Cell* **151**, 937–950 (2012).
118. Loboda, A. *et al.* EMT is the dominant program in human colon cancer. *BMC Med. Genomics* **4**, 9 (2011).
119. Weigelt, B. *et al.* Refinement of breast cancer classification by molecular characterization of histological special types. *J. Pathol.* **216**, 141–150 (2008).
120. Weigelt, B., Kreike, B. & Reis-Filho, J. S. Metaplastic breast carcinomas are basal-like breast cancers: a genomic profiling analysis. *Breast Cancer Res. Treat.* **117**, 273–280 (2009).
121. Geyer, F. C. *et al.* Molecular analysis reveals a genetic basis for the phenotypic diversity of metaplastic breast carcinomas. *J. Pathol.* **220**, 562–573 (2010).
122. Jung, S.-Y. *et al.* Worse prognosis of metaplastic breast cancer patients than other patients with triple-negative breast cancer. *Breast Cancer Res. Treat.* **120**, 627–637 (2010).
123. Prat, A. *et al.* Phenotypic and molecular characterization of the claudin-low intrinsic subtype of breast cancer. *Breast Cancer Res. BCR* **12**, R68 (2010).
124. Taube, J. H. *et al.* Core epithelial-to-mesenchymal transition interactome gene-expression signature is associated with claudin-low and metaplastic breast cancer subtypes. *Proc. Natl. Acad. Sci. U. S. A.* **107**, 15449–15454 (2010).
125. Iwatsuki, M. *et al.* Epithelial-mesenchymal transition in cancer development and its clinical significance. *Cancer Sci.* **101**, 293–299 (2010).
126. Moody, S. E. *et al.* The transcriptional repressor Snail promotes mammary tumor recurrence. *Cancer Cell* **8**, 197–209 (2005).
127. Van Nes, J. G. H. *et al.* Co-expression of SNAIL and TWIST determines prognosis in estrogen receptor-positive early breast cancer patients. *Breast Cancer Res. Treat.* **133**, 49–59 (2012).
128. Huijbers, I. J., Krimpenfort, P., Berns, A. & Jonkers, J. Rapid validation of cancer genes in chimeras derived from established genetically engineered mouse models. *BioEssays News Rev. Mol. Cell. Dev. Biol.* **33**, 701–710 (2011).
129. Sequist, L. V. *et al.* Genotypic and histological evolution of lung cancers acquiring resistance to EGFR inhibitors. *Sci. Transl. Med.* **3**, 75ra26 (2011).
130. Uramoto, H., Shimokawa, H., Hanagiri, T., Kuwano, M. & Ono, M. Expression of selected gene for acquired drug resistance to EGFR-TKI in lung adenocarcinoma. *Lung Cancer Amst. Neth.* **73**, 361–365 (2011).
131. Gupta, P. B. *et al.* Identification of selective inhibitors of cancer stem cells by high-throughput screening. *Cell* **138**, 645–659 (2009).
132. Zhou, B.-B. S. *et al.* Tumour-initiating cells: challenges and opportunities for anticancer drug discovery. *Nat. Rev. Drug Discov.* **8**, 806–823 (2009).
133. Lapidot, T. *et al.* A cell initiating human acute myeloid leukaemia after transplantation into SCID mice. *Nature* **367**, 645–648 (1994).
134. Visvader, J. E. & Lindeman, G. J. Cancer stem cells in solid tumours: accumulating evidence and unresolved questions. *Nat. Rev. Cancer* **8**, 755–768 (2008).
135. Kelly, P. N., Dakic, A., Adams, J. M., Nutt, S. L. & Strasser, A. Tumor growth need not be driven by rare cancer stem cells. *Science* **317**, 337 (2007).

136. Quintana, E. *et al.* Efficient tumour formation by single human melanoma cells. *Nature* **456**, 593–598 (2008).
137. Al-Hajj, M., Wicha, M. S., Benito-Hernandez, A., Morrison, S. J. & Clarke, M. F. Prospective identification of tumorigenic breast cancer cells. *Proc. Natl. Acad. Sci. U. S. A.* **100**, 3983–3988 (2003).
138. Stingl, J. *et al.* Purification and unique properties of mammary epithelial stem cells. *Nature* **439**, 993–997 (2006).
139. Shackleton, M. *et al.* Generation of a functional mammary gland from a single stem cell. *Nature* **439**, 84–88 (2006).
140. Shafee, N. *et al.* Cancer stem cells contribute to cisplatin resistance in Brca1/p53-mediated mouse mammary tumors. *Cancer Res.* **68**, 3243–3250 (2008).
141. Pajic, M. *et al.* Tumor-initiating cells are not enriched in cisplatin-surviving BRCA1;p53-deficient mammary tumor cells in vivo. *Cell Cycle Georget. Tex* **9**, 3780–3791 (2010).
142. Zhang, M. *et al.* Identification of tumor-initiating cells in a p53-null mouse model of breast cancer. *Cancer Res.* **68**, 4674–4682 (2008).
143. Herschkowitz, J. I. *et al.* Comparative oncogenomics identifies breast tumors enriched in functional tumor-initiating cells. *Proc. Natl. Acad. Sci. U. S. A.* **109**, 2778–2783 (2012).
144. Lim, S. *et al.* SNAI1-Mediated Epithelial-Mesenchymal Transition Confers Chemoresistance and Cellular Plasticity by Regulating Genes Involved in Cell Death and Stem Cell Maintenance. *PLoS One* **8**, e66558 (2013).
145. Mani, S. A. *et al.* The epithelial-mesenchymal transition generates cells with properties of stem cells. *Cell* **133**, 704–715 (2008).
146. Morel, A.-P. *et al.* Generation of breast cancer stem cells through epithelial-mesenchymal transition. *PLoS One* **3**, e2888 (2008).
147. Scheel, C. *et al.* Paracrine and autocrine signals induce and maintain mesenchymal and stem cell states in the breast. *Cell* **145**, 926–940 (2011).
148. Li, X. *et al.* Intrinsic resistance of tumorigenic breast cancer cells to chemotherapy. *J. Natl. Cancer Inst.* **100**, 672–679 (2008).
149. Diehn, M. *et al.* Association of reactive oxygen species levels and radioresistance in cancer stem cells. *Nature* **458**, 780–783 (2009).
150. Schott, A. F. *et al.* Preclinical and clinical studies of gamma secretase inhibitors with docetaxel on human breast tumors. *Clin. Cancer Res. Off. J. Am. Assoc. Cancer Res.* **19**, 1512–1524 (2013).
151. Pham, C. G. *et al.* Upregulation of Twist-1 by NF-kappaB blocks cytotoxicity induced by chemotherapeutic drugs. *Mol. Cell. Biol.* **27**, 3920–3935 (2007).
152. Valsesia-Wittmann, S. *et al.* Oncogenic cooperation between H-Twist and N-Myc overrides failsafe programs in cancer cells. *Cancer Cell* **6**, 625–630 (2004).
153. Joesse, S. A. *et al.* Prediction of BRCA1-association in hereditary non-BRCA1/2 breast carcinomas with array-CGH. *Breast Cancer Res. Treat.* **116**, 479–489 (2009).
154. Waddell, N. *et al.* Subtypes of familial breast tumours revealed by expression and copy number profiling. *Breast Cancer Res. Treat.* **123**, 661–677 (2010).
155. Stefansson, O. A. *et al.* Genomic profiling of breast tumours in relation to BRCA abnormalities and phenotypes. *Breast Cancer Res. BCR* **11**, R47 (2009).
156. Jönsson, G. *et al.* Distinct genomic profiles in hereditary breast tumors identified by array-based comparative genomic hybridization. *Cancer Res.* **65**, 7612–7621 (2005).
157. Birkbak, N. J. *et al.* Telomeric allelic imbalance indicates defective DNA repair and sensitivity to DNA-damaging agents. *Cancer Discov.* **2**, 366–375 (2012).
158. Abkevich, V. *et al.* Patterns of genomic loss of heterozygosity predict homologous recombination repair defects in epithelial ovarian cancer. *Br. J. Cancer* **107**, 1776–1782 (2012).
159. Popova, T. *et al.* Ploidy and large-scale genomic instability consistently identify basal-like breast carcinomas with BRCA1/2 inactivation. *Cancer Res.* **72**, 5454–5462 (2012).
160. Warmoes, M. *et al.* Proteomics of mouse BRCA1-deficient mammary tumors identifies DNA repair proteins with potential diagnostic and prognostic value in human breast cancer. *Mol. Cell. Proteomics MCP* **11**, M111.013334 (2012).

161. Graeser, M. *et al.* A marker of homologous recombination predicts pathologic complete response to neoadjuvant chemotherapy in primary breast cancer. *Clin. Cancer Res. Off. J. Am. Assoc. Cancer Res.* **16**, 6159–6168 (2010).
162. Asakawa, H. *et al.* Prediction of breast cancer sensitivity to neoadjuvant chemotherapy based on status of DNA damage repair proteins. *Breast Cancer Res. BCR* **12**, R17 (2010).
163. Mukhopadhyay, A. *et al.* Development of a functional assay for homologous recombination status in primary cultures of epithelial ovarian tumor and correlation with sensitivity to poly(ADP-ribose) polymerase inhibitors. *Clin. Cancer Res. Off. J. Am. Assoc. Cancer Res.* **16**, 2344–2351 (2010).
164. Singh, K. K. *et al.* Regulating cardiac energy metabolism and bioenergetics by targeting the DNA damage repair protein BRCA1. *J. Thorac. Cardiovasc. Surg.* (2013). doi:10.1016/j.jtcvs.2012.12.046
165. Marangoni, E. *et al.* A new model of patient tumor-derived breast cancer xenografts for preclinical assays. *Clin. Cancer Res. Off. J. Am. Assoc. Cancer Res.* **13**, 3989–3998 (2007).
166. Zhang, X. *et al.* A Renewable Tissue Resource of Phenotypically Stable, Biologically and Ethnically Diverse, Patient-Derived Human Breast Cancer Xenograft Models. *Cancer Res.* **73**, 4885–4897 (2013).
167. DeRose, Y. S. *et al.* Tumor grafts derived from women with breast cancer authentically reflect tumor pathology, growth, metastasis and disease outcomes. *Nat. Med.* **17**, 1514–1520 (2011).
168. Singh, M., Murriel, C. L. & Johnson, L. Genetically engineered mouse models: closing the gap between preclinical data and trial outcomes. *Cancer Res.* **72**, 2695–2700 (2012).
169. Van Miltenburg, M. H. & Jonkers, J. Using genetically engineered mouse models to validate candidate cancer genes and test new therapeutic approaches. *Curr. Opin. Genet. Dev.* **22**, 21–27 (2012).
170. Wang, H. *et al.* One-step generation of mice carrying mutations in multiple genes by CRISPR/Cas-mediated genome engineering. *Cell* **153**, 910–918 (2013).
171. Rajan, A. *et al.* A phase I combination study of olaparib with cisplatin and gemcitabine in adults with solid tumors. *Clin. Cancer Res. Off. J. Am. Assoc. Cancer Res.* **18**, 2344–2351 (2012).
172. Ledermann, J. *et al.* Olaparib maintenance therapy in platinum-sensitive relapsed ovarian cancer. *N. Engl. J. Med.* **366**, 1382–1392 (2012).
173. Issaeva, N. *et al.* 6-thioguanine selectively kills BRCA2-defective tumors and overcomes PARP inhibitor resistance. *Cancer Res.* **70**, 6268–6276 (2010).
174. Fisher, R., Pusztai, L. & Swanton, C. Cancer heterogeneity: implications for targeted therapeutics. *Br. J. Cancer* **108**, 479–485 (2013).

SUMMARY



Resistance to anti-cancer drugs is one of the biggest challenges in clinical oncology. In addition to classical DNA-damaging chemotherapeutic agents, novel specific inhibitors have been developed in the route towards personalized medicine. Unfortunately, resistance to these new drugs is also frequently observed. My thesis describes our work on several aspects of drug resistance in mouse models of breast cancer. This includes acquired and intrinsic resistance, and biomarker discovery for anti-cancer drugs that are frequently used in the clinic as well as for a novel therapeutic approach: in genetically engineered mouse models of BRCA1/2-associated hereditary breast cancer we have studied intrinsic and acquired resistance to poly(ADP-ribose) polymerase (PARP) inhibitors (PARPi); a promising therapy for BRCA1- and BRCA2-deficient breast and ovarian cancer. **Chapter 1** provides an introduction to triple-negative breast cancer (TNBC), the subtype to which most of the BRCA1-related breast cancers belong. Tumors of this subtype do not express the estrogen and progesterone receptors and have no HER2 amplification. In the absence of these drug targets no targeted therapies are currently available for this group of patients. TNBC is a very heterogeneous group and several new drug targets have been proposed, such as EGFR- and PARP inhibitors. In **Chapter 1** we focus on BRCA1/2-related breast cancers and discuss why these tumors are sensitive to DNA-damaging therapy. Despite this therapy sensitivity, patients with metastatic disease are rarely cured and also BRCA1/2-deficient mouse tumors are usually not eradicated. Here we discuss several potential mechanisms of resistance, how these could be targeted and which assays could predict a good response to chemotherapy or PARP inhibitors.

Due to their defect in the error-free double-strand break (DSB) repair using homologous recombination (HR), BRCA1/2-deficient cells are highly sensitive to inhibitors of PARP. PARP1 is involved in single-strand break (SSB) repair and inhibition of PARP1 leads to toxic PARP-DNA complexes and unrepaired SSBs that become DSBs during replication, inducing synthetic lethality in BRCA1/2-deficient cells that lack HR. Cells with functional BRCA1 and BRCA2 can repair this damage and tolerate PARP inhibition, which makes PARP inhibition a tumor-specific therapy with few side effects. In **Chapter 2** we show that BRCA1-deficient mouse mammary tumors are sensitive to the PARPi olaparib as single agent, but eventually acquire resistance. Olaparib turned out to be a substrate for the drug efflux transporter P-glycoprotein (Pgp) and up-regulation of Pgp was largely responsible for the resistance, as tumors could be re-sensitized to olaparib by applying a Pgp inhibitor. Combining olaparib with a platinum drug prolonged the relapse-free survival, but also increased the toxicity. Unfortunately, also with this combination treatment the BRCA1-deficient tumors were usually not eradicated.

Clinical studies have confirmed the benefit of PARPi for patients with BRCA1- or BRCA2-related breast and ovarian cancer. But not all patients with a BRCA1/2 mutation responded well to PARP inhibition or responded initially and relapsed on treatment later, underlining

the importance of studying potential mechanisms of resistance. To study other PARPi resistance mechanisms than Pgp, we produced a cohort of Pgp-deficient *Brca1*^{-/-};*p53*^{-/-} mouse mammary tumors (**Chapter 3**). These tumors responded longer to olaparib, but still acquired resistance. The response of Pgp-deficient *Brca1*^{-/-};*p53*^{-/-} tumors to olaparib was comparable to the response of Pgp-proficient tumors to a novel PARPi AZD2461, which is a poor substrate for Pgp. We found that 25% of the PARPi-resistant tumors were negative for 53BP1, a key regulator of non-homologous end joining. The PARPi-resistant BRCA1-deficient tumors that had lost 53BP1 protein were able to form RAD51 foci, a marker for HR. The restoration of HR abolishes the synthetic lethality and, therefore, PARPi sensitivity. In **Chapter 3** we also studied the effects of long-term PARPi treatment and found that this could suppress the development of resistance in BRCA1-deficient mouse mammary tumors.

Resistance to all classes of anti-cancer drugs (also called pan-resistance) is a major problem as it severely limits the treatment options for patients. In many cancer types, including breast cancer, epithelial-to-mesenchymal transition (EMT) is linked to resistance to various chemotherapeutic and targeting agents, suggesting a role in pan-resistance. We have used a *Brca2*-mutated mouse mammary tumor model to study the role of EMT on drug resistance. These tumors are HR-deficient and, therefore, sensitive to PARP inhibition and DNA damaging therapy. Intriguingly, we show in **Chapter 4** that some BRCA2-deficient mouse mammary tumors are upfront resistant to olaparib, topotecan, docetaxel and doxorubicin, but still highly sensitive to cisplatin. These multi-drug resistant tumors had an EMT-like, sarcomatoid phenotype, and are therefore called carcinosarcomas. This phenotype correlates with a high expression of the efflux transporter genes *Abcb1a* and *Abcb1b* (both encoding Pgp), and *Abcg2* (also known as breast cancer resistance protein, BCRP). By pre-treating these carcinosarcomas with a Pgp inhibitor, we could partly re-sensitize them to olaparib, doxorubicin and docetaxel. Together, this suggests that EMT may play a role in multi-drug resistance. In addition, we demonstrate that EMT is associated with high expression of Pgp in several other mouse models of breast cancer.

The cancer stem cell (CSC) hypothesis provides a model to explain intrinsic resistance of a small subpopulation of tumor cells with stem cell-like properties (also called tumor-initiating cells, TICs), which is responsible for tumor re-growth. In several cancers, including breast cancer, TICs have been identified as a sub-fraction of tumor cells characterized by specific cell surface markers. Nevertheless, there is an ongoing debate whether the CSC model is applicable to all cancer (sub)types. In **Chapter 5** we investigated the tumor-initiating capacity of different cell populations in p53-deficient mouse carcinomas and carcinosarcomas. For this purpose, cells were sorted for the presence of the mammary stem cell markers CD24 and CD49f and transplanted in the mammary fat pad of syngeneic, immunocompetent mice. In contrast to the carcinomas, all four subpopulations (cells with both markers, one marker or none of the two markers) of the EMT-like carcinosarcomas had

equal tumorigenic capacity. EMT has been linked to an increase in TICs, but we show here that also cells that are negative for CD24 and CD49f and therefore identified as ‘non-TICs’ have tumorigenic potential. This indicates that the utility of these CSC markers to identify TICs is context dependent.

Since patients with tumors that have a defect in the HR pathway may substantially benefit from DNA-damaging therapy or PARP inhibitors, it would be useful to have a reliable tool to identify these patients upfront. Several groups have reported on genomic signatures for the identification of BRCA1-like or BRCA2-like breast cancers. We have used a proteomic approach to identify proteins that are differentially expressed between BRCA1-deficient and -proficient mouse mammary tumors (**Chapter 6**). Proteins that were higher expressed in BRCA1-deficient tumors were associated with DNA replication, recombination and repair pathways. The set of higher expressed proteins could classify BRCA1-related breast cancers with high sensitivity. The BRCA1-deficiency signature of 45 proteins also had prognostic value for clinical outcome in four gene expression data sets from breast cancer patients.

HR-deficiency sensitizes tumors not only to PARP inhibition, but also to platinum-based chemotherapy. Therapy-induced RAD51 foci formation is a marker for functional HR and predictive for a poor treatment response. In **Chapter 7** we aimed to find other proteins that discriminate between a good and poor response to cisplatin. We used a proteomic approach to analyse BRCA1-proficient and -deficient mammary tumors 24 hours after cisplatin versus untreated control tumors. We found that proteins that were up-regulated in the BRCA1-proficient cisplatin-resistant tumors were involved in fatty acid metabolism. Moreover, knock-down of fatty acid synthase (FASN) in BRCA1-proficient cell lines sensitized them to cisplatin *in vitro*. This led us to propose fatty acid metabolism as predictive marker for cisplatin resistance when analyzed shortly after treatment. It also highlights the potential of studying predictive markers by analyzing treatment-induced changes rather than untreated tumors.

The final chapter (**Chapter 8**) is a general discussion of the work presented in this thesis, with a special emphasis on PARPi resistance in HR-deficient breast cancer. The functions of BRCA1, BRCA2 and PARP and the treatment of HR-deficient tumors with PARP inhibitors are described. The current knowledge about potential mechanisms of PARPi resistance is discussed in detail, with a big role for restoration of HR, which may be the major way to lose PARPi sensitivity. In addition, I discuss the role of EMT and TICs in drug resistance and the importance of biomarkers to identify HR deficiency in tumors. The usefulness of preclinical models and clinical samples are put in perspective. Finally, I discuss strategies to optimize PARPi treatment and to overcome PARPi resistance.

APPENDICES



Nederlandse samenvatting

Curriculum vitae

List of publications

Dankwoord

NEDERLANDSE SAMENVATTING

Resistentie tegen anti-kanker medicijnen vormt een groot probleem binnen de klinische oncologie. In aanvulling op de klassieke chemotherapeutica zijn nieuwe specifieke remmers ontwikkeld om steeds meer een behandeling op maat te kunnen geven. Helaas is er vaak sprake van resistentie, ook tegen deze nieuwe remmers. Mijn proefschrift beschrijft ons werk aan verschillende aspecten van resistentie in muismodellen voor borstkanker, waaronder primaire (intrinsieke) resistentie, secundaire resistentie en de zoektocht naar biomarkers voor het voorspellen van een goede respons op anti-kanker medicijnen. In muismodellen voor erfelijke vormen van borstkanker die worden veroorzaakt door mutaties in de borstkankergenen *BRCA1* en *BRCA2*, hebben we primaire en secundaire resistentie tegen poly(ADP-ribose) polymerase (PARP) remmers bestudeerd. PARP remmers zijn nieuwe, veelbelovende medicijnen voor BRCA1- en BRCA2-gerelateerde borst- en eierstokkanker. **Hoofdstuk 1** geeft een introductie over het subtype triple-negatieve borstkanker (TNBC), waartoe de meeste BRCA1-gerelateerde borsttumoren behoren. Deze tumoren zijn negatief voor de oestrogeen- en progesteronreceptoren en HER2. Door de afwezigheid van deze markers zijn er op dit moment geen doelgerichte therapieën voor deze tumoren beschikbaar. TNBCs vormen een zeer heterogene groep en er worden verschillende nieuwe medicijnen getest voor een deel van de TNBCs, zoals EGFR remmers en PARP remmers. In **Hoofdstuk 1** richten we ons voornamelijk op BRCA1/2-gerelateerde borstkanker en bespreken we waarom deze vormen van borstkanker gevoelig zijn voor PARP remmers en therapieën die schade aan het DNA aanrichten. Maar ondanks deze gevoeligheid worden patiënten met uitzaaiingen niet vaak genezen en ook in de muizen gaan tumoren met een mutatie in *Brca1* of *Brca2* meestal niet helemaal weg. We bespreken hier een aantal mogelijke resistentiemechanismen, hoe deze zouden kunnen worden bestreden en welke testen een goede chemotherapierespons zouden kunnen voorspellen.

Homologe recombinatie (HR) is een mechanisme dat cellen gebruiken om op een foutloze manier dubbelstrengs breuken (DSB) in het DNA te repareren. Door een defect in HR zijn BRCA1- en BRCA2-deficiënte cellen erg gevoelig voor PARP remmers. PARP1 is essentieel voor de reparatie van enkelstrengs breuken (SSB) in het DNA. Remming van PARP1 zorgt voor toxische PARP-DNA complexen en een ophoping van SSB die DSB worden tijdens replicatie, wat leidt tot synthetische letaliteit in BRCA1/2-deficiënte cellen. Cellen met functioneel BRCA1 en BRCA2 kunnen deze DNA schade wel repareren, wat zorgt voor een tumorspecifiek effect van de PARP remmer en weinig bijwerkingen. In **Hoofdstuk 2** laten we zien dat BRCA1-deficiënte mammatumoren van muizen eerst gevoelig zijn voor de PARP remmer olaparib, maar later resistentie ontwikkelen. Olaparib bleek een substraat te zijn voor de efflux transporter P-glycoproteïne (Pgp). Een verhoogde activiteit van Pgp veroorzaakte de resistentie, want tumoren werden weer gevoelig voor olaparib wanneer

dit middel in combinatie met een Pgp remmer gegeven werd. Wanneer olaparib werd toegediend in combinatie met platinum chemotherapie duurde het langer voordat de tumor teruggroeide, maar er waren ook meer schadelijke bijwerkingen. Daarnaast kon ook met deze combinatietherapie de tumor niet helemaal uitgeroeid worden.

Klinische studies hebben laten zien dat PARP remmers in patiënten met BRCA1- of BRCA2-gerelateerde borst- en eierstokkanker effectief kunnen zijn. Maar ook bij deze patiënten werden tumoren resistent nadat ze in eerste instantie goed reageerden, terwijl in andere gevallen tumoren in het geheel niet op de behandeling reageerden. Deze wisselende resultaten onderstrepen het belang van het vinden van resistentiemechanismen tegen PARP remmers. Om naast Pgp activatie ook andere mechanismen te kunnen identificeren, hebben we een cohort van BRCA1-deficiënte tumoren gegenereerd waarin Pgp was uitgeschakeld (**Hoofdstuk 3**). Deze tumoren reageerden langer op olaparib, maar ontwikkelden nog steeds resistentie. Dit was vergelijkbaar met de respons van Pgp-proficiënte tumoren op de nieuwe PARP remmer AZD2461, dat een slecht substraat voor Pgp is. We vonden in 25% van de resistente tumoren een verlies van het eiwit 53BP1, dat betrokken is bij de reparatie van dubbelstrengs DNA breuken via non-homologe recombinatie (NHEJ). De resistente BRCA1-deficiënte tumoren met verlies van 53BP1 konden nu RAD51 foci vormen, een marker voor HR. Het herstel van HR heft de synthetische letaliteit en daarmee de gevoeligheid voor PARP remmers op. In **Hoofdstuk 3** hebben we ook de effecten van langdurige behandeling met PARP remmers op tumorgroei bestudeerd en vonden dat dit de ontwikkeling van resistentie kon onderdrukken.

Resistentie tegen verschillende soorten medicijnen tegelijk is een groot probleem, omdat het de behandelingsmogelijkheden voor de patiënt sterk vermindert. Epitheliale-naar-mesenchymale transitie (EMT) is in diverse kankersoorten, inclusief borstkanker, gerelateerd aan resistentie tegen verscheidene chemotherapieën en doelgerichte medicijnen. We hebben een muismodel met BRCA2-deficiënte mammatumoren gebruikt om een verband tussen EMT en resistentie te onderzoeken. Deze tumoren zijn HR-deficiënt en daarom gevoelig voor PARP remmers en chemotherapie. In **Hoofdstuk 4** laten we echter zien dat een deel van deze tumoren intrinsiek resistent is tegen olaparib, topotecan, docetaxel en doxorubicine, maar nog steeds zeer gevoelig voor cisplatine. In tegenstelling tot de gevoelige tumoren hebben de resistente tumoren een EMT-achtig fenotype, en worden daarom carcinosarcoma genoemd. De carcinosarcoma's hebben ook een hogere expressie van de efflux transporter genen *Abcb1a* en *Abcb1b*, die beide coderen voor Pgp, en *Abcg2* (ook wel "breast cancer resistance protein" of BCRP genoemd). Slechts een deel van de carcinosarcoma's werden weer gevoelig voor olaparib, docetaxel en doxorubicine wanneer deze medicijnen in combinatie met een Pgp remmer werden gegeven. Dit suggereert dat EMT misschien een rol speelt bij resistentie tegen meerdere medicijnen. Daarnaast laten we zien dat EMT ook is geassocieerd met een hoge Pgp expressie in diverse andere muismodellen voor borstkanker.

De kankerstamcelhypothese postuleert dat in iedere tumor slechts een klein deel van de tumorcellen in staat is om een nieuwe tumor te laten uitgroeien. Deze tumorinitiërende cellen (TIC) hebben stamcel eigenschappen en zijn intrinsiek resistent tegen antikanker medicijnen. TIC zouden daarom verantwoordelijk zou zijn voor de teruggroei van tumoren. In leukemie en diverse epitheliale kankersoorten, inclusief borstkanker, is een tumor sub-fractie als TIC geïdentificeerd met behulp van celmembraaneiwitten. Het is echter onduidelijk in hoeverre het kankerstamcelmodel op alle kanker (sub)typen van toepassing is. In **Hoofdstuk 5** onderzochten we de tumorinitiërende capaciteit van p53-deficiënte carcinoma's en carcinosarcoma's door de cellen te sorteren aan de hand van de stamcelmarkers CD24 en CD49f en te transplanteren in de mammapluis van immuuncompetente muizen van dezelfde genetische achtergrond. In tegenstelling tot de carcinoma's vormen alle vier subpopulaties (dat wil zeggen cellen met beide markers, één van beide markers, of geen marker) van de EMT-achtige carcinosarcoma's nieuwe tumoren met vergelijkbare efficiëntie. Anderen hebben laten zien dat EMT de populatie met TIC vergroot, maar hier laten we zien dat ook cellen zonder stamcelmarkers nieuwe tumoren kunnen vormen. Dit duidt er op dat het gebruik van de stamcelmarkers CD24 en CD49f om TIC te identificeren context afhankelijk is.

Omdat patiënten met HR-deficiënte borstkanker baat kunnen hebben bij therapie die gericht is op het induceren van DNA schade (zoals platinum chemotherapie of PARP remmers), is het belangrijk om deze patiënten vooraf te kunnen identificeren. Anderen hebben laten zien dat classificatie met een DNA profiel op basis van specifieke afwijkingen in het aantal DNA kopieën hiervoor gebruikt kan worden. In **Hoofdstuk 6** presenteren we een methode om eiwitten te detecteren die in verschillende hoeveelheden voorkomen in BRCA1-deficiënte versus -proficiënte mammatumoren in muizen. Een groot deel van de eiwitten die verhoogd aanwezig waren in BRCA1-deficiënte tumoren waren gerelateerd aan DNA replicatie, recombinatie en reparatie. Deze groep van verhoogd voorkomende eiwitten kon BRCA1-gerelateerde borstkanker identificeren in een genexpressie dataset van borstkankerpatiënten. Het BRCA1-deficiënte cluster van 45 eiwitten had ook prognostische waarde voor overleving in vier genexpressie datasets met overlevingsdata van borstkankerpatiënten.

Een defect in HR maakt tumoren gevoelig voor PARP remmers, maar ook voor platinum chemotherapie. De vorming van RAD51 foci geïnduceerd door DNA-schade is een marker voor functioneel HR en kan een slechte therapierespons voorspellen. In **Hoofdstuk 7** probeerden we andere eiwitten te vinden die onderscheid kunnen maken tussen een goede en slechte respons op cisplatine. We hebben met proteomics de eiwitten geanalyseerd in BRCA1-deficiënte en -proficiënte tumoren 24 uur na behandeling met cisplatine versus onbehandelde controle tumoren. We vonden dat eiwitten die na behandeling specifiek in de BRCA1-proficiënte, cisplatine-resistente tumoren verhoogd aanwezig waren, betrokken zijn bij vetzuurmetabolisme. De remming van één van deze eiwitten, FASN, maakte BRCA1-

proficiënte cellen gevoelig voor cisplatine *in vitro*. Dit suggereert een mogelijke rol voor actief vetzuurmetabolisme als voorspellende marker voor cisplatine resistentie. Het laat ook de potentie zien van het bestuderen van therapie-geïnduceerde veranderingen in de eiwitsamenstelling, in plaats van enkel het bestuderen van onbehandelde tumoren.

Het laatste hoofdstuk (**Hoofdstuk 8**) is een algemene discussie van het werk dat in dit proefschrift wordt gepresenteerd, met speciale aandacht voor resistentie tegen PARP remmers in HR-deficiënte borstkanker. De functies van BRCA1, BRCA2 en PARP worden beschreven, evenals de behandeling van HR-deficiënte tumoren met PARP remmers. Dan volgt een gedetailleerde bespreking van de huidige kennis over mogelijke mechanismen van resistentie tegen PARP remmers, waarin het herstel van HR een grote rol speelt, wat misschien de belangrijkste manier is om gevoeligheid voor PARP remmers te verliezen. Daarnaast bespreek ik de rol van EMT en TIC in resistentie en het belang van biomarkers om HR deficiëntie vast te stellen in tumoren. Ik probeer het gebruik van muismodellen en klinische tumormonsters in perspectief te plaatsen. Ten slotte, bespreek ik diverse strategieën om therapie met PARP remmers te optimaliseren en resistentie tegen te gaan.

CURRICULUM VITAE

Janneke Elisabeth Jaspers (Eindhoven, 25 November 1983) started her studies Biomedical Sciences at Utrecht University in 2001, after completing the high school gymnasium at the Christelijk College in Zeist. After graduating from the Bachelor study *cum laude*, she participated one year in the board of the student association S.S.R.-N.U. in Utrecht. In 2005 she started with the Master program Biology of Disease. The first research internship was performed in the laboratory of Vascular Medicine at the University Medical Center in Utrecht, where she worked on endothelial progenitor cells in diabetes under supervision of Dr. Peter Westerweel and Prof. dr. Marianne Verhaar. For her second internship she has worked for seven months in the laboratory of Prof. Roberto Pili at the Sidney Kimmel Comprehensive Cancer Center at Johns Hopkins University in Baltimore, MD, which was co-supervised by Prof. dr. Henk Verheul (Medical Oncology, VUmc, Amsterdam). Here she studied the sensitivity of renal cell carcinoma cells to angiogenesis inhibitors.

After obtaining her Master of Science diploma *cum laude*, Janneke started in January 2008 as a PhD student in the laboratories of Dr. Jos Jonkers and Dr. Sven Rottenberg at the Netherlands Cancer Institute in Amsterdam. For her PhD project, she received a Toptalent fellowship from the Netherlands Organization for Scientific Research (NWO). She has studied several aspects of drug resistance in mouse models of breast cancer, which are described in this thesis.

LIST OF PUBLICATIONS

During PhD training

1. **Proteomics of genetically engineered mouse mammary tumors identifies fatty acid metabolism members as potential predictive markers for cisplatin resistance**
Warmoes M*, [Jaspers JE*](#), Xu G, Sampadi BK, Pham TV, Knol JC, Piersma SR, Boven E, Jonkers J, Rottenberg S, Jimenez CR. (2013) *Mol Cell Proteomics* 12(5):1319-34
* Contributed equally to this work
2. **Loss of 53BP1 causes PARP inhibitor resistance in Brca1-mutated mouse mammary tumors**
[Jaspers JE](#), Kersbergen A, Boon U, Sol W, van Deemter L, Zander SA, Drost R, Wientjens E, Ji J, Aly A, Doroshov JH, Cranston A, Martin NM, Lau A, O'Connor MJ, Ganesan S, Borst P, Jonkers J, Rottenberg S. (2013) *Cancer Discovery* 3(1):68-81
3. **Impact of intertumoral heterogeneity on predicting chemotherapy response of BRCA1-deficient mammary tumors**
Rottenberg S, Vollebergh MA, de Hoon B, de Ronde J, Schouten PC, Kersbergen A, Zander SA, Pajic M, [Jaspers JE](#), Jonkers M, Lodén M, Sol W, van der Burg E, Wesseling J, Gillet JP, Gottesman MM, Gribnau J, Wessels L, Linn SC, Jonkers J, Borst P. (2012) *Cancer Res* 72(9):2350-61
4. **Proteomics of mouse BRCA1-deficient mammary tumors identifies DNA repair proteins with potential diagnostic and prognostic value in human breast cancer**
Warmoes M, [Jaspers JE](#), Pham TV, Piersma SR, Oudgenoeg G, Massink MP, Waisfisz Q, Rottenberg S, Boven E, Jonkers J, Jimenez CR. (2012) *Mol Cell Proteomics* 11(7):M111.013334
5. **6-thioguanine selectively kills BRCA2-defective tumors and overcomes PARP inhibitor resistance**
Issaeva N, Thomas HD, Djureinovic T, [Jaspers JE](#), Stoimenov I, Kyle S, Pedley N, Gottipati P, Zur R, Sleeth K, Chatzakos V, Mulligan EA, Lundin C, Gubanov E, Kersbergen A, Harris AL, Sharma RA, Rottenberg S, Curtin NJ, Helleday T. (2010) *Cancer Res* 70(15):6268-76
6. **Sensitivity and acquired resistance of BRCA1;p53-deficient mouse mammary tumors to the topoisomerase I inhibitor topotecan**
Zander SA, Kersbergen A, van der Burg E, de Water N, van Tellingen O, Gunnarsdottir S, [Jaspers JE](#), Pajic M, Nygren AO, Jonkers J, Borst P, Rottenberg S. (2010) *Cancer Res* 70(4):1700-10

7. **Therapeutic options for triple-negative breast cancers with defective homologous recombination**

Jaspers JE, Rottenberg S, Jonkers J. (2009) *Biochim Biophys Acta* 1796(2):266-80

8. **High sensitivity of BRCA1-deficient mammary tumors to the PARP inhibitor AZD2281 alone and in combination with platinum drugs**

Rottenberg S, Jaspers JE, Kersbergen A, van der Burg E, Nygren AO, Zander SA, Derksen PW, de Bruin M, Zevenhoven J, Lau A, Boulter R, Cranston A, O'Connor MJ, Martin NM, Borst P, Jonkers J. (2008) *Proc Natl Acad Sci USA* 105(44):17079-84

During Master training

9. **Impaired endothelial progenitor cell mobilization and dysfunctional bone marrow stroma in diabetes mellitus**

Westerweel PE, Teraa M, Rafii S, Jaspers JE, White IA, Hooper AT, Doevendans PA, Verhaar MC. (2013) *PLoS One* 8(3):e60357

10. **Reversible epithelial to mesenchymal transition and acquired resistance to sunitinib in patients with renal cell carcinoma: evidence from a xenograft study**

Hammers HJ, Verheul HM, Salumbides B, Sharma R, Rudek M, Jaspers J, Shah P, Ellis L, Shen L, Paesante S, Dykema K, Furge K, Teh BT, Netto G, Pili R. (2010) *Mol Cancer Ther* 9(6):1525-35

DANKWOORD

Het is af! Dit is dan echt het laatste wat ik nog moet en ook graag wil schrijven. Want de afgelopen bijna zes jaren waren een mooie en gezellige, ook moeilijke en uitdagende, en zeker een leerzame tijd. En nu is dat waar je al die tijd naar toe werkt helemaal af. Heel veel mensen hebben op vele manieren bijgedragen aan de totstandkoming van dit proefschrift en ook aan mijn ontwikkeling, zowel als onderzoeker als persoonlijk. Allereerst mijn collega's. Het Nederlands Kanker Instituut is een fantastische plek om onderzoek te doen, waar altijd ruimte is voor samenwerking en om elkaar verder helpen vanuit ieders expertise. Ik heb hier dan ook vele inspirerende mensen leren kennen, die ik graag wil bedanken!

Als eerste natuurlijk het gouden trio: **Sven**, **Jos** en **Piet**. Jullie hebben alle drie op een eigen manier bijgedragen aan mijn onderzoek en zonder jullie was dit boekje er niet geweest! **Sven**, de Rottenberg groep bestaat nu eindelijk officieel! Maar helaas niet voor lange tijd hier op het NKI... Het was erg fijn dat je er altijd was voor grote en kleine vragen, ook toen het lab steeds groter werd. Ik heb veel van je geleerd en vond het leuk om regelmatig met elkaar van gedachten te wisselen over van alles binnen en buiten de wetenschap! Ik heb goede herinneringen aan San Francisco (waar je ons meenam naar Chinatown en een jazzconcert) en Keystone! Ik ben heel blij voor je dat je zo'n mooie positie in Bern hebt gekregen. Heel veel succes met het opzetten van je lab daar!

Jos, vanaf onze eerste kennismaking, op de AACR in Los Angeles in 2007, wist ik dat ik graag wilde werken met jouw muismodellen. Dat het er zoveel verschillende zouden worden, had ik toen nog niet kunnen vermoeden! Je eindeloze enthousiasme voor onderzoek is mooi om te zien, ook omdat je daarbij altijd oog houdt voor mogelijke klinische toepassingen. Ik heb veel bewondering voor de manier waarop je zoveel verschillende onderzoekslijnen aanstuurt. Je hebt een enorme hoeveelheid kennis en soms lijkt het wel alsof je weet waar ieder ander lab mee bezig is! Jouw grote netwerk is denk ik een groot voordeel voor het hele lab. Ik heb jouw enthousiasme en optimisme als heel fijn ervaren. Als het even tegen zat, had ik altijd weer veel positieve energie en nieuwe plannen na een bespreking! Bedankt voor je inzet en vertrouwen!

Beste **Piet**, helaas mag je geen co-promotor zijn, maar ook aan jou heb ik veel te danken. Je kunt verbanden leggen als geen ander en weet de essentie van een proef, van ons of in de literatuur, feilloos te doorgronden en interpreteren. Veel uitspraken zullen me nog lang bij blijven, zoals 'Zullen wij...!', 'Controls, controls, controls!' en 'Back to work!'. Bedankt voor je kritische blik op mijn projecten en verhelderende inzichten!

Beste **René Medema**, bedankt dat je vanaf het begin al mijn promotor wilde zijn en dat je in de tussentijd naar het NKI bent gekomen! Ook wil ik jou en de overige leden van mijn oio begeleidingscommissie, **Jan Schellens**, **Hein te Riele** en **Maarten van Lohuizen**, bedanken voor de waardevolle en kritische vragen en suggesties voor mijn onderzoek in de afgelopen jaren. Ook dank aan de leden van mijn promotiecommissie **Sabine Linn**, **René**

Bernards, Jan Hoeijmakers, Paul van Diest en wederom **Jan Schellens** voor het kritisch lezen en beoordelen van mijn proefschrift.

En dan te beginnen met het Borst/Rottenberg lab! Dear **Charlotte**, I was so happy when you came to our lab! You are one of the sweetest and most social persons I know. You are always willing to take over cell culture or mouse work when necessary. Pipetting a 384wells plate and endless clonogenic assays is so much more fun with you around to discuss about a million different things. Many thanks for all the laughter and tears that we (I ;-)) have shared and for the great dinners, movies, drinks, games and much more! And most of all, thanks for standing next to me as my paranimf! Lieve kamergenoten, bedankt voor de ontzettend gezellige tijd! **Koen**, als enige ben jij al die tijd mijn kamergenoot geweest! Bij jou denk ik aan je droge humor, roddelkoningin, luidruchtige besprekingen en gestamp, maar bovenal aan veel gezelligheid, passie voor je experimenten (liever gisteren dan vandaag) en hoe je zichtbaar smelt zodra je aan Gijs denkt! **Robert**, jij hebt altijd weer mooie verhalen over 'een vriendje van je'. Laat je het weten als je weer de marathon van New York gaat lopen? Misschien kom ik je aanmoedigen:-). Veel succes met de zoektocht naar substraat X! **Asli**, mijn positiviteitsgoeroe a.k.a. peptalk-koningin! Altijd behulpzaam en sociaal, zo fijn dat je de afgelopen tijd naast me zat! **Sunny**, bedankt voor alle bestellingen en het ordenen van het lab! En je hebt nog een hoop chocola en dropjes van me tegoed...

Guotai, you keep surprising me again and again! I really enjoyed our discussions about Chinese habits and cultural differences. You have worked hard and I really hope this will result in a few nice papers! Good luck with finishing your thesis and all the best for you and your wife! Dear **Ewa**, great that you continue the search for mechanisms of PARPi resistance! Good luck with the huge amount of tumors to analyze... I thought about writing this to you in Dutch, as you are taking lessons, but you suffered too much already from our Dutch during the lunch breaks...:-) **Wendy**, hoeveel autopsies jij inmiddels wel niet gedaan hebt... Bedankt voor je hulp met een aantal cohorten, zeker ook in de afgelopen maanden, zodat ik me kon focussen op het schrijven. Veel succes met (het vinden van) je volgende baan! **Marco**, al snel was duidelijk dat je een rustige en harde werker bent. En sportief..! Volgend jaar Alp d'HuZes? Succes met al je projecten!

Henri, wat doe jij veel! Je bent ongeveer overal wel bij betrokken en doet ook nog onderzoek. Geen wonder dat je elk weekend op H5 te vinden bent. Maar ondanks je bergen werk blijf je rustig en gezellig! Bedankt voor de administratieve rompslomp met het UMC en voor de gezellige lunches (om klokslag 12.00 uur)! **Tom**, je doet veel achter de schermen, maar dat zorgt er wel voor dat H5 er piekfijn uitziet! Bedankt voor al je praktische hulp met het versturen van vele pakketjes! **Linda**, je werkt alweer een tijdje ergens anders, maar ook jij bedankt voor je hulp en gezelligheid op P2!

Lieve **Ariena K.**! Voor mijn gevoel hoor je niet in het rijtje oud-collega's... een soort ontkenningfase. Ik had niet verwacht dat jij eerder weg zou gaan dan ik! Vijfentwintig jaar

lief en leed gedeeld en dan ben je niet eens bij mijn verdediging... Bedankt voor veel: lol, hulp met de muizen, ultraasmomenten, paarse invloeden, luisterend oor, dansjes in het lab, snoeprooftochten, etc... Ik wens je een superfijne tijd in Melbourne, maar gezien alle feestfoto's op Facebook zit dat wel goed. Tot over een paar weken!! En dan onze ongekroonde celkweekkoningin! **Liesbeth**, wat fijn dat jij altijd tot laat werkte! Ik bewaarde mijn kweekwerk vaak tot het eind van de dag en dan was jij er ook. Bedankt natuurlijk voor het maken van de o zo veel gebruikte cellijnen, maar nog meer voor de vele mooie gesprekken over heel veel verschillende dingen! **Marcel**, op P2 was je de eeuwige vraagbaak voor alle grote en kleine vragen. Bedankt voor alle hulp! Gelukkig kun je nu gewoon weer experimenten doen:-). **Petra**, good luck with your research and all the best! **Serge**, ik bewonder je doorzettingsvermogen en volharding in het doen van experimenten. Ik ben benieuwd waar jouw carrière je zal brengen. Veel succes! Also thanks to my former colleagues **Nikola, Jay and Marina**. **Marina**, as you can see, the TIC experiments have resulted in a chapter, and hopefully a paper soon. Thanks for setting up the FACS sorts! **Wouter**, als ik AZ zie, moet ik toch nog altijd aan jou denken. **Maaïke**, ik zal niet snel vergeten hoe toegewijd jij als dierenarts en –vriend de strijd aanging voor een extra tissue in de kooi. Succes in de epidemiologie!

Ik wil ook graag de twee studenten die ik heb mogen begeleiden, bedanken. **Thijs**, je kwam bij ons voor een eerste kennismaking met onderzoek. Het was erg leuk om je een aantal basistechnieken te leren (hoe werkt een pipet:-)), zeker ook omdat jij zo leergierig en enthousiast bent! **Marieke**, jij werkte al snel heel zelfstandig en ondanks dat die knock-downs maar niet wilden lukken, heb je veel gedaan. Allebei bedankt voor jullie bijdrage aan hoofdstuk 3!

Ik ben ook de **Jonkers groep** dankbaar voor alle discussies, feedback en ideeën, retraites en werkbereprekingen en natuurlijk de gezelligheid, ook nadat we na P2 helaas niet meer op dezelfde afdeling zaten. Ik heb met zoveel van jullie mooie gesprekken gehad over werk en andere dingen en het is mooi om te zien dat de sfeer in de groep zo goed is, waarvan ook de etentjes, BBQs, baby-showers en vrijgezellenetentjes getuigen!

Peter, ik bewonder je enorme hoeveelheid kennis en belezenheid. Bedankt voor al je input. Wat mooi was het dat jouw hit 53BP1 een vervolg kreeg in onze PARPi-resistente tumoren! Mooi blad hè, Cancer Discovery;-). **Hanneke, Ingrid en Ellen**, bedankt voor jullie praktische hulp en adviezen door de jaren heen. **Hanneke**, ik heb met bewondering gezien hoe sterk je je door de afgelopen periode hebt heengeslagen. Ik hoop dat je snel weer helemaal terug bent op C2! De muizenanalisten **Eline, Tanya, Eva en Ute**, bedankt voor de gezelligheid op G2Zuid tijdens de vele uren transplanteren (wat ik lang geleden van jou, **Tanya**, heb geleerd!), tumoren opmeten en autopsies. **Ute**, bedankt voor je hulp met de CD3 en TIC cohorten! **Linda en Martine**, bedankt voor de goede samenwerking voor het EMT-Pgp verhaal. **Martine**, wat fijn dat je regelmatig kritische vragen stelt tijdens werkbereprekingen. En jammer dat je straks nou net in China zit! Veel succes met je beursaanvragen! **Sjoerd**,

Sjors, Petra, Mirjam, Lisette en **Julian**, bedankt voor alle waardevolle discussies en mooie momenten! **Marieke**, jou enthousiasme is echt aanstekelijk. Bedankt voor de enorme hoeveelheid energie die je verspreidt!:-) **Julian**, wat fijn dat de grote hoeveelheid verzamelde sequencing data nu systematisch door jou geanalyseerd wordt! Ik ben erg benieuwd welke nieuwe hits er uit komen! **Mirna**, bedankt voor de vele afspraken en andere dingen die je voor mij geregeld hebt!

Ook de oud-collega's wil ik graag bedanken: **Rinske**, jouw bergen werk afgelopen jaren hebben tot mooie dingen geleid! Ik ben benieuwd wat je in 'onze' tumoren allemaal gaat zien door het raampje. Bedankt voor je enthousiasme en vrolijke lach (die aan onze kant van P2 regelmatig te horen was;-)). Veel succes in Utrecht! **Bastiaan**, met jouw vertrek werden de werkbeprekingen een stuk korter. Bedankt voor je scherpe, kritische vragen en veel succes op B7! **Henne**, bedankt voor de mooie concerten en last-minute CGH data! **Marieke**, het was inspirerend om te zien hoe jij hard werken met veel gezelligheid kon combineren. Veel succes met je opleiding! **Chiel**, ik herinner me jou als aardig en rustig, en ook rechtvoor-zijn-raap en je bekommert je om het welzijn van anderen. Ik heb je oprechte interesse en soms bezorgdheid als heel warm ervaren. **Mark, Marco, Xiaoling** and **Gilles**, thanks for a great time! **Chris**, bedankt voor de EMT genexpressie analyses (lang geleden..) en voor de gastvrijheid in SF, samen met **Sietske**. Veel geluk met zn drieën! Dear **Ewa**, I am very happy for you that your hard work and piles of data resulted in a very nice paper. Besides all the complaints about the Dutch weather (ok, Dutch complain too...), clothes, habits, institute etc. etc. ;-P it was great to have you here! Good luck in Melbourne and hopefully see you in a few weeks!

Met het verdwijnen van P2 verhuisde ook de De Visser groep naar een andere afdeling. Maar gelukkig zag ik jullie gewoon nog bij de C2 werkbeprekingen en natuurlijk in het muizenhuis. **Karin**, mooi om te zien dat jouw groep zich steeds verder uitbreidt! Bedankt dat je iedereen er gewoon op blijft wijzen dat de tumor microenvironment ook nog een rol speelt. **Metamia**, je bent een topper! Succes met de laatste loodjes. Wie weet tot straks in NY! **Chris**, bedankt voor de gesprekken over wetenschap en alles daar omheen. Veel succes straks weer in de kliniek! Of toch in het onderzoek...? **Seth**, I am confident you will find a great place in the US! **Kelly** en **Tisee**, bedankt voor jullie gezelligheid en hulp!

Both on P2 and H5 we were lucky to have the Schinkel group next to us. **Alfred, Dilek, Selvi, Seng, Anita** and **Els**, thanks for the great lab outings, Christmas dinners, drinks and cakes that I shared with you! **Dilek**, wat was ik verrast tijdens het laatste kerstdiner! Ik bewonder hoe relaxed je in het leven staat. Veel geluk met **Jorma** en Max en in je volgende baan! **Seng**, all the best in Malaysia and/or Amsterdam! **Els**, bedankt voor alle stroopwafels en mandarijntjes! Ik wil ook graag iedereen van de **Te Riele, Linn** en **Wessels** groepen bedanken voor de mooie en gezellige tijd op P2, met leuke labuitjes, kerstdiners, borrels en appelmeisjes. **Sabine**, wat is het waardevol om tijdens werkbeprekingen jouw input

vanuit de kliniek te krijgen, want uiteindelijk gaat het om de patiënt. Bedankt voor de goede discussies! **Philip**, bedankt voor je werk aan 53BP1 en EMT. Als die aantallen toch niet steeds zo laag waren... **Andi**, thanks a lot for the many analyses that you did with the EMT signature! **Lodewyk**, bedankt voor het fijne contact en je advies over statistische analyses voor diverse projecten. On H5 I am happy to share the department with the **Jacobs** and **Peeper groups**. Thanks to all of you for the very nice time!

Ook van andere afdelingen heb ik veel fijne mensen leren kennen en mee samen gewerkt. **John**, bedankt voor je hulp met diverse kleuringen! **Monique**, succes met de afronding van jouw onderzoek! **Jelle Wesseling**, bedankt voor je waardevolle aanvullingen over de humane pathologie in vergelijking tot onze muismodellen. **Jarich**, het is mooi om te zien hoe enthousiast je bent over de spectroscopie studies. Helaas heeft ons doxorubicine experiment niet tot iets moois geleid, maar ik vond het heel prettig om met je samen te werken! **Olaf**, bedankt voor de waardevolle discussies en je advies over de farmacokinetiek van doxorubicine en topotecan. **Levi**, bedankt voor je hulp met het opwerken van de samples voor HPLC. **Roel**, het was gezellig om samen de BioBusiness Summer School te doen. Succes de 13^e! **Nienke, Natalie, Andrej, Anja, Ingar, Esther, Petra, Rita, Jelle** en **Jorma**: thanks for a great time at the NKI! **André**, jou moet ik zeker bedanken, want dankzij jou ben ik met Jos in contact gekomen en zie wat er allemaal van gekomen is! Veel succes met jouw groep!

De faciliteiten op het NKI hebben een belangrijke bijdrage geleverd aan dit boekje. Daarom veel dank aan de medewerkers: **Lenny** en **Lauran**, bedankt voor de steeds terugkerende vragen als ik weer eens geen goed beeld had. **Anita** en vooral **Frank**, bedankt voor de vele uren en dagen dat de tumoren gesorteerd werden. **Ron, Marja** en de anderen van de Genomics Core Facility, bedankt voor het profilen en sequencen van heel veel samples! **Marja**, bedankt voor je hulp en geduld toen vorig jaar een grote serie heringedeeld moest worden... **Arno**, bedankt voor het last-minute analyseren van de CGH data! **Ellen** en **Joost**, bedankt voor de fijne samenwerking, ook wanneer een kleuring haast had of ik coupes op een bepaalde dag gesneden wilde hebben. **Tania** en **Bjørn**, wat een geluk dat jullie op G2Zuid werken! Dankzij jullie is het een prettige, opgeruimde afdeling om te werken, met een goede sfeer. Bedankt voor de goede zorgen voor mijn muizen!

Ook wil ik graag **Connie Jimenez** en **Marc Warmoes** van het VUmc bedanken voor de fijne samenwerking. De proteomics studies hebben tot twee mooie papers geleid! **Marc**, bedankt voor het oppakken van de data analyse van de behandelde tumoren. Veel succes met de afronding van je proefschrift en ik wens je een goede tijd in de VS! Dear **Mark** and others from KuDOS and AstraZeneca, thanks for the fruitful collaboration!

Ook buiten het NKI zijn er heel veel fantastische mensen die mij op allerlei manieren gesteund hebben en veel interesse hebben getoond in mijn onderzoek. **Bertine**, echt heel balen dat Rutte er nou net voor zorgt dat je er niet bij kan zijn... Maar alleen al uit het feit dat

je je ticket al geboekt had, blijkt wel wat een topvriendin je bent. Bedankt voor al je steun en gezelligheid! Heel veel plezier samen met Dirk in Beijing. Leve Skype en tot over een paar weken! Lieve **Miranda**, jij bent pas excellent! Ik ken weinig mensen zo attent als jij. Ik hoop dat je behalve aan al die andere mensen ook lekker aan jezelf zal denken! Hopelijk zitten we gauw weer met onze voeten in de vijver op Washington Square Park. **Aafke**, wat jammer dat ik net weg ben als jij naar het AvL komt! **Dominique**, bedankt voor je vriendschap! **Jacobine** en **José**, wat fijn dat jullie door jullie eigen promoties veel (niet alleen wetenschappelijke) dingen begrijpen. Ik kijk uit naar nog veel gezellige avonden, ook met de mannen! Lieve Tuffers, **Mathanja**, **Inge**, **Willemien**, **Jasper**, **Elmer**, **Bob** en **Wilco**, ondanks dat ik niet meer zo vaak naar Utrecht kom, vind ik het superfijn dat we elkaar nog regelmatig zien! Bedankt voor de vele gezellige feesten en borrels afgelopen jaren! **(Oud)kringgenoten**, dankzij jullie voelde ik me snel thuis in Amsterdam. Bedankt voor de goede gesprekken, ontspannende avondjes en broodnodige relativering! **Mady** en **Anjali**, ik heb veel mooie herinneringen aan Baltimore en dat is voor een groot deel aan jullie te danken! **Carlijn**, **Solange** en **Rolien**, ik zal de maandagavonden missen! Lieve **Adrienne**, heel erg bedankt voor het maken van de prachtige cover! Ik wist wel dat het bij jou in goede handen was! Heel fijn dat we elkaar zijn blijven zien sinds jullie in Hong Kong wonen, hopelijk blijft dat zo als wij weg gaan! Jullie zijn lieverds!

Lieve familie Visée, **Wim**, **Cobie**, **John**, **Annelies** en **Claire**, bedankt voor de warme ontvangst in de familie en jullie grote belangstelling voor mijn werk. Ook wil ik graag **Henk**, **Rolien**, **Eline**, **Marije**, **Jochem**, **Aletta**, **Louisa**, **Wendy** en **Jantje** bedanken voor jullie interesse en meelevens!

Annelieke, zo fijn dat jij de ins and outs van wetenschap kent en gewoon weet waar ik het over heb als ik over mijn werk vertel! Ik vind het geweldig dat je ons zoveel mogelijk laat meegenieten van jullie lieve schat Olivier. Bedankt voor alle steun en ik ben heel blij dat je 12 november naast mij staat als paranimf! An, **Daniel**, **Carlien** en **Jan Maarten**, bedankt voor jullie interesse, alle gezellige dagen en avondjes afgelopen jaren! En voor de drie liefste en leukste neefjes van de wereld!

Lieve **pap** en **mam**, jullie support is eindeloos! Ondanks soms wat eerste terughoudendheid, weet ik dat jullie altijd achter mij staan en heel trots op me zijn! En dat is echt heel fijn. Jullie moeten weten dat ik ook trots op jullie ben! En ik kan niet wachten om jullie straks onze nieuwe plek te laten zien (waar het ook zal zijn)!

Lieve, lieve, lieve **Tom**, de laatste woorden zijn voor jou. Wat ben ik ontzettend blij met je! Dank je wel voor al je liefde en steun. Jouw geduld (sorry voor de talloze keren dat ik je heb laten wachten met het eten...), je relativeringsvermogen, samen grapjes maken die niemand anders leuk vindt en de etentjes voor grote en kleine mijlpalen hebben mij de afgelopen jaren heel veel geholpen! Ik kijk er naar uit om eindelijk Down Under te gaan en daarna samen aan een nieuw avontuur te beginnen! Love you!

